Plasma is a kind of gaseous complex composed of electrons, negatively and positively charged particles, neutral atoms and molecules.

In the present research, curative powders were surface modified by plasma polymerization and their performance in the dissimilar rubber-rubber blends improved compared to the unmodified curatives.
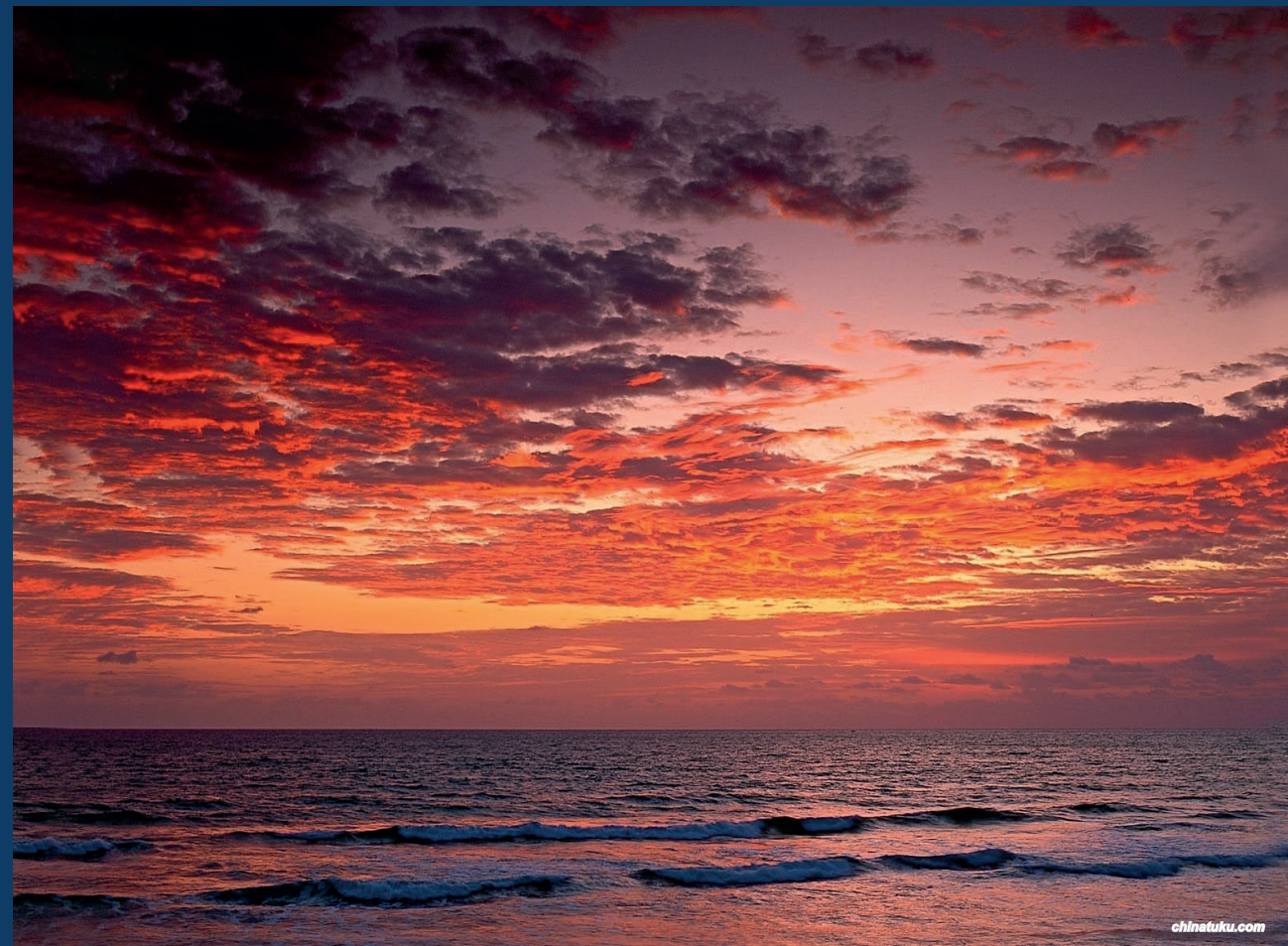
The nano-meter thick plasma polymer layer has changed the surface properties of the encapsulated curatives by forming a shell on the curative substrate. The imperfections on the shell layer acted as a gateway for further release of the curatives for vulcanization.
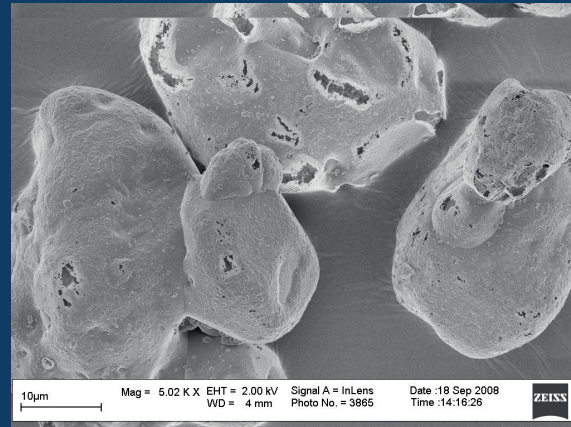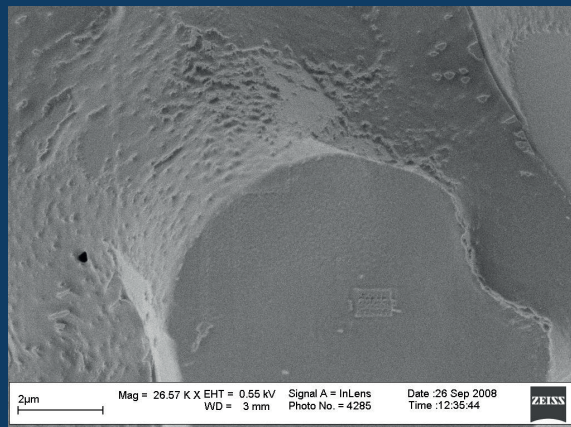
Improved Properties of Dissimilar Rubber-Rubber Blends using Plasma Polymer Encapsulated Curatives

A Novel Surface Modification Method to Improve Co-vulcanization

Rui Guo

Improved Properties of Dissimilar Rubber-Rubber Blends using Plasma Polymer Encapsulated Curatives

A Novel Surface Modification Method to Improve Co-vulcanization

Improved Properties of Dissimilar Rubber-Rubber Blends using Plasma Polymer Encapsulated Curatives: A Novel Surface Modification Method to Improve Co-vulcanization

By Rui Guo

Cover designed by Rui Guo & Chenglei Lu, which gives an example of the plasma in nature.

IMPROVED PROPERTIES OF DISSIMILAR RUBBER-RUBBER BLENDS USING PLASMA POLYMER ENCAPSULATED CURATIVES

A NOVEL SURFACE MODIFICATION METHOD TO IMPROVE CO-VULCANIZATION

DISSERTATION

to obtain

the degree of doctor at the University of Twente,

on the authority of the rector magnificus,

prof. dr. H. Brinksma,

on account of the decision of the graduation committee,

to be publicly defended

on Wednesday, 11th November 2009 at 13:15 hrs.

by

Rui Guo

born on 23rd March 1975

in Urumqi, Xinjiang, China

This dissertation has been approved by:

Promotor   : prof. dr. ir. J.W.M. Noordermeer

Assistant promoter   : dr. A. G. Talma

Table of Contents

Chapter 1

Introduction

This first chapter provides a general introduction into the research described in this thesis, from a historical perspective. The aim of the thesis is stated and a summary of the structure of this thesis is provided.

1.1 Introduction

Elastomers are a kind of polymers, which were initially made from caoutchouc ("weeping tree"). [3] The term "rubber" was assigned by the English scientist Joseph Priestley, for the ability of Natural Rubber (NR) to erase pencil or ink marks. The history of today's NR can be traced back to the time when pre-Columbian people of South and Central America used rubber for balls, containers, shoes and waterproofing fabrics. However, it did not appear useful until Charles de la Condamine and François Fresneau reported this material to the French Academy of Sciences between 1736 and 1751. [4, 5] After that, a series of breakthroughs in processing of this material have been achieved, while the most revolutionary one is still from 1839, when Charles Goodyear discovered a process, which involved the heating of rubber with sulfur and white lead, to overcome the stickiness and high degradability of uncured rubber: vulcanization. [5, 6] The process of vulcanization creates crosslinks between the loose rubber polymer chains, thereby rendering the rubber form-stable. This form stability is commonly called "set". Although the obtained vulcanized rubber had improved physical properties, the process of vulcanization took too long (>5 h) to become commercially acceptable until 1906, when the effect of the organic chemical accelerator, aniline, was discovered in sulfur vulcanization by Oenslager. [7]

Nowadays, rubber for almost all ordinary purposes is vulcanized; exceptions are rubber cement, crepe-rubber soles, and adhesive tapes. [4] It should be pointed out that the amount of crosslinks in elastomers should be under a certain level, otherwise the vulcanized rubbers will become a hard duromer, which is actually a thermoset material instead.

Initially synthetic rubbers, like styrene-butadiene rubber (SBR) and butadiene rubber (BR), were introduced as counterparts for NR during World Wars I and II. Normally, synthetic rubbers provide inferior mechanical properties compared to NR due to the lack of the specific strain-crystallization phenomena that NR provides. Nowadays, synthetic rubbers, like for instance nitrile rubber (NBR), ethylene-propylene rubber (EPM and EPDM) and Chlorinated polyethylene (CM) are

widely employed for their special properties, such as better ageing properties, ozone resistance, oil resistance and heat resistance. [3, 8] Along with the developments in synthetic rubbers, new vulcanization systems were also designed to achieve proper vulcanization conditions and resulting properties.

Fillers, which were originally used to reduce the production costs, now play an important role in the rubber industry as well. It is known that the incorporation of carbon black (CB) can stiffen and reinforce the amorphous elastomers due to chemical and physical interactions between the fillers and polymers. [9] Replacement of CB by silica was another important development in rubber technology in the late 20th century. [4] With the development of a silane coupling agent, silica started to be widely used in elastomeric compositions to reduce the rolling resistance of tyres, which will subsequently reduce the consumption of fuel. [10]

Although rubber technology has been established for more than one century, there are still intensive investigations being carried out today to bring this technology to a higher level of sophistication.

1.2 Aim of this research

In order to fine-tune or optimize properties of rubbers, often blends of dissimilar rubber species are employed. However, in rubber blends often a cure mismatch occurs. This is due to the difference in solubility of the curatives in the different rubbers in the blend, as well as different reactivities of the rubbers with the curatives employed. In this way an imbalance in crosslink densities of the different rubber phases in the blends are obtained. In most cases this results in poor mechanical and dynamic properties of the blends.

The main objective of this project is to apply a novel plasma polymerization surface coating technique in order to alter the solubility characteristics of the curatives sulfur (S_8) and N-cyclohexylbenzothiazole-2-sulfenamide (CBS). Coating of curatives by plasma polymerization with polar and apolar monomers, alters the surface tension and surface energy. Tuning the surface energy or tension, aims to improve the solubility of

curatives in those rubber phases, which they do not prefer. Therefore, it is expected to improve the properties of dissimilar rubber blends by creating a more balanced cross-linked network.

1.3 Structure of this thesis

There are 10 chapters in this thesis, which starts with a general introduction in **Chapter 1** and finishes with a summary as well as some final remarks in **Chapter 10.**

    Chapter 2 gives an overview of rubber blends, covulcanization in rubber blends, reinforcing fillers and the state of the art of micro-encapsulation.

    A solubility study is provided in **Chapter 3**, where the solubilities of various curatives in different rubbers are determined by both experimental measurements and theoretical calculations. This study provides valuable data for the prediction of the distribution of various curatives in dissimilar rubbers. The results can be used to interpret the improvements in the properties of the blends.

    Chapter 4 describes a mixing study. By applying the solubility data obtained in the previous chapter, mixing schemes are developed that may improve the properties of the blends.

    In **Chapter 5**, the surface modification of both sulfur and CBS is applied through plasma polymerization with acetylene. The performance of plasma polyacetylene encapsulated curatives in unreinforced rubber blends is evaluated and discussed.

    Chapter 6 provides a study of the surface modification by plasma polymerization of a fluoro-carbon monomer on sulfur and CBS. The behavior of plasma polyperfluorohexane encapsulated curatives in the unreinforced rubbers and rubber blends are discussed. Some specific properties are achieved with this monomer.

    Acrylic acid is chosen as the monomer for plasma polymerization in the study in **Chapter 7**, which provides significant improvements in the properties of unreinforced NBR/EPDM blends, where all previous methods were not so successful.

    In **Chapter 8**, several combinations of plasma coated sulfur and plasma coated CBS are applied in carbon black reinforced dissimilar rubber blends. The

improvements achieved in the unreinforced rubber blends are not compromised by using both plasma coated sulfur and plasma coated CBS in carbon black filled blends.

The blooming behavior of plasma polymer-encapsulated sulfur is described in **Chapter 9**. It is demonstrated that the plasma coating can also stop sulfur migration from the bulk to the surface of the rubbers, which results in a reduction of blooming.

1.4 References

[1]   W. Hofmann, *"Rubber Technology Handbook",* 2ed, Hanser Publishers, Munich, **1989**, 611.

[2]   Columbia University, *"Columbia Encyclopedia"*, 6th Edition, eds. L.G.P. Lagasse, A. Hobson, S.R. Norton, Columbia University Press, New York, **2001**.

[3]   W. Dierkes, Ph.D thesis, University of Twente, Enschede, the Netherlands, **2005**.

[4]   K.C. Baranwal, H.L. Stephens, *Meeting of the Rubber Division of the American Chemical Society,* New York, **2001**.

[5]   L. Bateman, C.G. Moore, M. Porter, B. Saville, *"Chemistry and Physics of Rubber-like Substances"*, Maclaren & Sons, London, **1963**, 405.

[6]   J.W.M. Noordermeer, *"Industrial Elastomers"* 4th edition, University of Twente Press, Enschede, the Netherlands, **2005**, 162.

[7]   N. Sombatsompop, S. Thongsang, T. Markpin, E. Wimolmala, *J. Appl. Polym. Sci.*, **2004**, 93, 2119.

[8]   A.R.R. Menon, C.K.S. Pillai, W.S. Jin, C. Nah, *Polym. Int.*, **2005**, 54, 629.

Chapter 2

Improving Properties of Elastomer Blends by Surface Modification of Curatives

A Literature Review

+

In this chapter rubber blends, curatives, reinforcing fillers and the developments of microencapsulation are reviewed. Special emphasis is put on plasma polymerization surface treatments, which are applied in this research to surface modify curative powders. The unique features of plasma polymerization are explained together with its mechanism. It looks promising to use this technique in surface modification of rubber additives in order to improve rubber blend properties.

2.1 Introduction to elastomer blends

Various rubber polymers are often blended to provide a property portfolio required for a successful performance of an end-article in a certain application. To obtain a desired combination of properties, both theoretical and technical aspects should be taken into account. Compatibility of rubber ingredients is vital for rubber blends in order to achieve optimum properties.

2.1.1 Elastomer blends

Blending of different rubber polymers is an effective and economic approach to achieve a desired combination of properties compared to synthesizing new elastomers. Potential merits of rubber blends are: (1) improved solvent resistance; (2) improved processability; (3) better product uniformity; (4) quick formulation changes and manufacture flexibility and (5) improved productivity.

Rubber blends, based on the miscibility of constituent polymers, can be divided into three broad classes: a) miscible blends (interpenetrating networks); b) partially miscible blends; and c) immiscible blends (e.g. polymer alloys which are immiscible but compatibilized). A polymer alloy has two or more different phases on a micro-scale. However, it exhibits macroscopic properties as a single-phase material. [11]

Rubber polymers are generally immiscible and phase separate into their constituent components. Fortunately, for most applications, homogeneity at a fairly fine level instead of molecular miscibility is sufficient for optimum performance. It is usually even desirable to have a certain degree of microheterogeneity to preserve the individual properties of the respective rubber components. [12]

2.1.2 Miscibility of polymers

Miscibility of polymers is determined by thermodynamic phenomena. It is determined by the Gibbs free energy change of mixing (ΔG_m), which is defined by equation 2.1:

$$\Delta G_m = \Delta H_m - T\Delta S_m \leq 0 \qquad \text{(Equation 2.1)}$$

Where, ΔH_m is the enthalpy of mixing (J), ΔS_m is the entropy change of mixing (J/K) and T is the absolute temperature (K). Polymers are miscible only when the free energy of mixing is negative. Most rubber polymer blends are immiscible because mixing is endothermic and the entropic contribution is small due to the high molecular weights of the constituent polymers.

Miscibility can also be predicted from the solubility parameters. The relationship between the enthalpy change of mixing and the solubility parameters is governed by equation 2.2.

$$\Delta H_m / V = k(\delta_1 - \delta_2)^2 \phi_1 \phi_2 \qquad \text{(Equation 2.2)}$$

In this equation, V is the volume of the two polymers, k is a constant close to 1, δ_1, ϕ_1 and δ_2, ϕ_2 are the solubility parameters and volume fractions of components 1 and 2, respectively. Polymer miscibility is possible only when the difference in solubility parameters is small enough (< 0.1 $(J/cm^3)^{1/2}$), or if there are specific interactions existing which contribute to a negative ΔH_m. [13] The solubility parameters of some relevant polymers, determined by Gas Liquid Chromatography (GLC), viscometry, swelling measurements together with the calculated data are given in Table 2.1. [14]

Table 2.1 Solubility parameters of various polymers determined with different methods. [14]

Elastomer types	Solubility parameters [$(J/cm^3)^{1/2}$]			
	GLC	Viscometry	Swelling	Calculated
EPDM	15.9	15.8	15.9	15.8
NR	16.6	16.8	16.7	16.7
Cis-BR	17.2	17.0	16.7	17.1
PS	19.9	-	-	19.0

2.1.3 Compatibility of rubber polymer blends

The lack of miscibility and technological compatibility of the component rubber polymers severely restricts the application of rubber blends. It is very often that components are grossly immiscible as well as technologically incompatible. [12, 15]

The mutual compatibility is essentially governed by the thermodynamic incompatibility of the rubber components involved in blending. [12, 15] The better the compatibility between two phases in the blend, the smaller are the dispersed phase domains. [14]

Concerning the morphology of phase separated rubber blends, the main influences governing the structure of the entire system are: (1) the interfacial tension, which influences the size of the phases; (2) the viscosity of the matrix; and (3) the shear stress. [14] Co-continuous blend morphology is observed only for rubbers with similar viscosities. [16] The relative mixing viscosities of the components affect the size and the shape of the domain zones. Generally, the matrix is formed by the phase with lower viscosity, while the one with higher viscosity forms the dispersed phase. Homogeneity of mixing can be controlled by using either proper mixing conditions or by addition of compatibilizers. [12, 15] The mechanical properties are determined by the homogeneity of the elastomer blends. [17]

2.1.4 Characterization of rubber polymer blends

It is important to use fundamentally powerful techniques to study the structure of rubber polymer blends once they are formed. The frequently used techniques for studying rubber blends can be classified as: Microscopic techniques, Visco-elastic characterization and optical characterization techniques. [18]

Significant improvements have been made in the analysis of elastomer blends for the determination of composition, morphology and filler inter-phase distribution. Gas Chromatography (GC), [19-21] Infrared spectroscopy (IR), [22-25] Nuclear Magnetic Resonance (NMR) [26-29] and thermal analyses: [30-34] Differential Thermal Gravimetry (DTG), Differential Scanning Calorimetry (DSC), Thermogravimetric Analysis (TGA) techniques can provide quantitative information on the composition. The latter three methods, along with Small-angle X-ray Scattering (SAXS), [35] Small-angle Neutron

Scattering (SANS), [36] Dynamic Mechanical Thermal Analysis (DMTA), optical microscopy, [37-44] Electron Microscopy (EM), [45, 46] Transmission Electron Microscopy (TEM), [44, 47-50] Scanning Electron Microscopy (SEM) [42, 43, 47-52] and Atomic Force Microscopy (AFM) [35, 36, 53-61] are also useful for resolving differences in blend homogeneity. [12] Time-of-flight Secondary Ion Mass Spectroscopy (ToF-SIMS) is a newly developed method to characterize elastomer blends and vulcanizates, where ToF-SIMS is applied to simultaneously map the rubber phase structure with detailed chemical information. ToF-SIMS is an extremely powerful tool for the analysis of the rubber surface structure. By scanning the surface, the top 1 to 2 nanometers are analyzed. A lateral resolution of 0.5 μm can be reached. It is a unique technique which is capable to distinguish all elements of the periodic table and their isotopes as well as a vast array of organic functional groups. [62]

2.2 Covulcanization of rubber polymer blends

Covulcanization plays an essential role and determines the properties of rubber blends. Generally, the respective rates of vulcanization in the different rubber polymer phases are different. The solubility of sulfur and accelerators in the two polymer phases determines their distribution and migration in rubber blends and consequently results in different rates of vulcanization and different crosslink densities for the different rubber polymers in the blend. Several methods are discussed here with the aim to improve the vulcanization compatibility of rubber blends. [12]

Covulcanization can be defined in terms of a single network structure encompassing crosslinked macromolecules of both rubbers. They should preferentially be vulcanized to similar levels with crosslinking across the micro-domain interfaces. The nature of the rubber polymers, e.g. level of unsaturation and polarity, determines the curative reactivity, which is also influenced by the solubility of the curatives in the various phases. Vulcanizates with components having similar curative reactivity generally give better properties than those with components having large differences in this respect. [12]

Chapman and Tinker [63] reviewed all the techniques to determine crosslink density in blends. They claimed that the diffusion of vulcanization intermediates probably plays an important role in defining the eventual crosslink distribution, while the eventual presence of carbon black as reinforcing filler does not significantly affect the crosslink distribution.

Shershnev [64] has summarized the various means to achieve good co-vulcanization in blends of high and low un-saturation elastomers in terms of:

(1)   Separate masterbatches with varied curative loadings;

(2)   Modified elastomers with chemically bound vulcanization agents;

(3)   Accelerators with a high degree of alkylation;

(4)   Use of ingredients that form insoluble compounds after reacting with accelerators and other vulcanizing agents;

(5)   Use of vulcanizing agents which distribute uniformly and have similar activities for different elastomers.

According to van Duin et al., [65] either the addition of compatiblizers like poly-trans-octenylene rubber, liquid Butadiene rubber (BR) and application of maleic anhydride grafted Ethylene-Propylene-Diene rubber (EPDM), or increasing the vulcanization time of natural rubber/EPDM blends are the only methods, that both improve covulcanization and seem technologically and environmentally feasible for this particular polymer combination.

2.2.1 Sulfur and sulfur donors

The most important vulcanization agent for rubber is sulfur, which is the oldest and most applied vulcanizing agent. It is only suitable to vulcanize unsaturated elastomers, such as natural rubber (NR), Isoprene rubber (IR), BR, Styrene-Butadiene rubber (SBR), Isoprene-Isobutylene copolymer (IIR), Acrylonitrile-Butadiene rubber (NBR), Chloroprene rubber (CR) and EPDM. [36]

Sulfur is normally added to rubber mixtures in concentrations of roughly 0.4 to 5 wt %, relative to the rubber polymer. [66] The quantity of sulfur used depends on the amount of accelerators used and the demand on properties of the vulcanizate.

Sulfur exists in various allotropic forms, but rubber technologists only differentiate between two types in the vulcanization of elastomers. These are known as "soluble" sulfur and "insoluble" sulfur, their designation reflecting their relative solubilities in carbon disulfide at room temperature.

Soluble sulfur is the most stable form of elemental sulfur, with the molecular structure S_8. At room temperature these eight membered rings are known to adopt an orthorhombic crystal structure which converts to a monoclinic crystal form at a temperature above 95.5 ^{o}C. If the orthorhombic form is heated rapidly, it melts at 112.8 ^{o}C before it has time to convert. The monoclinic form melts at 119 ^{o}C. [67]

Hendra et al. [67] applied Raman Spectroscopy to study the conversion of sulfur from the insoluble to the soluble form. As soluble and insoluble sulfur can be distinguished by the different positions of the Raman bands associated with each form, the conversion can be observed by changing the temperature.

Insoluble sulfur (IS) is relatively stable at room temperature due to the addition of chemical stabilizers. The structure of insoluble sulfur is less well established, but it is often described as a polymeric form of sulfur in order to explain its low solubility. [67]

The choice as to which of the two types of sulfur should be used in the process of vulcanization is based on their specific behavioral properties during mixing and maturation. Soluble sulfur may migrate to the surface and form crystals during storage of the compound: called blooming. This will prevent building tack (creating considerable difficulty in building articles such as tires); it will hinder lamination or rubber-metal bond formation and, even if the compound can be remixed, it may well result in an inhomogeneous cure. [67] Insoluble sulfur is more expensive than soluble sulfur and has to be used if sulfur blooming is expected to be a problem for the application. However, in this case the bulk temperature during mixing or compounding should be lower than the temperature of 120 ^{o}C at which insoluble sulfur converts to the soluble form within the timescale of the mixing cycle. [67-69]

Sulfur donors are sulfur-containing compounds that liberate sulfur at vulcanization temperature. Some of the sulfur donors can be a substitute for sulfur, while others are

simultaneously vulcanization accelerators. The use of sulfur donors can increase the vulcanization efficiency and improve sulfur blooming phenomena. [3, 70]

2.2.2 Accelerators

The addition of accelerators not only shortens the vulcanization process, but also suppresses undesired side reactions. In addition, the average number of sulfur atoms per crosslink is decreased and as a result the crosslinking efficiency is increased. [3] Over the years different types of accelerators were developed. Accelerators can be classified into two broad categories: primary accelerators and secondary accelerators. Primary accelerators like sulfenamides are generally efficient vulcanization catalysts and confer good processing safety to the rubber compounds, exhibiting a stable vulcanization plateau without reversion. Ultra-fast accelerators like thiurams belong to the primary accelerators, however, they are more scorchy. Secondary accelerators, amines, are only applied in combination with primary accelerators. These combinations cause faster vulcanization than each product separately and a considerable activation of cure, which is positive for the general property spectrum of the vulcanizate. [70]

Mastromatteo et al. [71] found that the use of accelerators with longer alkyl substituents, whose solubility ratio in different rubbers was close to unity, resulted in the best physical properties of NBR/EPDM blends. The study also indicated that these accelerators could be used to provide non-blooming cure systems for EPDM compounds and safer ultrafast cure systems for diene rubber compounds.

According to the research of van Ooij et al., [72] optimum covulcanizate properties of SBR/EPDM blends are obtained by using less polar accelerators which have minimum tendency of migrating to the more polar SBR phase. Sulfur, 2-mercaptobenzothiazole (MBT), and Tetramethylthiuram disulfide (TMTD) have higher solubility in the SBR phase than in the EPDM phase. On the other hand, sulfenamide-based accelerators: N-tert-butyl-benzothiazole-2-sulfenamide (TBBS), N-dicyclohexylbenzothiazole-2-sulfenamide (DCBS), N-cyclohexylbenzothiazole -2-sulfenamide (CBS) have higher solubility in the EPDM phase than in the SBR phase. As a result, the EPDM phase of the blends cured with sulfenamide type

accelerators had shorter scorch times and faster curing rates than the SBR phase. This overcame the effect coming from the lower polarity of EPDM and resulted in a compatibilized vulcanizate.

2.2.3 Migration of curing additives

Migration of curing additives is an important factor in the overall properties and performance of rubber articles containing a number of layers, for example a tire, a hose or a conveyor belt. There are at least two mechanisms, which explain the movement (migration) of chemical additives throughout a rubber article. [70]

2.2.3.1 Bloom

Bloom happens when a partly soluble additive is applied at a level higher than its solubility at a given temperature. It occurs because crystallization is more favorable at the surface than in the bulk. [70] It was patented that by use of insoluble sulfur, sulfur donors and metal alkylxanthate, blooming can be eliminated. [69]

2.2.3.2 Diffusion

Diffusion happens when the solubility equilibrium of soluble additives is disrupted. Soluble components diffuse to re-establish concentration equilibrium, which is similar to what happens for solutions of low molecular weight liquids and follows the same law. It also depends on the difference in solubility of the diffuzates between the dissimilar elastomers. [70]

Diffusion in an isotropic substance is based on the assumption that the rate of transfer, R, of the diffusing matter through a unit area is proportional to the concentration gradient, given in equations 2.3 and 2.4: Fick's first law.

$$R = -D \frac{\partial c}{\partial x} \qquad \text{(Equation 2.3)}$$

$$q = DA \int_0^t -(\frac{dc}{dx}) dt \qquad \text{(Equation 2.4)}$$

Where D is the diffusion coefficient; c is the concentration of diffusing matter; x is the space coordinate measured normal to the section and q is the amount of diffusing substance passing a section of surface area, A, in total time t. [73]

A lot of research has been done to obtain a proper understanding of migration. According to Gardiner [40], curatives diffuse from the less polar to the more polar elastomer phase, which occurs very quickly during both the mixing and the vulcanization processes. The diffusion coefficient of sulfur will change with concentration and the diffusion rate of sulfur does not vary significantly with polymer. Comparing the diffusion behavior in blends to that in a two-ply system, additives will come to equilibrium more rapidly in blends than in a two-ply system.[39] Sung-Seen Choi [74] found that for silica-filled NR compounds, the migration rate was dependent on the content of silica in the vulcanizate. Wax with a low molecular weight migrates faster than that with a high molecular weight. R.N. Datta [70] did his study on migration of soluble and insoluble sulfur between a tire tread compound and a belt compound. He found that the use of insoluble sulfur can prevent sulfur migration between adjacent rubber compounds at processing temperatures below 110 °C; consequently, the variation in compound performance was circumvented.

In certain cases, migration of compounding ingredients before, during and after vulcanization in rubber compounds can be beneficial. Waxes and antiozonants rely upon migration to provide optimum protection against degradation by ozone. Migration of compounding ingredients may also result in a change in physical properties, which can be an improvement or a detrimental change, like a loss in adhesion, antidegradant protection or staining of light-colored products. [70]

Migration of sulfur and curatives is essentially governed by the difference of their solubility in different rubber phases, which will be discussed in detail later. Techniques like radioisotope tracing and microinterferometry can be used for this study. The use of radioisotope tracing is limited due to its high cost and specialized procedure. Microinterferometry, an optical method, provides low accuracy.[75] ToF-SIMS is a new powerful technique for the study of curative migration by using cryogenically microtomed specimens. [62]

2.2.4 Solubilities of sulfur and other curatives

When being mixed into elastomer blends, curing additives have their own preferences to partition more into one phase than in the other. This difference in solubility is

influenced by the unsaturation and the degree of polarity of the different elastomers. Due to the polar nature of sulfur, sulfur donors, and most of the accelerators, they are readily gathering in the more polar phase or a phase with higher degree of unsaturation. The solubilities of several elastomers and curatives are given in Figure 2.1. These values are a little different compared to those in Table 2.1, as different determination methods were employed.
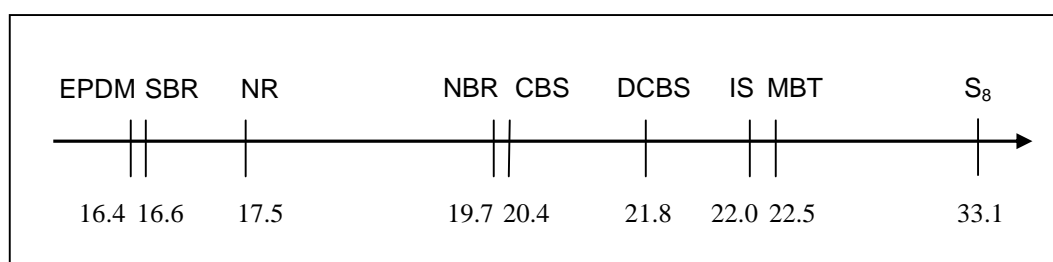

Figure 2.1 Polarity solubility parameters [(J/cm^3)$^{1/2}$] of various elastomers and some curatives. [72, 76]

Knowledge of the solubility of sulfur, insoluble sulfur (IS) and other curatives in rubber at various temperatures enables the prediction of whether blooming might occur in a particular rubber product and for example, whether it is necessary to use insoluble sulfur in a particular compound. [77] Furthermore, information on solubility will be beneficial for co-vulcanization also. It is assumed that the initial distribution of curatives before vulcanization is the same in the different rubber phases due to the extensive interface shared. However, the difference of solubility will consequently induce a very rapid migration of curatives at the vulcanization temperature. As more curatives diffuse to the more soluble phase, an unbalanced distribution will be created in a rubber blend. Consequently, an unbalanced vulcanization is created with the impoverished phase vulcanized more slowly and less completely. [78] To prevent the lack of co-vulcanization in rubber blends, accelerators with the same solubility in each elastomer component of the blends should be applied. [71, 79]

Attempts to determine the solubility of sulfur experimentally started a long time ago. Although quite some methods have been developed, there are still deficiencies

and disagreements among the published data. [77, 78] Morris and Thomas[77] used sheets of peroxide-vulcanized NR in both liquid and, more surprisingly, powdered solid curatives to determine the solubility of S_8 and accelerators. The results are listed in Table 2.2. These results fit the theoretical curve of solubility against temperature very well. It is quite informative for predicting blooming.

Table 2.2 Solubility of sulfur and accelerators (wt. %) in NR[77]

Temperature (^{o}C)	Sulfur	Temperature (^{o}C)	ZDBC*	ZDEC**
23	0.5 ± 0.2	23	0.33	-
40	1.2 ± 0.2	50	1.10	-
60	2.0 ± 0.2	60	-	24
73	3.3 ± 0.2	76	3.1	-
85	4.9 ± 0.2	90	7.75	-
100	7.1 ± 0.3	100	-	1.8
115	10.3 ± 0.3	110	49.2	-
125	11.8 ± 0.3	120	60.0	3.8
135	13.2 ± 0.3	130	71.1	-
		135	-	6.3

* ZDBC = Zinc dibutyl dithiocarbamate

** ZDEC = Zinc diethyl dithiocarbamate

Brimblecombe [80] applied Fourier Transform Raman Spectroscopy to determine the solubility of sulfur at 25 ^{o}C. This technique is quite promising because crystallized sulfur and soluble sulfur can be differentiated. As the EPDM involved in the testing is the same as the one used in the research described in this thesis, the results are more relevant for our current research. Table 2.3 gives the results of the solubilities of sulfur in different elastomers from this study.

Table 2.3 Solubility of sulfur in various elastomers at 25 $^{\circ}$C.

Elastomer	Solubility limit of sulfur (phr*)
NR (Latex Grade SMRL)	1.6
DPDR (deproteinised NR)	1.8
EPDM (Keltan 4703)	1.0
IR (Cariflex)	1.2
NR+5 phr ZnO	1.6

* phr = parts per hundred rubber

The solubilities obtained by Guillaumond [78] are quite valuable in studying the migration of curatives in rubber blends, which is most severe at vulcanization temperatures. As zinc oxide and stearic acid were not involved in the compounds investigated, it is hard to exclude the possibility that solubility might be different in a normal compounding system. Especially for the involvement of zinc oxide, which may react with accelerator and stearic acid to form complexes. The solubility of curatives is given in table 2.4. [78]

Table 2.4 Solubility of curatives in different elastomers and blends at 153 $^{\circ}$C

	Solubility at 153°C (phr)			Ratio of solubilities		
	SBR	EPDM	BR	SBR/EPDM	SBR/BR	BR/EPDM
S	17.3	10.7	16.8	1.62	1.03	1.57
MBT	5.2	1.1	2.4	4.65	2.16	1.92
TMTD	14.3	5	4.9	2.86	2.92	0.98

2.3 Rubber reinforcement with fillers

In practical applications, rubbers are generally applied with reinforcement fillers to improve the mechanical properties. The incorporation of fillers is on the other hand not just providing enhanced mechanical properties, but also reducing the cost of the final product, which is commercially appealing. For rubber blends, the final

mechanical properties are not only determined by the phase morphology but are also influenced by the distribution, dispersion and structure network formed by the fillers.

In most cases, elastomers are applied with fillers to improve properties like hardness, tensile strength and wear resistance in order to meet the requirements for practical applications. The mechanical properties of rubber compounds result from the admixture of these reinforcing fillers at quantities of 30% up to as much as 300% relative to the rubber part. [81] The maximum efficiency is obtained when a continuous, structured network of the filler is formed, homogeneously dispersed within the polymer matrix. [82] The distribution and dispersion of fillers into the rubber is influenced by the mixing process, which consequently changes the processing behavior, the non-linear viscoelastic properties as well as the ultimate properties. [14]

The most widely used fillers in the rubber industry are carbon black and silica. Carbon black can provide the highest polymer-filler interaction. Therefore, it provides the highest level of reinforcement. [36] Carbon black was introduced as a reinforcing agent in 1904. The use of carbon black not only imparts reinforcement effects but also reduces the necessary loading of zinc oxide, which is more expensive than carbon black. [3]

It is believed that there exists disorder-induced adsorption of polymer chains on the disordered or fractal carbon black surface, which is based on configurational entropy that is less restricted. This coupling is caused by entanglements formed between tightly adsorbed bound rubber polymers on the filler surface and the bulk rubber far removed from the surface. [83]

Quite a lot of research was done on the influence of carbon black on the vulcanization rate and crosslink density. Escalas and Borrós [84] found that the presence of carbon black can activate the breakdown of the accelerator. This could be related with a π-π interaction between the carbon black surface and the accelerator. They also found that vulcanization intermediates absorb on the carbon black surface.

There is an increased technological interest in the use of silica as a reinforcing filler in tire compounds due to its reduction of rolling resistance and improvement of wet grip. Silicas (silicic acids) are highly active and light colored fillers. [3] However,

strong hydrogen bonding formed between the surface silanol groups in silica itself, restrict the reinforcing ability of silica. It is generally more difficult to disperse silica into the elastomer matrix than carbon black. Fortunately, the dispersion problems can be overcome by modifying the silica surface with organosilane coupling agents which reduce the filler-filler interaction and promote filler-polymer interaction via physical and particularly chemical linkages. [82]

Another drawback of silica is its acidic nature, which de-activates the sulfur curing of rubber, which usually requires alkaline conditions. The cure retarding effect, the difficulty of mixing and the dispersion behavior of hydrophilic silica are often corrected again with the use of a silane coupling agent.

Choi et al. [85] found that TBBS can improve filler dispersion in silica-filled natural rubber (NR) compounds. The experimental results were explained by TBBS adsorption on the silica surface resulting in an improvement in silica dispersion.

2.4 Surface modification of rubber additives

Surface modification is applied on a large scale in many industrial applications. Materials such as polymer films, fabrics and to a lesser extent, metals are treated with various types of techniques. [86] There are numerous methods available to introduce a thin film coating on a surface. These thin film technologies can be used to modify surface properties such as wettability, hardness, hydrophobicity or hydrophilicity, abrasion, adhesion, resistance, permeability, refractive index and biocompatibility without changing the bulk properties. [86, 87] They are widely used in industry like for pharmaceuticals and food, for e.g controlled release and delivery.

2.4.1 Introduction into micro-encapsulation

The history of microencapsulation goes back to the 1950s when Green [88] attempted to microencapsulate tiny dye precursor droplets. At the same time, workers in other laboratories, facing other problems, were also developing methods for coating small droplets and particles. This was the beginning of the present microencapsulation processes. [88]

For a simple form of microcapsule, that is a single droplet or particle with a layer of wall material or coating around it, the internal material is usually called the "core" or the "internal phase", and the coating is usually called the "wall" or "shell". There are many types of microcapsules besides this idealized one. The size range for this technique is for particle diameters ranging from 2 μm to 2mm. [88]

The performance of a microcapsule always involves the method of release or activation of its contents. Typical methods include breaking the wall by crushing, shear, dissolution, melting, pH change, enzyme action. However, it is not always necessary to break the wall to release the contents. The release can also be controlled by the permeation rates of the encapsulated molecules through the intact walls. [88]

2.4.2 Microencapsulation methods

Various methods have been developed by different researchers and companies for a variety of applications. These techniques together with their specific features are given in Tables 2.5a-f. [88]

Table 2.5a Microencapsulation method: spray coating. [88]

Methods	Feature description
Pan coating	➢ Excellent for large irregular particles ➢ Particles tumbling in a spherical cyclinder
Fluid-bed coating	➢ Smaller particles fluidized by an opposite gas flow ➢ Batch process with a max. capacity of 500 kg ➢ Increased control of recycle time, more uniform
Wurster air-suspension coating	➢ Capable to coat particles varying greatly in size, shape and density ➢ Uniform product and rapid operation

Table 2.5b Microencapsulation method: deposition from aqueous solution. [88]

Methods	Feature description
The core particles/droplets are suspended in solution before a polymer forms.	
Complex coacervation	➤ Effective for hydrophobic liquid cores from microns to over a centimeter ➤ Batches can be as large as 75000 liters ➤ Hydrophilic wall and contains residual water
Organic phase separation coacervation	➤ For water-soluble solids in the pharmaceutical industry ➤ Coacervate of ethyl cellulose is formed after cooling and then proceed at room temperature ➤ Particle size from a few microns to 1cm
Cross-linked reverse-solubility cellulosics	➤ Used to encapsulate the dye precursor for carbonless copy paper ➤ Special coating materials, which are soluble in water at low temperature, but become insoluble as the temperature exceeds 40-44 ℃ ➤ Droplet emulsified in the coating material and heated up to form the coating and then crosslinked
Urea-formaldehyde polymerization	➤ For coating hydrophobic liquid drops ➤ Polymer coating starts to form when pH < 2 ➤ The wall formed has high thermal stability and excellent barrier properties
Liposome (lipid vesicles) formation	➤ Core is aqueous and wall is phospholipid bilayer membrane ➤ Multilamellar vesicles are formed

Table 2.5c Microencapsulation method: interfacial polymerization. [88]

Methods	Feature description
Forms walls around droplets/particles by carrying out chemical reactions directly at their surface.	
Interfacial polycondensation	➤ Polycondensation happens at the interface of two liquid phases ➤ The walls obtained are the most uniform
Isocyanate hydrolysis and condensation	➤ Polymer walls formed by using only one reactant ➤ The reaction is fast
Free-radical condensation	➤ Various solid substrates, even those with irregular surface can be modified ➤ Vacuum is used to give long-lived free radicals in vapor, which will then condense on any cool surface before polymerization takes place
Alginate polyelectrolyte formation	➤ For droplets of fluid containing living cells
Direct olefin polymerization	➤ Forming polyolefin coating on cellulose ➤ Ziegler-Natta catalyst formed on the particle, then the olefin gases are admitted, for high MW polymers
Surfactant cross-linking	➤ For microcapsules $\Phi < 1\mu m$ ➤ Hollow spheres reflect light, good opacifiers for paper
Clay-Hydroxy complex walls	➤ Useful for preparation of paints ➤ Clay particles and polymer complexes react to form ultrathin stable walls

Table 2.5d Microencapsulation method: matrix solidification. [88]

Methods	Feature description
The products are particles of material in which microcrystals or microdroplets of the dispersed core phase are imbedded, which are called microcrystals or microdroplets.	
Spray drying and spray cooling	➢ Used for food mixes, like flavors, soups, and drinks ➢ Less expensive, give enough control of solubility and controlled release
Prilling	➢ Similar to spray cooling, while the technique to form the droplet is different
Solvent evaporation from emulsions	➢ Walls are formed around the matrix after evaporation of the solvent
Starch – based processes	➢ Useful for hydrophobic liquid droplets, such as pesticides in matrix particles based on starch
Cellulose acetate particles	➢ Highly porous sheets of cellulose acetate, pores can be filled with different materials via diffusional exchange with water.
Nanoparticle formation	➢ Martrix particles produced by polymerization of microemulsions ➢ Typically used in the medical field

Table 2.5e Microencapsulation method: plasma polymerization. [88]

Methods	Feature description
Plasma polymerization	➢ Tight and ultra-thin polymer films can be obtained ➢ Operational parameters play a vital role in determination of the film properties ➢ Both saturated and unsaturated monomers can be used ➢ Especially useful for micro-sized powders

Table 2.5f Microencapsulation method: physical processes. [88]

Methods	Feature description
Vacuum metallization	➤ To apply thin coats of metal on nearly any substrate
Annular jet encapsulation	➤ To coat large droplets of liquid with a solid wall
Gas-filled capsules	➤ To encapsulate gases in hollow bubbles of various materials
Suspension separation	➤ Works well for solid particles approximately 30 μm to 2mm.

Although all these microencapsulation methods are widely used in the food, pharmaceutical and paint industry, their applications in the rubber industry are in the phase of laboratory investigations. [88]

2.4.3 Encapsulation of rubber additives

2.4.3.1 Encapsulation of curatives

Early researchers patented several methods of encapsulating sulfur with the aim to reduce scorch and blooming problems involved in rubber vulcanization. Dolezal and Johnson [89] invented a method to coat sulfur with film forming resins, e.g. water soluble resins: urea formaldehyde, melamine formaldehyde and methyl cellulose resins; water insoluble resins: nitrocellulose, ethyl cellulose and mixtures of nitrocellulose with curing resins. The properties required for these resins are: (1) film forming; (2) sulfur insoluble; (3) insoluble in rubber; (4) not softened by contact with rubber compounds and inert at the temperatures encountered during milling; and (5) lose sealing effect at vulcanization temperature. No data about the size of the coated sulfur particles were given in this article.

According to the patent of Toshio, [90] microencapsulates of a mixture of soluble and insoluble sulfur were obtained by applying thermoplastic resins, e.g. polyvinylalcohol, with softening temperatures ranging from 100 to 250 $^{\circ}$C. The sulfur

mixture contained more than 80 wt % of insoluble sulfur with Mw: 100,000 to 300,000. Microencapsulates of sulfur mixtures were mixed into NR and IR, respectively. Results showed that both blooming and scorch were eliminated.

Kenji et al. [91] filed a patent of sulfur microencapsulation by using an epoxy resin. The aim of the invention was to improve the dispersion of sulfur and increase its adhesion to the rubber matrix. The average size of the microencapsulates was below 500 μm, and the weight percent of epoxy resin to sulfur was from 0.05 to 0.5. The testing of the effect of microencapsulates in preventing blooming was carried out in NR/SBR (w/w 70/30) blends.

Menting and Stone [92] filed a patent in 1999, in which processes for microencapsulating sulfur and other curatives were given. The coating materials being used were polyethylene (PE)-wax and/or Polyvinyl alcohol (PVA) for sulfur and PE-wax for accelerators or activators. The techniques employed were: spray-drying, fluid bed coating and precipitation from emulsions or suspensions.

M. Errasquin [93] patented a process to encapsulate the crosslinking agent in a polymer network by mixing the crosslinking agent with an uncured resin and cure the resin to form the polymer network to provide a slow release system. The release of the curing agent is controlled by the rate of degrading the polymer network. By keeping the available concentration of crosslinker low initially, the initial "burst" in reaction rate is avoided. Later on, the concentration of the crosslinker may be permitted to increase to maintain similar reaction kinetics. This process is simple and the results showed some increase in properties of the vulcanizate. However, no information about the structure of the polymer layer was given.

2.4.3.2 Encapsulation of Carbon black and Silica

Borrós et al. [94] found that the application of plasma polymerization was able to modify and tailor the surface properties of carbon black by introducing different functional groups to achieve an enhanced interaction with the polymer matrix. [95] Their further study showed that not only the surface composition could be modified in an atmospheric plasma reactor, but the vulcanization characteristics could also be influenced by changing the polarity of the filler surface.[94]

A new surface-modification process based on in situ polymerization of organic monomer(s) in surfactant layers adsorbed from an aqueous solution onto the surface of precipitated silica has recently been proven successful in improving rubber compound cure and cured physical properties. Thammathadanukul et al. [96] applied a so-called admicelles method to obtain an ultra-thin film on precipitated silica to reduce its polarity in order to make it more compatible with elastomers. In this way, "rubber-ready-fillers" with improved reinforcing capabilities can be prepared. Four basic steps are involved in this method:

(1)   Adsorption of the surfactant,

(2)   Adsolubilization of the monomer in the surfactant surface aggregate,

(3)   Polymerization of the monomer(s),

(4)   Washing to remove the surfactant.

Menting and Stone [66] patented a method for the microencapsulation of rubber additives, which achieved the encapsulating process in a reactor by emulsion polymerization or by spray-drying of the mixture, and resulted in a multilayered coating. It is claimed that rubber additives after coating are easily workable into the rubber and well compatible with the rubber material, display a high effectiveness in rubber or rubber mixtures and are characterized by good dispersability in the rubber material. The stability during storage is also increased.

Tiwari et al. [97] have done quite some work on the plasma surface modification on both carbon black and silica. According to their results, carbon black appears to be more difficult to be modified compared to silica as there are less functional groups present. However, plasma polymerization onto carbon black is successful using a special kind of carbon with fullerenic active sites. [98] Appreciable improvements are achieved in rubber blends with silica coated with different plasma polymers. [99]

2.4.4 Plasma polymerization

Amongst all the modification techniques, plasma enhanced chemical vapor deposition is particularly promising. [87] Hereinafter, a detailed introduction on plasma polymerization is given. It should be pointed out that although either plasma treatment

or a coating technique such as a fluidized bed or a tumbler reactor have existed for a long time, the combination of the plasma polymerization and these techniques is really a breakthrough. But still there are a lot of technical issues to be dealt with.

Plasma polymerization was observed for the first time at the beginning of the 20th century when the deposition of some organic compounds on the walls of a reactor in which a discharge was generated in acetylene, was observed. [100] People did not recognize until the beginning of the 1960's that electrical discharge could initiate monomers to form polymer products and that the products possessed distinguished properties such as pinhole-free thin films (0.01-100micrometers), chemical and thermal stability, integrity, excellent adhesion, high optical and electrical parameters, mechanical strength, insoluble films in organic solvents and a relative ease of production [101, 102]. During the last decades, plasma polymerization by a variety of means has been an active area of research due to its industrial importance.

Plasma is a partially ionized gas that contains positively and negatively charged particles, the whole plasma is neutral. Plasma is considered as being a state of materials. The state is more highly activated than in the solid, liquid or gas state. In this sense, the plasma state is frequently called the fourth state of materials. To achieve this state, either electron separation from atoms or molecules in the gas state, or ionization is required. [2]

To reach the plasma state of atoms and molecules, energy for the ionization must be put into the atoms and molecules from an external energy source. Further, the plasma state is not stable at atmospheric pressure, but at a low pressure of $1-10^{-2}$ torr. Thus, three essential items are necessary for plasma generation: (1) an energy source for the ionization; (2) a vacuum system for maintaining a plasma state; and (3) a reaction chamber. [102] Yasuda [103] proposed the 'elementary' or 'atomic' mechanism, because the initial substance, monomer, can undergo extensive fragmentation in a plasma, whereas the polymer may not include elements or parts of the 'monomer', playing at the same time a significant role in sustaining a discharge. Plasma polymerization is a nanometer film forming process, where thin films deposit directly on the surfaces of the substrates. [101]

2.4.4.1 Plasma polymers

Materials formed by a plasma polymerization process are not composed of repeating units, but of complicated units containing cross-linked and fragmented units or rearranged products from the monomers. In most cases, free radicals are trapped into the network. The plasma polymers possess a rather disordered structure which composition depends on the operational conditions, e.g., magnitude of the input radio frequency (RF) power to maintain the glow discharge, the flow rate of the organic gases introduced into the plasma and the pressure in the reaction chamber. [2, 104, 105]

Nevertheless plasma polymers have oxygen incorporated into the structure, although the corresponding monomers may not contain oxygen. Also the hydrogen concentration for the plasma polymers is lower than in the monomers.

a. Hydrocarbon films

Methane, ethane, ethylene, acetylene and benzene are widely used in the generation of plasma polymerised hydrogenated carbon films. They give outstanding physical properties such as microhardness, high optical refractive index and impermeability. [106, 107]

b. Halocarbon films

Plasmas of fluorine containing inorganic gases, such as hydrogen fluoride, nitrogen trifluoride, perfluorohexane, bromine trifluoride, sulfur tetrafluoride and sulfur hexafluoride monomers are used mainly to produce hydrophobic polymers. [106] These coatings offer very interesting characteristics such as low surface energy, high thermal stability, biocompatibility and chemical resistance. [108]

The polymerization on glow discharge produces a gaseous by-product: fluorine. According to the competitive ablation and polymerization scheme developed by Yasuda and Hsu [103], these by-product gasses sustain the glow discharge during polymerization. Fluorine abstraction is more difficult than hydrogen abstraction due to the higher bond energy. When the C-F bond is broken, the very reactive fluorine gas (F_2) is produced. Fluorine plays an important role in the etching effect, which competes with polymerization. High energy input tends to produce more F_2 and

enhances the etching effect, which is not desirable especially during deposition processes.

c. Organosilicon films

There are various organo-silicon precursors like silane, disilane (SiSi), disiloxane (SiOSi), disilazane (SiNHSi) and disilthiane (SiSSi). Plasma polymers formed using organo-silicon monomers have excellent thermal and chemical resistance and outstanding electrical, optical and biomedical properties. [106, 107]

2.4.4.2 Mechanism of plasma polymerization

Although, terms like "radical polymerization", "ionic polymerization", mean that the propagating species in the polymerization process is a radical or an ionic species, respectively, this is not the case for the term "plasma polymerization". Different from conventional polymerization processes, in plasma polymerization the term plasma means the energy source for initiation. [2, 101]

A comparison shows that the propagation reaction in plasma polymerization is not a chain reaction through double bonds, triple bonds or a cyclic structure, but a step-wise reaction of recombination between biradicals that are formed from fragmentation of the starting compounds by the plasma. Plasma polymerization is schematically illustrated in Figure 2.2. [2]
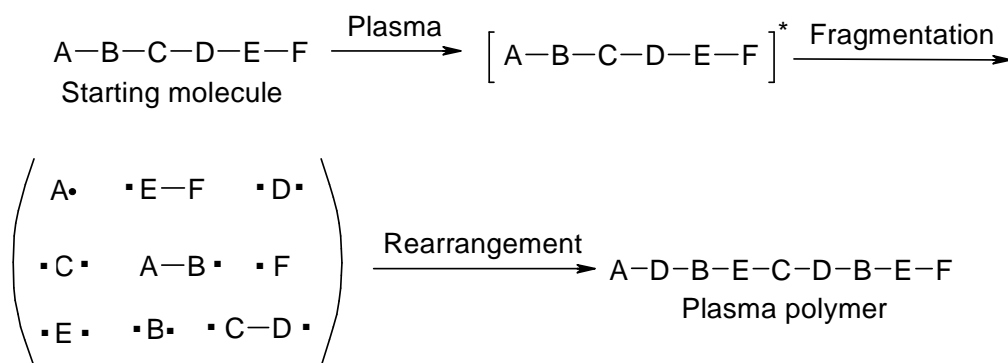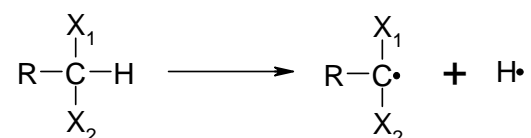

Figure 2.2 Schematic representation of plasma polymerization [2]

In an extreme case, starting molecules are fragmented into atoms and restructured into large molecules. Therefore, the sequence of the formed polymer chains is not identical to that of the starting molecules. How the starting molecules are fragmented

into activated small fragments depends on the level of plasma and the nature of the starting molecules. Two types of reactions can happen during the fragmentation of the starting molecules in plasma, as shown in Figure 2.3. Hydrogen elimination is considered to contribute primarily to the polymer forming process and secondly to C-C scission. [2]

(1) Hydrogen elimination

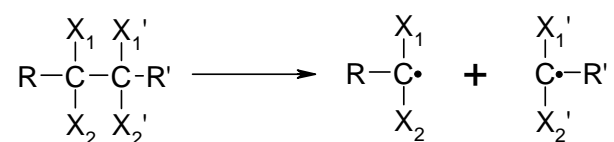$$R-\underset{\underset{X_2}{|}}{\overset{\overset{X_1}{|}}{C}}-H \longrightarrow R-\underset{\underset{X_2}{|}}{\overset{\overset{X_1}{|}}{C}}\cdot \quad + \quad H\cdot$$

(2) C—C bond scission

$$R-\underset{\underset{X_2}{|}}{\overset{\overset{X_1}{|}}{C}}-\underset{\underset{X_2'}{|}}{\overset{\overset{X_1'}{|}}{C}}-R' \longrightarrow R-\underset{\underset{X_2}{|}}{\overset{\overset{X_1}{|}}{C}}\cdot \quad + \quad \underset{\underset{X_2'}{|}}{\overset{\overset{X_1'}{|}}{C}}\cdot-R'$$

Figure2.3 Fragmentation reactions of the starting molecules

Yasuda [2] proposed the overall polymerization mechanism as shown in Figure 2.4. For atomic polymerization, step reactions via radicals form the polymers. A ceiling temperature is also existing which is frequently lower in the low pressure environment than the corresponding one at 1atmosphere.
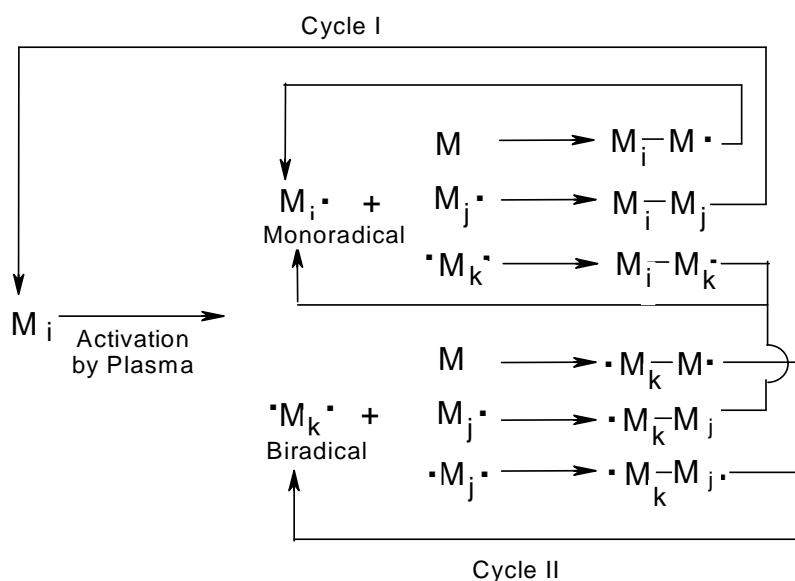

Figure 2.4 Overall plasma polymerization mechanism. [2]

2.4.4.3 Operational parameters

Plasma polymerization is highly system-dependent: the results depend on the reactor and operational conditions. Accordingly, one starting material (monomer) does not yield a well-defined polymer, but yields a variety of depositions depending on operational conditions. The composite parameter: $W/(F \cdot M)$ is the most appropriate to represent the power input parameter for plasma treatment and plasma polymerization. Here W is the electrical power input given in Watt, F is the molar or volume flow rate and M is the molecular weight of the gas. The units of this composite parameter are J/kg, i.e. energy per mass of gas.

The polymer formation rate or polymer deposition rate increases with increasing W/FM parameter in the operational condition where the activated species have a far lower concentration than the monomer molecules in the plasma (monomer sufficient region); afterwards, the polymer formation rate levels off (competition region); subsequently, the polymer formation rate decreases with increasing W/FM parameter because of the lack of monomer molecules (monomer deficient region). The domains of plasma polymerization are schematically illustrated in Figure 2.5. [2]
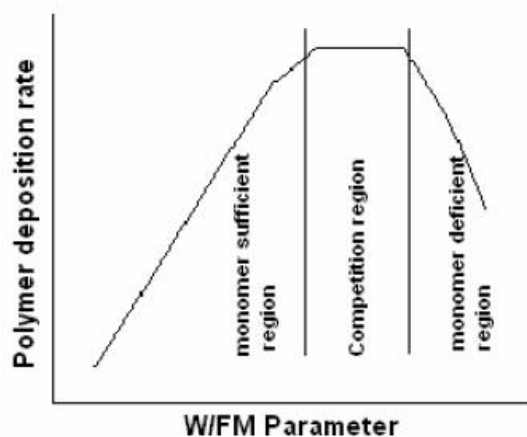

Figure 2.5 Domain of plasma polymer deposition [2]

The monomer flow rate is an important factor to control plasma polymerization. At a constant level of RF power, increase of the monomer flow rate results in a decrease of the W/FM parameter. As the monomer flow rate increases, the domain of the

plasma polymerization changes from the monomer deficient region to the monomer sufficient region. [2]

The hydrodynamic factor that influences plasma polymerization is complicated and depends on the specific features of the reactor used. The shape and size of the reactor, the relative position of the plasma zone, the monomer inlet and the plasma polymer-collecting location all influence the hydrodynamic factor for the system. It is of importance in the application of plasma polymerization of thin film coatings, to realize that two plasma polymers formed in two different reactors are never identical because of the difference in hydrodynamic factor. In this sense, plasma polymerization is a reactor-dependent process. [2]

2.4.4.4 Plasma reactor for powders

To get a powder-like substrate modified completely by plasma polymerization, special designs in reactors are required to break down the aggregation of powders and make each particle exposed to plasma. Inagaki et al. [2] reported the first surface modification on polyethylene powders using a fluidized bed plasma reactor. Later, Nutsch et al. [109] introduced an "induction plasma deposition method" to deposit plasma polymer films on powder substrates.

A vertical tubular reactor with RF excitation used for the plasma polymerization in the present research is schematically shown in Figure 2.6.
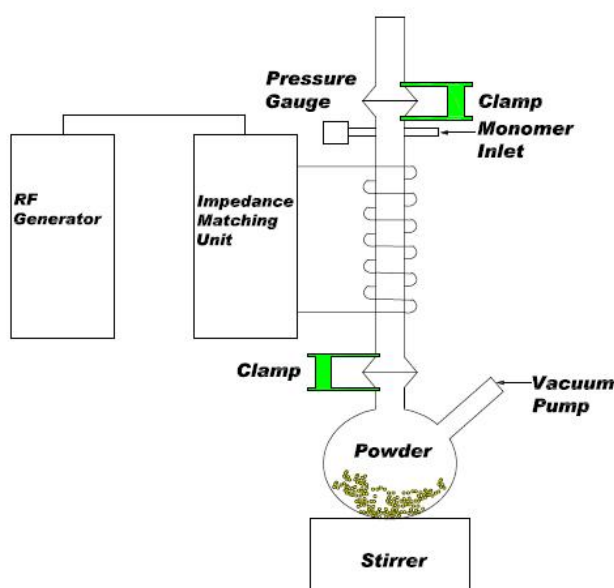

Figure 2.6 Schematic representation of vertical tubular reactor with RF excitation for treatment of fine powders.[1]

The plasma chamber is made of Pyrex glass, which consists of a flat bottom flask connected to a long cylindrical tube and closed with a glass lid with a valve on the top. The round bottom flask has an outlet for the vacuum pump. There are two inlets on the top of tubular region. One slot is for connection to the monomer source, and the other for the pressure gauge. The tubular part is surrounded by a copper coil, which is maintained in a Faraday cage to avoid electromagnetic radiation. [1]

An impedance matching unit with an operational power range of 40-500 W at 13.56 MHz, is used to connect the copper coil with the RF generator. The matching unit controls the transfer of RF-power between the RF-generator and the plasma chamber. [1]

The RF generator has a working frequency of 13.56 MHz. The alternating current input range is from 100 to 240 V and 50-60 Hz, and the power input 0-300 W. [1]

The pressure inside the plasma reactor is determined by an absolute pressure transducer (MKS Baraton® type 627B). The measurements are independent of gas composition. The device operates with ±15 V DC input at ≤250 mA, and provides 0-10 V DC output linear with pressure. The transducer unit is connected to a display unit. To maintain vacuum a DuoSeal vacuum pump from Welch vacuum, model number 1402B, is used. [1]

2.5 References

[1]   M.J. Folkes, P.S. Hope, "*Polymer blends and Alloys*", 1st edition, Blackie Academic & Professional, London, 1993.

[2]   W.M. Hess, C.R. Herd, P.C. Vegvari, *Rubber Chem. Technol.*, **1993**, 66, 329.

[3]   D. Mangaraj, *Rubber Chem. Technol.*, **2002**, 75, 365.

[4]   R.H. Schuster, H.M. Issel, V. Peterseim, *Rubber Chem. Technol.*, **1996**, 69, 769.

[5]   G.N. Avgeropoulos, F.C. Weissert, *Rubber Chem. Technol.*, **1976**, 49, 93.

[6]   S. Datta, *"Polymer Blends"*, editors: D.R. Paul, C.B. Bucknall, John Wiley &

Sons, Inc., New York, USA, 2000.

[7]   G.A. Buxton, A.C. Balazs, *Interf. Sci.*, **2003**, 11, 175.

[8]   S.Y. Hobbs, V.H. Watkins, *"Polymer blends"*, editors.: D.R. Paul, C.B.
        Bucknall, John Wiley & Sons, Inc., New York, USA, 2000.

[9]   G. Cotton, L.J. Murphy, *Kautsch. Gummi Kunstst.*, **1988**, 41, 54.

[10]   E.A. Ney, A.B. Heath, *Rubber Chem. Technol.*, **1969**, 42, 1350.

[11]   J.J. Leyden, J.M. Rabb, *Rubber Chem. Technol.*, **1980**, 53, 383.

[12]   H. Feuerberg, D. Gross, A. Zimmer, *Kautsch. Gummi Kunstst.*, **1962**, 16, 199.

[13]   J. Clark, R. Scott, *Rubber Chem. Technol.*, **1970**, 43, 1332.

[14]   R. Hampton, *Rubber Chem. Technol.*, **1972**, 45, 546.

[15]   D. Gross, *Rubber Chem. Technol.*, **1975**, 48, 289.

[16]   R. Komoroski, *Rubber Chem. Technol.*, **1983**, 56, 959.

[17]   D.D. Wrestler, *Rubber Chem. Technol.*, **1980**, 53, 119.

[18]   G.P.M. Van Der Velden, J. Kelm, *Rubber Chem. Technol.*, **1990**, 63, 215.

[19]   R. Kinsey, *Rubber Chem. Technol.*, **1990**, 63, 407.

[20]   D.W. Brazier, *Rubber Chem. Technol.*, **1980**, 53, 437.

[21]   A. Sircar, T. Lamond, *Rubber Chem. Technol.*, **1972**, 45, 329.

[22]   A. Sircar, T. Lamond, *Rubber Chem. Technol.*, **1975**, 48, 631.

[23]   J. Maurer, *Rubber Chem. Technol.*, **1969**, 42, 110.

[24]   A. Sircar, *Rubber Chem. Technol.*, **1992**, 65, 503.

[25]   P. Mele, S. Marceau, D. Brown, Y. de Puydt, N.D. Alberola, *Polymer*, **2002**, 43,
        5577.

[26]   Y. Zhang, *Macromolecules*, **2001**, 34, 7056.

[27]   J. Callan, W. Hess, C. Scott, *Rubber Chem. Technol.*, **1971**, 44, 814.

[28]   W. Hess, C.Scott, J. Callan, *Rubber Chem. Technol.*, **1967**, 40, 329.

[29]   J.B. Gardiner, *Rubber Chem. Technol.*, **1968**, 41, 1312.

[30]   J.B. Gardiner, *Rubber Chem. Technol.*, **1969**, 42, 1058.

[31]   J.B. Gardiner, *Rubber Chem. Technol.*, **1970**, 43, 370.

[32]   P. Marsh, A. Voet, L. Price, T. Mullens, *Rubber Chem. Technol.*, **1968**, 41**,** 344.

[33]   P. Marsh, A. Voet, L. Price, *Rubber Chem. Technol.*, **1970**, 43, 400.

[34]   J. Kruse , *Rubber Chem. Technol.*, **1973**, 46, 653.

[35]   P. Marsh, A. Voet, L. Price, *Rubber Chem. Technol.*, **1967**, 40, 359.

[36]   G. Binning, H.Rohrer, Ch. Gerber, E. Weibel, *Phys. Rev. Lett.*, **1982**, 49, 57.

[37]   W.M. Hess, *Rubber Chem. Technol.*, **1991**, 64, 386.

[38]   E.H. Andrews, *J. Polym. Sci.*, **1966**, 10, 47.

[39]   E. Kresge, *J. Appl. Polym. Sci.*, **1984**, 39, 37.

[40]   L.L. Ban, M.J. Doyle, G.R. Smith, *Rubber Chem. Technol.*, **1986**, 59, 176.

[41]   J.S. Trent, J.I. Scheinbein, P.R. Couchman, *Macromol.*, **1983**, 16, 589.

[42]   L.C. Ban, K.S. Campo, *Rubber Chem. Technol.*, **1991**, 64, 126.

[43]   G. Binning, C. Quate, C. Gerber, *Phys. Rev. Lett.*, **1986**, 56, 930.

[44]   A. Knoll, R. Magerle, G. Krausch, *Macromolecules*, **2001**, 34, 4159.

[45]   N. Yerina, S. Magonov, *Rubber Chem. Technol.*, **2003**, 76, 846.

[46]   A. Galuska, R. Poulter, K. McElrath, *Surf. Interface Anal.*, **1997**, 25, 418.

[47]   A. Bhowmick, S. Ray, S. Bandyopadhyay, *Rubber Chem. Technol.*, **2003**, 76, 1091.

[48]   I. Jeon, H. Kim, S. Kim, *Rubber Chem. Technol.*, **2003**, 76, 1.

[49]   S. Maas, W. Gronski, *Rubber Chem. Technol.*, **1995**, 68, 652.

[50]   Q. Zhang, L.A. Archer, *Langmuir*, **2002**, 18, 10435.

[51]   D. T. van Haeringen-Trifonova, H. Schönherr, J. Vancso, L. van der Does, J.W.M. Noordermeer, P.J.P. Janssen, *Rubber Chem. Technol.*, **1999**, 72, 862.

[52]   A.J. Dias, A.J. Galuska, *Rubber Chem. Technol.*, **1996**, 69, 615.

[53]   A. Chapman, A. Tinker, *Kautsch. Gummi Kunstst.*, **2003**, 56, 533.

[54]   V.A. Shershnev, *Rubber Chem. Technol.*, **1982**, 55, 537.

[55]   M. van Duin, J.C.J. Krans, J. Smedinga, *Kautsch. Gummi Kunstst.*, **1993**, 46, 445.

[56]   R. Datta, *"Rubber curing systems",* Smithers Rapra Technology, Shawbury, UK, 2002.

[57]   US 6984450 (2006), to Schill & Seilacher (GmbH & Co.), Hamburg, DE, invs.: K. Menting, C. Stone.

[58]   P. Hendra, P. Wallen, A. Chapman, K. Jackson, J. Loadman, *Kautsch. Gummi*

Kunstst., **1993**, 46, 694.

[59]   US 4242472 (1980), to Bridgestone Tire Co. Ltd., Tokyo, JP, invs: H. Taakashi, I. Setsuko, T. Seisuke.

[60]   US 4238470 (1980), to Stauffer Chemical Co. Ltd, Westport, CT, USA, inv: A.Y. Randall.

[61]   W. Hofmann, *"Rubber Technology Handbook",* Carl Hanser Verlag, München, Germany, 1989.

[62]   R. Mastromatteo, J. Mitchell, T. Brett, *Rubber Chem. Technol.*, **1971**, 44, 1065.

[63]   W.J. van Ooij, S. Luo, A. Ditya, J. Zhao, NSF Design and Manufacturing Research Conference, **2000**, Vancouver, BC, Canada.

[64]   W.M. Hess, C.R. Herd, P.C. Vegvari, ACS Rubber Division Meeting, **1992**, Nashville, Tennessee.

[65]   S.-S. Choi, *J Appl. Polym. Sci.*, **1998**, 68, 1821.

[66]   N.M. Huntink, R.N. Datta, *Kautsch. Gummi Kunstst.*, **2003**, 56, 310.

[67]   R.Guo, A.G. Talma, R.N. Datta, W.K. Dierkes, J.W.M. Noordermeer, *Eur. Pol. J.,* **2008**, 44, 3890.

[68]   M.D. Morris, A.G. Thomas, *Rubber Chem. Technol.*, **1995**, 68, 794.

[69]   F.X. Guillaumond, *Rubber Chem. Technol.*, **1976**, 49, 105.

[70]   U.S. 3706 819 (1972), to Sumitomo Chemical Co. Ltd. Osaka, Japan, invs.: T. Usamoto, Y. Hatada, I. Furuichi and M. Matsuo.

[71]   A. Brimblecombe, *Kautsch. Gummi Kunstst.*, **1996**, 49, 354.

[72]   L.A.E.M. Reuvekamp, Ph.D Thesis, University of Twente, Enschede, The Netherlands, **2003**.

[73]   G. Costa, G. Dondero, L. Falqui, M. Castellano, A. Turturro, *Macromol. Symp.*, **2003**, 193, 195.

[74]   G. Heinrich, *Rubber Chem. Technol.*, **1995**, 68, 28.

[75]   E.V. Escalas, S. Borros, ACS Rubber Division Meeting, **2002**, Savannah, Georgia.

[76]   S.-S. Choi, C. Nah, B.W. Jo, *Polym. Int.*, **2003**, 52, 1382.

[77]   W.J. Van Ooij, N. Zhang, S. Guo, S. Luo, Meeting: Functional Fillers and Fibers for Plastics, **1998**, Beijing, China.

[78]   A. Chityala, W.J. Van Ooij, 2nd International Conference on Plasma Polymerization, **1999**, Newark, USA.

[79]   R.E. Sparks, "*Encyclopedia of Chemical Processing and Design"*, editor: J.J. McKetta, CRC press, San Jose, USA, 1998.

[80]   P.T. Dolezal, P.S. Johnson, *Rubber Chem. Technol.* **1980**, 53, 252.

[81]   JP 52-69454 (1977), to Bridgestone Tire Co. Ltd., Tokyo, JP, inv.: S. Toshio.

[82]   JP 61-129039 (1986), to Yokohama Rubber Co.Ltd., Yokohama, JP, invs.: Y. Kenji, K. Tetsuo, N. Tatsuo, N. Kiyome.

[83]   WO 9927013 (1999), to Schill & Seilacher (GmbH & Co.), Hamburg, DE, invs.: K. Menting, C. Stone.

[84]   US 7388043 (2008), inv. M. Errasquin, Seabrook, TX, USA.

[85]   S. Borrós, N. Tricas, E.V. Escales, M. Gerspacher, IRC Meeting, **2003**, Nürnberg, Germany.

[86]   N.T. Rosell, Ph.D. Thesis, Ramon Llull University, Barcelona, 2008.

[87]   V. Thammathadanukul, J.H. O'Haver, J.H. Harwell, S. Osuwan, N. N. Ronong, W.H. Waddell, *J. Appl. Polym. Sci.*, **1996**, 59, 1741.

[88]   M. Tiwari, T. Mathew, J.W.M. Noordermeer, W.K. Dierkes, R.N. Datta, A.G. Talma, W.J. van Ooij, *Kautsch. Gummi Kunstst.*, **2008**, 61,502.

[89]   T. Mathew, R.N.Datta, W.K Dierkes, W.J. van Ooij, J.W.M. Noordermeer, T.M. Gruenberger, N. Probst, *Carbon*, **2009**, 47,1231.

[90]   M. Tiwari, J.W.M. Noordermeer, W. J. van Ooij, W.K. Dierkes, *Polym. Adv. Technol.*, **2008**, 19,1672.

[91]   S. Kinoshita, *Phys. Zeits.*, **1907**, 8, 35.

[92]   N. Inagaki, S. Tasaka, H. Abe, *J. Appl. Polym. Sci.*, **1992**, 46, 595.

[93]   L.S. Polak, Y.A. Lebedev, *"Plasma Chemistry"*, Cambridge International Science Publishing, Cambridge, UK, 1998

[94]   N. Inagaki, *"Plasma surface modification and plasma polymerization"* Technomic Publishing Company, Inc., Lancaster, USA, 1996.

[95]   H. Yasuda, *"Plasma polymerization"* 1st edition, Academic Press, Inc., Orlando, USA,1985.

[96]   H. Biederman, Y. Osada, *"Plasma Polymerization Processes"*, Elsevier Science, Amsterdam, The Netherlands, 1992.

[97]   H. Biederman, D. Slavinska, *Surf. Coatings Technol.*, **2000**, 125, 371.

[98]   C.-M. Chan, *Surf. Sci. Rep.*, **1996**, 24, 1.

[99]   P.K. Chu, J.Y. Chen, L.P. Wang, N. Huang, *Mater. Sci. Eng.*, **2002**, 36, 143.

[100]   N.D. Tran, N.K. Dutta, N.R. Choudhury, *Thin Solid Film*, **2005**, 491, 123.

[101]   G. Nutsch, B. Dzur, H. Wilhelmi, *J. Thermal Spray Technol.*, **2001**, 10, 637.

[102]   T. Mathew, Ph.D. Thesis, University of Twente, Enschede, Netherlands, **2008**.

Chapter 3

Solubility Study of Curatives in Various Rubbers

The solubility study provides indications for the distribution and dispersion of curatives (curing agents and accelerators) in rubber blends. The solubilities of sulfur, insoluble sulfur, and several accelerators *N*-cyclohexylbenzothiazole-2-sulphenamide (CBS), *N*-dicyclohexylbenzothiazole-2-sulphenamide (DCBS), and 2-mercaptobenzothiazole (MBT) are measured at room temperature and at 60 ^{o}C, in slightly with dicumyl peroxide vulcanized Styrene-Butadiene rubber (SBR), Acrylonitrile-Butadiene rubber (NBR) and Ethylene-Propylene-Diene rubber (EPDM). The experimental results can be correlated with the calculated solubility parameters, as determined using the method of Hoftijzer and van Krevelen. The absolute solubility parameter differences between rubbers and curatives are used to judge the solubilities of the curatives in specific rubbers in blends.

3.1 Introduction

Attempts to determine the solubility of curatives in rubbers have been made for quite some time. First values of sulfur solubility in natural rubber (NR) were measured by Venable and Greene [2] in 1922. Since then, various methods, e.g. equivalent solvents: solvents with similar structure as the rubber polymers [3], weight uptake, microscopy [4-7], radioactively labeled sulfur [8-11], ToF-SIMS [12] etc. were used to determine the solubility of curatives, in most cases the solubility of sulfur in rubbers. Amongst all these methods, the method of Morris and Thomas [13] is most effective to give reliable solubility results. Crystallization of sulfur is excluded due to the isothermal experimental procedure. Further, the peroxide cure applied in the method limits modification of the chain structure of rubbers, which consequently reduces its influence on the solubility compared to sulfur curing.

Although quite some experimental data have been obtained, an apparent lack of consistence exists due to the drawbacks of each method and the experimental conditions. On the other hand, the wide-spread use of rubber blends makes people become more interested in the solubility of sulfur in rubbers other than NR. Especially EPDM is interesting due to its excellent ozone- and oxygen-resistance. As the distribution and dispersion of curatives other than sulfur in blends of dissimilar rubbers is also vital for the properties of such vulcanized blends, it is of interest to determine the solubility of accelerators in various rubbers, in an attempt to obtain some insight into the mechanistic aspects involved in curing such blends.

The present paper covers an extended experimental study into the solubility of sulfur and various accelerators in SBR, NBR and EPDM, slightly pre-crosslinked with peroxide, at room temperature and at 60 ^{o}C, making use of the method of Morris and Thomas [1,13]. The experimental results are verified with theoretical solubility calculations using the group contribution theory of Hoftijzer and van Krevelen [14].

The solubility parameters of the rubbers and the curatives involved in this study can be calculated by the method of Hoftijzer and van Krevelen [14], by adding the contributions from all functional groups. The solubility parameter δ ($J^{1/2}/cm^{3/2}$) can then be used to predict the mutual solubilities. The solubility parameter can be divided into three parts:

$$\delta^2 = \delta_d^2 + \delta_p^2 + \delta_h^2 \tag{1}$$

Where the sub-parameter δ_d is the component from the dispersive forces, δ_p is the component from polar forces and δ_h is from hydrogen bonding. The three components are calculated as follows:

$$\delta_d = \frac{\Sigma F_{di}}{\Sigma V_i}$$

$$\delta_p = \frac{\sqrt{\Sigma F_{pi}^2}}{\Sigma V_i} \qquad (2)$$

$$\delta_h = \sqrt{\frac{\Sigma E_{hi}}{\Sigma V_i}}$$

Wherein F_{di}, F_{pi}, and E_{hi} are the dispersive force, the polar force and hydrogen bonding contribution from each group; V_i is the volume contribution from each group.

The mutual solubility between two materials 1 and 2 can be predicted from $\overline{\Delta\delta}$, defined as:

$$\overline{\Delta\delta} = [(\delta_{d1} - \delta_{d2})^2 + (\delta_{p1} - \delta_{p2})^2 + (\delta_{h1} - \delta_{h2})^2]^{1/2} \qquad (3)$$

For a good mutual solubility the value of $\overline{\Delta\delta}$ should be small: < 5 $J^{1/2}/cm^{3/2}$.

3.2 Experimental Part

3.2.1 Materials

In this study, three different kinds of rubbers: S-SBR (Buna[®] VSL 5025-0HM from LANXESS Corp, Germany), NBR (Perbunan[®] 3446F also from LANXESS), and EPDM (Keltan[®] 4703 from DSM Elastomers, the Netherlands) were employed. Zinc-oxide and elemental sulfur were purchased from Sigma Aldrich and polymeric sulfur (Crystex® HS OT 20) was obtained from Flexsys, Blegium; accelerators (Santocure[®] CBS, Santocure[®] DCBS and Perkacit[®] MBT) were also provided by Flexsys and stearic acid was of commercial type. Dicumyl peroxide (Perkadox[®] BC-40B) was provided by Akzo Nobel, the Netherlands, with a purity of 40%.

3.2.2 Methods

All the rubber samples were slightly crosslinked by peroxide before the solubility

measurements were carried out. The curative formulations are shown in Table 3.1. The amount of Dicumyl peroxide (purity 40%) was varied from rubber to rubber, in order to cure the rubbers to similar torque levels, i.e. similar crosslink densities. The vulcanization was carried out at 160 ^{o}C for 15 minutes. The gel content was measured after extraction with toluene in a Sohxlet extractor for 2 days: 96.6% for SBR, 99.6% for NBR, and 98.2% for EPDM. The levels of crosslinking were kept low and in a similar range for the three different rubbers to exclude an influence of crosslink density on solubility.

Table 3.1 General formulation for gum rubber compounds.

Component	Amount (phr)		
SBR	100	0	0
NBR	0	100	0
EPDM	0	0	100
ZnO	5	5	5
Stearic acid	2	2	2
Dicumyl peroxide　（40% pure on inert carrier）	1	4.8	6.25

The vulcanized samples were then cut into sheets with a size of 10mm×10mm×2mm. These sheets were extracted with acetone in a Sohxlet extractor for two days to remove the non-rubber contents. Finally, all the samples were dried in a vacuum oven for 24 hrs at room temperature. Samples were stored and protected from light before use.

The solubility measurements were carried out in triplo by placing accurately weighed samples of vulcanizate in a glass bottle such that they were packed on all sides with either sulfur or the accelerators of interest in the form of fine powders. The glass bottle was placed in a thermo-stated oven at room temperature or 60 ^{o}C. These are representative temperatures for rubber storage and the temperature generated by mixing on a two-roll mill. The sample weights were measured every day. The sample surfaces were cleaned with a sharp blade, followed by treatment with an adhesive tape before weighing in order to remove remaining adhering material. Blank experiments were carried out by inserting rubber samples into the

curatives for a few seconds and weighing the sample after the cleaning procedure. The aim of a blank experiment was to check if the cleaning procedure was good enough to remove all the adhered powders from the surface of the samples. This proved to be the case: no weight increase was observed.

The solubilities of both elemental sulfur and polymeric sulfur (OT20) were measured with these materials as received. Images of elemental sulfur particles from light-microscopy showed that in most cases the particle size was in the range of 25-50μm; the particle size of polymeric sulfur was smaller than 30μm according the product information provided by Flexsys.

The solubilities of the accelerators CBS, DCBS, and MBT were determined using the same procedure. CBS and DCBS were first ground into fine powders before use. MBT was used as received in powder form. With light-microscopy the particle sizes of the powders were determined: for CBS mostly in the range of 25-50μm; 10-25μm for DCBS; and 5-25μm for MBT.

3.3 Results and Discussion

First, the solubility parameters of the different elastomers and curatives are calculated based on the method of Hoftijzer and van Krevelen [14]. Then the solubilities of the curatives in the different elastomers are presented as percentage weight increase, plotted against time for two temperatures: room temperature (RT) and 60 $^{\circ}$C. Finally, these experimental results will be compared with the calculated solubility parameters of the elastomers and curatives.

The example of EPDM is given to illustrate the solubility parameter calculations, by taking the ratio of each monomer into account. The composition of the EPDM used in this study is: 48 wt% ethylene, 43 wt% propylene and 9 wt% ethylidene norbornene. Taking the molecular weight of the monomers into account, the molar ratio was calculated to be: 61:36:3. F_{di}, F_{pi}, E_{hi}, and V_i were summed up from the contributions of the functional groups of each monomer, by taking the molar ratios into account.

The calculated solubility parameter components of the polymers involved in this study are shown in Table 3.2. It should be mentioned that both the content of more polar groups (e.g.

the styrene group in SBR, the acrylonitrile contained in NBR) and the molar ratio of the copolymers influence the polarity and amount of hydrogen bonding in these polymers. Consequently, the solubility parameters for elastomers of different composition will differ to some extent. For example, the solubility parameter of SBR would be 18.7 [$J^{1/2}/cm^{3/2}$], if the styrene units were of equal molar amounts as the butadiene units in this copolymer. However, in the case of the SBR used in this study, where the molar ratio of styrene to butadiene monomers is 15:85, the overall solubility parameter is calculated to be 16.6 [$J^{1/2}/cm^{3/2}$].

Table 3.2 Calculated solubility parameter components of rubbers [$J^{1/2}/cm^{3/2}$] .

	SBR	NBR	EPDM
δ_d	16.6	17.2	16.4
δ_p	0.5	8.6	0
δ_h	0	4.3	0

The solubility parameters of the curatives are summarized in Table 3.3. From the values of δ_p it can already be deduced that the polarities of the accelerators are much higher than that of sulfur.

Table 3.3 Calculated solubility parameter components of curatives [$J^{1/2}/cm^{3/2}$].

	S_8	OT20	CBS	DCBS	MBT
δ_d	33.1	22.0	20.4	21.8	22.5
δ_p	0	0	4.0	2.2	7.5
δ_h	0	0	6.3	6.2	6.8

The mutual solubilities between rubbers and sulfur or curatives as reflected in the calculated values of $\overline{\Delta\delta}$, are given in Table 3.4. It illustrates the preference of each curative towards the three rubbers used in this study at room temperature: $\overline{\Delta\delta}$ should be < 5 $J^{1/2}/cm^{3/2}$ for good solubility.

Table 3.4 Calculated $\overline{\Delta\delta}$ between rubbers and curatives at room temperature [$J^{1/2}/cm^{3/2}$].

	S_8	OT20	CBS	DCBS	MBT
BR	16.5	5.4	8.1	8.3	11.4
NBR	18.6	10.7	5.9	8.1	6.0
EPDM	16.8	5.6	8.5	8.5	11.8

The weight up-take of sulfur (S_8) and polymeric sulfur (OT20) increases with time, as shown in Figures 3.1 and 3.2. The solubility of sulfur increases with increasing temperature. The percentage weight increase at room temperature for elemental sulfur is in the range of experimental error: below 0.2 wt%. It is clear from Figure 3.1 that the solubility of sulfur is very low at room temperature in all three types of rubber. When the temperature is increased to 60 °C, the solubility increases substantially in SBR and EPDM; however the solubility in NBR rubber remains low. It shows that the preference of sulfur is SBR>EPDM>>NBR. Therefore, it can be expected that in case of blends of dissimilar rubbers, a homogeneous dispersion of sulfur is achieved for the blend SBR/EPDM, while in NBR/EPDM sulfur is expected to accumulate in the EPDM phase.
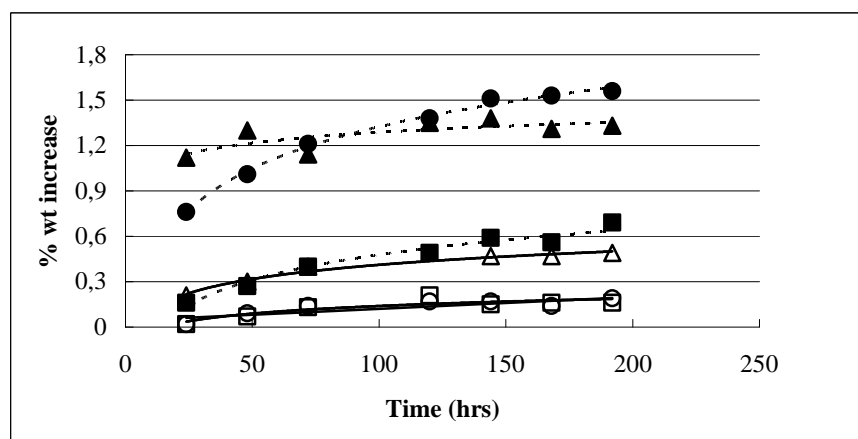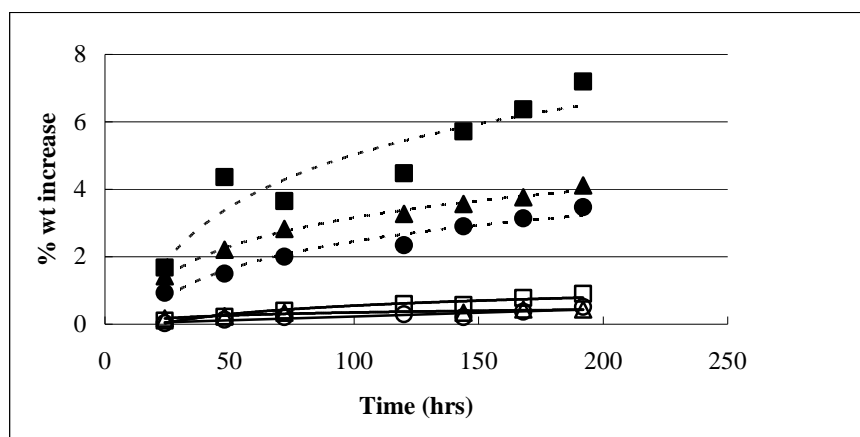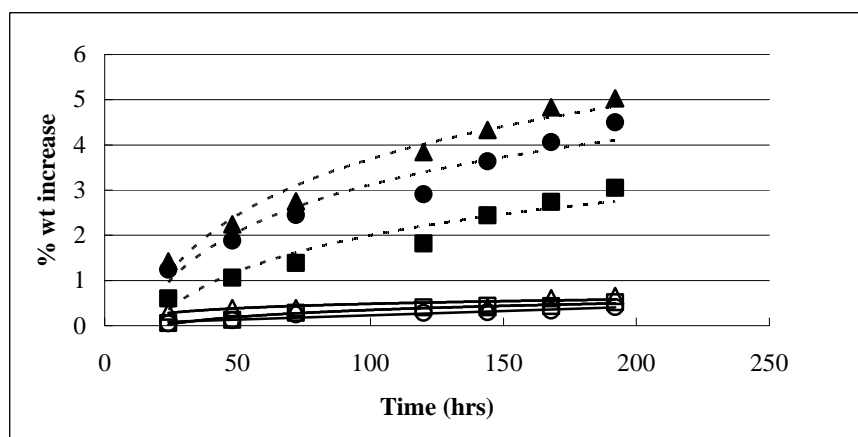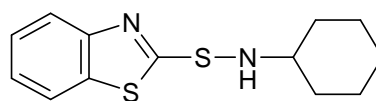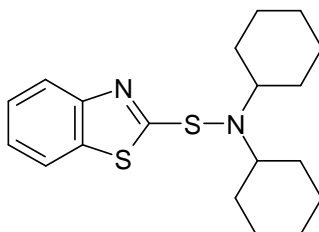

Figure 3.1 Solubility of sulfur (S_8) in gum rubbers at room temperature and 60 °C.
(○) SBR RT; (□) NBR RT; (△) EPDM RT;
(●) SBR 60 °C; (■) NBR 60 °C; (▲)EPDM 60 °C.
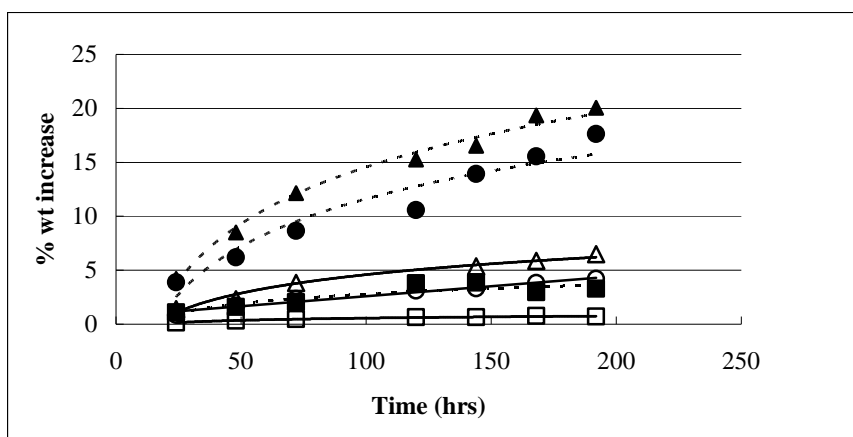
Figure 3.2 Solubility of polymeric sulfur (OT20) in gum rubbers at room temperature and 60 ^{o}C. (○) SBR RT; (□) NBR RT; (△) EPDM RT; (●) SBR 60 ^{o}C; (■) NBR 60 ^{o}C; (▲)EPDM 60 ^{o}C.

In Figure 3.2 it can be seen that the solubility of polymeric sulfur (OT20) is 10-fold higher than that of elemental sulfur for SBR and EPDM. However, it is still poorly soluble in NBR. This can partially explain the reduced blooming tendency of polymeric sulfur. The other reason for reduced blooming is that polymeric sulfur is not migrating, which is not accounted for in this study. A substantial increase in solubility of polymeric sulfur is observed at 60 ^{o}C. The preference of polymeric sulfur is EPDM>SBR>>NBR. The higher solubility of polymeric vs. elemental sulfur observed in EPDM can be related to the fact that there is some 20% oil mixed in OT20, which has a high solubility in EPDM. However, the solubilities of OT20 in EPDM and SBR are still very close, so that it will still result in a good dispersion of OT20 in a blend of SBR/EPDM. In a NBR/EPDM blend the OT20 will partition more to the EPDM phase than the NBR phase, similar to elemental sulfur.

The solubility measurement of the curatives was also done at the two temperatures: RT and 60 oC. Although a colour change was observed of the curative powders after several days of solubility measurement, Differential Scanning Calorimetric analysis of the powders showed no evidence of decomposition at 60 oC. The solubility behaviour of CBS in the different rubbers at the two temperatures is shown in Figure 3.3. The highest solubility of CBS is in NBR at both temperatures. This correlates with the fact that the polarity of CBS is much higher than that of sulfur, as demonstrated by the higher value of δp of CBS.

Figure 3.3 Solubility of CBS in gum rubbers at room temperature and 60 $^{\circ}$C.
(○) SBR RT; (□) NBR RT; (△) EPDM RT;
(●) SBR 60 $^{\circ}$C; (■) NBR 60 $^{\circ}$C; (▲)EPDM 60 $^{\circ}$C.

The solubility results for DCBS are shown in Figure 3.4. The highest solubility is found for EPDM at 60 $^{\circ}$C, different to CBS. This may be explained by the molecular structures of CBS and DCBS, shown in Figure 3.5. The decrease in polarity as reflected in the δ_p in Table 3.3 can be attributed to the presence of two cyclohexane rings in the DCBS molecular structure.

Figure 3.4 Solubility of DCBS in gum rubbers at room temperature and 60 $^{\circ}$C.
(○) SBR RT; (□) NBR RT; (△) EPDM RT;
(●) SBR 60 $^{\circ}$C; (■) NBR 60 $^{\circ}$C; (▲)EPDM 60 $^{\circ}$C.

CBS

DCBS

Figure 3.5 Structure of sulfenamide curatives.

A solubility measurement was also done for MBT, which is a thiazole-type curative. MBT is a decomposition product of all sulfenamide accelerators. Its solubility is shown in Figure 3.6. It demonstrates that MBT has the highest solubility in NBR at room temperature as well as at 60 oC. The polarity of MBT is quite high as reflected in the δp in Table 3.3, so that it has a preference to partition into the NBR phase in rubber blends like NBR/SBR and NBR/EPDM.
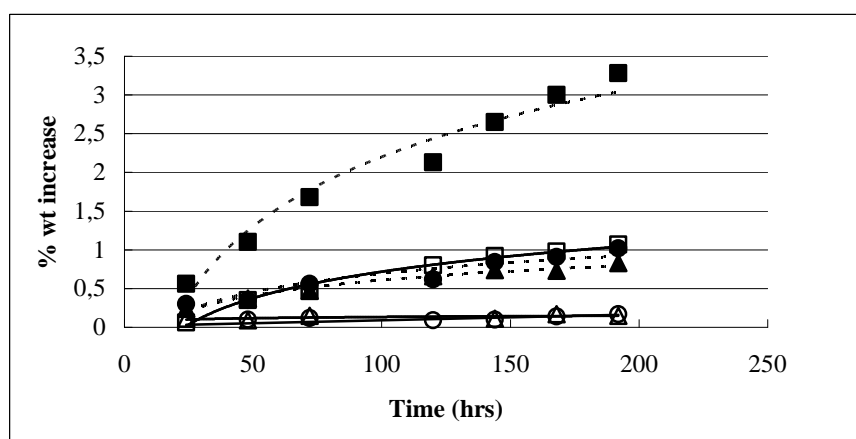
Figure 3.6 Solubility of MBT in gum rubbers at room temperature and 60 ^{o}C.
(○) SBR RT; (□) NBR RT; (△) EPDM RT;
(●) SBR 60 ^{o}C; (■) NBR 60 ^{o}C; (▲)EPDM 60 ^{o}C.

A comparative overview of the solubilities, the highest values taken from the measurements, of the three accelerators for a certain temperature is given in Figure 3.7a and 3.7b, for the

three rubbers involved in this study. It is clear that CBS and MBT have the highest solubilities in NBR at both RT and 60 $^{\circ}$C. The solubility preference of DCBS is quite different from that of CBS. The similar level of solubility of DCBS in SBR and EPDM at 60 $^{\circ}$C should be positive for co-vulcanization of SBR/EPDM blends. As the solubility of CBS and MBT in NBR is much higher than in SBR and EPDM, these curatives will tend to accumulate in the NBR phase in NBR/SBR and NBR/EPDM blends.
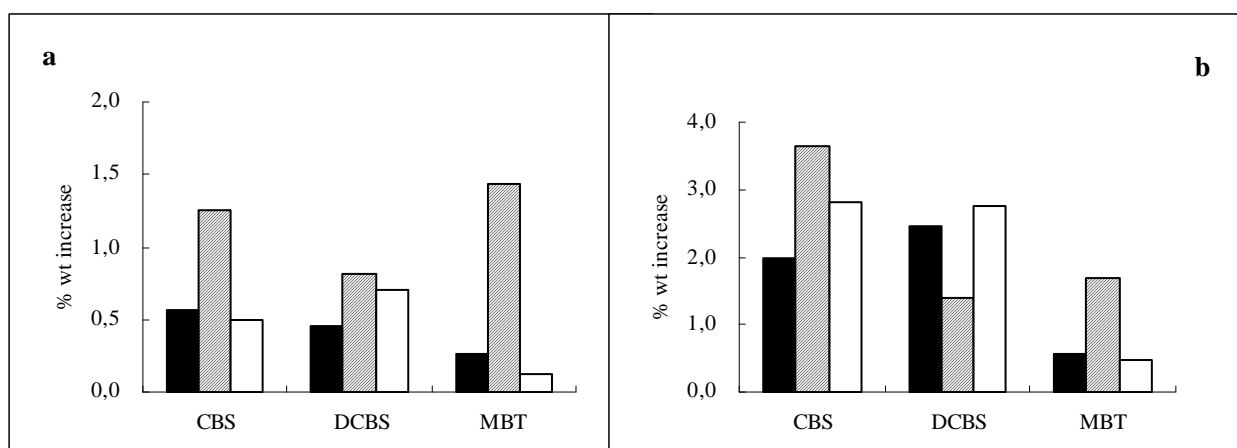
Figure 3.7 Comparison of solubility of accelerators in (■) SBR; (▨) NBR; (□) EPDM.

(a) at room temperature; (b) at 60 $^{\circ}$C

As stated before, mutual solubility occurs only when the value of $\overline{\Delta\delta}$ is smaller than 5 $J^{1/2}/cm^{3/2}$. This rule can now be used in this study, to check if the calculated $\overline{\Delta\delta}$, as shown in Table 3.4, is sufficiently predictive for the experimental values. In Figures 3.8a and 3.8b the solubility data are plotted against the value of $\overline{\Delta\delta}$ for both RT and 60 $^{\circ}$C. Due to the complexity involved in calculating the solubility parameters at 60 $^{\circ}$C, especially the solubility parameter components, δ_d, δ_p and δ_h, the solubility measured at 60 $^{\circ}$C is also plotted against the $\overline{\Delta\delta}$ at room temperature. It is still possible to observe the same trend in Figure 8b as in Figure 8a. It is clear from Figures 8 that a higher solubility is found with smaller $\overline{\Delta\delta}$ value, regardless what rubbers or curatives are involved. An extremely high solubility is observed for OT20, but this must most probably be attributed to the 20% oil contained.
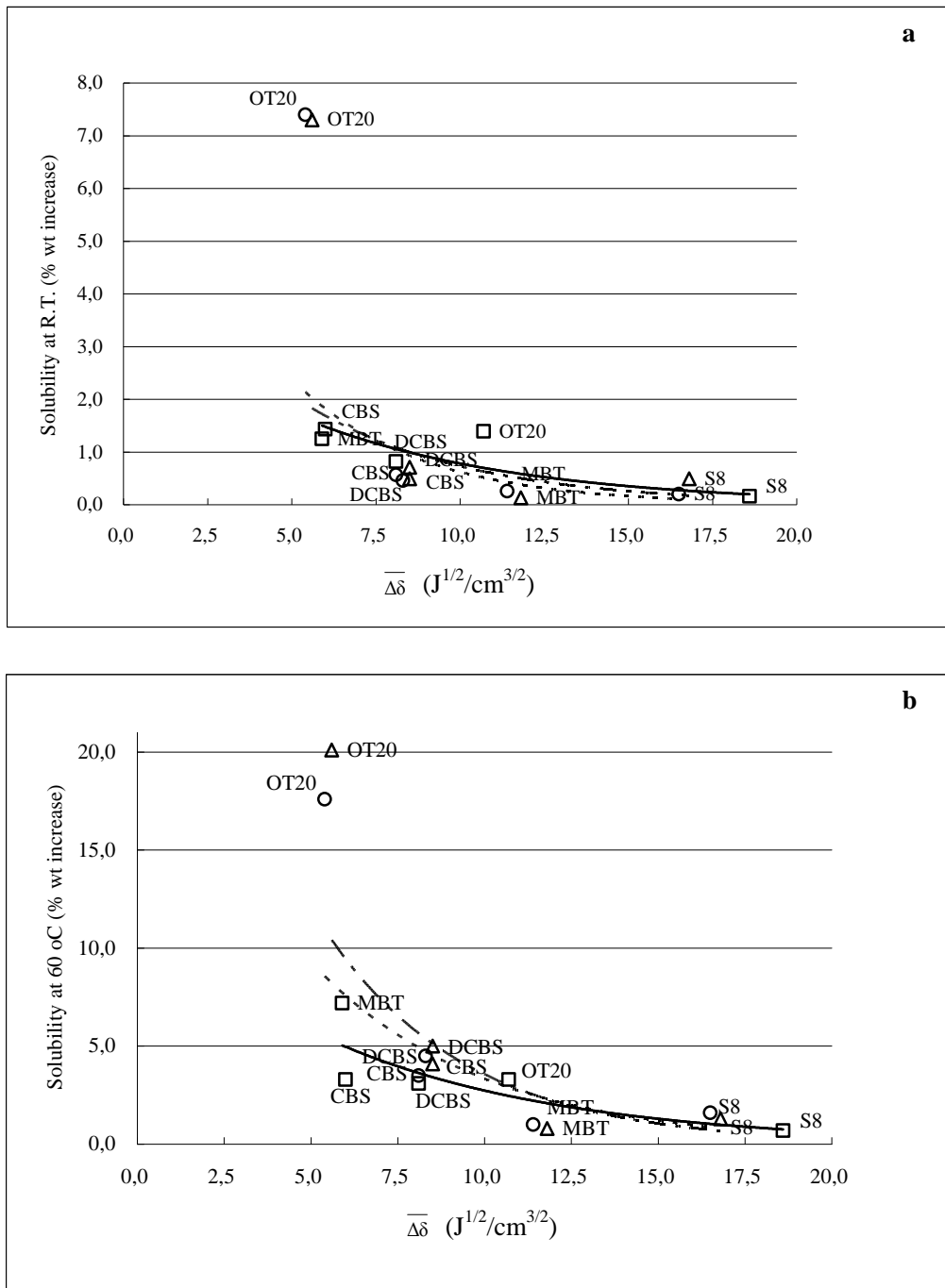
Figure 3.8 Correlation between the calculated solubility parameters and the experimental

data. (a) at RT; (b) at 60 $^{\circ}$C.   (····◦····) SBR; (──□──) NBR; (──△──) EPDM.

3.4 Conclusions

Elemental sulfur does not dissolve well in any of the rubbers investigated. The difference in solubility of sulfur in the different rubbers is more pronounced at higher temperatures (SBR>EPDM>>NBR). This is the main reason for cure incompatibility in rubber blends.

Polymeric sulfur shows a 10-fold higher solubility than elemental sulfur, although the order is only slightly changed (EPDM>SBR>>NBR). This partially explains the ability of polymeric sulfur to prevent blooming.

The solubility of accelerators is much higher than that of elemental sulfur in NBR, SBR and EPDM rubber. CBS and MBT are very polar, which gives them a preference towards NBR rubber (NBR>>SBR>EPDM). However, in the case of DCBS, the solubility sequence is SBR>EPDM>NBR, explained by the molecular structure of DCBS, where the two benzene rings cause symmetry and therefore less polarity.

The experimental data of solubility of curatives at room temperature can be correlated with the $\overline{\Delta\delta}$ values calculated by the method of Hoftijzer and van Krevelen, as shown in Figures 8, where a lower value of $\overline{\Delta\delta}$ correlates with a higher solubility.

3.5 References

[1]   R.Guo, A.G. Talma, R.N. Datta, W.K. Dierkes, J.W.M. Noordermeer, *Eur. Pol. J.,* **2008**, 44, 3890.

[2]   C.S. Venable and C.D. Greene, *Ind. Eng. Chem.*, **1922**，14, 319.

[3]   F. Guillaumond, *Rubber Chem. Technol.*, **1976**，49, 105.

[4]   J.B. Gardiner, *Rubber Chem. Technol.*, **1968**，41**,** 1312.

[5]   H.J. Graf and H.M. Issel*, Kautsch. Gummi Kunstst.*, **48**, 600.

[6]   T.C. Morris, *Ind. Eng. Chem.,* **1995**，24**,** 584.

[7]   A.R. Kemp, F.S. Malm, and B. Stiratelli, *Ind. Eng. Chem.*, **1944**，36, 109.

[8]   L. Baldi and R. Zannetti, *Rubber Chem. Technol.*, **1962**，44, 1350.

[9]   R.N. Datta, et al., *Rubber Chem. Technol.,* **2003**，76, 747.

[10]   M. Mozisek, *Pol. Eng. Sci.*, **1970**，10, 383.

[11]   B.S. Berry and J.R. Susko, *IBM J. Res. Develop*, **1977**.

[12]   A.J. Dias and A.A. Galuska, *Rubber Chem. Technol.*, **1996**，69, 615.

[13]   M.D. Morris and A.G. Thomas, *Rubber Chem. Technol.*, **1995**，68, 794.

[14]   D.W. van Krevelen and P.J. Hoftijzer, "*Properties of polymers".* 3rd edition, Elsevier, Amsterdam, 1990, p. 189.

Chapter 4

A Phase Blending Study on Rubber-Rubber Blends Based on the Solubility Preference of Curatives

Previous chapter gave a detailed picture of the solubilities of curatives in Styrene-Butadiene rubber (SBR), Ethylene-Propylene-Diene rubber (EPDM) and in Acrylonitrile-Butadiene rubber (NBR). Using these data, different mixing procedures were performed on 50/50 blends: SBR/EPDM (SE) and NBR/EPDM (NE). Different from a previous phase-mixing study, the curatives were added to separate phases before final blending, in an attempt to control the curatives' distributions in the blends for optimal mechanical properties. Fillers were not applied in the system to exclude their influence on the dispersion of the curatives. The properties of such blends compounded by selective phase mixing are superior to those of blends compounded with normal mixing procedures.

4.1 Introduction

Rubbers often consist out of a blend of various elastomers to provide a property portfolio required for a good performance of a rubber article. The properties of such rubber blends are influenced by both their mutual compatibility and their cure compatibility. [13, 110, 111] As the nature of various rubber phases involved in the blends is different, the distribution or dispersion of curatives and lateron their reactivities towards the different rubber polymers will never be the same in the two phases. The solubilities of various curatives in SBR, NBR and EPDM from our previous study, as expressed in their absolute difference in Hildebrand solubility parameters $\overline{\Delta\delta}$, are shown in Table 4.1. The smaller the $\overline{\Delta\delta}$, the higher the solubility. A $\overline{\Delta\delta} < 5$ [$J^{1/2}/cm^{3/2}$] was shown to generally be required for a good solubility. It is clear that the sequence of solubilities of N-cyclohexylbenzothiazole-2-sulfenamide (CBS) is in decreasing order: NBR>>SBR~EPDM, and the solubility sequence of sulfur (S_8): SBR~EPDM>NBR, where for sulfur the $\overline{\Delta\delta}$ are very high and the solubility very low in all rubber-types compared to CBS. [4] As a consequence, a homogeneous dispersion of curatives cannot be achieved in blends of SBR and EPDM, and even worse so of NBR and EPDM. Furthermore, curatives will readily migrate across rubber/rubber interfaces in blends following the classical laws of diffusion with a rate proportional to temperature. [5,6] Consequently, for a sulfur curing system, the ratio of accelerators to sulfur in each phase is different; neither will it be in correspondence with the formulation given in the overall recipe.

Table 4.1 $\overline{\Delta\delta}$ between rubbers and curatives at room temperature [$J^{1/2}/cm^{3/2}$]. [4]

	S_8	CBS
SBR	16.5	8.1
NBR	18.6	5.9
EPDM	16.8	8.5

Although earlier studies show that the solubilities of sulfur [7,8] and accelerators [9,10] are

different from rubber to rubber type, attempts to employ these data in improving the properties of rubber blends have been limited. Researchers have tried several options: e.g. applying accelerators that have the same solubility towards different phases in the blend; grafting accelerator-segments onto EPDM; and changing the polarity of accelerators by alkylation. [11-13] In a study of Zhao et al., different formulations were used for blends of SBR and EPDM. Their results show that the use of sulfonamide-based accelerators is beneficial due to their high solubility in the EPDM phase in the blend. [112]

The aim of the present study is to explore the influence of the distribution and dispersion of sulfur and CBS, as used for the earlier solubility measurements, on the rubber blend properties by varying the mixing procedures. By first adding all CBS or S_8 to the rubber phase wherein they have the lower solubility, it may compensate for the solubility difference and generate a more homogeneous dispersion. Consequently, it may benefit the co-vulcanization of such blends and consequently provide better properties of the blends.

4.2 Experimental Part

4.2.1 Materials

The following types of rubber were employed: S-SBR (Buna® VSL 5025-0HM from LANXESS Corp., Germany), NBR (Perbunan® 3446F from LANXESS Corp., Germany), and EPDM (Keltan® 4703 from DSM Elastomers, the Netherlands). Zinc-oxide and elemental sulfur were purchased from Sigma Aldrich; accelerator (Santocure® CBS) was provided by Flexsys, Belgium and stearic acid used as commercial grade.

4.2.2 Methods

The general formulations for the compounds used in this study are given in Table 4.2, where 1, 2, 3 are the codes for SBR, NBR, EPDM compounds and 4, 5 are the codes for 50/50 SBR/EPDM (SE) and 50/50 NBR/EPDM (NE) blend compounds. For all the compounds, the non-productive first mixing step was carried out in a Brabender Plasticorder internal mixer with a chamber volume of 390ml for 10 mins. The starting temperature was 50 $^{\circ}$C, the rotor speed 70 rpm, and a load factor of 70% was applied. Zinc-oxide and stearic acid were added into the internal mixer after 5 mins. mastication of rubber or rubber blends. The compounds

were then dropped onto a Schwabenthan two roll mill (15×33 cm, Polymix 80) with a friction ratio of 1:1.25, cooled and slabbed. After this step the "rubber masterbatches" (rubbers with activator ZnO and co-activator stearic acid) were ready. The second and/or third mixing step were performed on the same two roll mill for about 15 mins. with a finishing temperature around 40 ^{o}C. Each "rubber masterbatch" was first homogenized for 1min. before the incorporation of the curatives.

Table 4.2 General formulations for the rubber compounds

Component	Amount (phr)				
	1	2	3	4	5
SBR	100	0	0	50	0
NBR	0	100	0	0	50
EPDM	0	0	100	50	50
ZnO	5	5	5	5	5
Stearic acid	2	2	2	2	2
Sulfur	2.5	2.5	2.5	2.5	2.5
CBS	1.7	1.7	1.7	1.7	1.7

The flow charts, which describe the sequences of mixing and the strategy of adding the curatives to the elastomer blends (e.g. SE-0, SE-1); to the pure elastomers before final blending (SE-2, SE-3); or a combination of the two procedures (e.g. SE-4 and SE-5), are shown in Figures 1 a-f, using the SE blends as examples. The flow chart of the mixing procedure SE-0, shown in Figure 1a, encompasses first mastication and blending of the two rubbers: SBR and EPDM, then incorporation of ZnO and stearic acid into the SE blend in the internal mixer. The curatives are added in one step on the two roll mill into the blend.
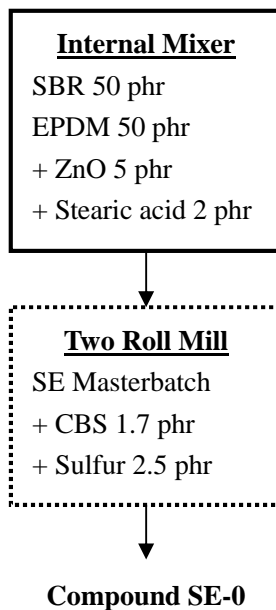
Figure 4.1a Mixing methods for SE-0.

Figure 4.1b schematically shows the mixing procedure for SE-1. SBR and EPDM are separately masticated and mixed with ZnO and stearic acid, before they are blended on the two-roll-mill. Sulfur and CBS are then added as the last step into the blend on the two roll mill.
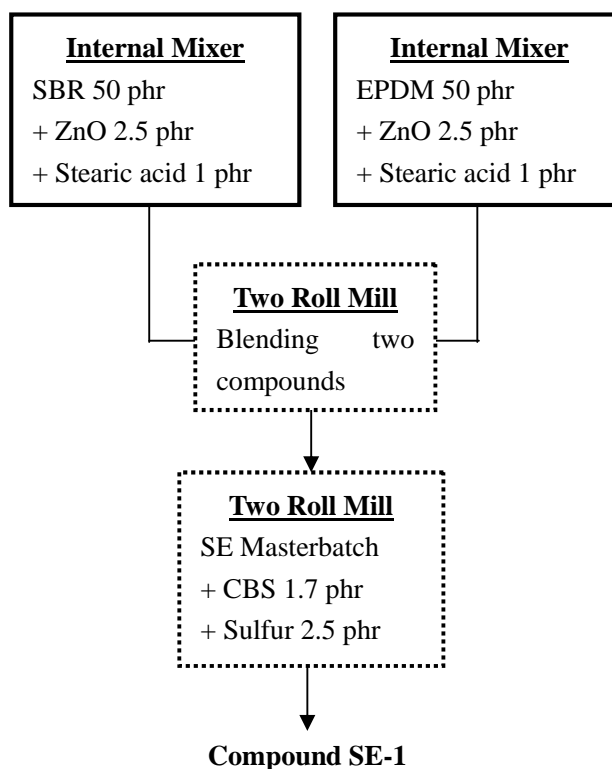
Figure 4.1b Mixing methods for SE-1.

The mixing procedure for SE-2 is shown in Figure 4.1c. Two separate masterbatches of SBR and EPDM are prepared in the same way as SE-1, and then sulfur is added to the EPDM-masterbatch, while CBS is added to the SBR-masterbatch, both on the two roll mill. Finally, the two masterbatches are mixed together to form the final blend.

Compound SE-2
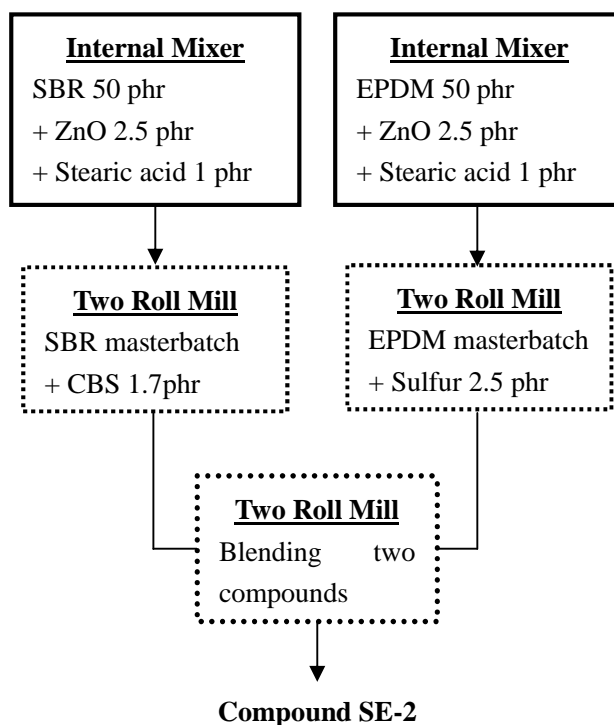
Figure 4.1c Mixing method for SE-2.

The mixing procedure for SE-3, as shown in Figure 4.1d, is similar to SE-2. However, sulfur is now added to SBR and CBS to EPDM, opposite to SE-2.

In the mixing procedure for SE-4 in Figure 4.1e, all CBS is added to the SBR masterbatch. Then EPDM masterbatch with ZnO and stearic acid is blended with the SBR masterbatch, which already contains CBS. In a last step, sulfur is added to that blend. A similar procedure is applied for SE-5, in Figure 4.1f, only switching the sulfur and CBS relative to SE-4.

Changing SBR to EPDM; and EPDM to NBR in the flowcharts, shown in Figure 4.1, these mixing procedures can readily be used also for NE-0, NE-1, NE-2, NE-3, NE-4 and NE-5, respectively.
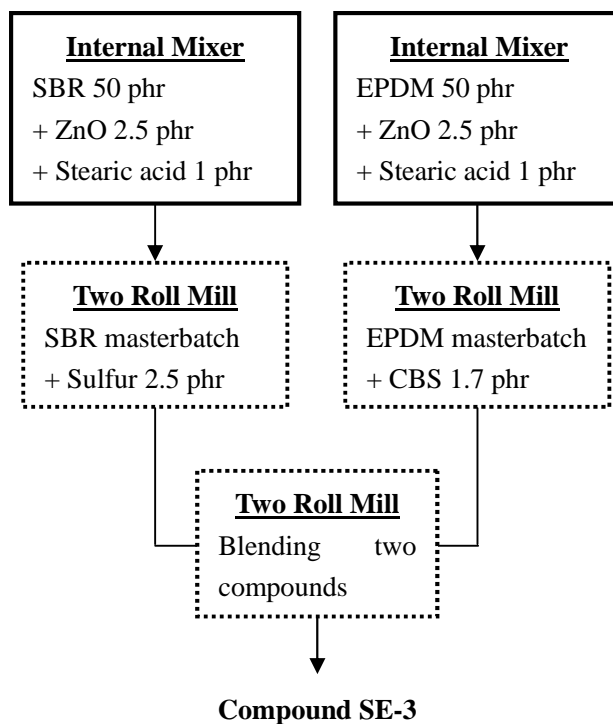
Figure 4.1d Mixing method for SE-3.
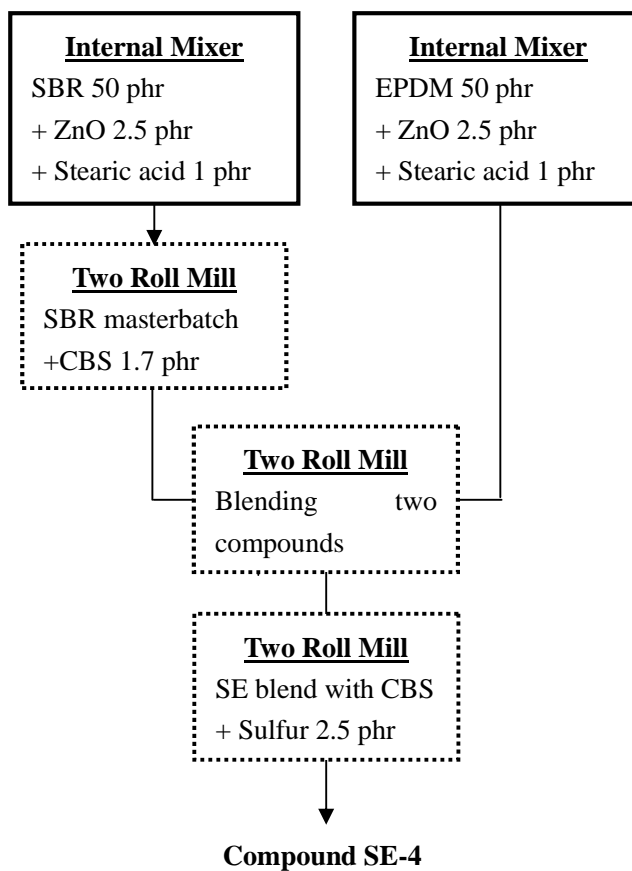
Figure 4.1e Mixing method for SE-4.

```
┌─────────────────────────┐        ┌─────────────────────────┐
│     Internal Mixer      │        │     Internal Mixer      │
│  SBR 50 phr             │        │  EPDM 50 phr            │
│  + ZnO 2.5 phr          │        │  + ZnO 2.5 phr          │
│  + Stearic acid 1 phr   │        │  + Stearic acid 1 phr   │
└─────────────────────────┘        └─────────────────────────┘
```

Two Roll Mill
SBR masterbatch
+Sulfur 2.5 phr

Two Roll Mill
Blending   two
compounds

Two Roll Mill
SE blend with Sulfur
+ CBS 1.7 phr
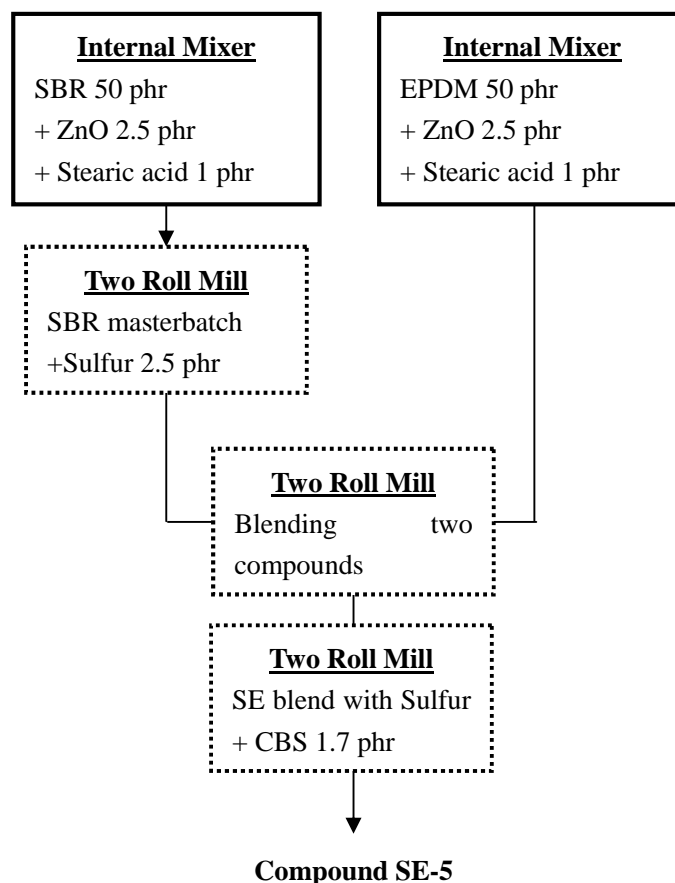
Compound SE-5

Figure 4.1f Mixing method for SE-5.

The curing properties of the compounds were determined using a RPA 2000 rheometer from Alpha Technologies to determine the optimum vulcanization time: t_{90} and time till beginning of vulcanization: t_{10}. The compounds were subsequently cured in a Wickert Laboratory press at 160 $^{\circ}$C and 100 bar pressure. Stress-strain behaviors of the vulcanizates were determined using a Zwick Z 1.0/TH1S tensile tester according to the ISO 37 standard.

4.3 Results and Discussion

4.3.1 SE blends

As shown in Figure 4.1, the SE rubber blends are composed of the same formulation, however different mixing procedures. Different from the normal mixing sequence SE-0, the mixing methods SE-1 to SE-5 may create different phase sizes since they are executed on the two roll mill instead of in the internal mixer. Further, SE-2 aims to direct more sulfur into the EPDM phase, opposite to its solubility preference. SE-3 is performed in order to obtain the opposite

effect of curatives' distribution compared to SE-2: more CBS in the EPDM phase. The mixing procedure according to SE-4 aims at creating a distribution of curatives in between that of SE-2 and SE-0, and SE-4 in between that of SE-3 and SE-0.
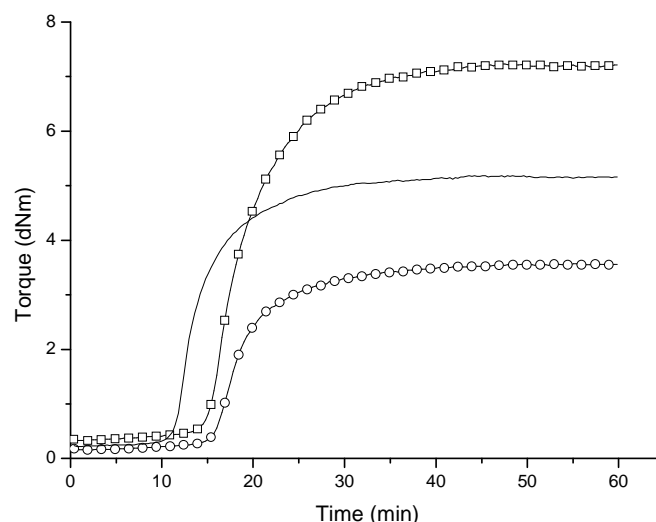
Figure 4.2 Curing properties of (—○—) SBR; (—□—) EPDM; (——) SE-0, at 160 $^\circ$C.

The curing properties of the SBR and EPDM straight rubbers and the SE-0 blends are presented in Figure 4.2. It can be observed that a sulfonamide-based accelerator like CBS provides scorch safety for all compounds; t_{10} for SBR is 13.6 mins., for EPDM 12.2 mins., and for SE-0 11.4 mins. Considering t_{10} as a period in which the curatives still may migrate through the compounds, curatives have enough time to diffuse to the phase in which they find their higher solubility in the SE blend. Typical migration speeds of curatives in rubbers are of the order of μm/s. [15, 16] So, the curatives migrate across the phase boundaries in order of seconds, which is far shorter than the time needed for scorch, of the order of minutes, see Table 3. On the other hand, the curing reactions in the SBR and the EPDM phases are simultaneous, as shown in Table 4.3. It demonstrates that the influence of reactivity on the cure compatibility of the SE blends can be neglected. Solubility plays the determinant role in migration and, consequently, the cure compatibility of this system. As SE-0 has a SBR: EPDM ratio of 50 to 50, it is reasonable to expect its' highest torque value somewhere in between of those of SBR and EPDM, as observed. However, SE-0 shows a shorter t_{10} than SBR and EPDM, which gives evidence for a cure mismatch of this blend. As the curatives are preferentially dispersed in double quantities in one phase, such a phase becomes more scorchy

compared to the straight rubbers.

Table 4.3 t_{10}, t_{90}, curing speed $(t_{90}-t_{10})$ and the maximum torque of SBR, EPDM and SE series.

Compound name	t_{10} (min)	t_{90} (min)	$(t_{90}-t_{10})$ (min)	Torq. Max. (dNm)
SBR	13.6	22.5	8.9	3.3
EPDM	12.2	23.1	10.9	7.2
SE-0	10.6	22.2	11.6	5.1
SE-1	11.4	25.1	13.7	5.0
SE-2	11.6	23.1	11.5	5.2
SE-3	14.7	27.7	13.0	5.0
SE-4	13.5	27.5	14.0	5.0
SE-5	15.3	28.8	13.5	5.0

The various curing curves obtained for the SE rubber blends with the same formulation, however prepared with different mixing procedures are shown in Figure 4.3. Although the detailed mixing steps are varied from blend to blend, the common feature in the mixing processes is that all blends are finalized on the two-roll-mill expect for SE-0. Taking the SE-0 mixing procedure as control, the scorch time for SE-1 is also short, as for both curatives were added into the pre-blended rubbers. The reason why the scorch time for SE-2 is so low is a bit unclear, other than that this procedure is the only case where all sulfur was purposely premixed into the EPDM-phase. The highest torque is also obtained for SE-2. All other mixing procedures give slightly lower, but still comparable maximum torque values. However, longer scorch delays are observed for SE-1 and SE-2, and even much longer delays in scorch are obtained for SE-3, SE-4 and SE-5 compared to that of SE-0.
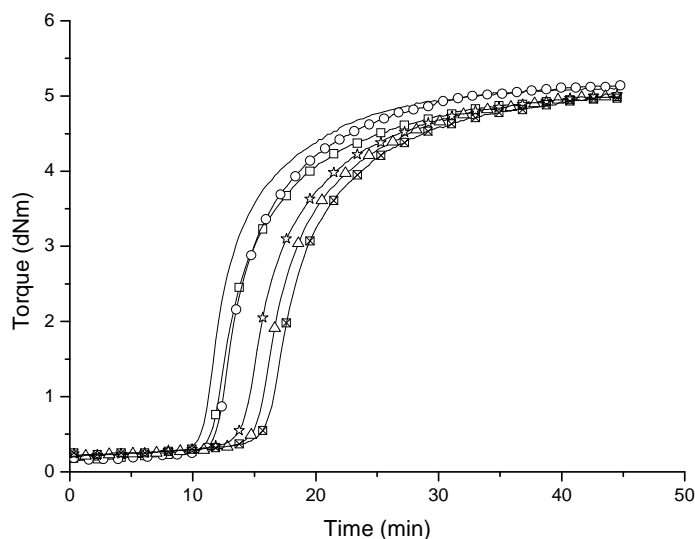
Figure 4.3 Curing properties of SE blends as function of various mixing procedures

at 160 °C. (——) SE-0; (–□–) SE-1; (–○–) SE-2; (–△–) SE-3; (–⋆–) SE-4; (–⊠–) SE-5.

The stress-strain properties of straight SBR, EPDM and blend SE-0 are presented in Figure 4.4. It can be seen that EPDM has the highest modulus; SBR has the highest elongation at break and tensile strength over the three vulcanizates. The stress-strain properties of SE-0 are closest to the SBR properties relative to EPDM.
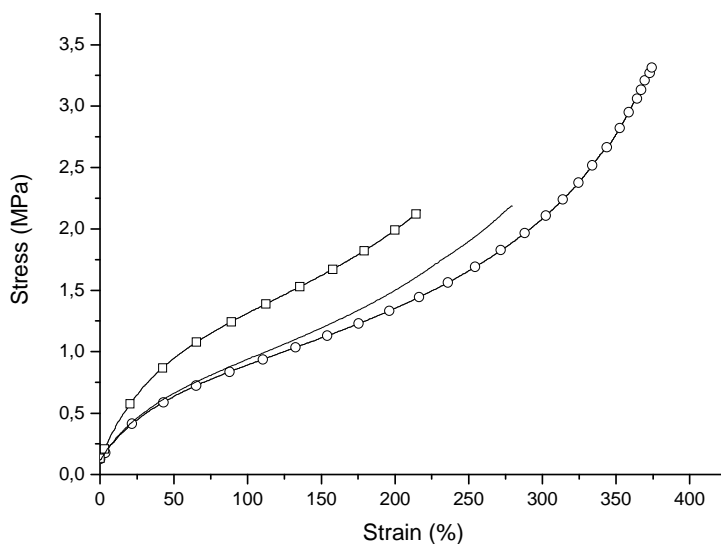
Figure 4.4 Stress-strain behaviors of (–○–) SBR; (–□–) EPDM; (——) SE-0.

:

The stress-strain properties of all SE rubber blends are shown in Figures 4.5 and 4.6. In SE-0 and SE-1, where the curatives were added to the pre-blended compound, the two phases

have an equal chance to obtain curatives. However, the curatives will preferentially distribute themselves into the phase with highest compatibility. It is surprising though that SE-1, blended on the two roll mill, shows so much better stress-strain properties than SE-0, blended in the internal mixer.
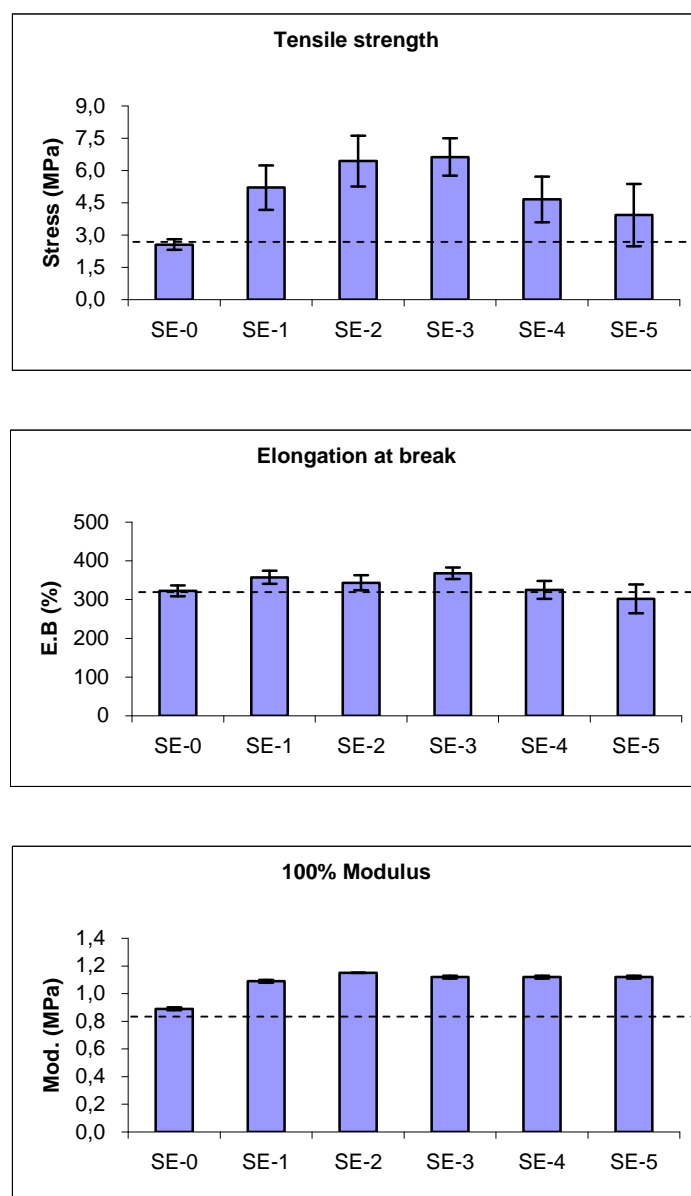
Figure 4.5 Tensile strength, elongation at break and 100% moduli of SE blends.
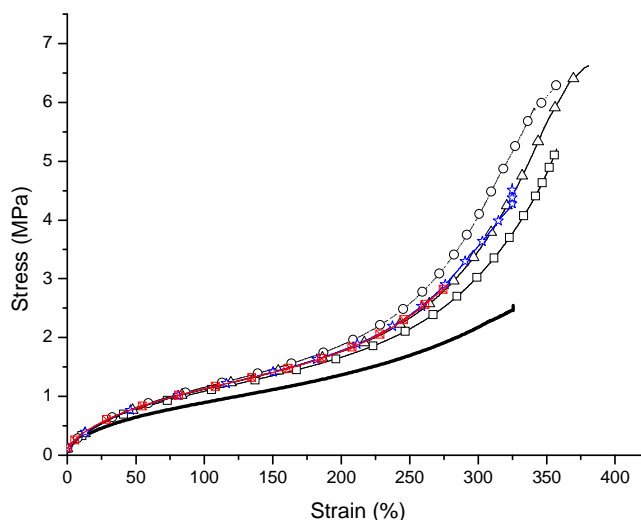
Figure 4.6 Stress-strain curves of SE blends:

(——) SE-0; (—□—) SE-1; (—○—) SE-2; (—△—) SE-3; (—☆—) SE-4; (—⊠—) SE-5.

The mechanical properties SE-2 and SE-3 are practically the same. Although this might be surprising at first sight, a closer look at the solubility parameter differences in Table 1 shows that the actual preferences of sulfur and CBS for either rubber phase are only very little different. So, it does not make much difference during final blending on the mill at about 40 ^{o}C whether e.g. sulfur was pre-mixed into the EPDM-phase (SE-2) or into the SBR-phase (SE-3); and CBS the reverse. Apparently, sulfur and CBS need to migrate each from their respective phases into the other at the curing temperature of 160 ^{o}C, and while doing so meet each other to form an effective curing system for either rubber-phase. Whether most of the crosslinking takes place in the respective rubber-phases or primarily in the interface between the phases is a question to be investigated in a later stage.

It is the more surprising that the mechanical properties of SE-4 and SE-5 are so much worse than SE-2 and SE-3, although still better than SE-0. However, in terms of the explanation given here before, either the sulfur (SE-4) or the CBS (SE-5) is only added when the SBR/EPDM blend is already fully developed. The curatives added in the final stage will preferentially partition into the phase they prefer, even though the solubility differences are only small. So, no migration is needed anymore and most probably one phase becomes overcured, and the other undercured, just like SE-0 and SE-1.

The rupture energies calculated by integrating of the area under the stress-strain curves are shown in Figure 4.7. Comparing the highest rupture energy of SE-3 to that of SE-0, an

increase of nearly 100% is obtained.
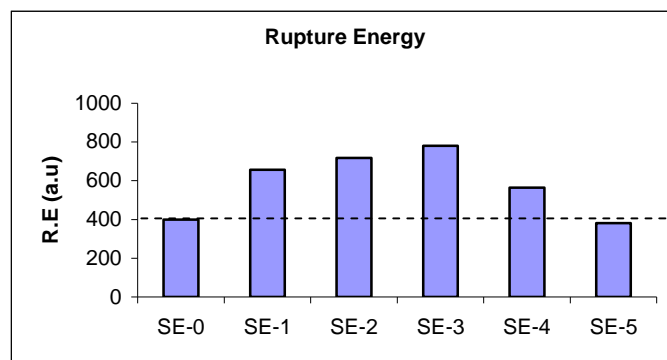
Figure 4.7 Rupture energy [arbitrary units(a.u)] of the SE blends.

4.3.2 NE blends

Although the mixing strategies used for the NE blends can simply be described by replacing SBR with EPDM, and EPDM with NBR, the performances of the NE blends are quite different from the SE blends. The compatibility of NBR and EPDM is very poor, so that the mutual phase sizes, after being blended using the internal mixer, are so large that they can be observed by the eye. The curing properties of NBR and EPDM together with NE-0 are shown in Figure 4.8. Clearly, NBR has a much shorter scorch safety than EPDM. The vulcanization of NBR is completed before the curing of EPDM starts. Further, the curing behavior of NE-0 is surprisingly similar to that of the straight NBR rubber.
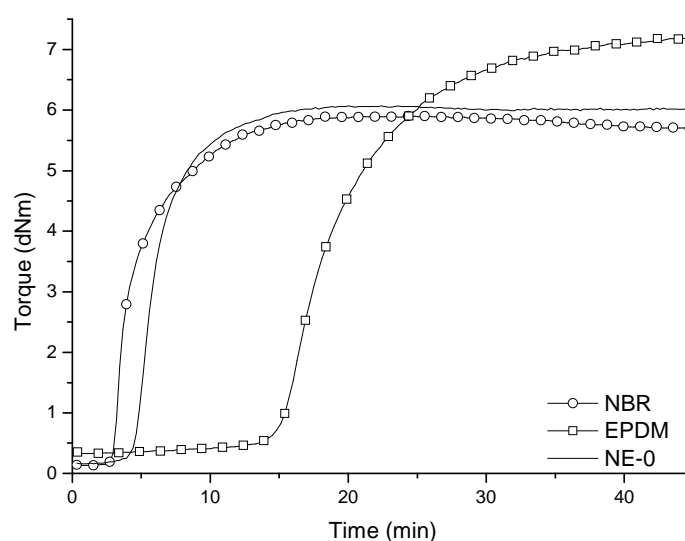
Figure 4.8 Curing properties of (─○─) NBR; (─□─) EPDM; (──) NE-0, at 160 $^{\circ}$C.

The much shorter scorch of NBR is reflected in t_{10}, as shown in Table 4.4. The optimal curing time of NBR: t_{90} is also much shorter than the t_{90} of EPDM, even slightly shorter than the t_{10} of EPDM. This large mismatch in cure rate does play an equally important role along with the solubility of the curatives in determining the curing properties of the blends. Consequently, it will lead to a situation that in a NE blend the NBR phase is grossly over-cured while the EPDM phase stays far under-cured.

Table 4.4 t_{10}, t_{90}, curing speed (t_{90}-t_{10}) and the torque maximum of NBR, EPDM and NE series.

Compound name	t_{10} (min)	t_{90} (min)	(t_{90}- t_{10}) (min)	Torq. Max. (dNm)
NBR	3.2	10.4	7.2	5.9
EPDM	12.2	23.1	10.9	7.2
NE-0	4.6	12.0	7.4	4.6
NE-1	5.2	13.3	8.1	5.0
NE-2	5.1	11.9	6.8	5.2
NE-3	5.4	11.5	6.1	5.0
NE-4	5.0	12.1	7.1	5.0
NE-5	5.7	11.9	6.2	5.0

The rheograms of the NE-0 to NE-5 blends are shown in Figure 4.9. Only a small delay in scorch time and a slight decrease in maximum torque are obtained by applying the mixing procedures of NE-1 to NE-5 compared to NE-0. The rheograms of NE-1 to NE-5 grossly overlap. Different from the SE blends, there is no pronounced effect of the different mixing strategies. Apparently, the properties of the blends are primarily governed by the NBR phase, wherein CBS has a much higher solubility and the curatives show a much faster reaction speed than in the EPDM phase. The maximum torques and t_{10} are summarized in Table 4.4. As mixing methods NE-2 to NE-5 can only compensate for the solubility differences to some

extent, no appreciable improvement is observed in the maximum torques by using any of these mixing strategies.
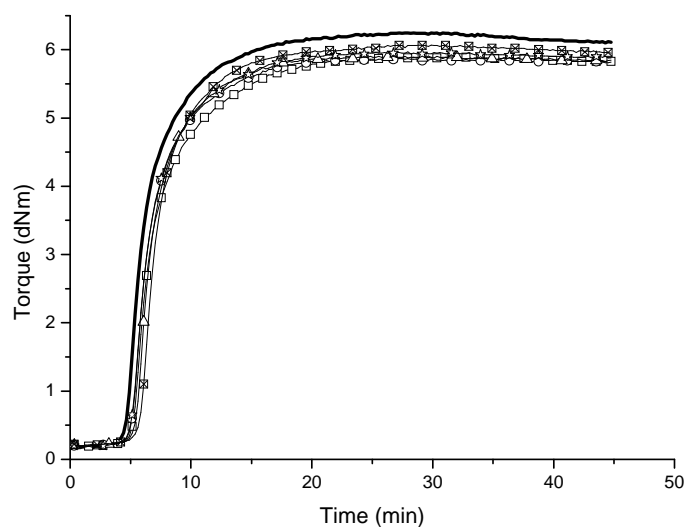
Figure 4.9 Curing properties of NE Blends.
(——) NE-0; (—□—) NE-1; (—○—) NE-2; (—△—) NE-3; (—☆—) NE-4; (—▣—) NE-5.

The accumulation of the curatives in the NBR, and practically not in the EPDM phase is different from that given in the overall recipe. Taking the large difference in $\overline{\Delta\delta}$ between CBS and the two rubber polymers into account, an efficient curing system with much higher ratio of CBS/sulfur may be generated in the NBR-phase during the vulcanization process. This could further speed up the curing.

The stress-strain properties of the NBR, EPDM and NE-0 are shown in Figure 4.10. It is clear that NE-0 shows almost the same features of the stress-strain curve of EPDM with only a longer elongation at break.
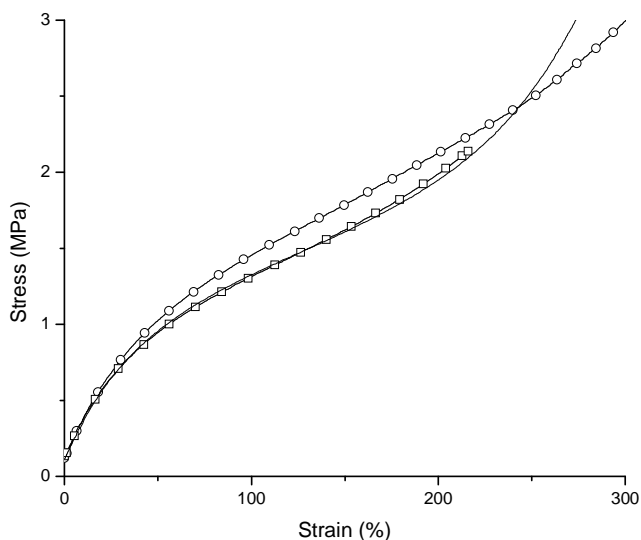
Figure 4.10 Stress-strain properties of (─○─) NBR; (─□─) EPDM; (──) NE-0.

The stress-strain properties of the full NE series are shown in Figure 4.11. Only NE-3 shows somewhat inferior tensile strength compared to NE-0. The rest of the NE blends all show some improvements in tensile strength relative to NE-0. For the elongation at break and 100% modulus, all the NE compounds show similar values.
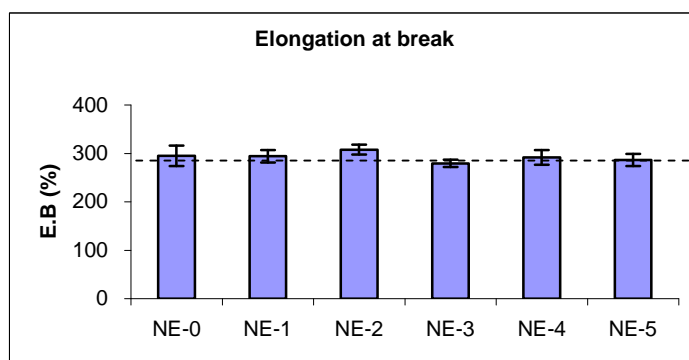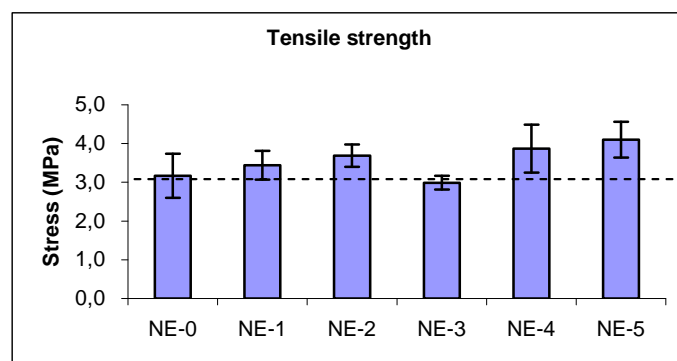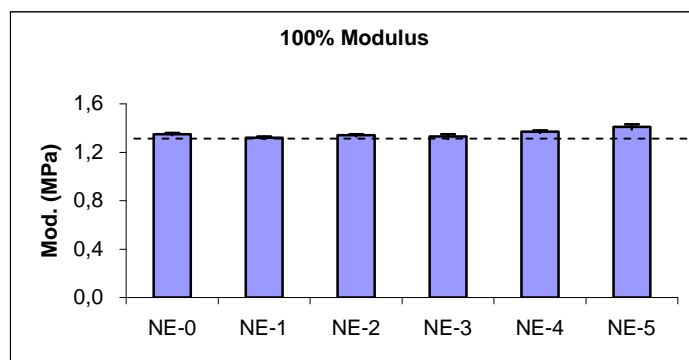
Figure 4.11 Tensile strength, elongation at break and 100% moduli of NE blends.

The tensile curves and the rupture energies are shown in Figures 4.12 and 4.13. Except for NE-3, the rest of the NE blends show better properties relative to NE-0. However, the improvement is small compared to that of the SE blends. The highest value of rupture engergy is found for NE-2 with an increase of 9%. The sequence of rupture energy from high to low is quite different from the one for the SE series. Although NE-2 does not give the best properties like SE-2 did for the SE rubber blends, it is still superior compared to NE-3, which gives the lowest rupture energy of all.
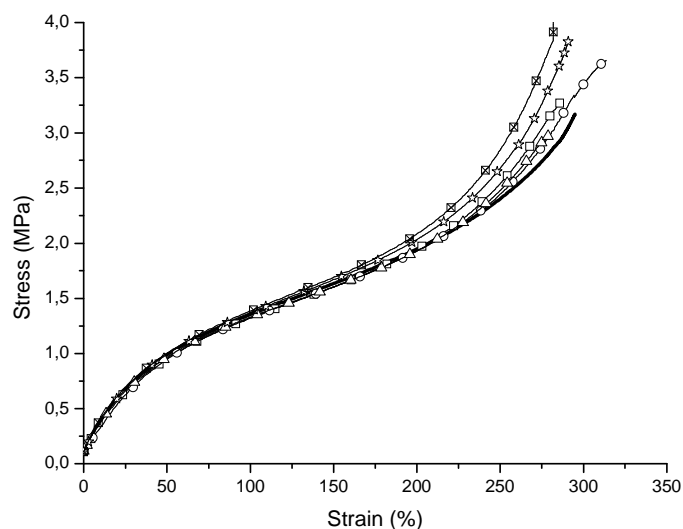
Figure 4.12 Stress-strain properties of NE blends.
(——) NE-0; (—□—) NE-1; (—○—) NE-2; (—△—) NE-3; (—☆—) NE-4; (—⊠—) NE-5.
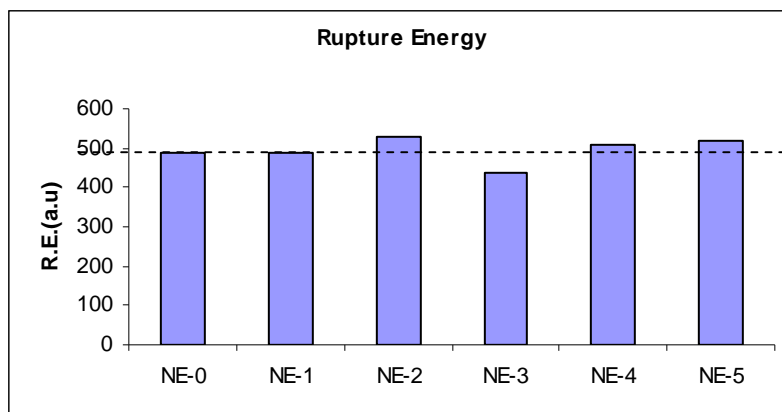
Figure 4.13 Rupture energy [arbitrary units(a.u)] of the NE blends.

4.4 Conclusions

In this chapter, it was shown that the distribution of curatives plays a vital role in the properties of 50/50 SBR/EPDM rubber blends. By using solubility information of the curatives in different rubber phases, it is possible to improve the performance of such blends by intentionally introducing seprate curatives in opposite rubber phases, e.g. SE-2 and SE-3. The calculated and measured solubilities of sulfur in SBR and EPDM are practically the same, and a similar argument applies for CBS. Also the t_{10} of the cure system in either phase is equivalent. The fact that the cure and mechanical properties of SE-2 and SE-3 are so outstanding, apparently is the result of the two separate curatives sulfur and CBS added to separate phases before final blending. Mutual migration of the curatives into the opposite phases is held responsible for the improved properties.

   Although the same mixing methods are applied to the 50/50 NBR and EPDM blends as well, quite different results are obtained. Compared to the SE blends the solubility difference and scorch times of these two rubber phases are far more different. The curing reaction of the NBR phase is much faster than that of the EPDM phase, reflected by (t_{90}-t_{10}). As a result, the EPDM phase remains seriously under-cured in the NE blends, and the properties of the NE (50/50) blends are mainly dominated by the properties of the NBR. On the other hand, the large difference in polarity of the two rubber polymers results in a very poor compatibility, where the phases are so coarse as to be observable by the eye. All this explains why the mixing methods, which work well in the SE blends, do not give appreciable improvements for the NE blends.

In summary, both solubility and reactivity of curatives in the different phases of rubber blends play a role in the cure compatibility. When a very large difference in reactivity of curatives towards the two rubber phases exists, the influence of solubility is an overruling factor. That explains the fact that by applying knowledge of mutual solubility between curatives and rubber polymers into mixing, the properties of the SE blends could be improved. However, in the case of the NE blends, the situation is much more complicated and less successful.

4.5 References

[1]   W.M. Hess, C.R. Herd and P.C. Vegvari, *Rubber Chem. Technol.*, **1993,** 66, 329.

[2]   D.Mangaraj, *Rubber Chem. Technol.*, **2002,** 75, 365.

[3]   R.H. Schuster, *Angew. Makromol. Chemie*, **1992**, 202**,** 159.

[4]   R. Guo, A.G. Talma, R.N. Datta, W.K. Dierkes and J.W.M. Noordermeer, *Eur. Pol. J.*, **2008,** 44, 3890.

[5]   J.B. Gardiner, *Rubber Chem. Technol.*, **1969,** 42, 1058.

[6]   D.A. Lederer, K.E. Kear, and G.H. Kuhls, *Rubber Chem. Technol.*, **1982,** 55, 1482.

[7]   C.S. Venable, and C.D. Greene, *Ind. Eng. Chem.*, **1922**, 14, 319.

[8]   M.D. Morris, and A.G. Thomas, *Rubber Chem. Technol.*, **1995**, 68, 794.

[9]   F. Guillaumond, *Rubber Chem. Technol.*, **1976**, 49, 105.

[10]   H.J. Graf, and H.M. Issel, *Kautsch. Gummi Kunstst.*, **1995**, 48, 600.

[11]   R.P. Mastromatteo, J.M. Mitchell, and T.J. Brett, *Rubber Chem. Technol.,* **1971**,44, 1056.

[12]   U.S. 3706 819 (1972), to Sumitomo Chemical Co. Ltd. Osaka, Japan, invs.: T. Usamoto, Y. Hatada, I. Furuichi and M. Matsuo.

[13]   K.C. Baranwal, and P.N. Son, *Rubber Chem. Technol.*, **1974**, 47, 88.

[14]   J. Zhao, G. Ghebremeskel, and J. Peasely, *Kautsch. Gummi Kunstst.*, **2001**, 54**,** 84

[15]   R. Byron Bird, Warren E. Steward, Edwin N. Lightfoot, *"Transport Phenomena"* 2nd edition, John Wiley & Sons, Inc., New York, 2007, 518.

[16]   C. Rosca, U. Giese, R.H. Schuster, *Kautsch. Gummi Kunstst.*, **2004**, 57, 593.

Chapter 5

Acetylene Plasma Encapsulated Sulfur and CBS

in Rubber-Rubber Blends

In this chapter, the surface modification of curatives by plasma polymerization with acetylene is described with the aim of changing the surface properties of these curatives without losing their bulk properties and reactivities in the vulcanization process. Significant improvements are obtained in both pure rubbers and elastomer blends using encapsulated sulfur and N-cyclohexylbenzothiazole-2-sulphenamide (CBS) powders. The conditions for the plasma polymerization of acetylene are varied in order to obtain the optimal performance of the modified curatives. The imperfections in the shell structure, obtained with plasma polyacetylene, act as gateways to release sulfur for the vulcanization reaction.

5.1 Introduction

Blending is a convenient method for the development of new polymeric materials. Blends may combine the beneficial properties of the different components. One of the main problems with dissimilar rubber/rubber blends is the difference in the retention of the curatives in each phase. A large cure mismatch results from the migration of curatives across phase boundaries due to solubility differences and reactivity imbalances. A few methods for adjusting the amounts of curatives in the different phases are described in literature. These methods can be divided into three categories: 1) modification of the elastomers; 2) defining the surface chemistry of the fillers, e.g. by encapsulation; and 3) adjusting the mixing procedure. [76, 113]

Although the history of encapsulation began in the 1950's, the application for fillers and curatives by plasma polymerization is a relatively new approach. Plasma polymerization uniquely deposits an ultra-thin film on a substrate in a clean process. Encapsulation of a powdery substrates with a highly crosslinked plasma polymer layer can retain the bulk properties of the substrate, while selectively modifying the surface tension, polarity, morphology and electrical conductivity. [114, 115]

Several studies were performed on the surface modification of reinforcing fillers, like Carbon Black (CB) and silica, using plasma treatment. The deposition of a plasma polymer layer on a filler can reduce the filler-filler interaction and enhance the filler-polymer interaction, respectively. [7-16] As there are less functional groups on the substrate of CB, its surface modification is much more difficult compared with silica. [12, 13] Being different from CB and silica, sulfur has a higher density and the application of encapsulation to sulfur is even more complicated as the encapsulated sulfur needs to be released from inside its shell to take part in the vulcanization process.

Van Ooij and also Borrós et al. have applied plasma polymerization on curatives and checked their reactivity towards squalene in a model compound study. [17, 18] In the present chapter, plasma polymerization of acetylene is carried out on pre-ground curatives: sulfur and CBS, in a Radio Frequency (RF) plasma vertical tubular reactor.

The aim of the study was to improve the co-vulcanization and mechanical properties of dissimilar rubber blends with the plasma polyacetylene modified sulfur ($PPAS_8$).

5.2 Experimental Part

5.2.1 Materials

The following types of rubber are employed: Solution Styrene-Butadiene rubber (S-SBR, Buna® VSL 5025-0HM from LANXESS Corp., Germany), Nitrile-Butadiene rubber (NBR, Perbunan® 3446F from LANXESS Corp.), and Ethylene Propylene Diene rubber (EPDM, Keltan® 4703 from DSM Elastomers, the Netherlands). Zinc oxide was purchased from Sigma Aldrich; stearic acid was used as commercial grade, and accelerator CBS (Santocure® CBS) was provided by Flexsys, Belgium. Elemental sulfur (S_8) was purchased from Sigma Aldrich, with a particle size smaller than 100 mesh. Acetylene (99.6% purity) was supplied by Matheson tri gas, USA.

5.2.2 Methods

a. Grinding by ball mill

The sulfur powders were ground using a ball mill and the powders were sieved to a size smaller than 50 μm before the plasma treatment. CBS pellets were ground without sieving, as the particle size was already smaller than 50 μm.

b. Plasma polymerization

Plasma polymerizations on pre-ground sulfur/CBS were carried out in a vertical tubular reactor. A schematic representation of this reactor is shown in Figure 5.1. The amount of curatives to be treated was fixed at 20 grams for each batch. The glass reactor was evacuated with an oil pump to a pressure of 3.6 Pa. Subsequently, acetylene gas was introduced under steady flow conditions, and the monomer pressure was maintained at approximately 26-31 Pa by applying a flow rate of 20 sccm (standard cubic centimeter). Finally, the coil was brought down to position 2 and a discharge power (13.56MHz frequency) was applied, which turned the monomer gas into the plasma state. Subsequently, plasma polymerization of acetylene took place and a plasma polyacetylene layer was deposited on the sulfur/CBS substrate. The

reaction conditions are summarized in Table 5.1 for sulfur and 5.2 for CBS.
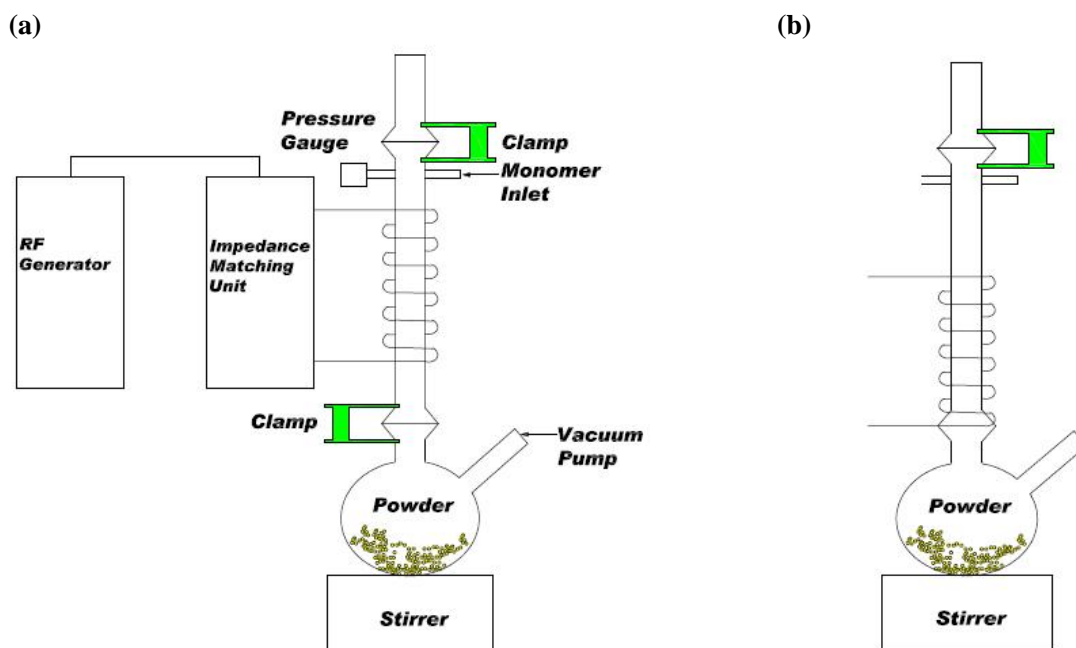
(a)   (b)

Figure 5.1 (a) Schematic representation of a vertical tubular RF plasma reactor with coil position 1; (b) coil position 2.

Table 5.1 Plasma polymerization conditions for sulfur

Sample code	RF power (W)	Monomer concentration (Pa)	Reaction time (hr)
$PPAS_8$-1	150*	26	1
$PPAS_8$-2	150	31	1
$PPAS_8$-3	150	26	1.5
$PPAS_8$-4	125	26	1.5

In condition $PPAS_8$-1, the coil was left at the higher position 1; while in the other cases it was brought down to position 2.

Table 5.2 Plasma polymerization conditions for CBS

Sample code	RF power (W)	Monomer concentration (Pa)	Reaction time
PPACBS-1	150	29	1.5 hr
PPACBS-2	180	28	15 min
PPACBS-3	180	28	30 min
PPACBS-4	180	29	45 min
PPACBS-5	180	28	1.0 hr
PPACBS-6	180	29	1.5 hr
PPACBS-7	180	29	2.0 hr
PPACBS-8	250	29	1.0 hr

c. Scanning Electron Microscopy (SEM)

Digital images were obtained for both uncoated and coated sulfur/CBS, deposited on carbon tape, using a LEO 1550 FEG/Thermo Noran Instruments, with accelerating voltage 2 kV. To obtain the images of cross sections of coated sulphur, 0.55 kV was applied. The cross-sections were created using a shape knife, cutting through the sulfur agglomerates under a stereo light microscope. The cross section CBS was not measured.

d. Wetting behaviors with liquids of known surface energy

Glycerol, formamide, ethylene glycol and toluene were used as the comparative liquids. For this analysis, about 50 ml of liquids were put in a beaker and 1 g of unmodified and modified sulfur/CBS was added to the liquids. The powder sample sinks if it has a surface tension higher than that of the liquid; otherwise it floats on the liquid.

e. Thermogravimetric analysis (TGA)

A Perkin Elmer TGA 7 was used to investigate the plasma modified curative samples. The samples were heated in nitrogen from 50 $^{\circ}$C to 700 $^{\circ}$C with a heating rate of 10

^{o}C/min. The quantitative measurement of the amount of coating was carried out by heating in nitrogen from 50 ^{o}C to 180 ^{o}C, followed by an isothermal step at 180 ^{o}C for 5 hours to complete the sublimation of sulfur. Finally, the remaining weight was all from the polyacetylene coating.

f. Rubber mixing and testing

Samples were prepared in a similar way as described in Chapter 4 of this thesis. The formulations used for this study are given in Table 5.3. S_0, N_0, E_0 are the codes for pure SBR, NBR, EPDM compounds; while SE, NE are the abbreviations for the 50/50 w/w SBR/EPDM and 50/50 w/w NBR/EPDM blends. The curing properties of the compounds were determined at 160 ^{o}C using a rheometer (RPA 2000) from Alpha Technologies. Stress-strain properties were determined using a Zwick Z 1.0/TH1S tensile tester according to the ISO 37 standard.

Table 5.3 Compound formulations in phr.

Component	S_0	N_0	E_0	SE	NE
SBR	100	0	0	50	0
NBR	0	100	0	0	50
EPDM	0	0	100	50	50
ZnO	5	5	5	5	5
Stearic acid	2	2	2	2	2
Sulfur	2.5	2.5	2.5	2.5	2.5
CBS	1.7	1.7	1.7	1.7	1.7

5.3 Results and Discussion

5.3.1. Plasma polyacetylene modified sulfur and its performance in straight rubbers and dissimilar elastomer blends

5.3.1.1 Optimization of the stirrer in the plasma reactor

Sulfur has the tendency of becoming plasticized and forming lumps during mixing. Therefore, it is very difficult to achieve a good mixing of sulfur powders in order to

have a proper plasma coating deposited on each sulfur powder particle.

Several designs were made with the stirrer and one with a triangle-shaped magnetic stirrer bound with three flexible plastic tubes with different lengths seemed to provide the best mixing effect. The longest tube had the length of the diameter of the bottom of the reaction flask. The stirrer works as a broom and the powders are all the time being swept to the plasma.

5.3.1.2 Scanning Electron Microscopy (SEM)

The morphologies of ground uncoated sulfur and the plasma polyacetylene modified sulfur particles are shown in Figures 5.2. The images in Figures 5.2a to 5.2d, were obtained using an accelerating voltage of 2 kV. Compared to the images of uncoated sulfur, Figures 5.2a and 5.2b, an amorphous layer is deposited on top of the sulfur agglomerates after the plasma polymerization with acetylene, Figures 5.2c and 5.2d. The size of the encapsulated particles ranges from 10 to 100 μm. However, different from what has been described in the literature, [5, 6, 18] the layer is not pin-hole free. Instead, there are quite some flaws present, as demonstrated in Figure 5.2d. As sulfur needs to be released from the shell before the vulcanization process in a rubber system, the flawed encapsulation is actually a gateway for future release of the active sulfur.

The images in Figures 5.2e and 5.2f are obtained with a lower accelerating voltage of 0.55 kV. No conductive coating was applied for the SEM anaylsis of these two samples. The shells in Figure 5.2e seem to be more perfect compared to those in Figures 5.2c and 5.2d. A core-shell structure with a shell-thickness of about 100 nm is shown in Figure 5.2f, which represents a cross-section of a coated sulfur aggregates.
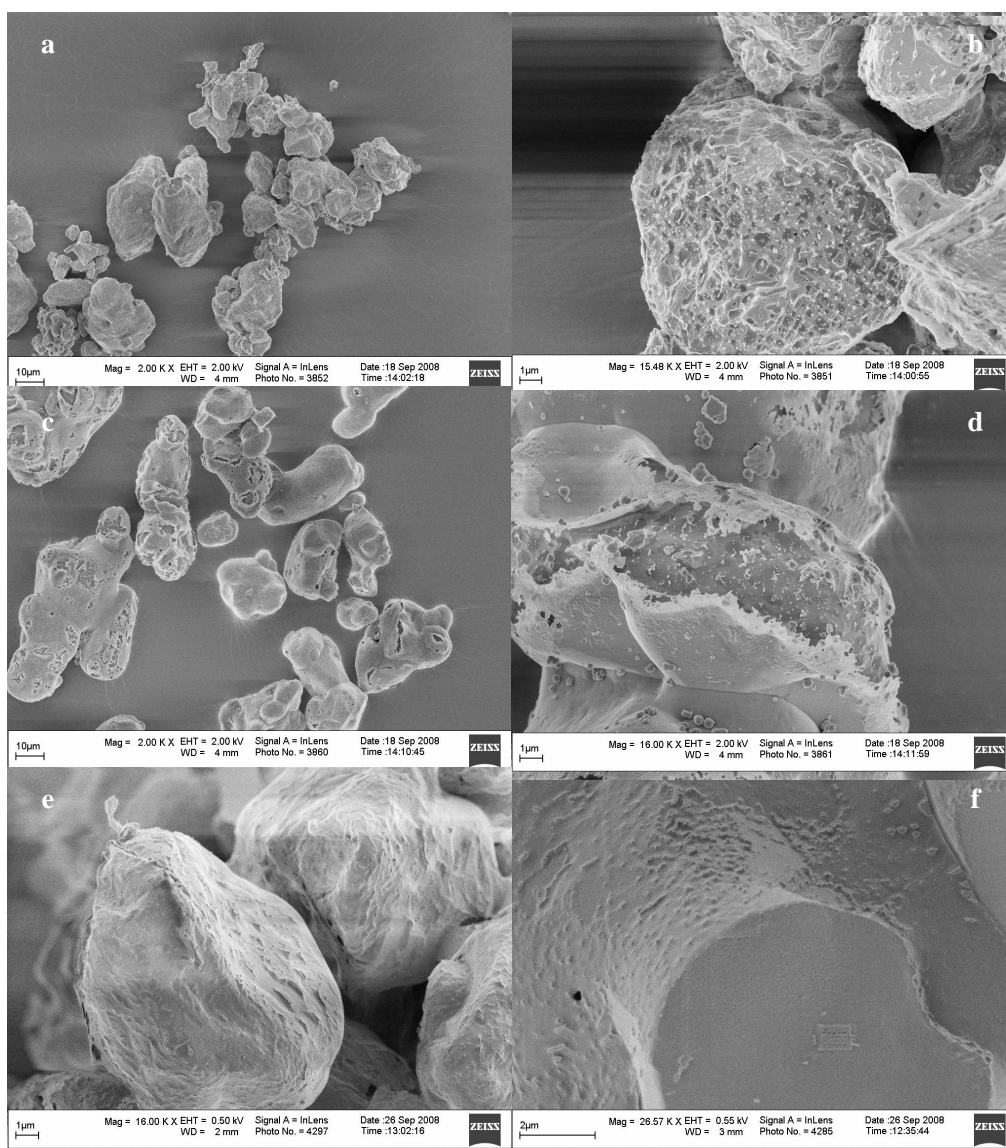
Figure 5.2 SEM images: (a) & (b) uncoated sulfur; (c) - (e) plasma polyacetylene coated sulfur; (f) cross-section of the plasma polyacetylene coated sulfur.

5.3.1.3 Surface energy

In literature the surface energy of polystyrene is given as 43 mJ/m^2 and that of polybutadiene as 32.5 mJ/m^2. [19] Calculated on basis of the weight ratio of styrene and butadiene in SBR, the surface energy of SBR is estimated to be 34.1 mJ/m^2. The surface energies of EPDM and NBR are derived in the same way and given in Table 5.4. Surface energies can also be calculated from the parachor per structural unit by applying equation 5.1 according the method described by Van Krevelen. [19]

$$\gamma = \left(\frac{P_s}{V} \right)^4 \qquad \text{(Equation 5.1)}$$

In this equation, P_s is the parachor with a unit of $(m^3/mol) \times (J/m^2)^{1/4}$ and V is the molar volume of a particular atom or structure. The calculated surface energies are summarized in Table 5.4. The average values of the surface energies from the two methods are used for further discussion.

Table 5.4 Surface energies of SBR, EPDM and NBR.

Polymer	γ_w	γ_p	$\bar{\gamma}$
	From weight ratio	From parachor	Average
SBR	34.1	29.7	31.9
EPDM	32.0	29.0	30.5
NBR	44.5	41.9	43.2

After the plasma polyacetylene surface modification, sulfur floats on top of ethylene glycol, while the untreated sulfur sinks immediately. The surface energy of uncoated sulfur can be therefore scaled in the range of 47.7 to 50 mJ/m^2; polyacetylene encapsulated sulfur in the range of 28.4- 47.7 mJ/m^2 indicated in Figure 5.3. As the surface energy of sulfur after being encapsulated with polyacetylene layer is brought closer to those of rubbers, better compatibility with these rubbers is to be expected.
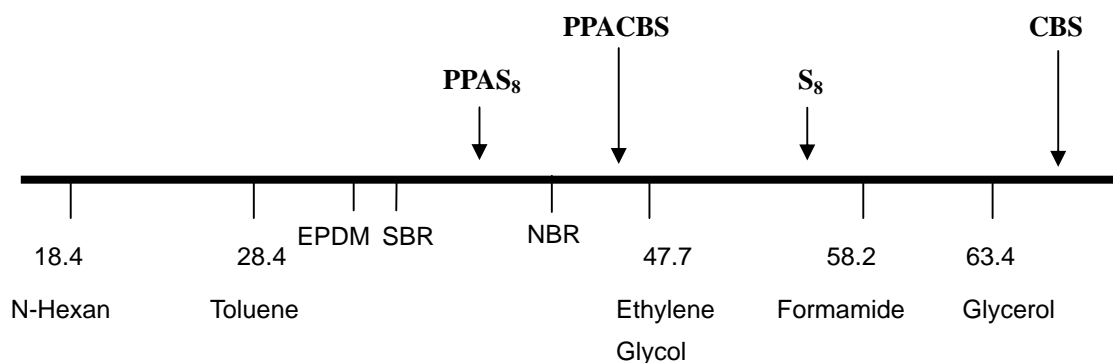
Figure 5.3 Surface energies [mJ/m^2] of uncoated and plasma acetylene encapsulated sulfur and CBS.

5.3.1.4 Thermogrametric analysis

The thermogrametric curves of uncoated sulfur and sulfur encapsulated under different experimental conditions are given in Figure 5.4. The weight losses in the TGA curves of the different encapsulated sulfur powders are all shifted to a higher temperature compared to uncoated sulfur. This can be attributed to the fact, that pure polyacetylene has a higher onset weight loss temperature of 265 ^{o}C relative to the sublimation temperature of sulfur. [13] The sequence of the stability is PPAS$_8$-3> PPAS$_8$-4> PPAS$_8$-2> PPAS$_8$-1>S$_8$. The amounts of deposition are summarized in Table 5.5.
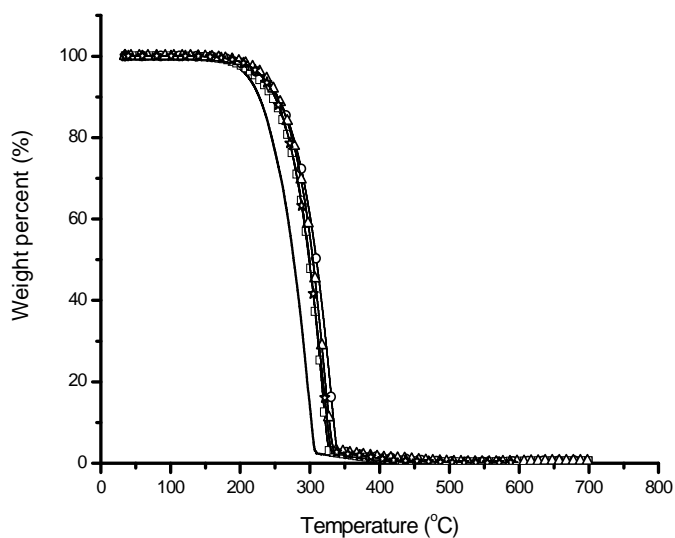
Figure 5.4 TGA thermograms of uncoated and plasma acetylene coated sulfurs.

(———) S$_8$; (—□—) PPAS$_8$-1; (—○—) PPAS$_8$-2; (—△—) PPAS$_8$-3; (—☆—) PPAS$_8$-4.

Table 5.5 Estimated coating amount (wt %) for sulfur samples.

Sample code	Amount of coating (%)
PPAS$_8$-1	n.a.
PPAS$_8$-2	1.32
PPAS$_8$-3	1.51
PPAS$_8$-4	n.m.

n.a. = not available

n.m. = not measurable

5.3.1.5 Performance of the plasma polyacetylene treated sulfur powders in rubbers

5.3.1.5a In straight SBR, EPDM and NBR rubbers

The rheograms of SBR, EPDM and NBR are represented in Figure 5.5. It is clear that the coated sulfurs show longer scorch times as compared to the uncoated sulfur in SBR, shown in Figure 5.5a. The only exception is $PPAS_8$-4, which shows a similar rheogram as uncoated sulfur. As $PPAS_8$-4 was modified with a lower discharge power, the not measurable thickness of the coating may be too thin to provide an effect on its performance in rubbers. This assumption is supported by the fact that only a very minor change in color was obtained for this sample after the coating. For EPDM and NBR rubber, there is no appreciable difference in the shape of the curing curves. Only a minor delay is observed in the scorch time for $PPAS_8$-3 in EPDM. For NBR, a small increase of the ultimate state of cure (maximum torque) is shown for coated sulfur samples in Figure 5.5c. The rheological properties are summarized in Table 5.6.

Table 5.6a Rheological properties of SBR compounds with different sulfur samples.

Sample name	t_{s2} (min)	t_{90} (min)	Min. torque (dNm)	Max. torque (dNm)
S8	8.8	19.4	0.1	3.7
PPAS8-1	9.0	25.3	0.1	3.5
PPAS8-2	9.4	25.1	0.1	3.6
PPAS8-3	8.4	24.0	0.1	3.5
PPAS8-4	7.6	19.3	0.1	3.7

Table 5.6b Rheological properties of EPDM compounds with different sulfur samples.

Sample name	t_{s2} (min)	t_{90} (min)	Min. torque (dNm)	Max. torque (dNm)
S8	5.3	24.5	0.3	7.7
PPAS8-1	5.2	24.4	0.3	7.7
PPAS8-2	5.4	25.6	0.3	7.6
PPAS8-3	6.9	25.8	0.3	7.8
PPAS8-4	6.2	24.7	0.3	7.7

Table 5.6c Rheological properties of NBR compounds with different sulfur samples.

Sample name	t_{s2} (min)	t_{90} (min)	Min. torque (dNm)	Max. torque (dNm)
S8	2.7	8.9	0.1	6.0
PPAS8-1	2.8	7.3	0.1	6.2
PPAS8-2	2.8	7.3	0.1	6.1
PPAS8-3	2.6	8.8	0.1	6.0
PPAS8-4	2.7	7.5	0.1	6.1
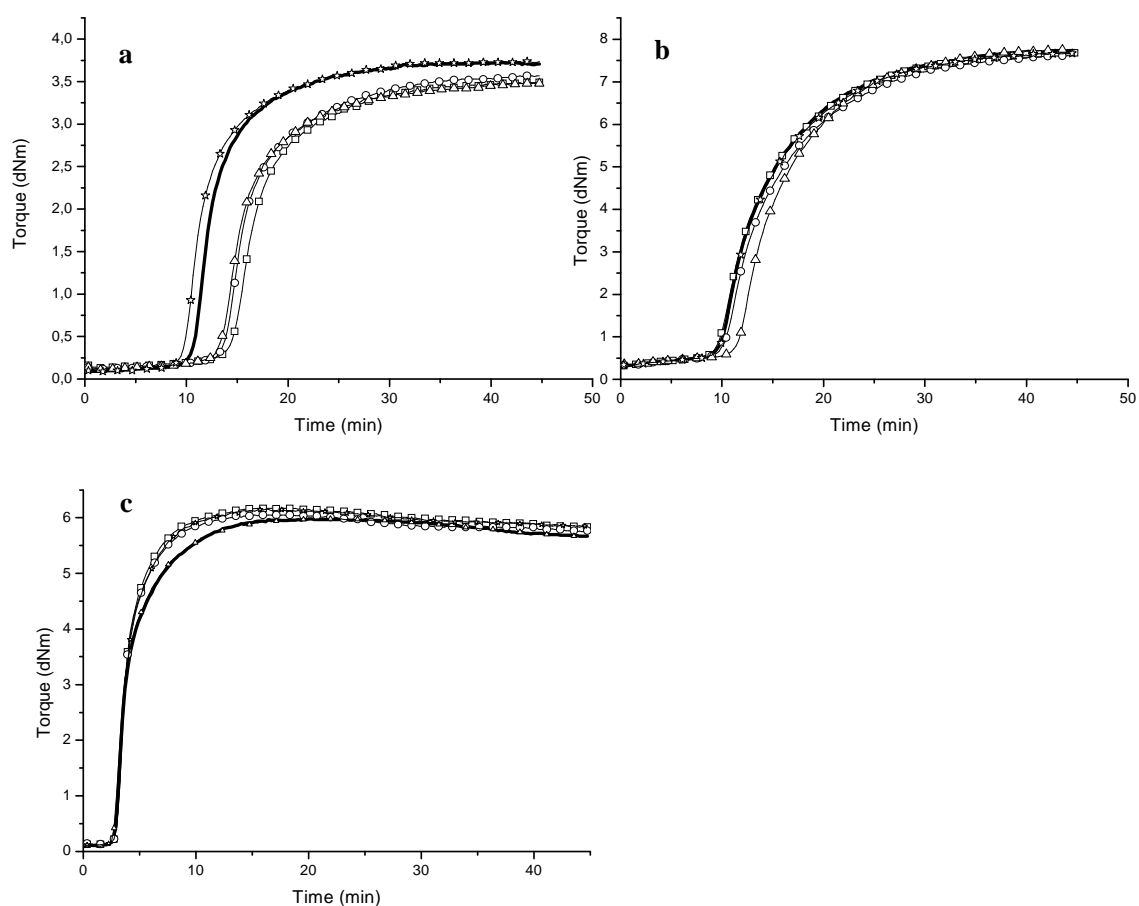
Figure 5.5 Rheograms of (a) SBR; (b) EPDM; (c) NBR cured with: (———) S_8; (—□—) PPAS$_8$-1; (—○—) PPAS$_8$-2; (—△—) PPAS$_8$-3; (—☆—) PPAS$_8$-4.

The stress-strain curves of SBR, EPDM and NBR straight rubbers cured with uncoated and coated sulfur are represented in Figure 5.6. The rupture energies calculated by integrating the area under the tensile curve are given in Table 5.7.
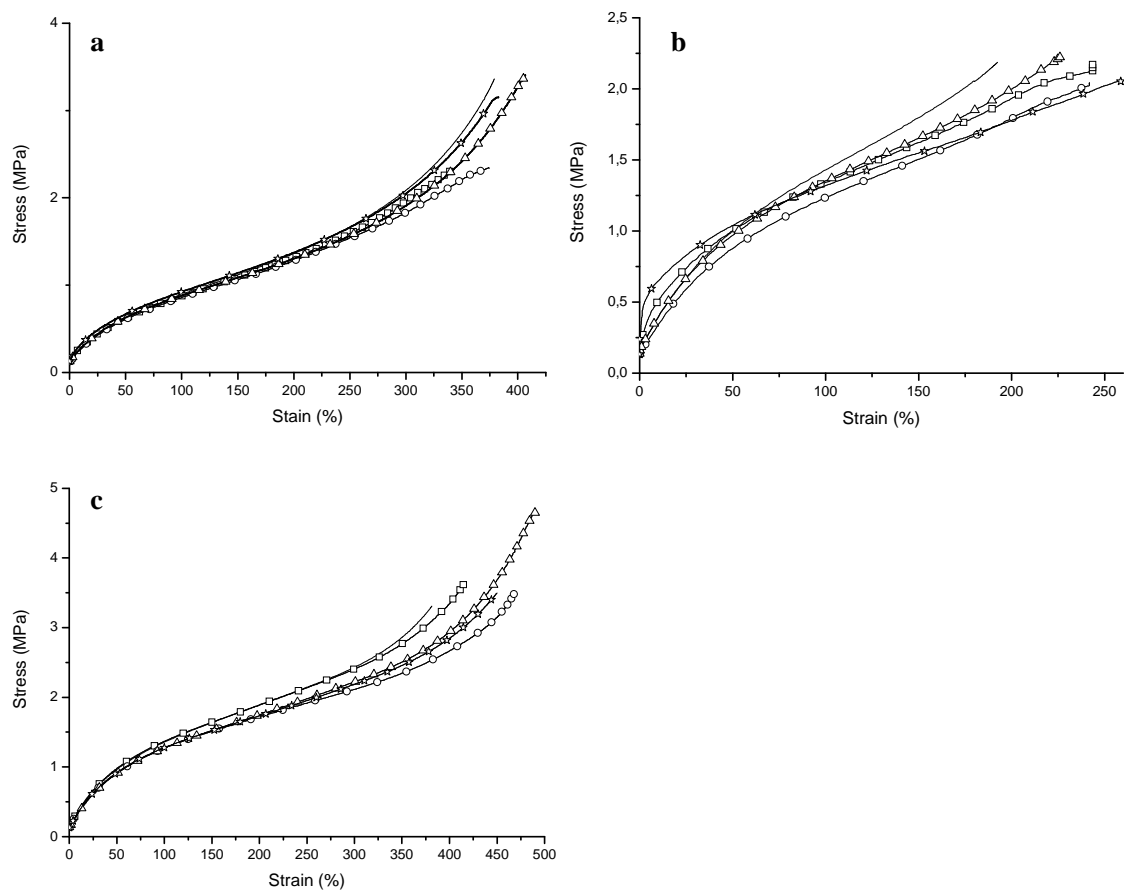
Figure 5.6 Stress-strain curves of (a) SBR; (b) EPDM; (c) NBR cured with:
(——) S_8; (—□—) PPAS$_8$-1; (—○—) PPAS$_8$-2; (—△—) PPAS$_8$-3; (—☆—) PPAS$_8$-4.

Table 5.7a Rupture energies of the SBR compounds with different sulfur samples.

Sample code	Rupture energy (a.u)
S_8	547
PPAS$_8$-1	404
PPAS$_8$-2	406
PPAS$_8$-3	595
PPAS$_8$-4	540

(a.u) = arbitrary units

Table 5.7b Rupture energies of the EPDM compounds with different sulfur samples.

Sample code	Rupture energy (a.u)
S_8	257
PPAS8-1	305
PPAS8-2	295
PPAS8-3	312
PPAS8-4	326

(a.u) = arbitrary units

Table 5.7c Rupture energies of the NBR compounds with different sulfur samples.

Sample code	Rupture energy (a.u)
S_8	695
PPAS8-1	803
PPAS8-2	869
PPAS8-3	1003
PPAS8-4	937

(a.u) = arbitrary units

It is clear that the microencapsulated sulfur powders give similar or somewhat reduced ultimate stress-strain properties compared to the uncoated sulfur in SBR, as shown in Figure 5.6a. The only improvements in tensile properties were obtained for $PPAS_8$-3. In case of EPDM and NBR, improvements in rupture energy are obtained for all compounds cured with coated sulfur samples. The best properties are measured with $PPAS_8$-4 for EPDM with an increase of 27 % in rupture energy as compared to uncoated sulfur. As shown in Figure 5.6c, NBR compounds cured with coated sulfur samples show appreciable improvements in tensile strength and elongation at break as compared to uncoated sulfur. The highest rupture energy in a NBR compound is obtained with $PPAS_8$-3 with an increase of 44 %. The improvement in the tensile properties of NBR can be related to the fact that the sulfur coated with polyacetylene

layer has a surface tension closer to NBR relative to the uncoated sulfur, which results in a better compatibility.

5.3.1.5b In SE blends

The rheograms of the SE blends are represented in Figure 5.7. For all SE compounds vulcanized with the encapsulated sulfur samples, a pronounced increase in the final state of cure (maximum torque) is observed. This demonstrates that SE blends cured with plasma acetylene encapsulated sulfur provide a better co-vulcanization behavior.
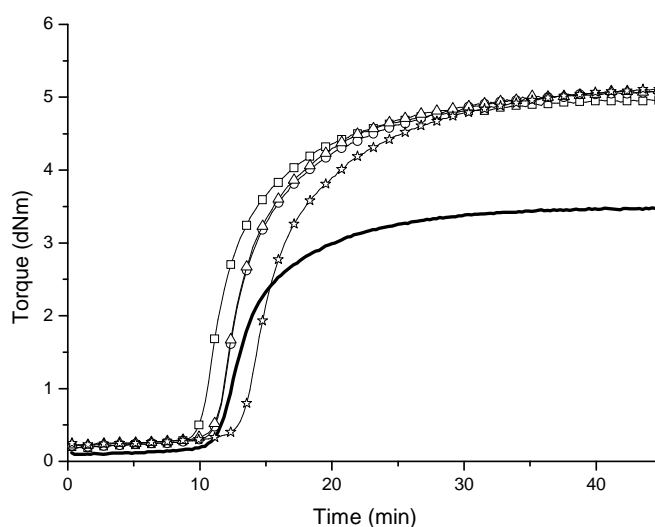
Figure 5.7 Rheograms of the SE blends cured with: (——) S_8; (—□—) $PPAS_8$-1; (—○—) $PPAS_8$-2; (—△—) $PPAS_8$-3; (—☆—) $PPAS_8$-4.

The tensile properties of the SE blends cured with uncoated and coated sulfur are shown in Figure 5.8. It is clear that the compounds with microencapsulated sulfur show significantly improved tensile strength, elongation at break and moduli. The rupture energies, calculated from the full stress-strain curves in Figure 5.9, are given in Table 5.8. The sequence of the rupture energies is: $PPAS_8$-3> $PPAS_8$-4> $PPAS_8$-2> $PPAS_8$-2>> S_8. The highest rupture energy is measured for $PPAS_8$-3 with an increase of 58% compared to S_8.

Previous work, as described in Chapter 3 of this thesis, has shown that the solubility of sulfur is somewhat higher in SBR than EPDM, and the difference becomes larger with increase in temperature. [1] This solubility difference acts as the driving force for

sulfur to migrate from EPDM to SBR before and during vulcanization. However, the deposition of the polyacetylene layer decreases the surface polarity of sulfur and meanwhile the crosslinked polyacetylene shell will also decrease the speed of migration by diffusion. [20]
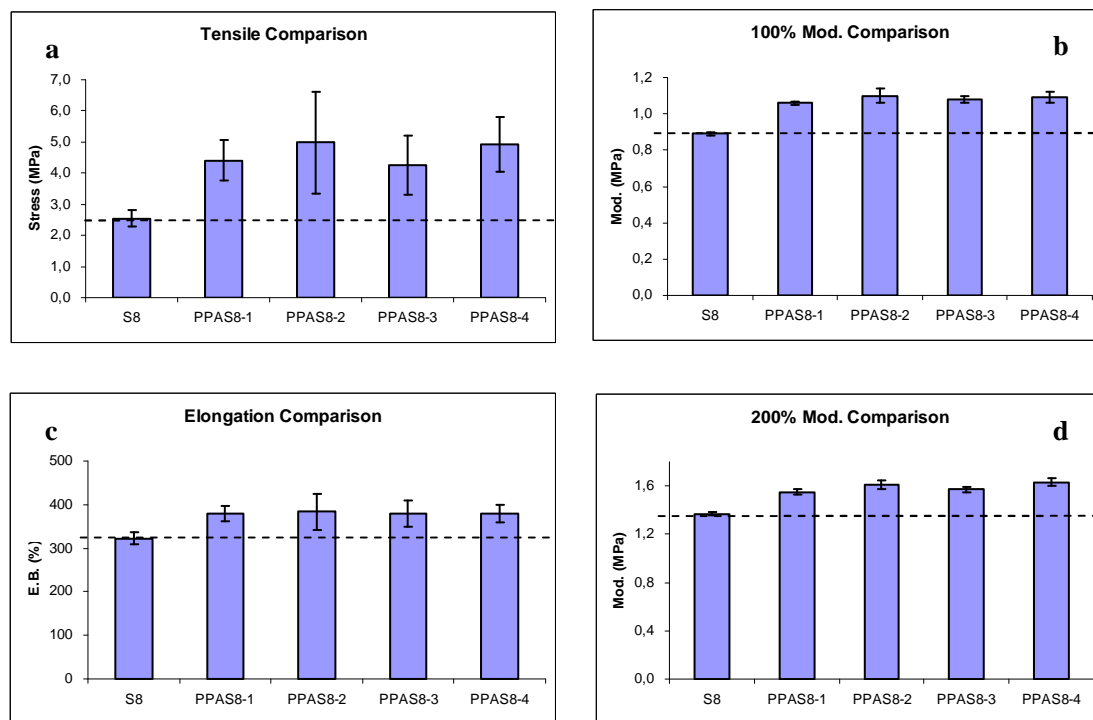
Figure 5.8 Stress-strain properties of the SE blends cured with different sulfur samples.
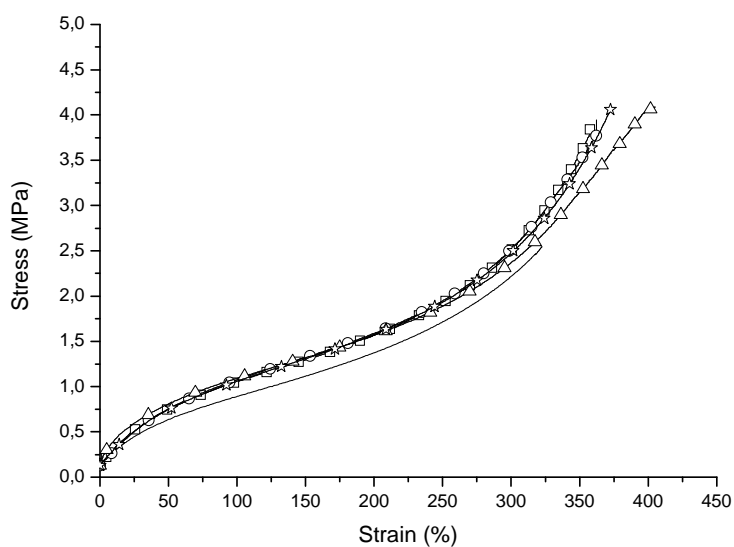
Figure 5.9 Stress-strain properties of the SE blends cured with: (——) S_8; (—□—) $PPAS_8$-1; (—○—) $PPAS_8$-2; (—△—) $PPAS_8$-3; (—☆—) $PPAS_8$-4.

Table 5.8 The rupture energies of the SE blends with different sulfur samples.

Sample code	Rupture energy (a.u)
S_8	399
$PPAS_8$-1	594
$PPAS_8$-2	598
$PPAS_8$-3	631
$PPAS_8$-4	606

(a.u) = arbitrary units

5.3.1.5c In NE blends

The rheograms of NE blends are represented in Figure 5.10. It is clear that all the NE compounds show similar characteristics, the rheograms of all the compounds coincide.
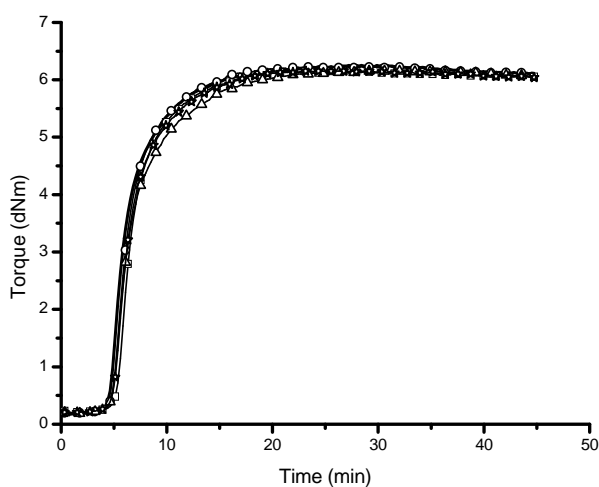
Figure 5.10 Rheograms of the NE blends cured with:(———) S_8; (—□—) $PPAS_8$-1; (—○—) $PPAS_8$-2; (—△—) $PPAS_8$-3; (—☆—) $PPAS_8$-4.

All the compounds with microencsulated sulfur show a higher tensile strength and elongation at break. However, the 300% moduli are lower compared to the compound cured with uncoated sulfur, as represented in Figure 5.11.
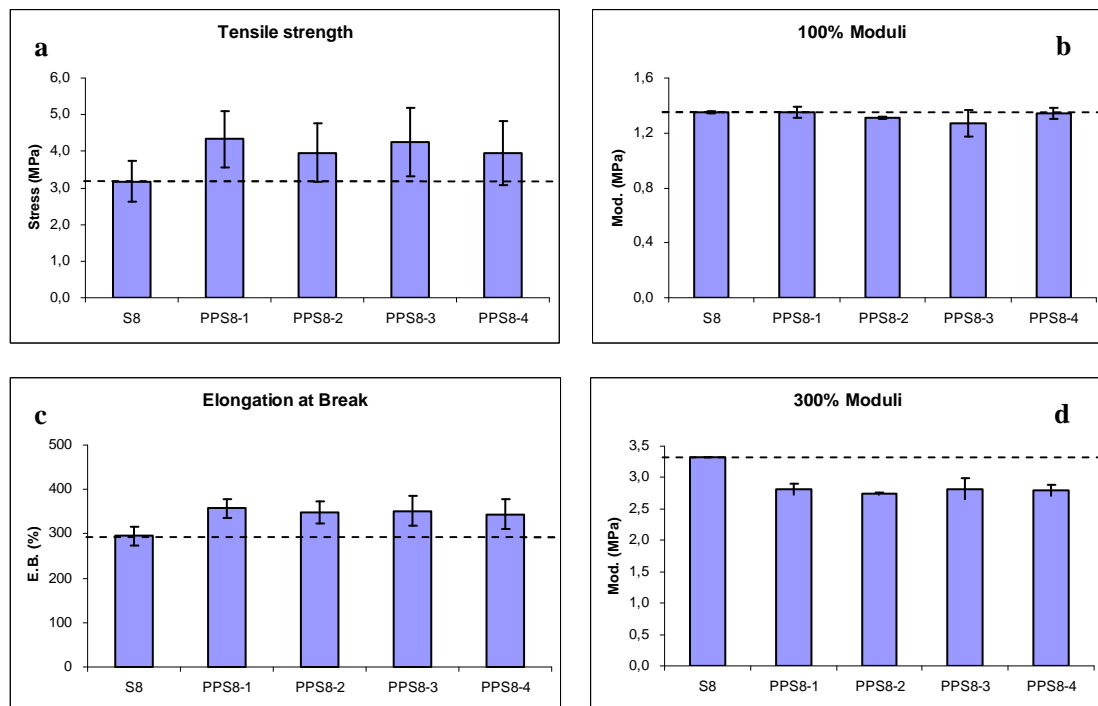
Figure 5.11 Stress-strain properties of the NE blends cured with sulfur samples.

The rupture energies, calculated by integrating the area under the full stress-strain curves in Figure 5.12, are given in Table 5.9. The sequence of the breaking energy is: $PPAS_8$-1> $PPAS_8$-2> $PPAS_8$-3> S_8> $PPAS_8$-4. The highest increase is from $PPAS_8$-1 with an increase of 27%.
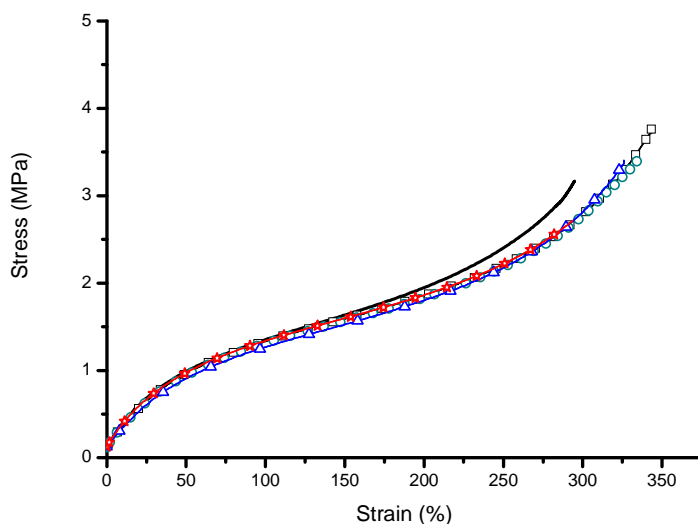
Figure 5.12 Stress-strain properties of the NE blends cured with: (———) S_8;
(—□—) $PPAS_8$-1; (—○—) $PPAS_8$-2; (—△—) $PPAS_8$-3; (—✶—) $PPAS_8$-4.

Table 5.9 The rupture energies of the NE blends with different sulfur samples.

Sample code	Rupture energy (a.u)
S_8	486
$PPAS_8$-1	616
$PPAS_8$-2	571
$PPAS_8$-3	546
$PPAS_8$-4	458

(a.u) = arbitrary units

5.3.2. The performance of plasma acetylene encapsulated CBS in rubber blends

5.3.2.1 Appearance and SEM images

The color of the CBS powders changes from pale white to brown after the acetylene plasma treatment. The color gets darker with increasing treatment time, as shown in Figure 5.13.

| 0min | 15 min | 30 min | 45 min | 60 min | 90 min | 2hrs |

Figure 5.13 Color of CBS coated with different reaction time.

The morphologies of the uncoated CBS particles and the acetylene plasma encapsulated CBS particles are shown in Figure 5.14. As CBS itself has already an amorphous morphology, the difference between the images before and after coating is not as pronounced as for sulfur. However, the encapsulated CBS as shown in Figure 5.14d, seems to have a much rougher structure compared to the untreated CBS morphology in Figure 5.14b. Although it is impossible to discern a morphology difference using a lower magnification, as represented in Figures 5.14a and b, a pronounced decrease in agglomerate size can be observed. The deposited layer from

plasma polymerization on CBS also has some cracks and holes, which act as gateways for a future release of the CBS particles.
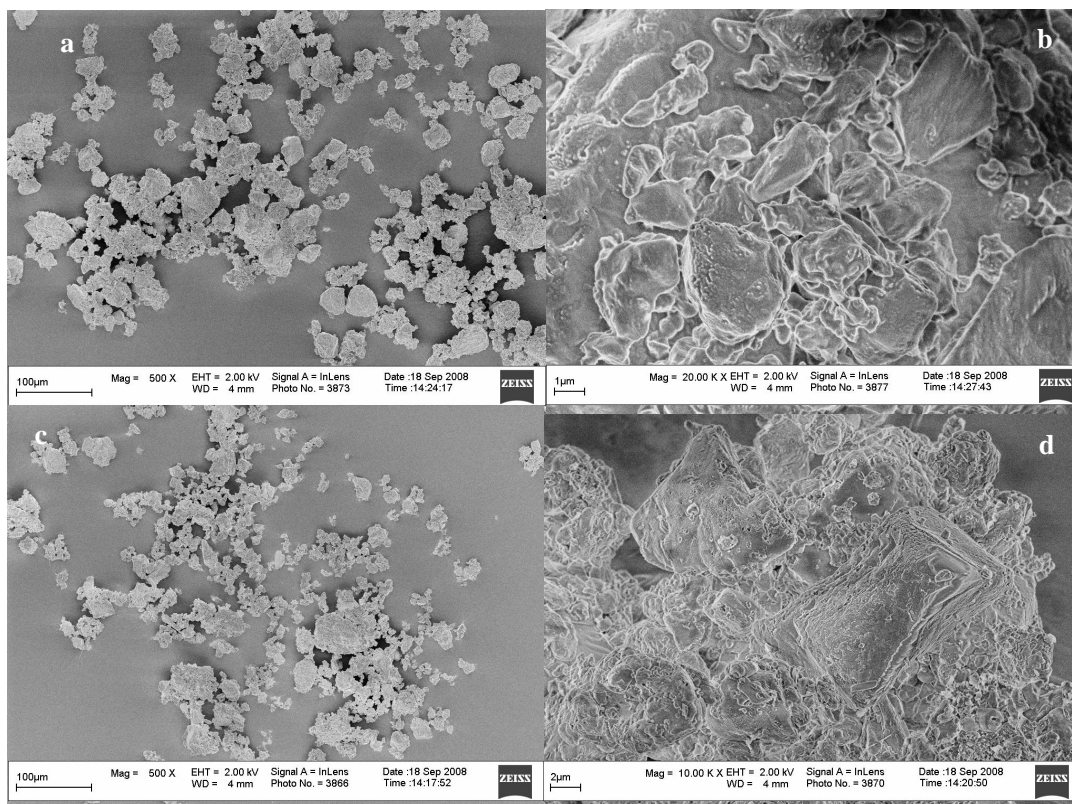
Figure 5.14 SEM images: (a)&(b) uncoated CBS; (c)&(d) plasma polyacetylene coated CBS.

5.3.2.2 Surface energy of plasma polyacetylene coated CBS

The surface energy of coated CBS is decreased compared to the uncoated CBS, which is proved by the fact that it can float on top of ethylene glycol, while the uncoated CBS sinks immediately. The surface energies of uncoated and coated CBS are also indicated in Figure 5.3. Compared to sulfur, the initial surface energy of CBS is very high which results also in a higher surface energy for encapsulated CBS compared to sulfur.

5.3.2.3 Thermogravimetric analysis

The thermogravimetric curves of uncoated and plasma polyacetylene coated CBS are shown in Figure 5.15, using PPACBS-5 as example. The weight loss curve shows some delay, which proves the presence of a layer of plasma polyacetylene. In spite of many attempts, unfortunately, it was not feasible to find a reproducible method to

quantify the amount of coating on CBS.
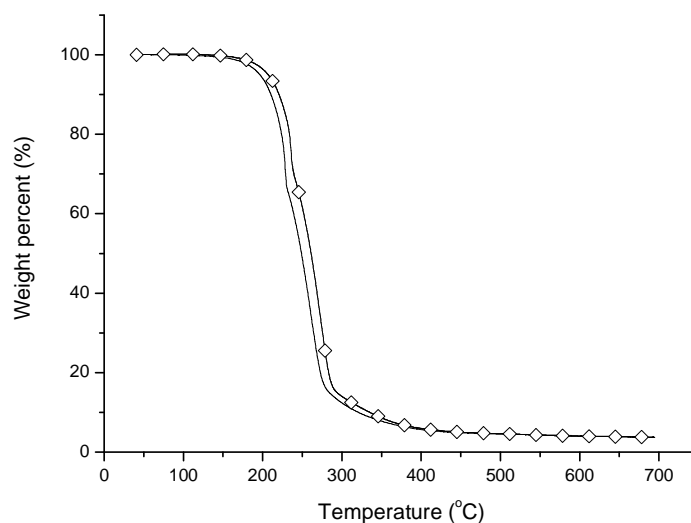
Figure 5.15 TGA thermograms of(──) CBS; (─◇─) PPACBS-5.

5.3.2.4 Performance of plasma polyacetylene encapsulated CBS in rubber blends

The performance of the encapsulated CBS samples was checked in the SE blends to select the best experimental conditions for plasma treatment for optimal performance. In NE blends, only PPACBS-1, PPACBS-5 and PPACBS-6 were tested.

5.3.2.4a In SE blends

The rheograms of the SE blends are represented in Figure 5.16. For all the SE compounds vulcanized with the polyacetylene encapsulated CBS samples, coated using a RF power of 150W and 180W, a pronounced increase in the final state of cure is observed. These samples also show a decreased scorch time. The CBS coated using 250 W also gives an increase in state of cure, however the increase is rather small. For the samples coated using a RF power of 180 W, but varied reaction time periods, the lowest torque plateau is reached for PPACBS-2, the sample that was coated for only 15 mins. The other CBS samples show similar curing properties and their rheograms overlap. Apparently, in case of applying the monomer flow rate of 20 sccm, the overall reaction speed (deposition rate) increases with the RF power, reaches a maximum and decreases again with increasing power, a phenomenon described by Yasuda. [21]
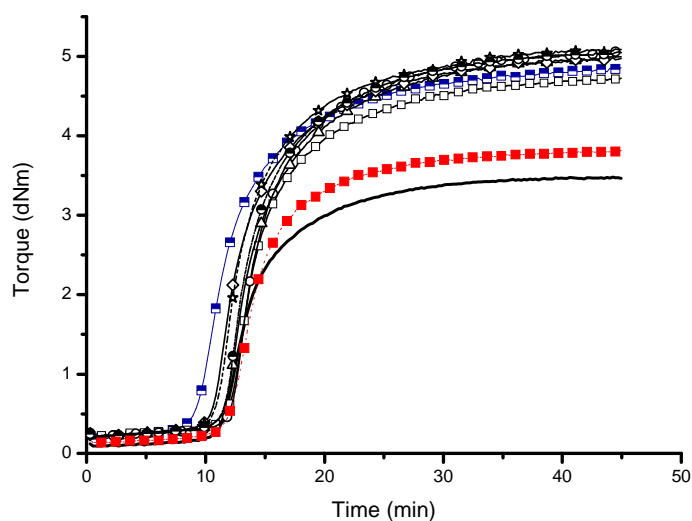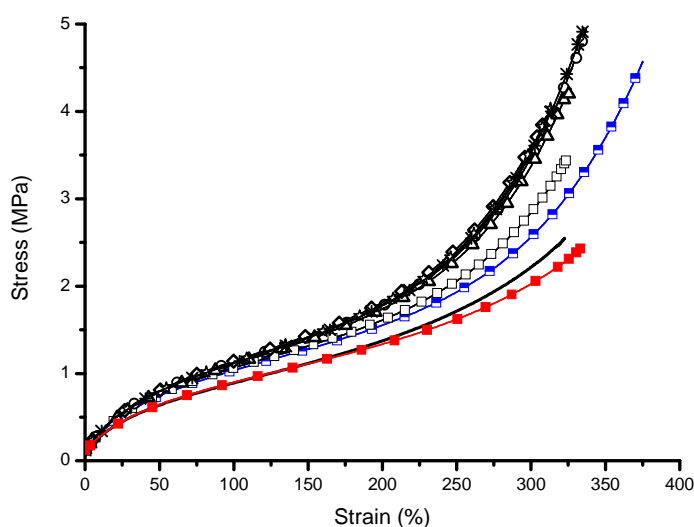
Figure 5.16 Rheograms of the SE blends cured with: (——) CBS; (—■—) PPACBS-1; (—□—) PPACBS-2; (—○—) PPACBS-3; (—△—) PPACBS-4; (—◇—) PPACBS-5; (—☆—) PPACBS-6; (—✳—) PPACBS-7; (—■—) PPACBS-8.

The stress-strain properties of all the SE compounds with uncoated and polyacetylene coated CBS are shown in Figure 5.17. All the compounds with microencapsulated CBS show higher tensile strengths, elongations at break and moduli values, compared to the uncoated CBS. PPACBS-1, coated with a RF power of 150 W and reaction time of 1.5 hr provides the highest elongation at break and a fairly good tensile strength; however it shows a much lower 300% modulus compared to the samples coated with a RF power of 180 W. A reaction time of 15 minutes (sample PPACBS-2) is obviously too short, as not much property improvements are obtained. Most likely the polyacetylene shell obtained under such a reaction condition is not thick enough or not even closed.
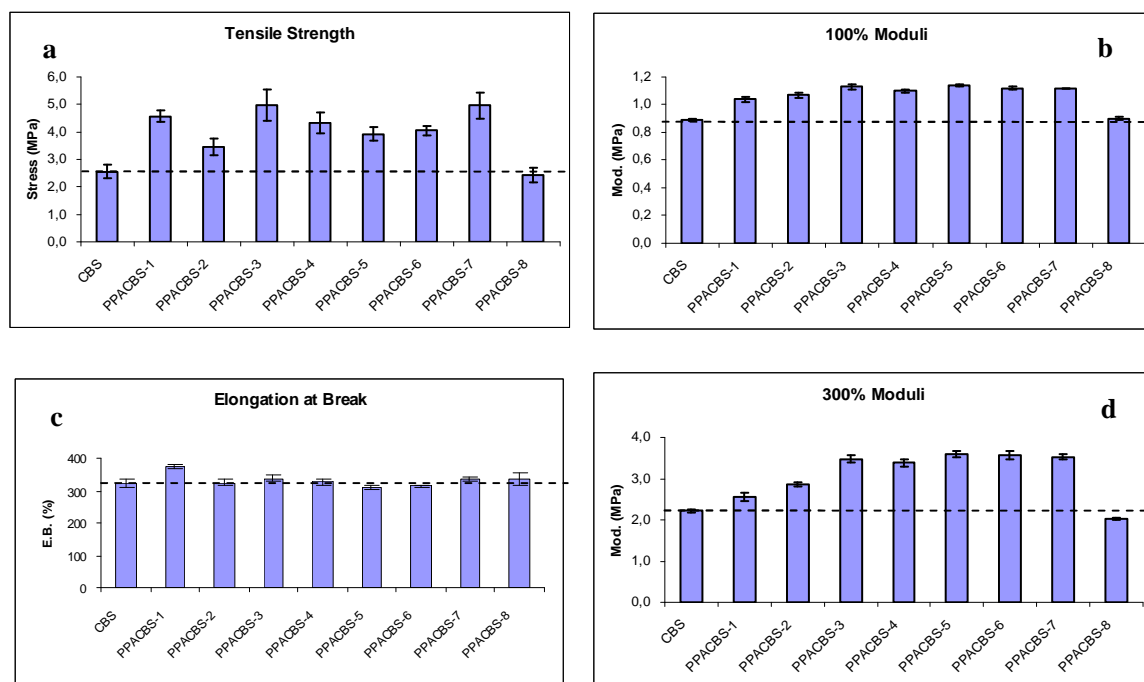
Figure 5.17 Stress-strain properties of the SE blends cured with different CBS samples.

The rupture energies of all the SE compounds calculated from the full stress-strain curves in Figure 5.18 are summarized in Table 5.10. Relative to the rupture energy of the control (uncoated CBS: 399 MPa), the highest increase of 63 % is obtained for PPACBS-1.

Figure 5.18 Stress-strain properties of the SE blends cured with: (——) CBS;
(—■—) PPACBS-1; (—□—) PPACBS-2; (—○—) PPACBS-3; (—△—) PPACBS-4;
(—◇—) PPACBS-5; (—☆—) PPACBS-6; (—✳—) PPACBS-7; (—■—) PPACBS-8.

Table 5.10 The rupture energies of the SE blends with different CBS samples.

Sample code	Rupture energy (a.u)	Sample code	Rupture energy (a.u)
CBS	399	-	-
PPACBS-1	652	PPACBS-5	506
PPACBS-2	490	PPACBS-6	519
PPACBS-3	616	PPACBS-7	611
PPACBS-4	554	PPACBS-8	410

(a.u) = arbitrary units

5.3.2.4b In NE blends

The rheograms of the NE blends are represented in Figure 5.19. For all the NE compounds, the curing curves are clustered together. The NE blend cured with untreated CBS shows a slightly higher value of the maximum torque compared to those with encapsulated CBS samples.
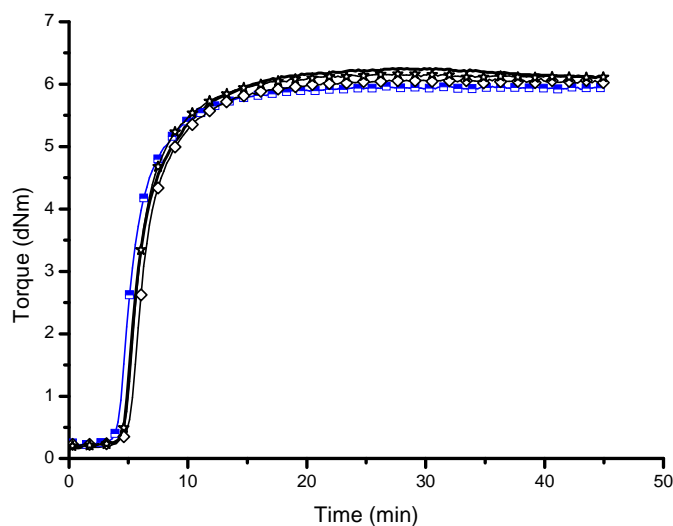
Figure 5.19 Rheograms of the NE blends cured with: (──) CBS;
(─■─) PPACBS-1; (─◇─) PPACBS-5; (─☆─) PPACBS-6.

The stress-strain properties of all the NE compounds with uncoated and plasma polyacetylene coated CBS are given in Figure 5.20. PPACBS-1, which gives quite a good performance in SE blends, shows inferior properties compared to uncoated CBS.

Although PPACBS-5 and PPACBS-6 give some better properties, the improvements are clearly not as pronounced as those achieved in SE blends.
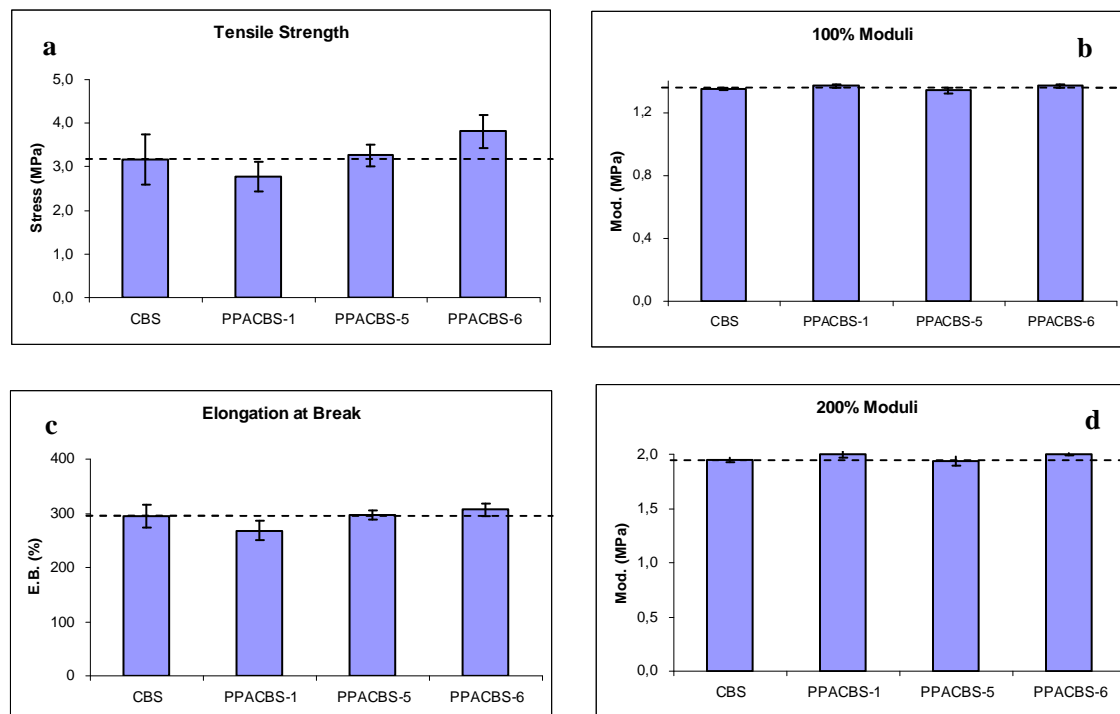
Figure 5.20 Stress-strain properties of the NE blends cured with different CBS samples.

The rupture energies calculated from the area under the full stress-strain curves in Figure 5.21 are given in Table 5.11. The difference between the uncoated and plasma polyacetylene coated CBS is rather small. The highest rupture energy is obtained for PPACBS-6, which is coated with 180 W and 90 mins., with an increase of only 8% compared to the uncoated CBS.

Table 5.11 The rupture energies of the NE blends with different CBS samples.

Sample code	Rupture energy (a.u)
CBS	486
PPACBS-1	418
PPACBS-5	492
PPACBS-6	526

(a.u) = arbitrary units
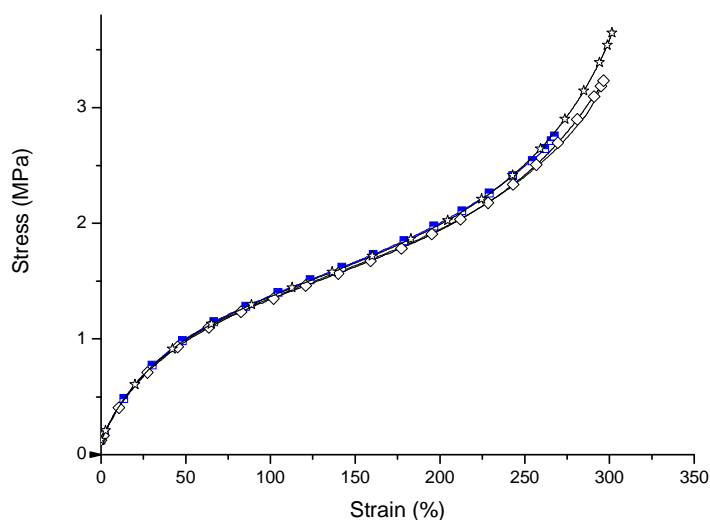
Figure 5.21 Stress-strain properties of the NE blends cured with:(——) CBS;
(—■—) PPACBS-1; (—◇—) PPACBS-5; (—☆—) PPACBS-6.

5.4 Conclusions

By applying plasma polymerization with acetylene, a layer is deposited on sulfur/CBS powders, resulting in a color change from their original colors to a brownish color. The longer the deposition time, the darker the color. The surface energies of sulfur/ CBS are decreased and brought closer to the range of the rubber polymers involved in this study. A better compatibility between the rubbers and sulfur and CBS is achieved by decreasing the surface energy difference. Improvements are obtained in straight NBR and EPDM compounds, which can be attributed to the better compatibility due to a closer surface energy between rubbers and sulfur and CBS. In case of SBR, the coated sulfur and CBS provide similar performance as the uncoated ones.

A better co-vulcanization is achieved in the SE blends with the plasma polyacetylene microencapsulated sulfur/CBS. As to CBS, the performance increases when the discharge power is increased from 150 W to 180 W, and then decreases again when the discharge power is further increased to 250 W. This is in accordance with the observations of Yasuda. [20]

There are practically no appreciable improvements obtained in the NE blends. As stated in Chapter 4, it is more difficult to improve the cure mismatch in the NE blends.

Therefore, monomers other than acetylene need to be applied in the plasma treatment in order to achieve better mechanical properties in the NE blend.

5.5 References

[1]   R. Guo, A.G. Talma, R.N. Datta, W.K. Dierkes, J.W.M. Noordermeer, *Eur. Pol. J.*, **2008,** 44, 3890.

[2]   J.E. Mark, B. Erman, and F.R. Eirich, *"Science and Technology of Rubber: Elastomer blends"*, 3 [rd] edition, Elsevier Academic Press, New York, **2005**, 565.

[3]   A.K. Ghosh, S.C. Debnath, N. Naskar, D.K. Basu, *J. Appl. Polym. Sci.*, **2001**, 81, 800.

[4]   B.G. Scares, A.S. Sirqueira, M.G. Oliveira, M.S.M. Almeida, Macromol. Symp., 2002, 189, 1, 45.

[5]   H.K Yasuda, *Plasma Process. Polym.*, **2005,** 2, 293.

[6]   N. Inagaki, S. Tasaka, H. Abe, *J. Appl. Polym. Sci.*, **1992,** 46, 595.

[7]   S.J. Park, J.S. Kim, *J. Colloid Interf. Sci.,* **2000**, 232, 311.

[8]   S.J. Park, J.S. Kim, *Carbon*, **2001**, 39, 2011.

[9]   G. Akovali, I. Ulkem, *Polymer*, **1999**, 40, 7417.

[10]   N. Tricás, E. Vidal-Escales, S. Borrós, M.Gerspacher, *ISPC Proceedings*, *Sicilia*, **2003**, 366.

[11]   N. Tricás, S. Borrós, *Kautsch. Gummi Kunstst.,* **2005**, 58, 511.

[12]   T. Mathew, R.N. Datta, W.K. Dierkes, J.W.M. Noordermeer, W.J. van Ooij, *Plasma Chem. Plasma Process.*, **2008**, 28, 273.

[13]   T. Mathew, Ph.D. Thesis, University of Twente, Enschede, The Netherlands, **2008**.

[14]   G. Mathew, *Polym. Adv. Technol.*, **2004**, 15, 400.

[15]   C. Nah, M-Y, Huh, J.M. Rhee, T-H. Yoon, *Polymer Int.*, **2002**, 51, 510.

[16]   M. Tiwari, T. Mathew, J.W.M. Noordermeer, W.K. Dierkes, R.N. Datta, A. Talma, W.J. van Ooij, *Kautsch. Gummi Kunstst.*, **2008**, 61, 502.

[17]   W.J. van Ooij, *Rubber world*, August 1, **2003**.

[18]   E. Vidal, S. Borros, N. Agullo, W.J. van Ooij, ACS Rubber Division Meeting,

2000, Cincinnati, Ohio, USA.

[19] D.W. van Krevelen, P.J. Hoftijzer, "*Properties of polymers*", 3rd edition, Elsevier, Amsterdam, **1990**, 231.

[20] R.B. Bird, W.E. Steward, E.N. Lightfoot, *"Transport Phenomena: Diffusivity and the Mechanisms of Mass Transport"* 2nd edition, John Wiley & Sons, Inc., New York, **2007**, 518.

[21] H. Yasuda, "*Plasma polymerization*", 1st edition, Academic press, Inc. Orlando, **1985**, 179.

Perfluorohexane Plasma Encapsulated Sulfur and CBS in Pure Rubbers and Rubber-Rubber Blends

Perfluorohexane (PFH), a very un-polar monomer, is used for the plasma encapsulation of sulfur and CBS in the current chapter. Unique features are achieved compared to the modification using acetylene as monomer. The rubber mechanical properties can be significantly improved for the SBR/EPDM blends using plasma PFH coated curatives; not much for the NBR/EPDM blend. Solubility measurements are carried out with plasma perfluorohexane microencapsulated sulfur and CBS in the different rubbers studied. The solubility changes as predicted from the theory can nicely be used to interpret the improved performance of the rubber blends by using these PFH coated additives for the SBR/EPDM blends. For the NBR/EPDM blends the very large difference in curing reactivities turns out to be an overruling factor, which cannot be compensated by coating of the curatives with perfluorohexane.

6.1 Introduction

Perfluorocarbon plasmas can readily produce hydrophobic polymers, either by fluorination of the surface layer or by deposition of plasma polymers, depending on the plasma gas composition or on the F/C ratio of the fluorocarbon monomer used for the plasma polymerization. [1-5] These coatings offer very interesting characteristics such as low surface energy, high thermal stability, biocompatibility and chemical resistance. [6]

Perfluorohexane is chosen as the monomer for the plasma encapsulation of sulfur and CBS. According to Hochart et al., a plasma of perfluorohexane leads to the deposition of a thin fluorocarbon polymerized film. [7] In the context of this thesis, it was of interest to investigate the specific features of deposited polymer layers based on this very hydrophobic perfluorohexane, and to compare these to those of polyacetylene. The C-F bond in the fluorocarbon species has a higher bonding energy (485.6 kJ/mol) than that of the C-H bond (413.6 kJ/mol). [8, 9] As a consequence a RF power of 180 W, instead of 150 W for acetylene, is needed for generating the plasma state of perfluorohexane. The appearance of fluorine gas also makes ablation a competitive reaction with plasma polymerization.

The performance of the microencapsulated curatives with perfluorohexance is checked in the pure rubbers and in 50/50 w/w SBR/EPDM (SE) and NBR/EPDM (NE) blends. The method of measuring the solubility, as described in Chapter 3, is applied to determine the solubility of the coated curatives in the different rubbers at both room temperature (RT) and 60 $^{\circ}$C. The objective is to decrease the solubility difference of the curatives in the two phases of the blends, to obtain better co-vulcanization. Consequently, better mechanical properties are to be expected.

6.2 Experimental Part

6.2.1 Materials

The following types of rubber were employed: S-SBR (Buna$^{®}$ VSL 5025-0HM from

LANXESS Corp., Germany), NBR (Perbunan® 3446F from LANXESS Corp.), and EPDM (Keltan® 4703 from DSM Elastomers, the Netherlands). Zinc-oxide was purchased from Sigma Aldrich; stearic acid was used as commercial grade from Sigma Aldrich, and accelerator (Santocure® CBS) was provided by Flexsys, Belgium. Elemental sulfur was purchased from Sigma Aldrich, with a particle size smaller than 100 mesh (150 μm). Perfluorohexane (PFH) (99.6% purity) was supplied by Sigma Aldrich.

6.2.2 Methods

a. Grinding by ball mill

See Chapter 5.

b. Plasma polymerization

As in Chapter 5. As the monomer perfluorohexane was in a liquid state, a new connection was made for monomers inlet. The operating conditions are given in Table 6.1. The amounts of sulfur and CBS were kept at 20 grams for each batch.

Table 6.1 Operational conditions for the plasma polymerization system with perfluorohexane.

Operational parameters	Conditions
Power Input	180 W
Vacuum	~ 5 Pa
Monomer pressure	27 Pa
Reaction Time	1 hr, 90 min, 2 hrs, 3 hrs

c. Scanning Electron Microscopy (SEM)

As in Chapter 5.

d. Wetting behaviors with liquids of known surface tension

As in Chapter 5.

e. Thermogravimetric analysis (TGA)

As in Chapter 5.

f. Scanning X-ray Photoelectron Spectroscopy (XPS)

XPS is also known as ESCA, an abbreviation for Electron Spectroscopy for Chemical Analysis. XPS determines the chemical bonding state at the surface of virtually all materials in a solid state. Information is available directly in a region to a depth of around 10 nm. Analysis of the content of material surfaces was carried in a Quantera SXM from Physical Electronics with a scanning Al-Kα source. The bonding energy region was from 0 to 1450 eV. The powders were investigated by XPS in order to prove the presence of fluor after plasma polymerization.

g. Rubber mixing and testing

As described in Chapter 5.

h. Solubility measurements

The solubilities of the microencapsulated curatives were measured following the methods described in Chapter 3.

i. Crosslink density measurements

The crosslink densities of the vulcanizates were measured as the level of gel content according to ASTM D 2765. The samples were made by cutting a 2mm thick film into small pieces. They were first extracted with acetone for 24 hours, using a Soxhlet to remove the un-reacted small molecular reagents. Afterwards, the samples were dried in a vacuum oven at 60 $^{\circ}$C for 2 days, and weighed. The dried films were then placed into a Teflon cage and immersed in toluene for 48 hours to extract the uncrosslinked rubber. The film samples were dried again in a vacuum oven at 100 $^{\circ}$C, and weighed. The gel content was calculated using equation 6.1, using the SE blend as an example.

$$Gel(\%) = 100 - \left[\frac{\left(W_{ac,residue} - W_{xy,residue} \right)}{W_{SE}} \right] \qquad \text{(Equation 6.1)}$$

In this equation, $W_{ac,residue}$ is the weight of the specimen after acetone extraction, $W_{xy,residue}$, weight after toluene extraction, W_{SE}, the weight of the rubber fraction

according to the original formulation used in the composition employed.

6.3 Results and Discussion

6.3.1. Plasma perfluorohexane modified sulfur and its performance in straight rubbers and elastomer blends

6.3.1.1 Surface energy by wetting behavior

As no appreciable change in the appearance color of sulfur was observed after being treated with perfluorohexane under plasma conditions (PFHS$_8$), a quick check on surface energy change was done by investigating the wetting behaviors of the treated samples. As shown in Figure 6.1, the modified sulfur floats on ethylene glycol while the uncoated sulfur does not. Compared with plasma acetylene treated sulfur (PPAS$_8$), the PFHS$_8$ floats on top of ethylene glycol for a longer time. This indicates a lower surface energy of PFHS$_8$ compared to PPAS$_8$.
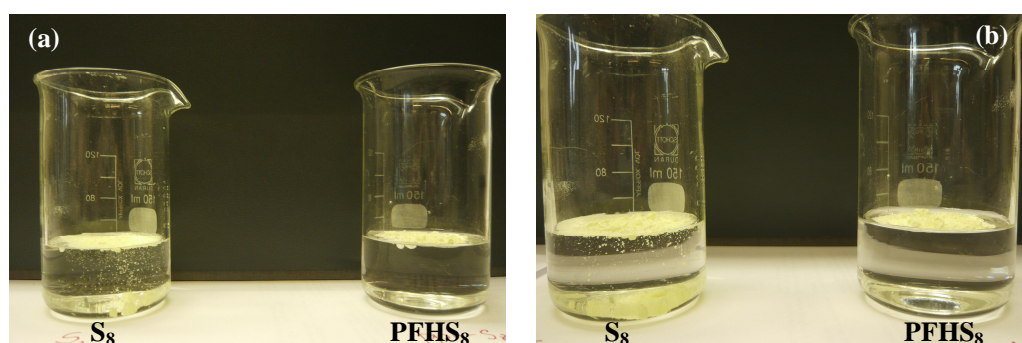
Figure 6.1 Wetting behavior of sulfur and plasma PFH treated sulfur in ethylene glycol: (a) 0 minute after addition; (b) 30 minutes after addition.

After the PFH plasma treatment, the surface energy of sulfur is brought down from the range of 48 - 58 mJ/m^2 to a value lower than 48 mJ/m^2, as can be seen in Figure 6.2. This measurement gives conclusive evidence that a perfluorohexane plasma film exists on the particles surfaces.
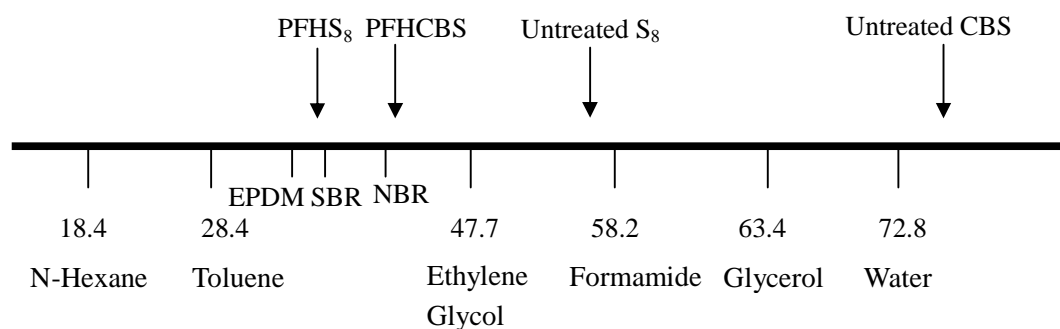
Figure 6.2 Surface energies [mJ/m^2] of uncoated and plasma PFH encapsulated sulfur and CBS.

6.3.1.2 Scanning Electron Microscopy (SEM)

To obtain more information on the deposited layer on the sulfur powders, scanning electron microscopy was used. The images are shown in Figure 6.3. A change in surface morphology can be observed, due to the deposited coating by plasma polymerization. The surface of untreated sulfur is rather smooth, as shown in Figure 6.3a, while the coated sulfur shows an amorphous morphology, as shown in Figures 6.3b and c. It is clear that the layer of coating formed on the sulfur is not closed using 60 minutes for modification, see Figure 6.3 b; while the layer is more homogeneous and perfect, after a longer treatment time, see Figure 6.3c. Figure 6.3d presents a cross section of PFHS$_8$. It shows that a layer of amorphous material is deposited on the substrate of sulfur. As elemental fluor is formed during the plasma polymerization process, ablation is competing with polymerization. This could account for the formation of a quite loose polymer shell as shown in Figure 6.3d.
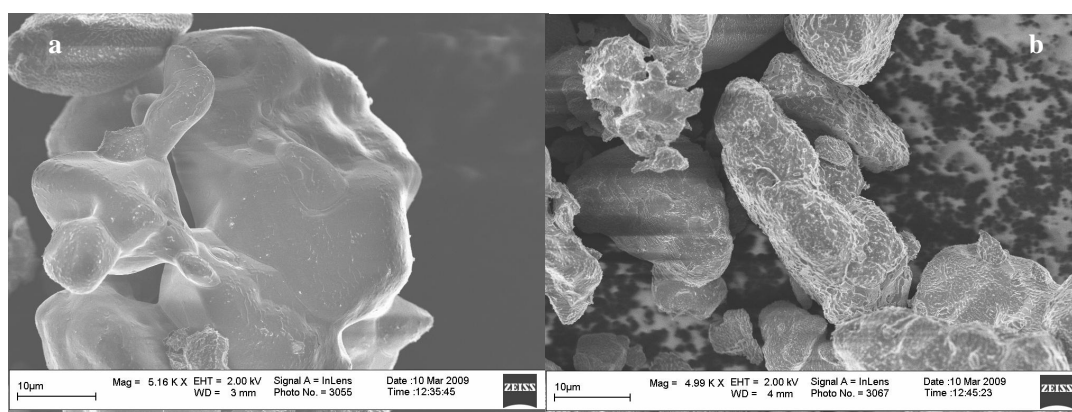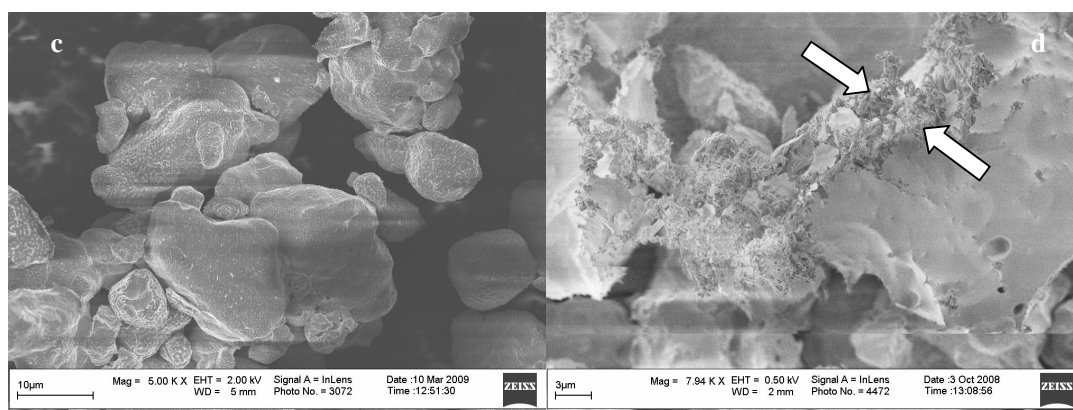
Figure 6.3 SEM images: (a) uncoated sulfur; (b) PFHS$_8$-1hr; (c) PFHS$_8$-90mins; (d) cross-section of the plasma PFH coated sulfur.

6.3.1.3 Thermogravimetric analysis (TGA)

The TGA thermograms of uncoated sulfur and sulfur coated by plasma polyperfluorohexane (PFHS$_8$) are shown in Figure 6.4. The samples were heated from 50 ^{o}C to 700 ^{o}C with a heating rate of 10 ^{o}C/min in N$_2$-atmosphere. The onset of weight loss of coated sulfur is shifted to a lower temperature after PFH coating. This is quite different from the plasma acetylene coated sulfur. Apparently the fusibility of the plasma polymerized perfluorohexane is different from the plasma polymerized acetylene, where delays in the onset of weight loss were observed.
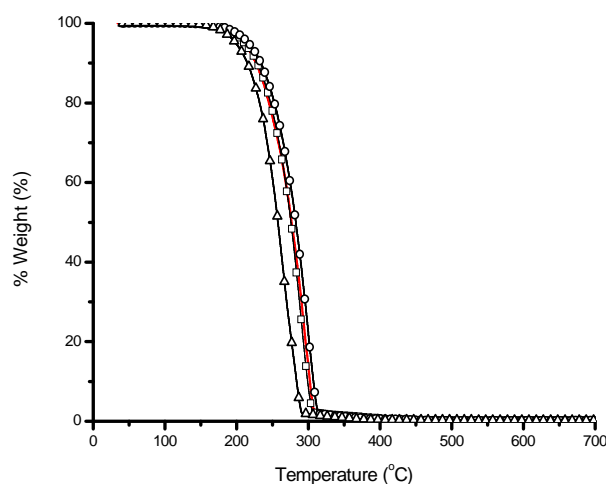
Figure 6.4 TGA thermograms in N$_2$ of different sulfur samples.
(——) S$_8$; (—□—) PFHS$_8$-1hr; (—○—) PFHS$_8$-90min.; (—△—) PFHS$_8$-3hrs.

To determine the amount of deposited coating, the samples were first heated to 180 ^{o}C and held at 180 ^{o}C for 300 mins. to let the sulfur sublimate completely. Then the samples were heated from 180 ^{o}C to 700 ^{o}C with a heating rate of 10 ^{o}C/min. Since the coating is stable at 180 ^{o}C, while sulfur changes its state from solid to gas and leaves the measuring plate, the remaining part of the sample measured above 180 ^{o}C is thus plasma polyperfluorohexane. The weight percentages of coating are presented in the Table 6.2.

Table 6.2 Estimated coating amount (wt %) for sulfur samples.

Sample code	Amount of coating (%)
Uncoated S_8	-
PFHS$_8$-1hr	1.23
PFHS$_8$-90min	4.97
PFHS$_8$-3hrs	5.43

6.3.1.4 Performance of the plasma polyperfluorohexane treated sulfur powders in rubbers

6.3.1.4a In straight SBR, EPDM and NBR rubbers

Figures 6.5a, b and c show the curing behaviors of the SBR, EPDM and NBR rubbers cured with sulfur and plasma PFH coated sulfur, respectively. It can be seen from Figure 6.5a, that all the SBR compounds show similar states of cure. However, the vulcanizates cured with PFHS$_8$ show a pronounced scorch reduction in curing. The same behavior is observed for EPDM cured with plasma PFH coated sulfur, as shown in Figure 6.5b. In Figure 6.5c, the maximum torque is much lower for the NBR vulcanized with PFHS$_8$-3hrs. As the scorch time of NBR is already very short, no further decrease in scorch time is observed.

Apparently, the PFH-coating acts as a kind of accelerator in the vulcanization process of SBR and EPDM. This can be explained by fact that a large amount of radicals is contained in the perfluorocarbon plasma polymers. The maximum torque is dependent on

the amount of reactive sulfur left for the vulcanization, while the scorch time is more related to the properties and structures of the plasma polymer formed on the sulfur surface. Further investigations are needed to get a clearer picture of the mechanism.

As demonstrated in Chapter 4, there is a large cure rate mismatch present in the NBR-phase and the EPDM-phase in the NE blend. It can be observed that using the plasma PFH-treated sulfur samples the difference in the cure rate of NBR and EPDM remains large, see Figures 6.5b and c. NBR finishes the curing before the onset of EPDM vulcanization.
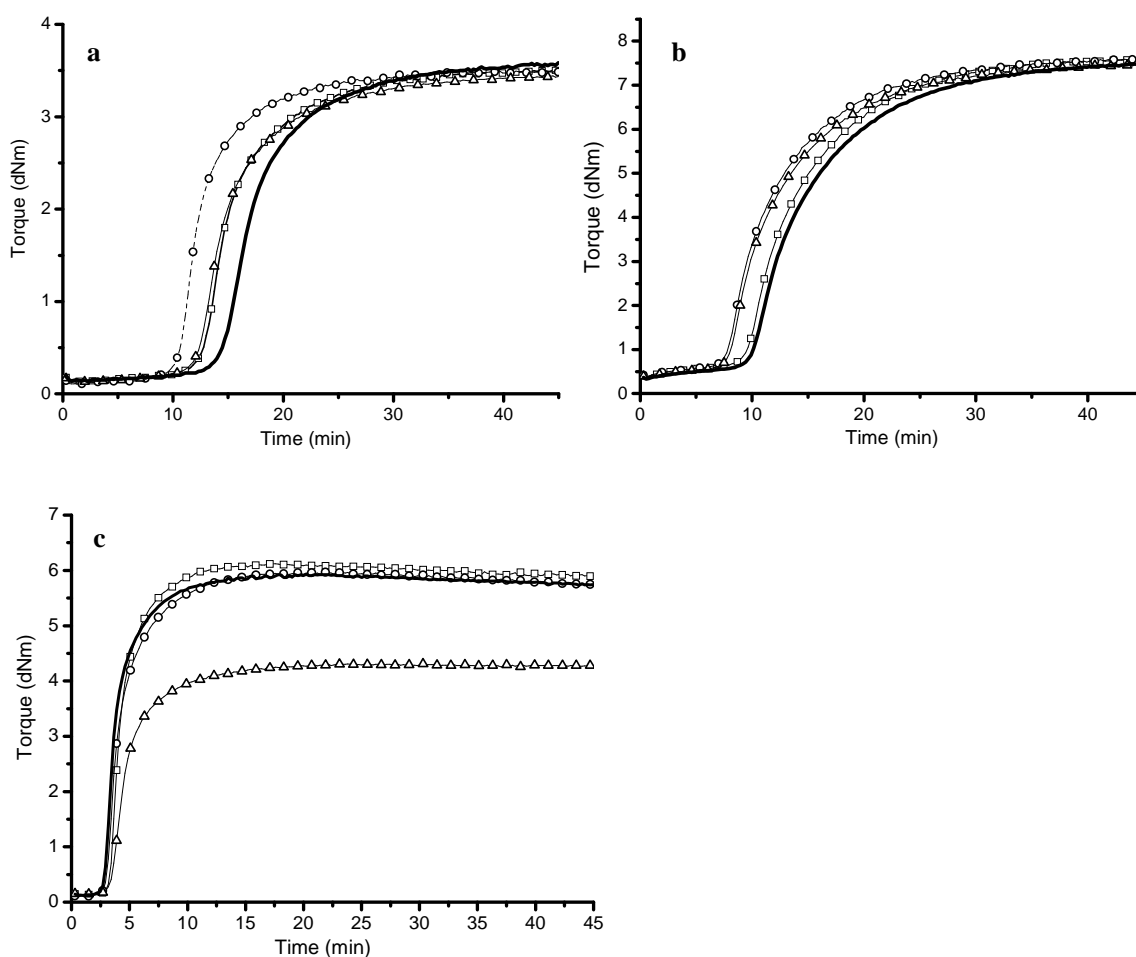
Figure 6.5 Rheograms of (a) SBR; (b) EPDM; (c) NBR cured with:
(——) S_8; (—□—) PFHS$_8$-1hr; (—○—) PFHS$_8$-90min; (—△—) PFHS$_8$-3hrs.

The stress-strain properties of the SBR vulcanizates are presented in Figures 6.6. SBR cured with $PFHS_8$-1hr has the lowest tensile strength and elongation at break. $PFHS_8$-90 min provides more or less equivalent performance as the untreated sulfur. The best mechanical properties are shown by SBR cured with $PFHS_8$-3hrs.

The properties of vulcanized EPDM, with various types of modified sulfur samples are shown in Figures 6.7. The differences amongst the various samples are not really significant in view of experimental error.
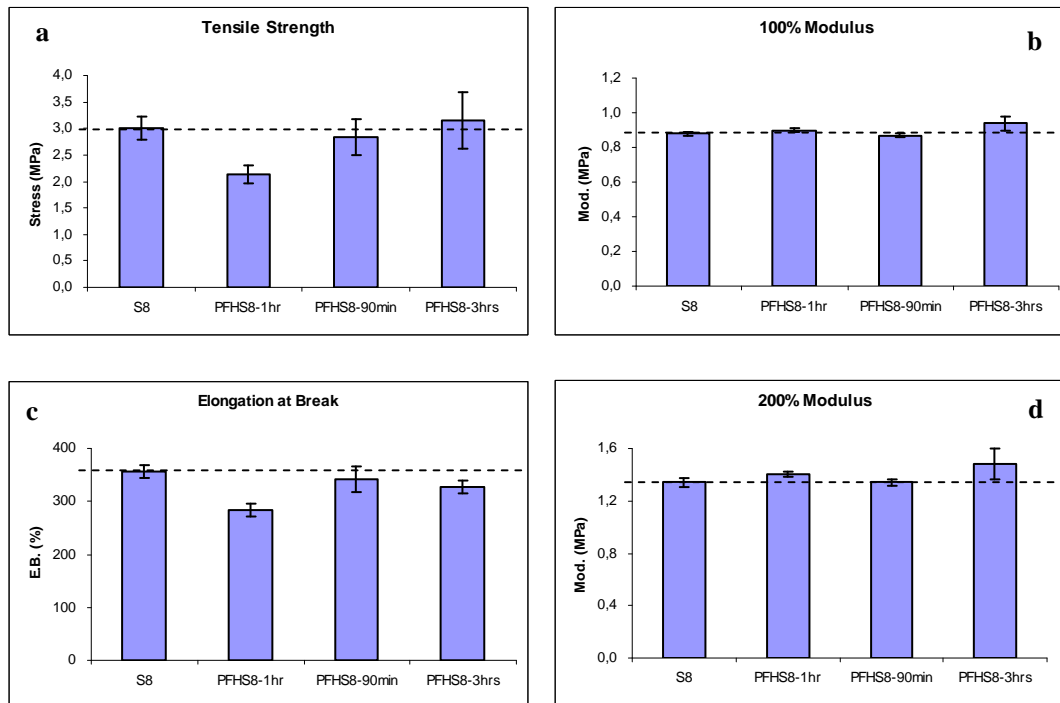
Figure 6.6 Stress-strain properties of SBR cured with different sulfur samples.
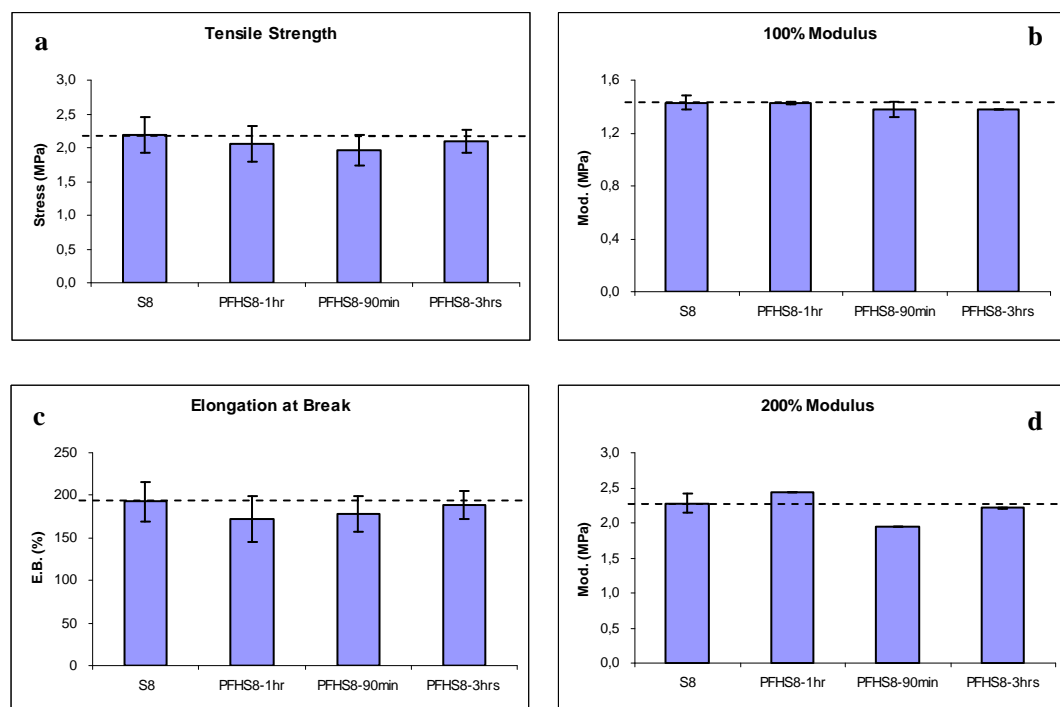
Figure 6.7 Stress-strain properties of EPDM cured with different sulfur samples.

The stress-strain properties of the NBR vulcanizates, with uncoated sulfur and plasma PFH coated sulfur using different plasma reaction times, are shown in Figures 6.8a to d, respectively. From Figure 6.8a, it can be seen that the tensile strengths of the NBR vulcanizates cured with different sulfur samples are similar. However, the NBR vulcanizate cured with $PFHS_8$-3hrs shows a very high elongation at break, Figure 6.8c, compared to the lowest 100% and 200% moduli of all, Figure 6.8b and d. This can be correlated with the curing characteristics of this compound, where the crosslink density was much lower for the NBR vulcanized with $PFHS_8$-3hrs, as given in Figure 6.5c.
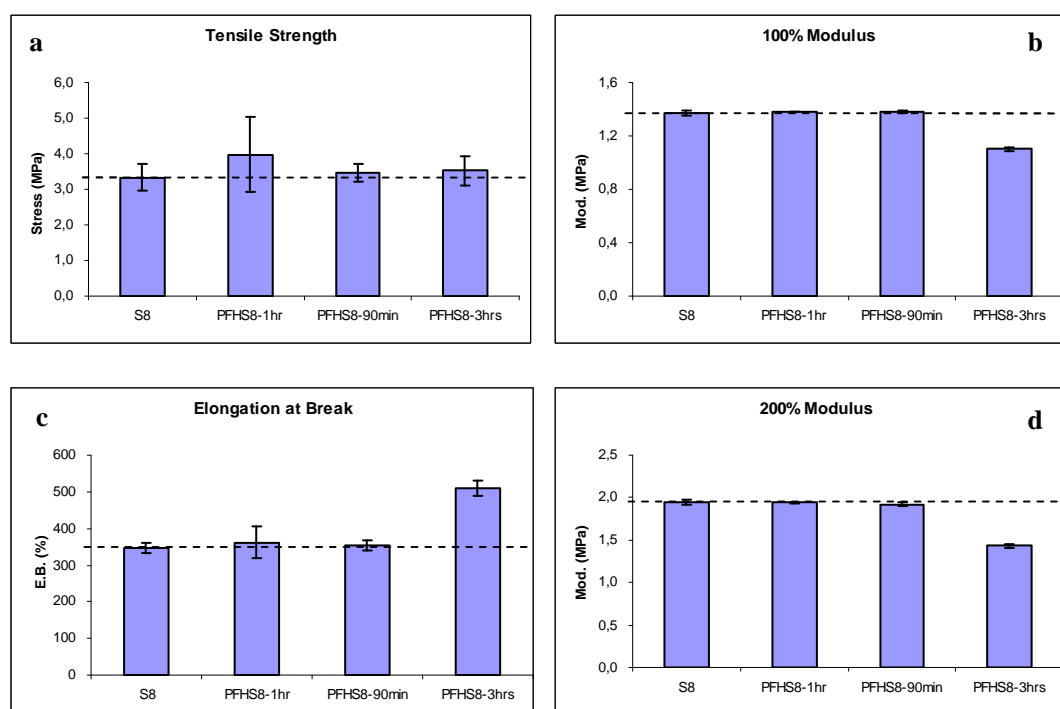
Figure 6.8 Stress-strain properties of NBR cured with different sulfur samples.

It is interesting that PFHS$_8$-3hrs, which demonstrates the best performance in SBR, shows the worst properties in NBR. The shift of PHS$_8$ in surface energy closer to SBR may result in a better match in surface energy between PFHS$_8$-3hrs and SBR. Considering the fact that the surface energy of NBR is quite far from that of SBR and EPDM, PFHS$_8$-3hrs may have become less compatible with NBR.

Figure 6.9 shows a comparison of the hardness for SBR, EPDM and NBR. As the samples are not reinforced with fillers, they are all rather soft. There are no significant differences among the same type of rubbers by using the plasma PFH modified sulfur. The only exception is for the NBR cured with PFHS$_8$-3hrs, which gives a much lower value in hardness. This low hardness value can again be correlated with its low state of cure.
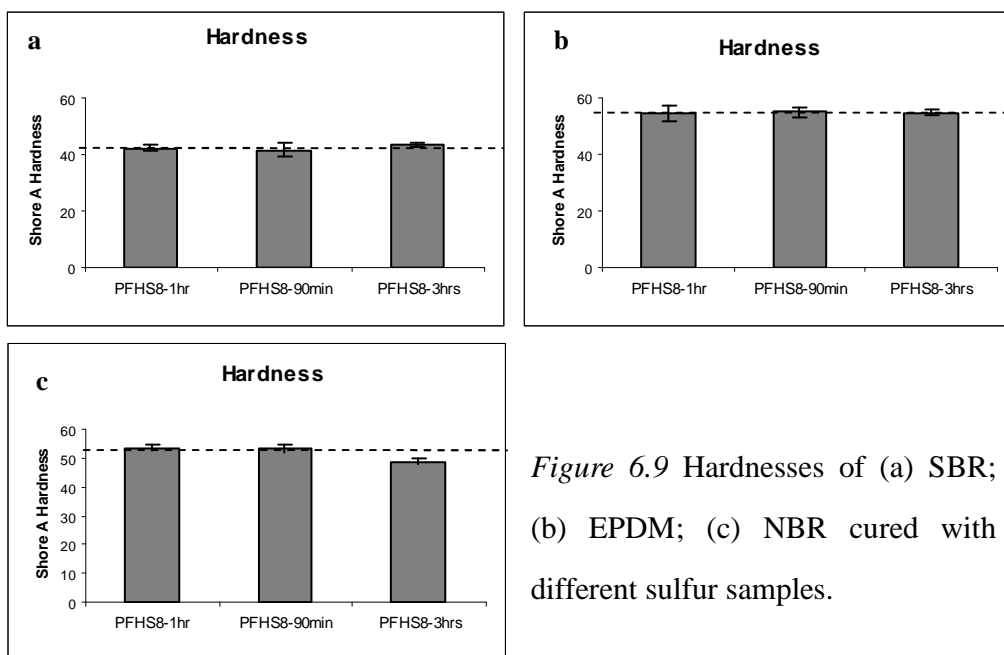
Figure 6.9 Hardnesses of (a) SBR; (b) EPDM; (c) NBR cured with different sulfur samples.

6.3.1.4b In SE and NE blends

Although a significant improvement in the performance of pure rubber vulcanizates was not expected and not found experimentally, an improvement in rubber blend properties is expected due to a possible reduction in solubility difference of the curatives between two rubber phases.

The tensile strength, elongation at break, 100% and 200% moduli of the SE and NE blends with both unmodified and plasma PFH modified sulfur using different plasma reaction times are summarized in Figures 6.10 and 6.11, respectively. Significant improvements in tensile strength are obtained for plasma PFH coated sulfur in SE blends compared to the uncoated one, Figure 6.10. The increases in the 100% and 200% moduli are also impressive. The improvements in NE blends are also clear, however, not as pronounced as those for SE blends. All samples have very similar 100% moduli, as shown in Figure 6.11b.
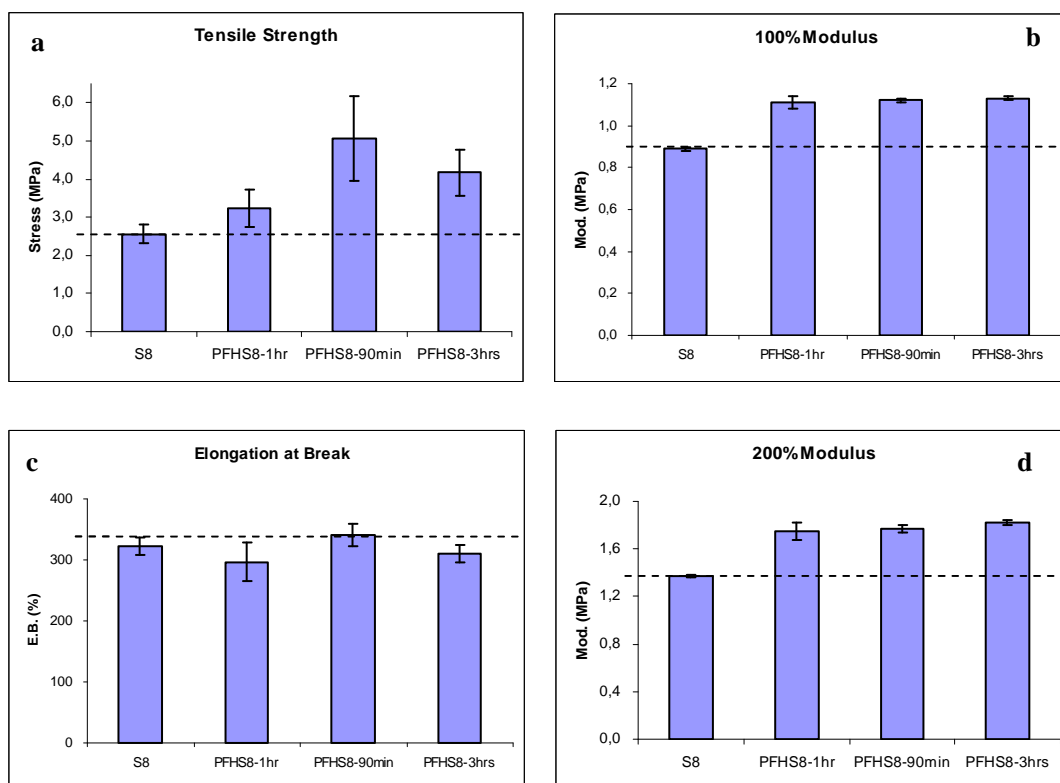
Figure 6.10 The stress-strain properties of the SE blends cured with different sulfur samples.
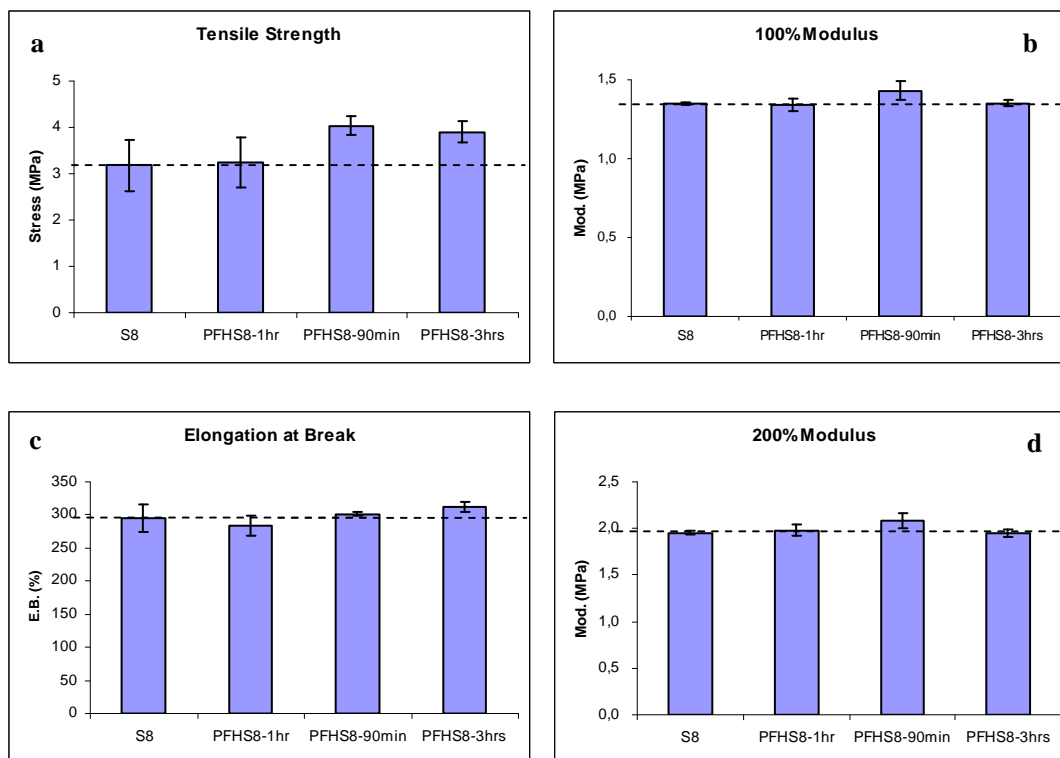

Figure 6.11 The stress-strain properties of the NE blends cured with different sulfur samples.

Figure 6.12 shows a comparison of the hardness for the different rubber blends. There are no significant differences among the values. The blend samples were prepared without a reinforcing filler, thus are rather soft. The modification of vulcanizing agent (S_8) does not have a large influence on the hardness results.
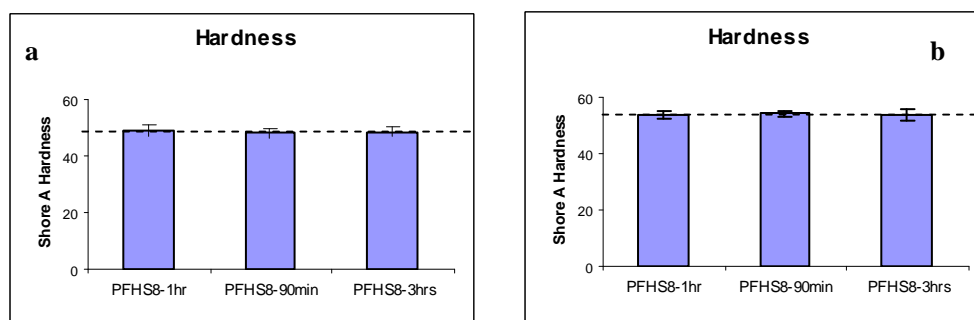
Figure 6.12 Hardnesses for the SE and NE blends cured with different sulfur samples.

The rupture energies of the SE blends, calculated from the full stress-strain curves in Figure 6.13, are given in Table 6.3. A general increase in rupture energy is found for all the SE blends cured with modified sulfur samples, with the highest value achieved for PFHS$_8$-90min. An increase of 63 % is obtained compared to the control.
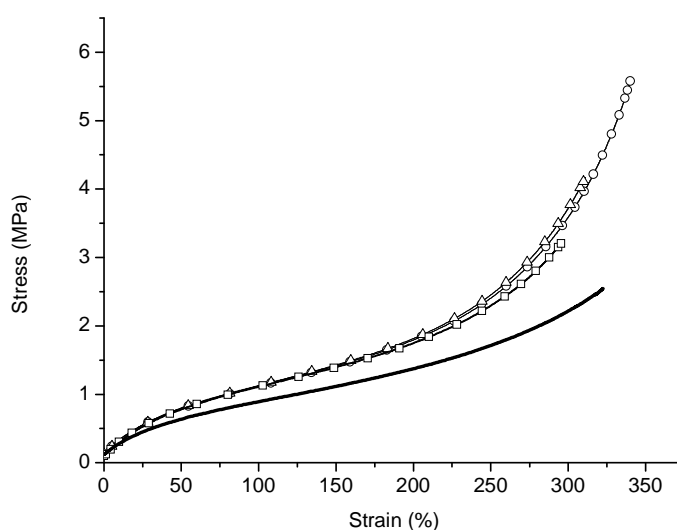

Figure 6.13 Stress-strain properties of the SE blends cured with:
(——) S$_8$; (—□—) PFHS$_8$-1hr; (—○—) PFHS$_8$-90min.; (—△—) PFHS$_8$-3hrs.

Table 6.3 Rupture energies of the SE blends cured with different sulfur samples.

Sample code	Rupture energy (a.u)
S_8	399
$PFHS_8$-1hr.	440
$PFHS_8$-90min.	650
$PFHS_8$-3hrs.	519

(a.u) = arbitrary units

The rupture energies of the NE blends, calculated from the area under the full stress-strain curves in Figure 6.14, are given in Table 6.4.
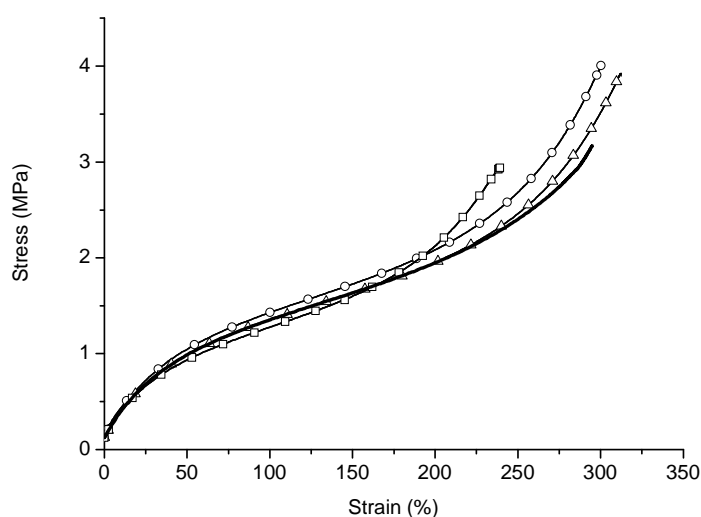

Figure 6.14 Stress-strain properties of the NE blends cured with:
(——) S_8; (—□—) $PFHS_8$-1hr; (—○—) $PFHS_8$-90min.; (—△—) $PFHS_8$-3hrs.

As can be seen in Table 6.4, the rupture energy corresponds with the mechanical properties of the NE blends. The NE blend cured with $PFHS_8$-1hr demonstrates the lowest rupture energy and tensile strength. The NE blends cured with $PFHS_8$-90min and $PFHS_8$-3h show similar rupture energies with a increase of some 14 % relative to the use

of non-coated sulfur. Apparently, the properties of the NE blends cannot be improved with both plasma polyacetylene and polyperfluorohexane coating. The large cure rate mismatch between the NBR-phase and the EPDM phase overrules the effects of plasma coating.

Table 6.4 Rupture energies of the NE blends cured with different sulfur samples.

Sample code	Rupture energy (a.u)
S_8	486
$PFHS_8$-1hr	350
$PFHS_8$-90min.	555
$PFHS_8$-3hrs	556

(a.u) = arbitrary units

The results of crosslink density measurements for the SE and NE blends are given in Table 6.5. There are no significant differences among the NE samples. The SE blends have the highest gel contents when they are cured with $PFHS_8$-3hrs and $PFHS_8$-90min. Only a slight increase in crosslink density values for the SE blend cured with $PFH-S_8$-90min and $PFH-S_8$-3hrs can be observed, corresponding with the minor differences in the hardness test results.

Table 6.5 The crosslink densities of the SE and NE blends cured with different sulfur samples.

Sample code	Gel (%)	Sample code	Gel (%)
$SE+S_8$	98.2	$NE+S_8$	-
$SE+PFHS_8$-1hr	99.7	$NE+PFHS_8$-1hr	99.8
$SE+PFHS_8$-90min	99.9	$NE+PFHS_8$-90min	99.8
$SE+PFHS8$-3hrs	99.9	$NE+PFHS_8$-3hrs	99.8

It demonstrates that the significant improvements observed for the SE blends using plasma PFH modified sulfur are not simply the results of a higher degree of crosslinking. Instead, it is more related to the fact that the crosslinks are more homogeneously distributed. A better co-vulcanization is therefore achieved by a more homogeneous distribution of sulfur, as a result of a balanced solubility in the two rubber phases and reduced migration.

6.3.2. Plasma PFH coated CBS and its performance in straight rubbers and elastomer blends

6.3.2.1 Surface energy by wetting behavior

Similar to sulfur, there is also no appreciable color change of the CBS powders after the plasma coating with perfluorohexane. Therefore, the surface energy was also determined for a quick confirmation of the presence of the coating.

Comparison of behaviors of CBS samples in liquids with known surface tension gives an indication of the surface energy reduction. The scales of the surface energies of CBS before and after coating are also shown in Figure 6.2. PFH-CBS, exhibits a lower surface energy compared to the uncoated one. The decrease in surface tension proves that a perfluorohexane film is present on the particles surface.

6.3.2.2 Scanning Electron Microscopy (SEM)

The SEM images of uncoated and coated CBS are shown in Figures 6.15a and b. It is difficult to distinguish the amorphous coating of the plasma polymerized perfluorohexane, because the surface of uncoated powders is already amorphous. However, the images taken at resolution of 50,000 show some difference of topography. The uncoated CBS has a much smoother surface compared to the PFH-CBS.
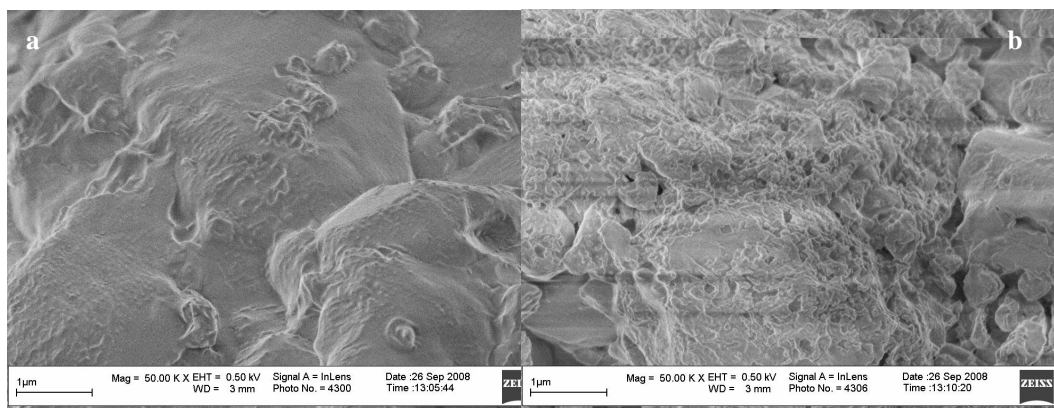
Figure 6.15 SEM images of (a) uncoated and (b) plasma PFH coated CBS.

6.3.2.3 Thermogrametric analysis (TGA)

The TGA thermograms of uncoated CBS and CBS coated with plasma polymerized perfluorohexane are given in Figure 6.16. The samples were heated in N_2 from 50 ^{o}C to 700 ^{o}C with a heating rate of 10 ^{o}C/min. The onset of weight loss of coated CBS is shifted to a slightly higher temperature due to the presence of the coating. It is hard to explain why PFHCBS-1hr shows more delay in the onset of weight loss temperature. The amount of plasma polymer deposited and also the composition of plasma polymer apparently have an influence on the shape of the curve.
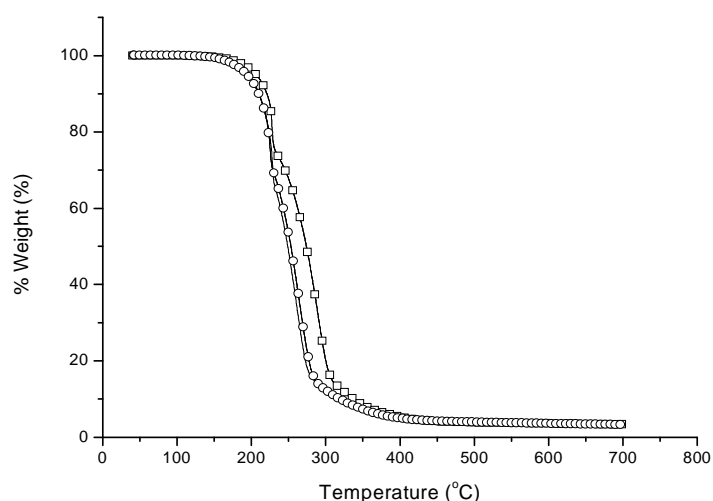

Figure 6.16 TGA thermograms of (——) CBS; (—□—) PFHCBS-1hr; (—○—) PFHCBS-2hrs.

The 10, 50 and 90 % weight losses are indicated in Table 6.6 to elucidate the influence of the deposited plasma PFH layer on weight loss. Clearly, the largest delay is obtained with PFHCBS-1hr, which again is a bit difficult to explain.

Table 6.6 Weight loss (%) of CBS vs. TGA temperature.

Weight loss (%)	Temperature (^{o}C)		
	CBS	PFHCBS-1hr	PFHCBS-2hrs
10 %	220	221	207
50 %	249	274	249
90 %	321	338	316

6.3.2.3 X-ray photonelectron spectroscopy (XPS)

XPS-analysis was performed to further prove the presence of the PFH-coating on CBS. The technique was also intended to give some insight into the structure of the plasma polymer. Both pure CBS and plasma polymerized perfluorohexane-CBS were investigated. The powder samples were pressed into indium foil and two acquisition areas were indicated. The XPS-spectrum for the uncoated CBS is shown in Figure 6.17. The presences of carbon, sulfur, nitrogen and oxygen are confirmed. The oxygen atoms are not involved in CBS structure; its concentration of 8.03 % can be attributed to carbonyl and hydroxyl groups incorporated through the reaction of free radicals distributed throughout the plasma polyperfluorohexance by oxygen from the air.
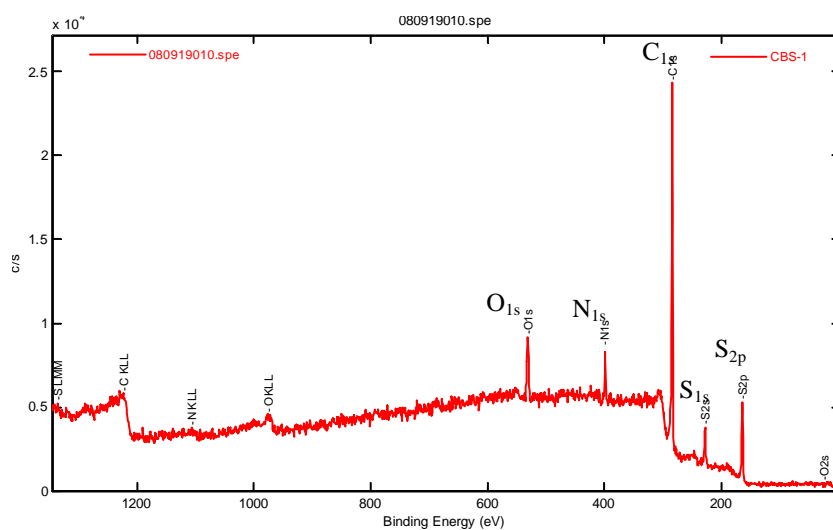
Figure 6.17 XPS spectrum of untreated CBS.

Figure 6.18 shows the XPS-spectrum of PFHCBS. The occurrence of fluor is observed. The average concentration of fluor is quite low: 2.72 %. Fluor shows two peaks in the F_{1s} spectrum. This means that the F-atoms are bonded in two different ways. The binding energies are 685.38 eV and 688.58 eV, respectively, which correspond to covalent CF bonding and ionic CF bonding.
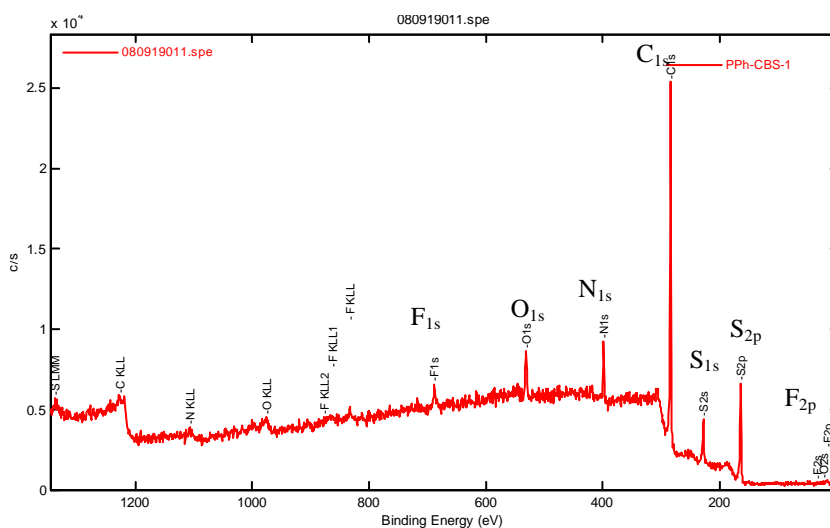

Figure 6.18 XPS spectrum of plasma PFH treated CBS.

Figure 6.19 shows the XPS-spectra for those bonding energies. There are no CF_2 and CF_3 groups/carbon atoms observed. A corresponding possible structure of the plasma polymerized perfluorohexane is shown in Figure 6.20.
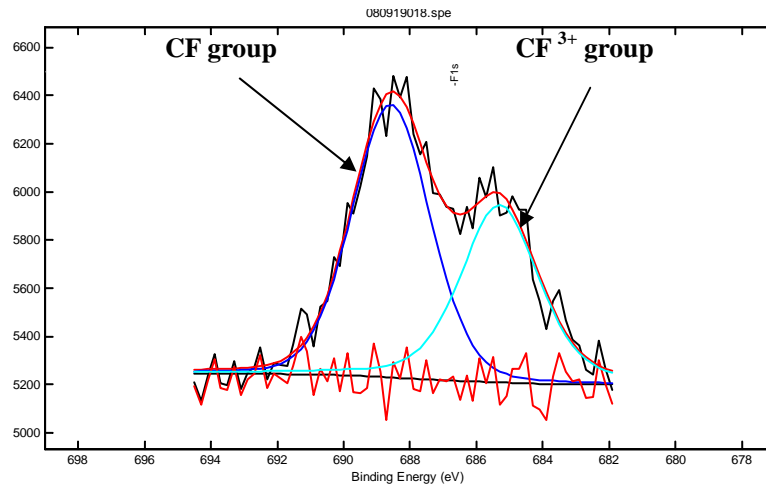

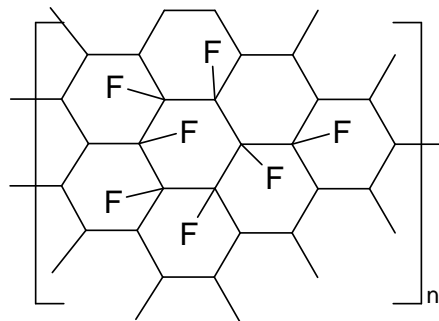*Figure 6.19* The F1s levels of plasma polymerized perfluorohexane.

Figure 6.20 Possible structure of plasma polymerized perfluorohexane.

6.3.2.4 Performance of plasma perfluorohexane treated CBS powders in rubbers

6.3.2.4a In straight SBR, EPDM and NBR rubbers

The curing behavior of straight rubbers cured with CBS and plasma PFH-coated CBS are presented in Figures 6.21a, b and c. It can be seen that the SBR compounds with PFHCBS show some longer scorch times, in Figure 6.21a. A slightly higher state of cure is observed for EPDM vulcanizates with PFHCBS in Figure 6.21b. The scorch time is

slightly longer for the SBR samples cured with PFHCBS, but shorter for the EPDM cured with PFHCBS-2hrs, compared with the vulcanizates cured with uncoated CBS. In Figure 6.21c, both scorch time and maximum torque for NBR vulcanized with the coated CBS show only minor differences from the one cured with uncoated CBS.
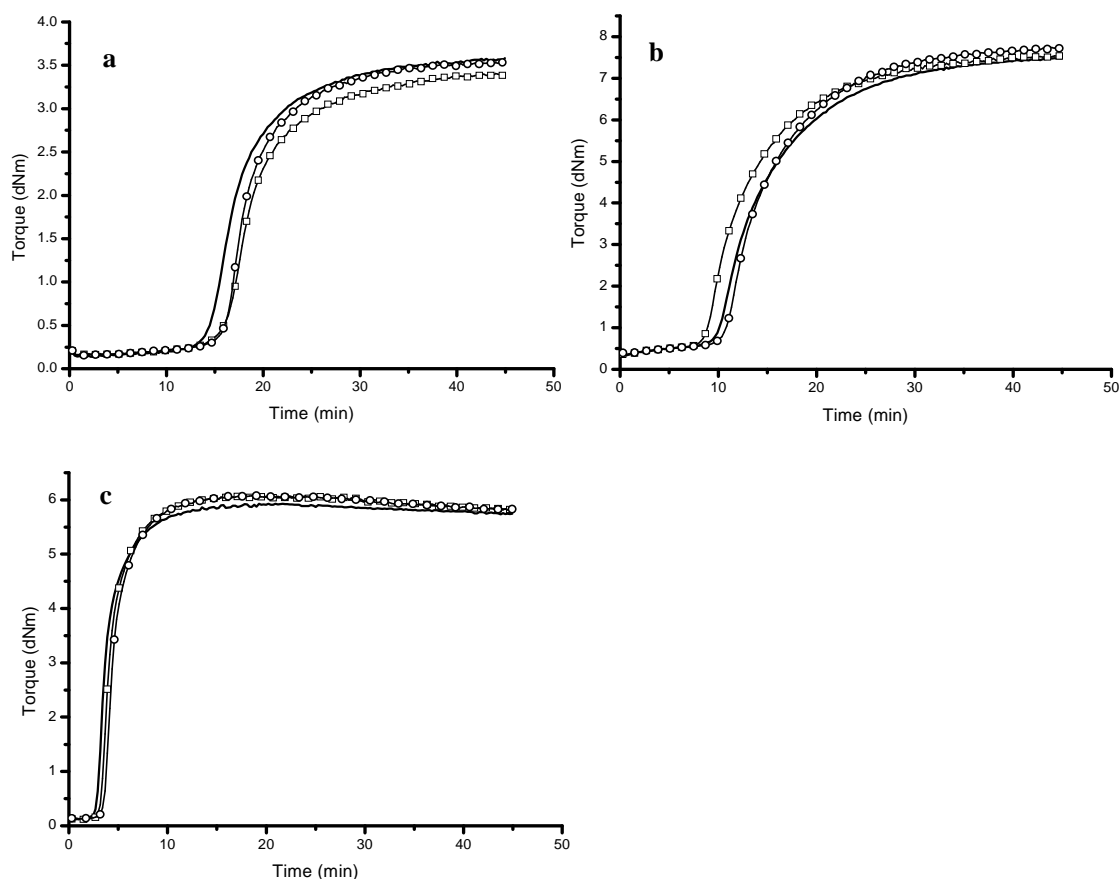

Figure 6.21 Rheograms of (a) SBR; (b) EPDM; (c) NBR cured with:
(——) CBS; (—□—) PFHCBS-1hr; (—○—) PFHCBS-2hrs.

The stress-strain behaviors of SBR, EPDM and NBR vulcanizates with both unmodified and plasma PFH-modified CBS with different plasma reaction times, are shown in Figures 6.22 to 6.24, respectively. It can be seen that SBR cured with PFHCBS-1hr has the lowest tensile strength and elongation at break value. The best mechanical properties are obtained for SBR cured with PFHCBS-2hrs. The 100% moduli are similar for all SBR vulcanizates. Overall the differences are minor.
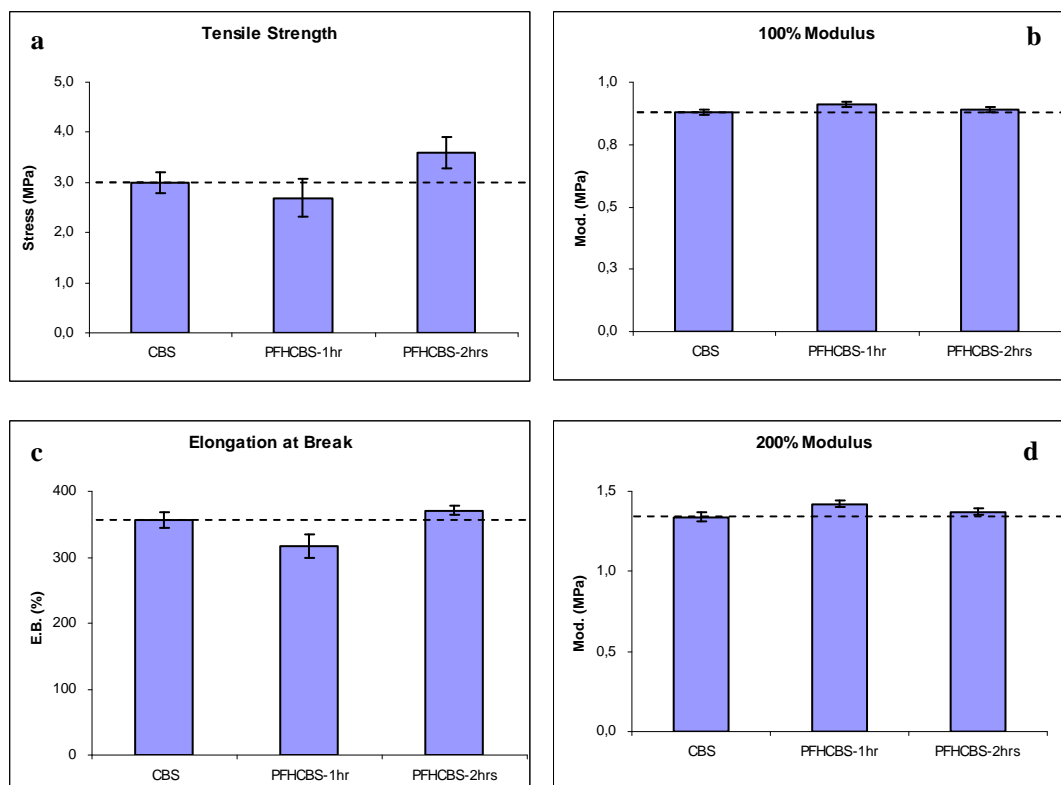
Figure 6.22 The stress-strain properties of SBR cured with different CBS samples.
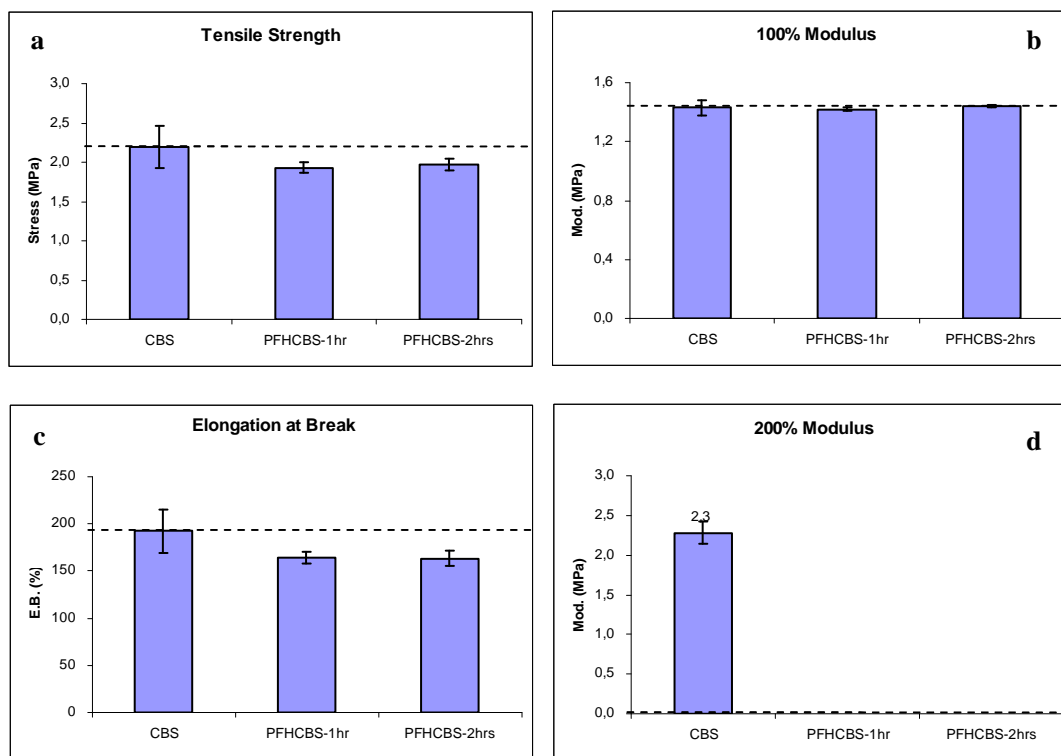

Figure 6.23 The stress-strain properties of EPDM cured with different CBS samples.

The properties of vulcanized EPDM with the various types of modified CBS together with the control unmodified CBS are shown in Figure 6.23. An appreciable decrease in the properties is found for all the PFHCBS cured EPDM vulcanizates.

CBS has the highest solubility in NBR among these three types of rubber as can be derived from Figure 6.2 and was confirmed in Chapter 3. From Figure 6.24, it can be seen that the stress-strain behavior of NBR vulcanizates cured with plasma PFH modified CBS show some improvement in stress-strain properties.

PFHCBS-1hr shows the best performance in NBR and the worst performance in SBR, opposite to the performance of $PFHS_8$ in these two rubbers. This may seem surprising since the two powder surfaces are treated by the same plasma monomer. However, as untreated CBS has a much higher initial surface energy than sulfur, and the surface of the powders is not covered to the full 100%, the surface energy of the substrate still shows some influence on the overall surface energy. Therefore, it is reasonable to expect a higher surface energy for PFHCBS than $PFHS_8$, and closer to NBR than SBR and EPDM.
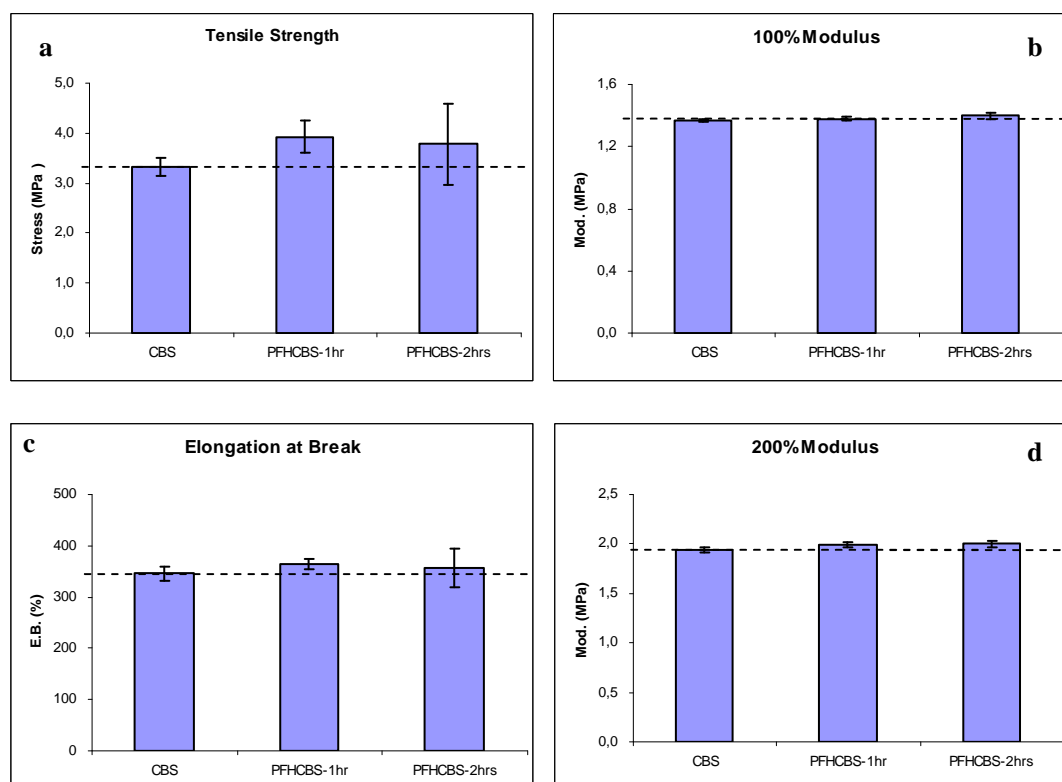

Figure 6.24 The stress-strain properties of NBR cured with different CBS samples.

6.3.2.4b In SE and NE blends

Figures 6.25a and b show the cure characteristics for SE and NE blends cured with unmodified and plasma PFH-modified CBS. A major improvement in the state of cure is observed for the SE blends cured with PFHCBS relative to the untreated CBS. PFHCBS-1hr provides a slightly shorter scorch time, while PFHCBS-2hrs shows a somewhat longer scorch time compared to uncoated CBS. In case of the NE blend, just slightly higher states of cure and somewhat longer scorch times are obtained for PFHCBS.
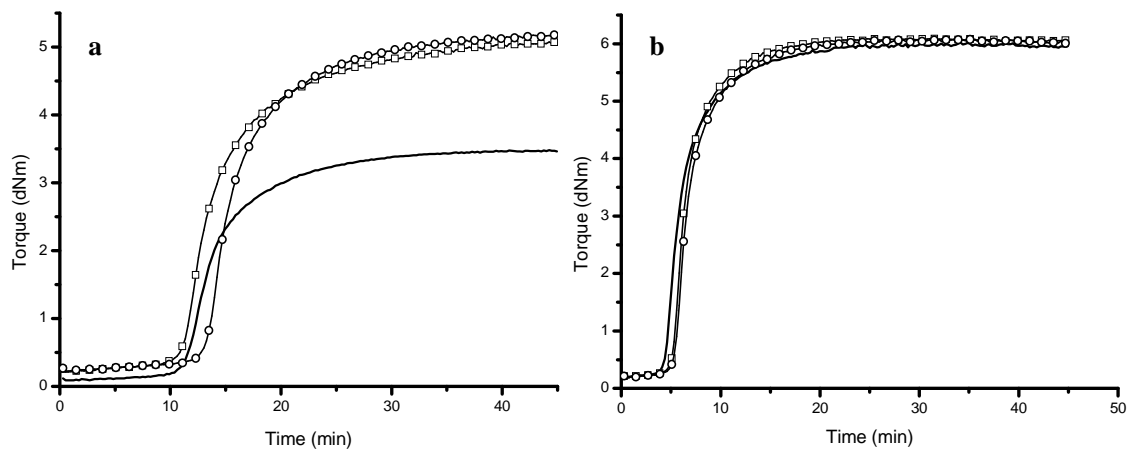

Figure 6.25 Rheograms of (a) the SE blends; (b) the NE blends cured with:
(——) CBS; (—□—) PFHCBS-1hr; (—○—) PFHCBS-2hrs.

The tensile strengths, elongations at break and 100% and 200% moduli of the SE and NE blends cured with both unmodified and modified CBS are summarized in Figures 6.26 and 6.27, respectively.

In the SE blends, as shown in Figure 6.26, it is clear that PFHCBS in general gives very pronounced improvements in the tensile strength, elongation at break and moduli. PFHCBS-2hrs demonstrates the best stress-strain properties. This can be interpreted as a consequence of a better co-vulcanization in the SE blends.

In the NE blends, a slight difference in tensile strength is obtained with PFHCBS-1hr and PFHCBS-3hrs, see Figure 6.27. All samples have very similar elongations at break

and moduli. From the solubilities, as discussed in Chapter 3, it is known that CBS has a much higher solubility preference for NBR than for the EPDM phase. The unpolar coating of plasma PFH could compensate for the solubility imbalance. However, the huge difference of the curing rate between the NBR and SBR phase, as seen in the curing curves in Figure 6.21, seems to play the determining role for the properties of the NE blends, as described earlier in Chapter 4 and seen for S_8 as well.
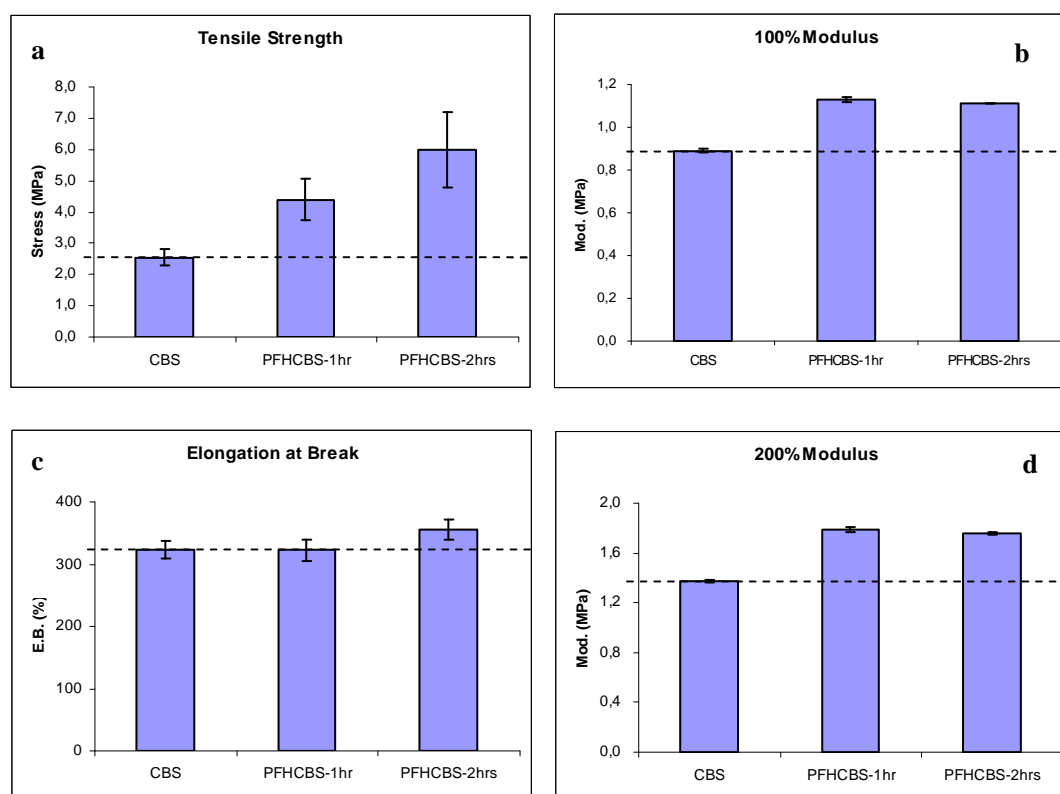
Figure 6.26 The stress-strain properties of the SE blends cured with different CBS samples.
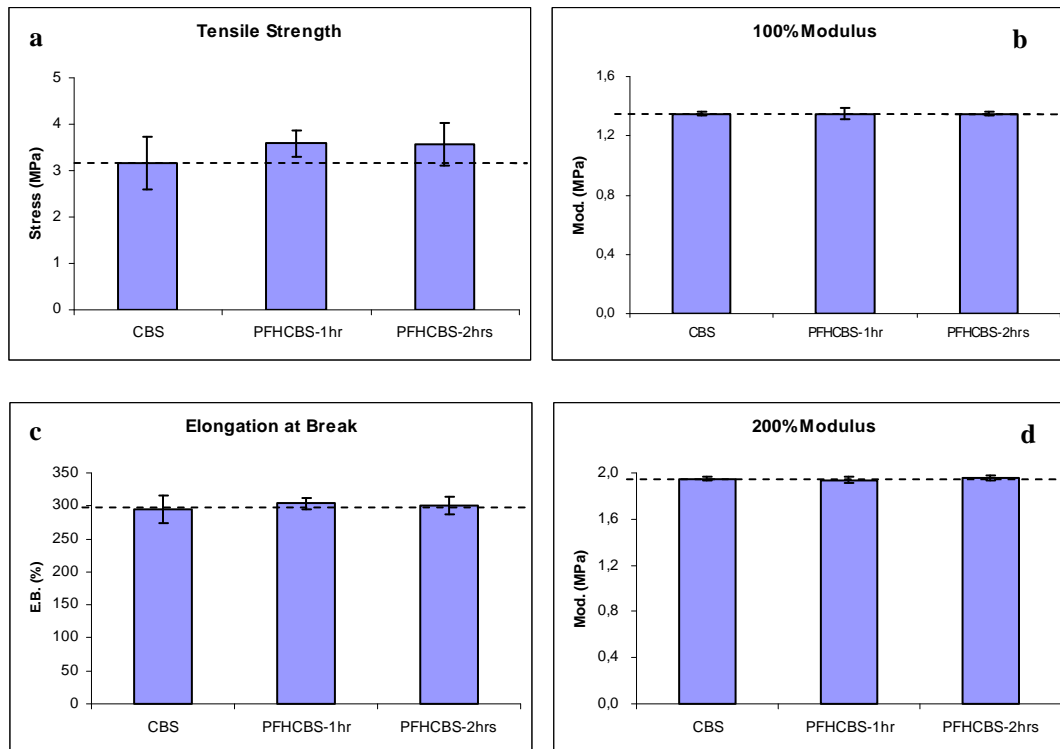
Figure 6.27 The stress-strain properties of the NE blends cured with different CBS samples.

The rupture energies of the SE blends are given in Table 6.7, as calculated from the full stress-strain curves in Figure 6.28. In general, plasma PFH-coated CBS gives a very pronounced increase in rupture energies. The highest value is found for PFHCBS-2hrs, with an increase of 71% compared to the control.

Figure 6.28 Stress-strain curves of the SE blends cured with:
(——) CBS; (—□—) PFHCBS-1hr; (—○—) PFHCBS-2hrs.

Table 6.7 Rupture energies of the SE blends cured with different CBS samples.

Sample code	Rupture energy (a.u)
CBS	399
PFHCBS-1hr.	554
PFHCBS-2hrs	683

(a.u) = arbitrary units

The rupture energies of the NE blends, calculated from the full stress-strain curves in Figure 6.29, are shown in Table 6.8. The NE blends cured with plasma PFH-coated CBS only show a slight increase compared to the control.

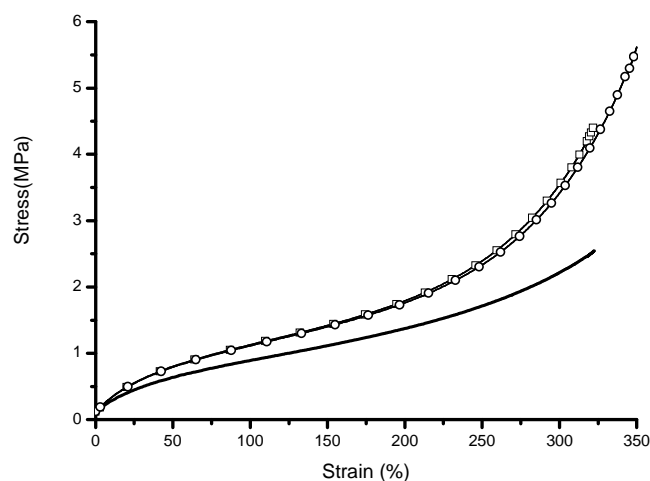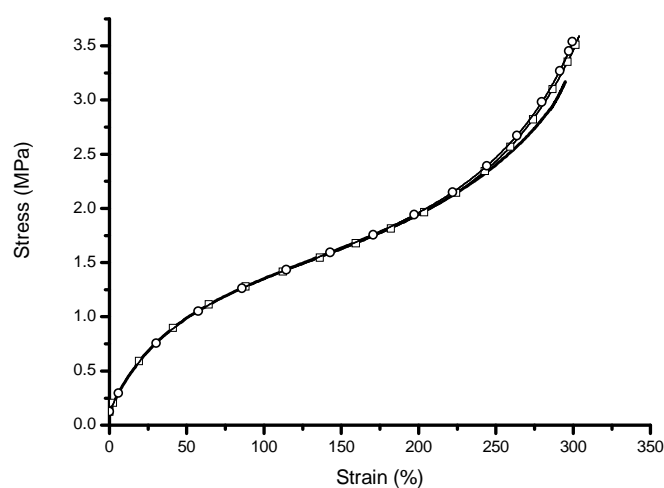*Figure 6.29* Stress-strain curves of the NE blends cured with:
(———) CBS; (—□—) PFHCBS-1hr; (—○—) PFHCBS-2hrs.

Table 6.8 Rupture energies of the NE blends cured with different CBS samples.

Sample code	Rupture energy (a.u)
CBS	486
PFHCBS-1hr.	512
PFHCBS-2hrs	520

(a.u) = arbitrary units

6.3.3 Solubilities of plasma PFH-coated sulfur and CBS in rubbers

6.3.3.1 Solubility of Plasma PFH coated sulfur in different rubbers

The solubilities of plasma PFH coated sulfur in SBR, EPDM and NBR rubbers are shown in Figures 6.30a-c. As expected, the plasma PFH coating has an effect on the solubilities of sulfur. Compared to the solubility data in our previous study, [10] as presented in Chapter 3, it is clear that the plasma PFH-coated sulfur shows a particularly pronounced decrease in solubility in SBR at 60 ^{o}C, but not in NBR and EPDM. At room temperature, there is a decrease in solubility seen for plasma PFH-coated sulfur in all three elastomers. Compared to the solubilities of sulfur in EPDM, Figure 6.30b, it is clear that the solubility of plasma PFH-coated sulfur in the SBR phase at 60 ^{o}C is even decreased below that of the EPDM. This will definitely benefit the EPDM phase in SE blends. This fact explains the improved mechanical properties of SE blends using plasma PFHS$_8$ as the curing agent. As not much difference in the solubility of plasma PFH-coated sulfur in NBR is observed, not in EPDM, in Figure 6.30b and c, it explains why the mechanical properties of the NE blend using plasma PFH-coated sulfur as the curing agent remained more or less unchanged.
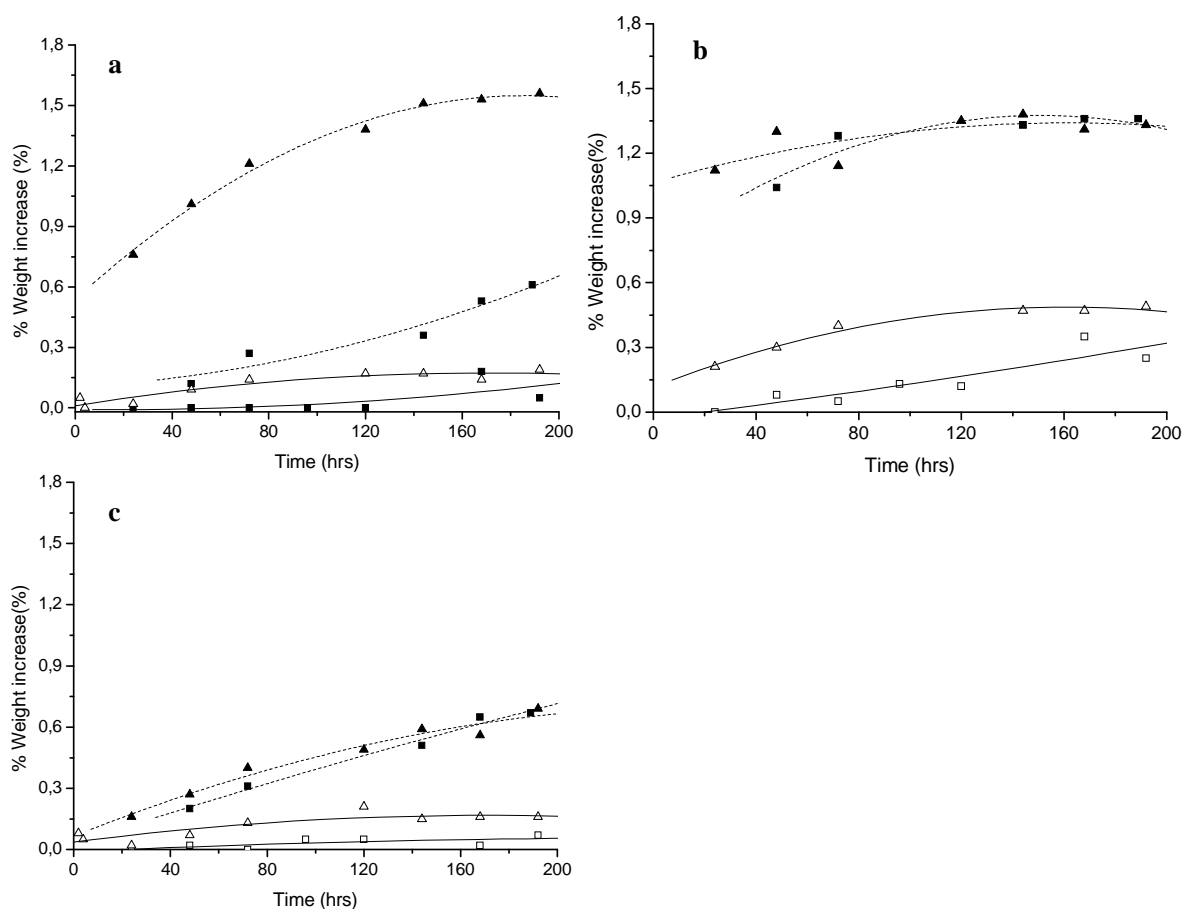
Figure 6.30 Solubility of S_8 and $PFHS_8$ in (a) SBR; (b) EPDM and (c) NBR.
(△) S_8 at RT; (▲) S_8 at 60 ^{o}C; (□) $PFHS_8$ at RT; (■) $PFHS_8$ at 60 ^{o}C.

6.3.3.2 Solubility of Plasma PFH-coated CBS in different rubbers

The polarity of CBS is much higher than that of the plasma PFH-coated CBS, so the solubility in rubbers is expected to change much more than seen with $PFHS_8$. The solubilities of CBS and PFHCBS in SBR, EPDM and NBR are shown in the Figures 6.31. The largest relative solubility difference is observed in SBR again at 60 ^{o}C, Figure 6.31a, where a pronounced decrease in solubility is found for PFH-CBS compared to uncoated CBS. In EPDM the solubility at 60 ^{o}C of plasma polymerized CBS is increased compared to the uncoated CBS. Like for $PFHS_8$, this benefits the EPDM phase in SE blends using a plasma PFH-coated CBS as accelerator. Consequently, again much better properties are

achieved due to improved co-vulcanization, as found in the stress-strain properties of the SE blends.

From Figure 6.31b and c, it is clear that the plasma PFH-coated CBS shows similar solubilities as uncoated CBS in EPDM and NBR. This explains the fact why only little improvements in the properties of the NE blends were achieved using PFHCBS as accelerator while the large cure mismatch remained the over-ruling factor.
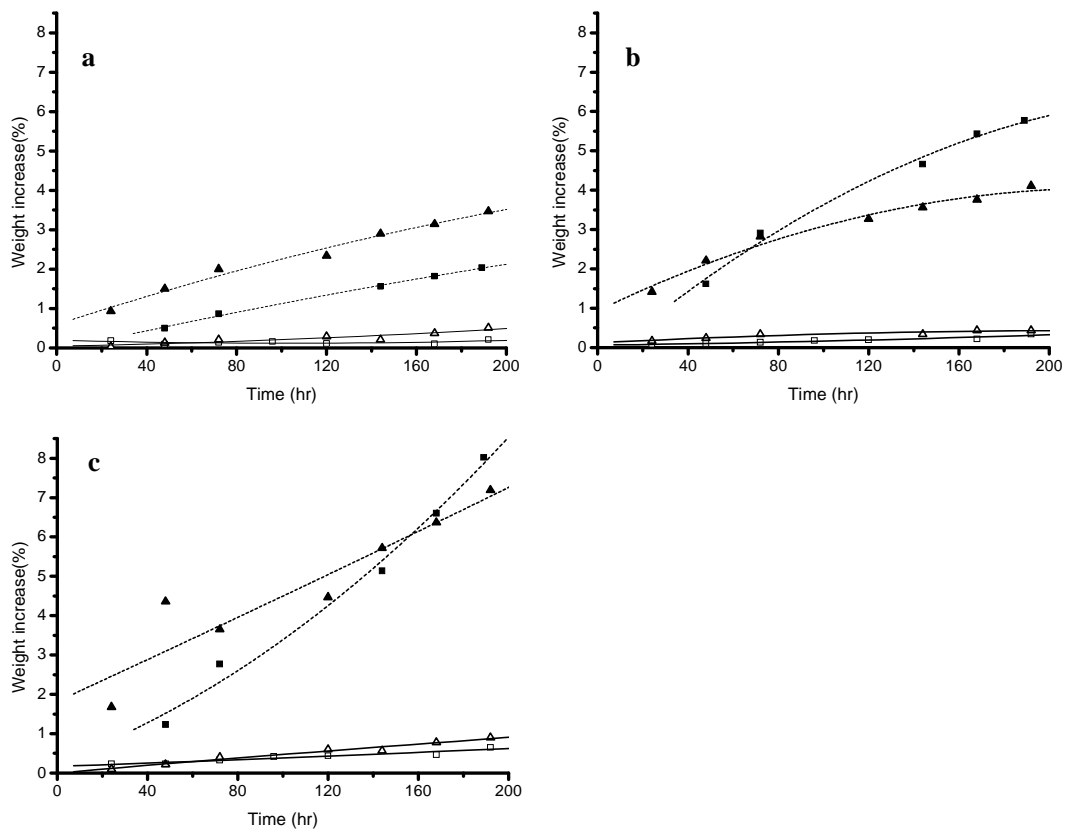

Figure 6.31 Solubility of CBS in (a) SBR, (b) EPDM and (c) NBR.
(△) CBS at RT; (▲) CBS at 60 ^{o}C; (□) PFHCBS at RT;
(■) PFHCBS at 60 ^{o}C.

6.4 Conclusions

A comprehensive study has been carried out on plasma polymerization using perfluorohexane on sulfur and CBS. The surface of sulfur and CBS was modified with an

nm thin layer of plasma polymerized perfluorohexane, which reduced the surface energies toward the levels of the elastomers.

For the unreinforced 50/50 SE blend, as discussed in Chapter 4, solubility of the curatives turns out to play a determing role in the mechanical properties of the blend due to the fact the SBR-phase and EPDM-phase have equivalent curing reactivities. Therefore, plasma PFH-encapsulation of these curatives overcomes the cure imbalance in such a dissimilar rubber blend by reducing the migration of polar curatives from the one phase to the other phase. In particular, a reduction of the higher temperature solubility of PHF-coated curatives in SBR benefits the cure of the EPDM-phase in the SE blends. By using the plasma PFH-coated sulfur and CBS, the mechanical properties of the 50/50 SE blend were improved very significantly.

The solubility study showed that the beneficial effect in the SE blend by PFH-encapsulation of the curatives was primarily due to a decrease of their solubility in the SBR-phase, even below that in the EPDM-phase; contrary to what had been aimed for: an increase of the solubility in the EPDM-phase. Still, it is the EPDM phase which benefits from this effect.

For the 50/50 NE blends, as there is a large difference in vulcanization reactivities of NBR and EPDM, as demonstrated in Chapter 4, and because there are no large changes in the relative solubilities of the sulfur and CBS in NBR and EPDM by the PFH-coating, the improvement by applying the plasma PFH-encapsulated curatives on mechanical properties of the NE blends is very limited compared to the SE blends.

The solubility of coated CBS is not decreased in NBR, but the coating did decrease the migration of the CBS into the NBR rubber somewhat in the first three days of testing.

It was proved that a reaction time of 90 minutes seems to be required for the full development of a complete coating shell. Otherwise, the curatives are too easy to diffuse out and migrate to their preferred phase, which results in cure mismatch.

Based on the results so far, it seems necessary to focus more on improving the

properties of the NE blends in the next chapters, for which all modifications discussed so far were not so successful in improving the properties.

6.5 References

[1]   C.-M. Chan, T.-M. Ko, H. Hiraoka, *Surf. Sci. Rep.*, **1996**, 24, 1.

[2]   M. Strobel, S. Corn, C.S. Lyons, G.A. Korba, *J. Polym. Sci. Part A: Polym. Chem.* 1**987**, 25, 1295.

[3]   I.H. Loh, M. Klausner, R.F. Baddour, R.E. Cohen, *Polym. Eng. Sci.* **1987**, 27, 861.

[4]   Y. Iriyama, T. Yasuda, D.L. Cho, H. Yasuda, *J. Appl. Polym. Sci.,* **1990**, 39, 249.

[5]   Y. Lin, H. Yasuda, M. Miyama, T. Yasuda, *J. Polym. Sci. Part A: Polym. Chem.*, **1996**, 34, 1843.

[6]   N.D. Tran, N.K. Dutta, N. Roy Choudhury, *Thin Solid Films*, **2005,** 491, 123.

[7]   F. Hochart, J. Levalois-Mitjaville, R. de Jaeger, L. Gengembre, J. Grimblot, *Appl. Surf. Sci.*, **1999**, 142, 574.

[8]   H. Yasuda, *"Plasma polymerization"*, 1st edition, Academic Press, Inc., Orlando,985.

[9]   N. Inagaki, *"Plasma surface modification and plasma polymerization"*, 1st edition, Technomic Publishing Company, Inc., Lancaster, 1996.

[10]   R.Guo, A.G. Talma, R.N. Datta, W.K. Dierkes, J.W.M. Noordermeer, *Eur. Pol. J.,* **2008**, 44, 3890.

Chapter 7

Acrylic Acid Plasma Encapsulated Sulfur

in Rubber-Rubber Blends

Acrylic acid was chosen as monomer for the plasma treatment of sulfur, for a study in blends of unreinforced Acrylonitrile-Butadiene rubber (NBR) and Ethylene-Propylene-Diene rubber (EPDM). Plasma acrylic acid modified sulfur has a smaller solubility difference between the NBR phase and the EPDM phase compared to untreated sulfur. A significant increase in mechanical properties of these blends is obtained using this micro-encapsulated sulfur as curative, while all other methods seemed not to be working in improving the properties of this blend.

7.1 Introduction

Plasma polymer surface-modified curatives with acetylene and perfuorohexane as monomers can successfully improve the properties of dissimilar rubber-rubber blends, e.g. SBR/EPDM, as discussed in the previous chapters. However, they were not so successful in improving the properties of NBR/EPDM (NE) blends.

As discussed in Chapter 3, the cure incompatibility in rubber blends partially results from the solubility difference of sulfur in the different rubber phases. The preference of sulfur in NE blends is in the following order: EPDM>>NBR. Acrylic acid, a polar monomer, may also be used in plasma polymerization to modify the surface of sulfur powder. As the resulting surface properties can be related to the starting monomer, acrylic acid is expected to modify the sulfur surface to become more polar, in order to increase its solubility in the NBR phase. Therefore, the aim of the work described in this chapter is to study the effect of a plasma polyacrylic acid (PAA) coating on the performance of sulfur powder in 50/50 NBR/EPDM blends.

7.2 Experimental Part

7.2.1 Materials

The following types of rubber were used: Acrylonitrile-Butadiene rubber (NBR, Perbunan® 3446F from LANXESS, Germany), and Ethylene Propylene Diene rubber (EPDM, Keltan® 4703 from DSM Elastomers, the Netherlands). Zinc-oxide was purchased from Sigma Aldrich; stearic acid was used as commercial grade, and accelerator N-cyclohexylbenzothiazole-2-sulphenamide (Santocure® CBS) was kindly provided by Flexsys, Belgium. Elemental sulfur (S_8) was purchased from Sigma Aldrich, with a particle size smaller than 100 mesh (150 μm). Acrylic acid (99 % purity) was supplied by Sigma Aldrich.

7.2.2 Methods

a. Plasma polymerization

The procedure as described in Chapter 5 was used. The reaction conditions are listed in Table 7.1

Table 7.1 Acrylic acid plasma polymerization conditions for sulfur.

Sample code	RF power (W)	Monomer concentration (Pa)	Reaction time (hr)
PAAS$_8$-1	180	27	1.5
PAAS$_8$-2	180	27	2

b. Scanning Electron Microscopy (SEM)

The procedure as described in Chapter 5 was used, except that cross-sections of the plasma acrylic acid modified sulfur were created by crushing the sulfur powders placed on top of a glass sample holder for light microscopy, by sliding another glass plate over the powder.

c. Wetting behavior with liquids of known surface tension

The same procedure as described in Chapter 5 was used.

d. Thermogravimetric analysis (TGA)

See Chapter 5.

e. Time-of-Flight Secondary Ion Mass Spectroscopy (ToF-SIMS)

After the plasma treatment, the untreated and plasma polyacrylic acid treated sulfur were examined by a CAMECA ION-ToF spectrometer (ToF-SIMS IV). The instrument was equipped with a reflection-type time-of-flight mass analyser and a pulsed 25 kV primary source of mono-isotopic $69Ga^+$ ions, with a minimum beam size of 50 nm. Positive and negative spectra were collected at 25 kV primary ion energy, a pulse width of 25 ns and a total integrated ion dose of ~1011 ions/cm^2. A sputter gun was also applied to eliminate the impurity ions from the atmosphere.

f. Rubber mixing and testing

Conditions were used as described in Chapter 5. The compound formulation of the NE blends is listed in Table 5.3 in Chapter 5.

g. Solubility measurements

The methods as described in Chapter 3 were applied.

7.3 Results and Discussion

7.3.1. Scanning electron microscopy (SEM)

The morphologies of the ground uncoated sulfur particles (<50μm) and the sulfur particles being plasma modified with acrylic acid are shown in Figure 7.1. No conductive coating of gold or carbon, as normally used in the SEM analysis, was applied on the sulfur samples. The images in Figure 7.1a and b were obtained using an accelerating voltage of 2 kV. Compared to the images of uncoated sulfur, in Figure 7.1a, an amorphous layer is deposited on the sulfur agglomerates after the plasma acrylic acid polymerization, as shown in Figures 7.1b and c. The morphology of the deposited plasma polymer layer has some sort of a filament structure, as can be observed in Figure 7.1b. The images in Figure 7.1c - f were obtained with an accelerating voltage of 0.5 kV. Figure 7.1c shows the morphology of the sulfur powders deformed under shear during the step to create the cross-sections. It is important to realize that most of the powder particles were only deformed without destroying the plasma polymer layer. As the shear forces are expected to be far less during a rubber mixing process, it is expected that most of plasma coated particles will survive during the mixing step. The encapsulated sulfur is then released via diffusion through the holes and cracks, later on during the vulcanization process. A core-shell structure can be seen in Figures 7.1d-f. The thickness of the shell is estimated to be in the nanometer range. The morphology of the cross-section of other coated sulfur particles is shown in Figures 7.1 e and f, where a sliced structure can be seen.
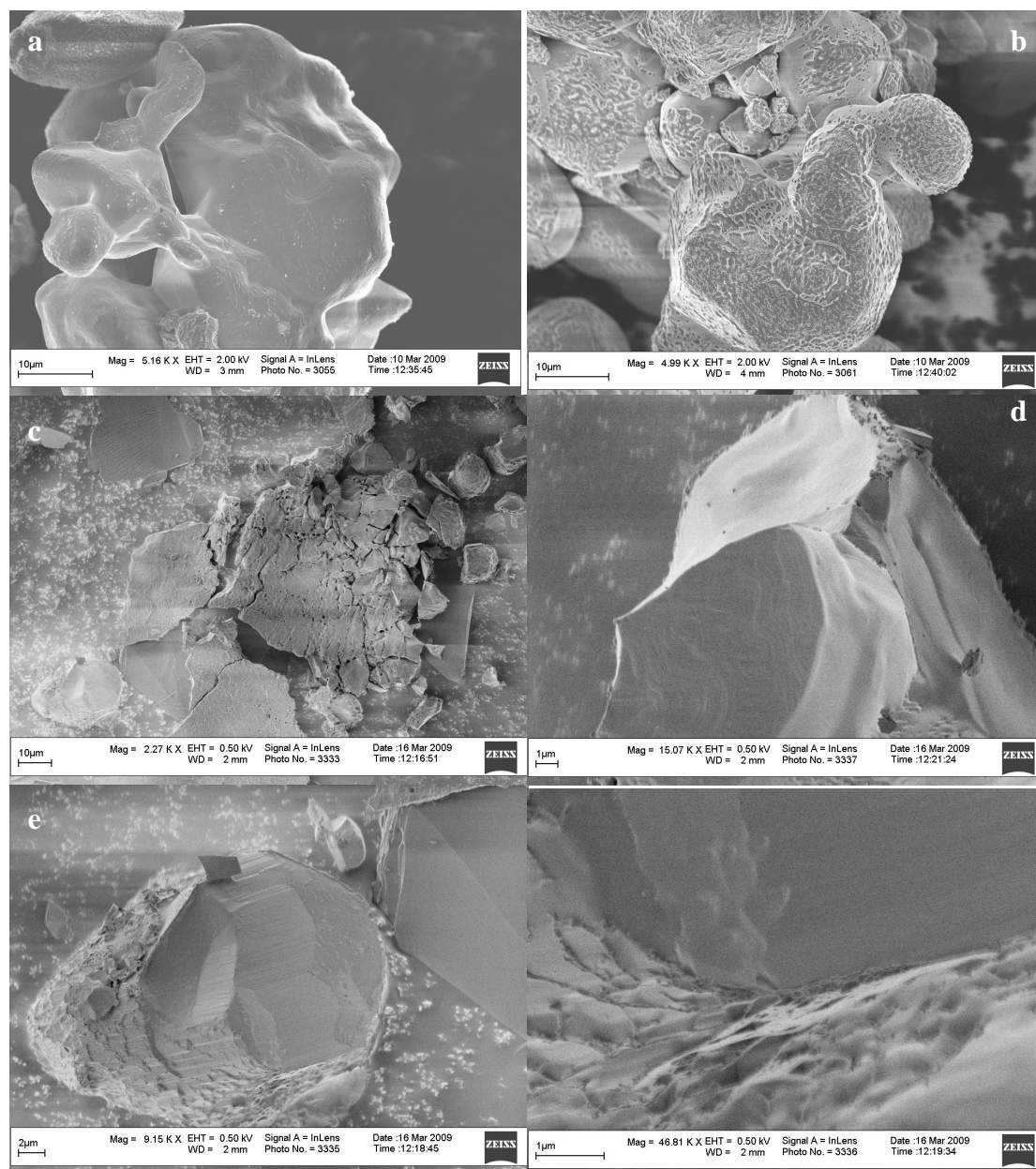
Figure 7.1 SEM images: (a) uncoated sulfur; (b) plasma polyacrylic acid coated sulfur; (c)-(f) cross-sections of the plasma acrylic acid coated sulfur.

7.3.2 Surface energy determination

The surface energy of the plasma acrylic acid modified sulfur was quite similar to the unmodified sulfur. Similar wetting behaviors are obtained for uncoated sulfur (S_8) and coated sulfur ($PAAS_8$) in ethylene glycol, as shown in Figure 7.2. Apparently the surface energy has not changed enough, to be outside the range coved by the selected solvents. The test is not discriminating enough to register small changes.

Figure 7.2 Wetting behaviors of PAAS$_8$ and uncoated sulfur in ethylene glycol.

7.3.3 Thermogravimetric analysis (TGA)

The thermogravimetric curves of uncoated and plasma PAA encapsulated sulfur samples are given in Figure 7.3. The weight losses of the PAAS$_8$ samples are all shifted slightly to a higher temperature compared to the uncoated sulfur, see Table 7.2, which demonstrates the presence of the plasma polymer layer deposited on top of the sulfur particles. The amount of the deposition, as determined by the residual weight at 180 ^{o}C is also given in Table 7.2.
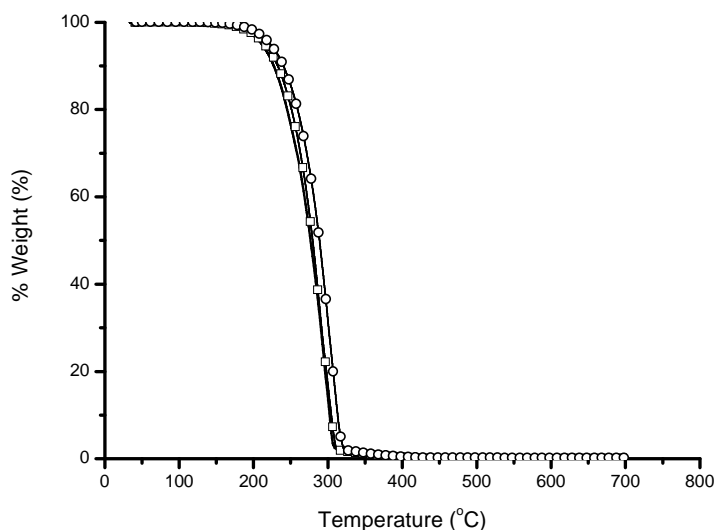

Figure 7.3 TGA thermograms of uncoated and plasma PAA coated sulfur.
(⎯⎯) S$_8$; (⎯□⎯) PAAS$_8$-1; (⎯○⎯) PAAS$_8$-2.

Table 7.2 Estimated coating amount (wt %) and 5% weight loss temperature for

      different sulfur samples.

Sample Code	Amount of coating (%)	Temperature (^{o}C) at 5% wt loss
S_8	0	211.0
PAAS$_8$-90min	1.4	214.5
PAAS$_8$-2hrs	2.2	222.5

7.3.4 ToF-SIMS

ToF-SIMS was applied to both the untreated sulfur and the PAAS$_8$-2hrs to obtain structural information of the outermost layer of the samples. The positive and negative spectra of untreated sulfur are presented in Figures 7.4 and 7.5, respectively. Compared to Figure 7.5, there are clearly more peaks in the positive spectra, in Figure 7.4, coming from hydrocarbon ions in the low molecular weight range. It is interesting to see that sulfur forms almost identical characteristic peaks of S_1, S_2 … up to S_{11} in both the positive and the negative spectra.
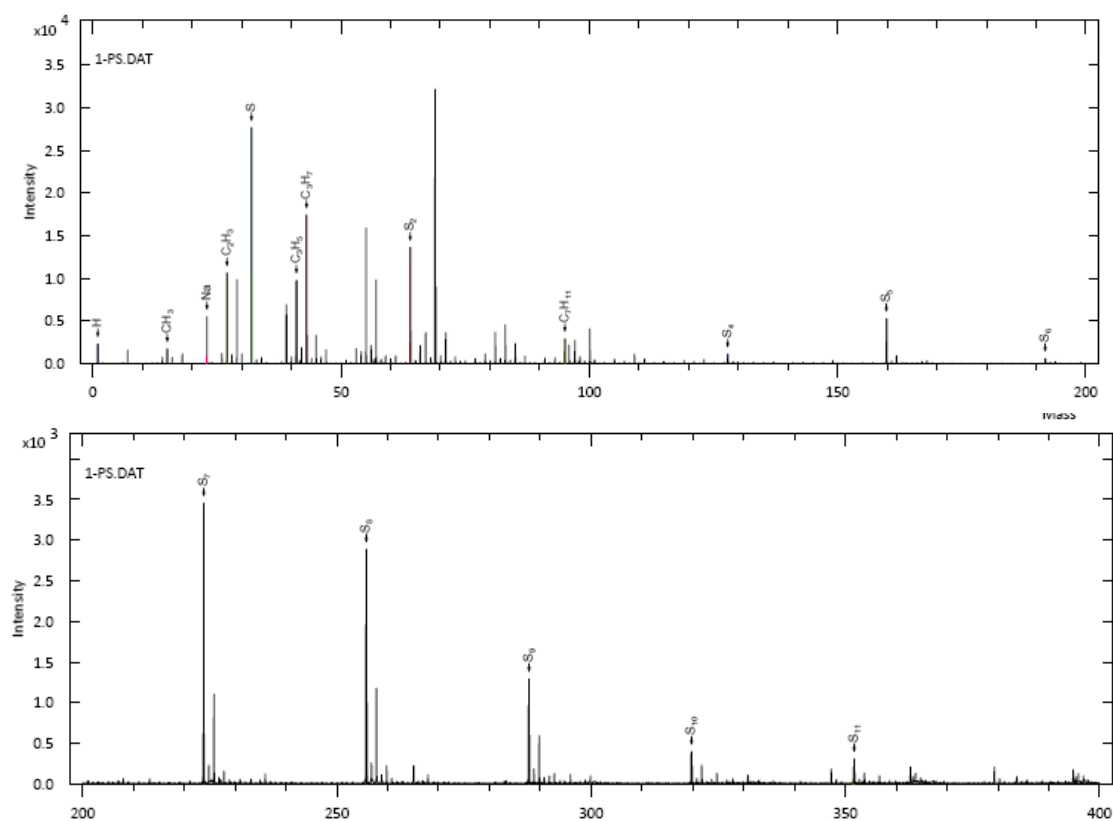

Figure 7.4 Positive ToF-SIMS spectrum of untreated sulfur.
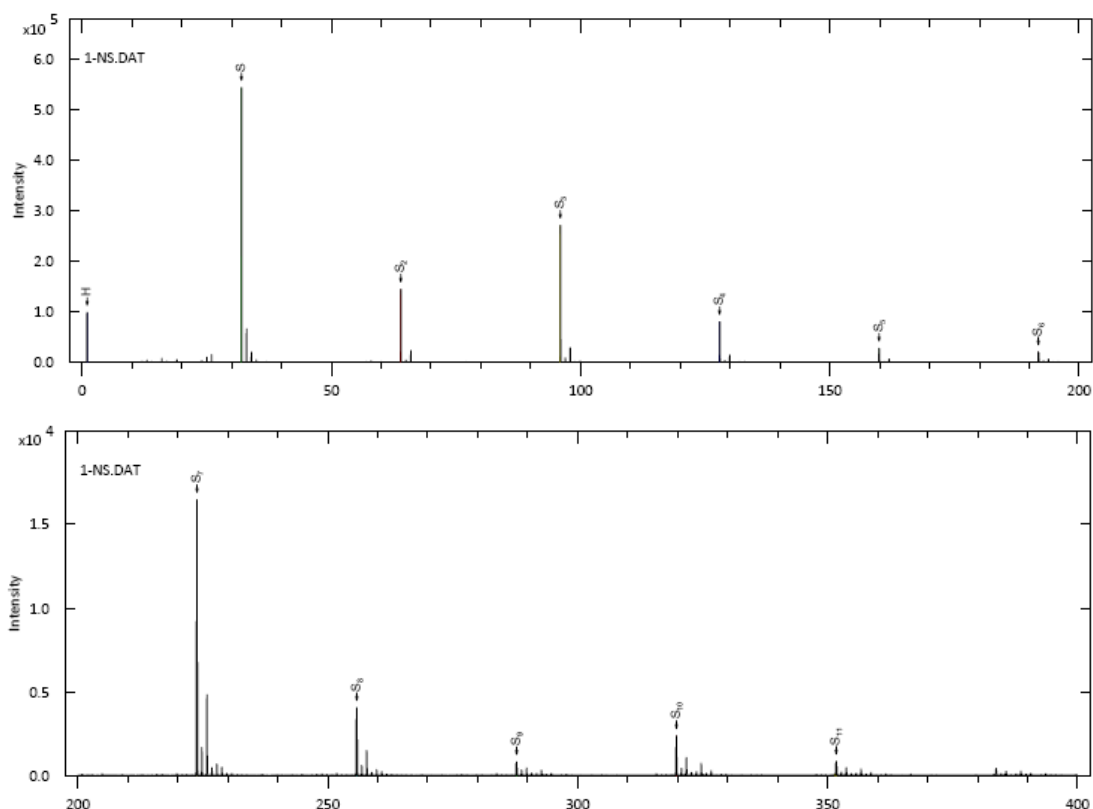
Figure 7.5 Negative ToF-SIMS spectrum of untreated sulfur.

The positive and negative spectra of plasma polyacrylic acid treated sulfur (PAAS$_8$-2) are given in Figures 7.6 and 7.7, respectively. Compared to the untreated sulfur, PAAS$_8$-2 shows a significantly reduced concentration of sulfur ion peaks, which is a sign of the presence of the coating. The presence of the coating is further evidenced by the characteristic cluster pattern of mass fragments, in the positive spectrum in Figure 7.6, especially in the higher mass fraction region from 200 to 400. No peaks coming from oxygen are detected. The absence of oxygen in the plasma polymer can be attributed to the very high RF power applied for the polymerization process. [1] Such a high power breaks the molecules of acrylic acid into atomical pieces and oxygen gas is formed as a byproduct. In former research, a much lower RF power was applied so that the original structure of the monomer was better preserved.[1]

Figure 7.6 Positive ToF-SIMS spectrum of PAAS$_8$-2.

Figure 7.7 Negative ToF-SIMS spectrum of PAAS$_8$-2.
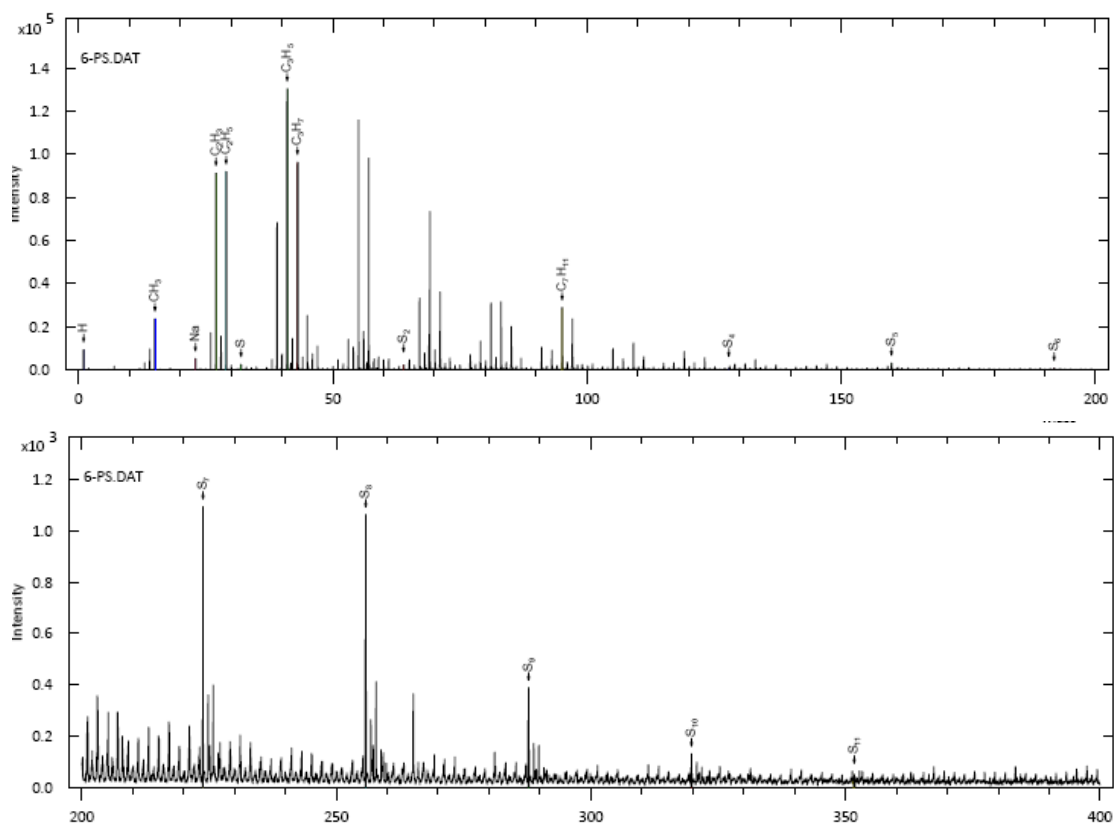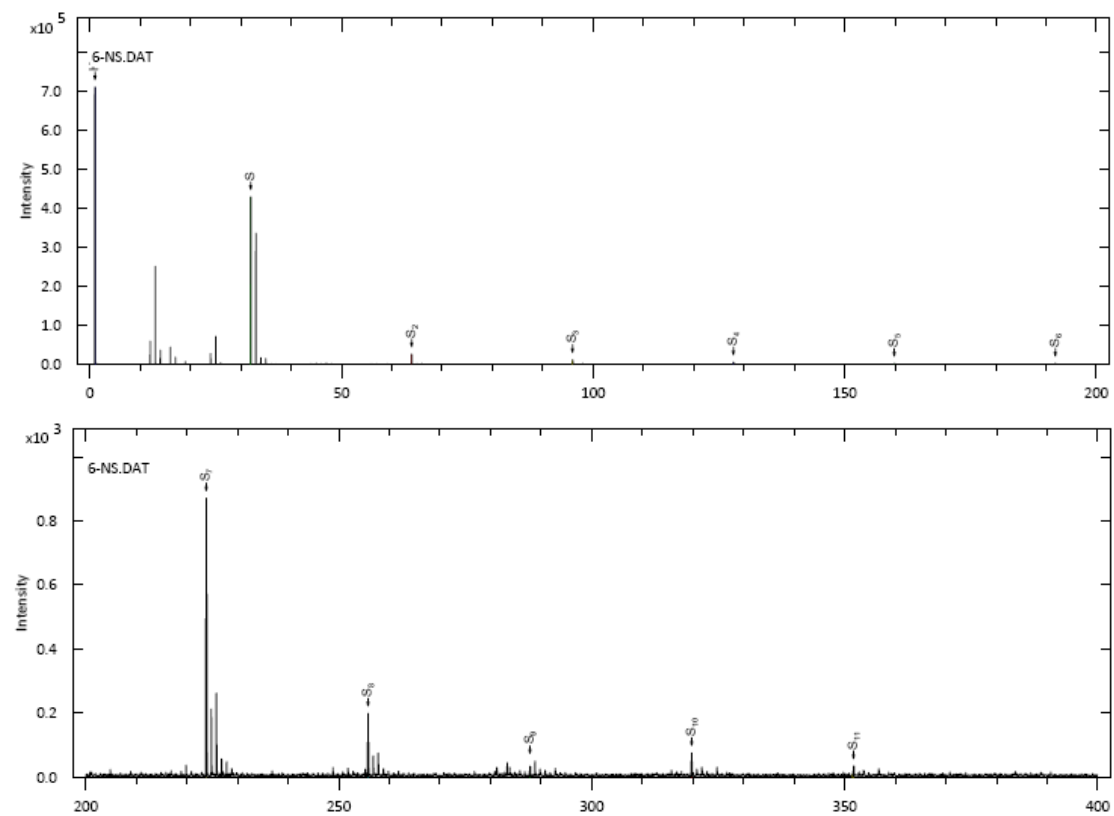
7.3.5 Performance of plasma polyacrylic acid modified sulfur in NE rubber blends

As discussed in Chapter 4, the properties of the NE blends are dominated by the NBR phase which has a much shorter scorch time t_{10} than that of the EPDM phase. The rheograms of the NE blends using polyacrylic acid modified sulfur are represented in Figure 7.8. It can be seen that the NE blends cured with plasma acrylic acid modified sulfur give a very small improvement in the maximum states of cure. Although the plasma acrylic acid modified sulfur has a smell of acrylic acid, which indicates the presence of a tiny amount of acid still present in the coatings, not much scorch delay was obtained.
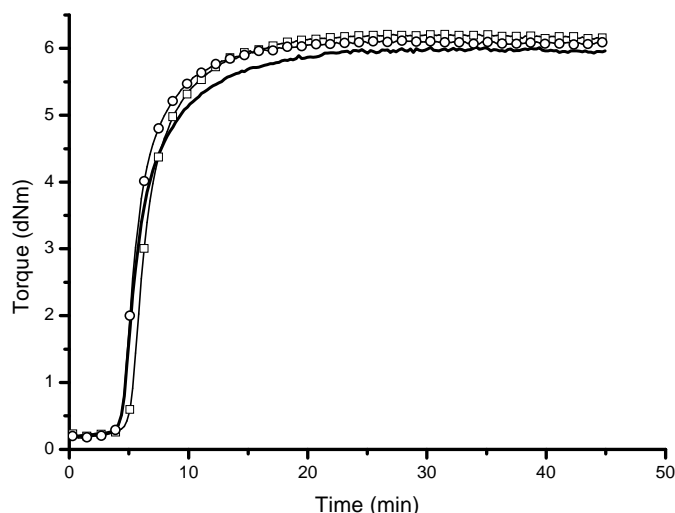
Figure 7.8 Rheograms of the NE blends cured with different sulfur samples: (——) S_8; (—□—) $PAAS_8$-1; (—○—) $PAAS_8$-2.

The tensile strength, elongation at break and 100% modulus of the NE blends cured with the plasma polyacrylic acid coated sulfur samples are given in Figure 7.9. The NE blend cured with uncoated sulfur is used as control. Both $PAAS_8$-1 and $PAAS_8$-2 provide better stress-strain properties compared to the control. A very pronounced increase is even found for $PAAS_8$-2, the sulfur powders treated for 2hrs. The NE vulcanizate cured with $PAAS_8$-2 shows a two times higher tensile strength compared to the control. It also gives a much higher elongation at break compared to the control. It is surprising to observe that a half an hour difference in treatment time can result in

such a large change in the performance of the modified sulfur.
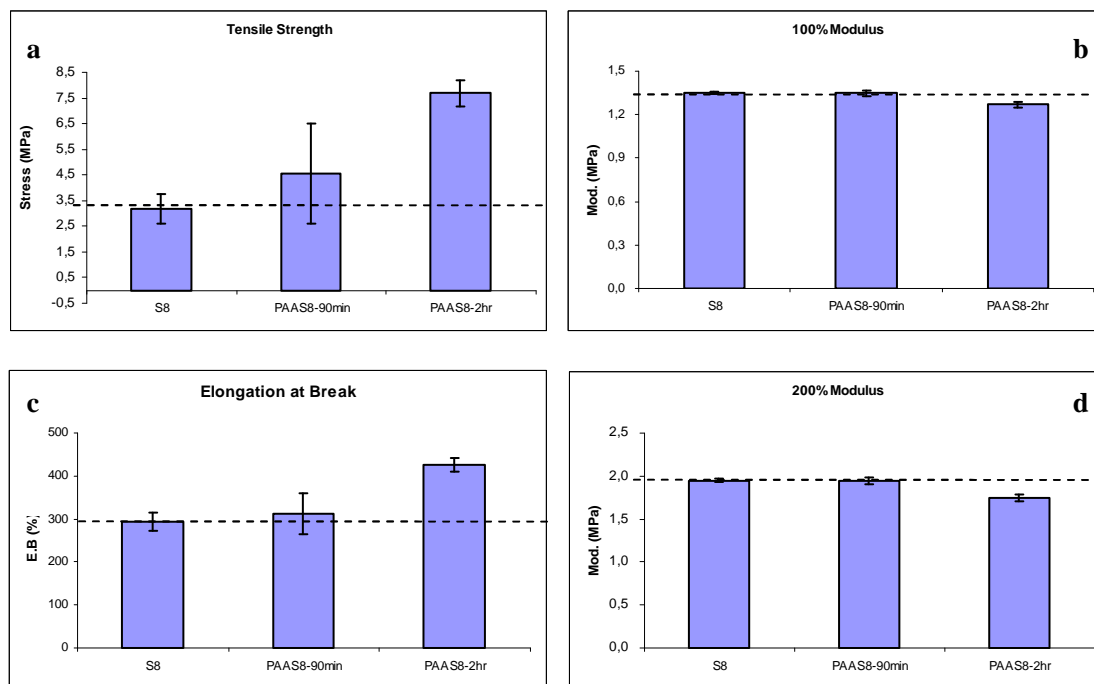
Figure 7.9 Stress-strain properties of the NE blends cured with uncoated and plasma polyacrylic acid coated sulfur samples.

The rupture energies calculated by integrating the areas under the stress-strain curves, as shown in Figure 7.10, are given in Table 7.3. The largest improvement is for $PAAS_8$-2 with an increase of 110 %.

Figure 7.10 Stress-strain properties of NE blends cured with:
(——) S_8; (—□—) $PAAS_8$-1; (—○—) $PAAS_8$-2.

Table 7.3 Rupture energies of the NE blends cured with different sulphur samples.

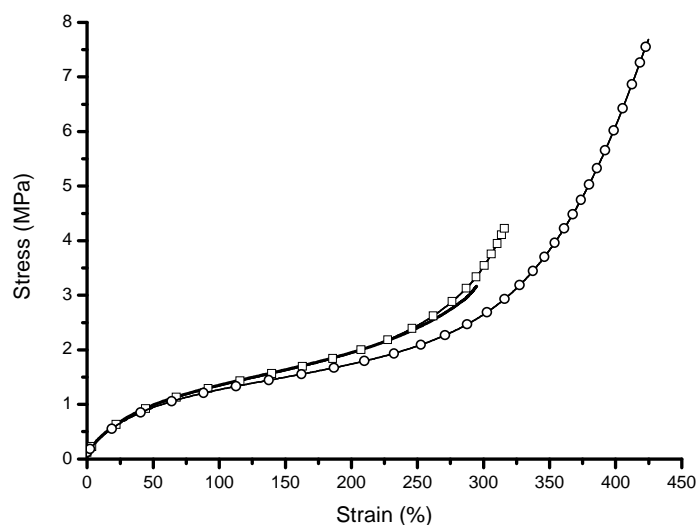| Sample code	Rupture energy (a.u)
S_8	485
$PAAS_8$-90min	571
$PAAS_8$-2hrs	1020

(a.u) = arbitrary units

7.3.6 Solubilities of the plasma polyacrylic acid coated sulfur in NBR and EPDM rubbers

Although the difference in surface energy was not significantly changed by the polyacrylic acid coating, the solubility of the coated sulfur materials was determined as described in Chapter 3. Figure 7.11 shows the weight increase of NBR and EPDM with S_8 and $PAAS_8$ vs. time at 60 ^{o}C. The solubility data of S_8 were taken from literature. [2] It can be seen from Figure 7.11 that $PAAS_8$-1 shows an increased solubility in NBR and a slightly decreased solubility in EPDM. As a result, the solubility differences for sulfur between the NBR and the EPDM rubber are decreased.

On a macroscopic level, treated sulfur is encapsulated in a shell of plasma polymer, whereby its migration into the bulk rubber is hampered during the solubility test. However, on a molecular level, encapsulated sulfur is a kind of mixture of virgin elemental sulfur molecules in the bulk of the sulfur agglomerate, together with treated sulfur molecules at the surface of the agglomerate reacted with tails of plasma polymers of different molecular weight. In case of the solubility of $PAAS_8$, apparently the tails of plasma oligomers which show affinity to NBR are responsible for the improved solubility of plasma treated sulfur in NBR rubber.

By using the plasma treated sulfur, it is expected to have a more balanced distribution of sulfur over the two rubber phases as the solubility differences are minimized as a result of the plasma surface treatment. The outstanding performance of the plasma polyacrylic acid coated sulfur in the NE blend can be partially explained by this solubility change induced by the plasma coating. In addition to the solubility

change, the presence of the plasma polymer shell further reduces the migration of $PAAS_8$ across rubber phases. Finally, the influence of some acidity due to remaining acidic acrylic acid groups in the coating on the vulcanization reaction may also be an influencing factor, as the treated sulfur samples gave a smell of acrylic acid.
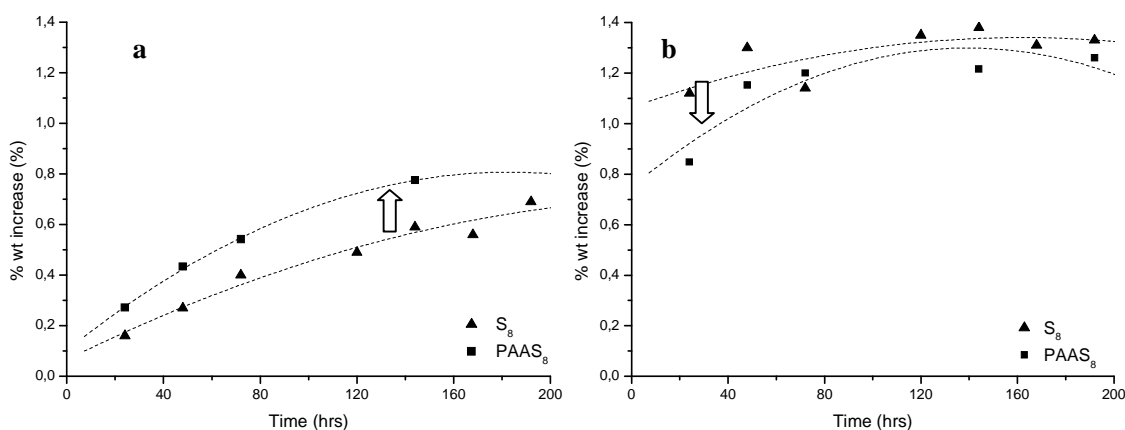
Figure 7.11 Solubility of (▲) S_8 and (■) $PAAS_8$-1 in (a) NBR and (b) EDPM at 60 °C.

7.4 Conclusions

It has been shown that the properties of the NE blends can be greatly improved by using plasma polyacrylic acid modified sulfur. A treatment time of 2 hrs under the conditions used, seems to be required to obtain the outstanding performance of the plasma polyacrylic acid coated sulfur. Using the plasma polyacrylic acid coated sulfur as curing agent reduces the solubility difference between the NBR-phase and the EPDM-phase. Consequently, a more homogeneous distribution of sulfur is expected to occur. As the coating also reduces the migration tendency of the sulfur, a better covulcanization is the result. The high polarity and acidity of acrylic acid may also account for the noteworthy increase in properties of the NE blends.

7.5 References

[1]   W.J. van Ooij, private communication.

[2]   R. Guo, A.G. Talma, R.N. Datta, W.K. Dierkes, J.W.M. Noordermeer, *Eur. Pol. J.,* **2008**, 44, 3890.

Chapter 8

Plasma Polymer Encapsulated Curatives

in Carbon Black Reinforced Rubber-Rubber Blends

In the previous chapters, it was proved that by surface modification by plasma polymers of curatives, the properties of unreinforced 50/50 SBR/EPDM (SE) and NBR/EPDM (NE) blends could be improved. In this chapter, different plasma polymer-treated curatives (sulfur and CBS) are applied in carbon black reinforced SE and NE blends. The effects of the plasma coating on the performance of the curatives as found in the unreinforced polymer blends were reproduced in the presence of carbon black. By using the plasma polymer-treated curatives, the same range of increase in tensile values was obtained for both unreinforced and carbon black reinforced SE blends. Interestingly, a higher improvement in mechanical properties was achieved for the carbon black reinforced NE blends than for the SE blends, opposite to what was observed for the unreinforced systems.

8.1 Introduction

Carbon black is essentially elemental carbon in the form of extremely fine, nano-scale particles having a partially amorphous structure among microcrystalline areas of condensed aromatic rings. [1] The reinforcement of carbon black comes from entanglements with the polymers in the rubber network and mechanical interlocking between carbon black aggregates. Gent and Hartwell [2] state that relatively strong bonds appear to be formed between rubber molecules and the surface of carbon black particles, which can withstand swelling stresses and temperatures up to 120 ^{o}C. The dispersion of carbon black in rubber, as obtained in the mixing operation, is well known to be of paramount importance for the final properties of the rubber after vulcanization. When carbon black is applied in a rubber-rubber blend, it will not be homogeneously dispersed. Instead, all black tends to become concentrated in the more unsaturated, somewhat more polar rubber phase. [3]

In the previous chapters different plasma polymer-treated curatives were applied in unreinforced 50/50 w/w SE and NE rubber blends. Improved properties of these blends were achieved by using the plasma-coated curatives (either sulfur or CBS) compared to the ones cured with uncoated curatives. In this chapter, carbon black (N550) is applied as most logical choice based on the reinforcement requirements for EPDM rubber. It is expected that the whole system of curing rubber-rubber blends with plasma-coated curatives becomes more complicated when carbon black is incorporated into the compounds, especially at a carbon black content of 40 phr, as is quite common in rubber technology. The aim of the work presented in this chapter is therefore to check the performance of the plasma-polymer surface modified curatives in carbon black reinforced rubber-rubber blends.

8.2 Experimental Part

8.2.1 Materials

The following types of rubber were used: Solution Styrene-Butadiene rubber (S-SBR, Buna$^{®}$ VSL 5025-0HM from LANXESS Corp., Germany), Acrylonitrile-Butadiene

rubber (NBR, Perbunan® 3446F from LANXESS Corp.), and Ethylene-Propylene-Diene rubber (EPDM, Keltan® 4703 from DSM Elastomers, the Netherlands). Zinc-oxide was purchased from Sigma Aldrich; stearic acid was from Aldrich, Germany and carbon black (N550) from Cabot, the Netherlands, was used as received. Accelerator N-cyclohexylbenzothiazole-2-sulphenamide (Santocure® CBS) and antioxidant oligomeric 2,2,4-Trimethyl-1,2-dihydroquinoline (Flectol® TMQ) were both provided by Flexsys, Belgium. Elemental sulfur (S_8) was purchased from Sigma Aldrich, with a particle size smaller than 100 mesh (150 μm). The different plasma polymer-coated curatives, which were applied in the carbon black reinforced rubber blends, are listed in Table 8.1. The codings of $PPAS_8$ and PPACBS correspond to the $PPAS_8$-3 and PPACBS-1 in Chapter 5, respectively; $PFHS_8$ and PFHCBS correspond to $PFHS_8$-90min and PFHCBS-2hrs in Chapter 6, respectively; and $PAAS_8$ corresponds to $PAAS_8$-1 in Chapter 7.

Table 8.1 Curatives being surface modified with plasma polymers

Sample Code	Plasma-treatment conditions			
	Monomer	**RF power**	**Monomer concentration**	**Reaction time**
$PPAS_8$	Acetylene	150 W	26 Pa	90 mins.
PPACBS	Acetylene	150 W	29 Pa	90 mins.
$PFHS_8$	Perfluorohexane	180 W	27 Pa	90 mins.
PFHCBS	Perfluorohexane	180 W	27 Pa	2 hrs
$PAAS_8$	Acrylic acid	180 W	27 Pa	90 mins.

8.2.2 Methods

a. Rubber mixing and testing

The compound formulations of the SE and the NE blends are given Table 8.2. The mixing and testing procedures are similar to those described in Chapter 4, with some difference in the mixing in the internal mixer. Taking the mixing procedure of SE

blends as example, this blend is prepared by pre-mixing of SBR and EPDM rubbers. After 3 mins. half the amount of the carbon black was added together with the ZnO, stearic acid and TMQ. After another 3mins. of mixing, the other half of the amount of carbon backed was incorporated. The mixing was stopped after 10 mins. of total mixing time. NE blends were prepared with the same procedure as described for the SE blend.

b. Crosslink density measurements

As described in Chapter 6.

Table 8.2 General compound formulations of the SE and NE blends.

Component	Amount (phr)	
	SE	**NE**
SBR	50	0
NBR	0	50
EPDM	50	50
ZnO	5	5
Stearic acid	2	2
TMQ	1	1
Carbon Black (N550)	40	40
Sulfur	2.5	2.5
CBS	1.7	1.7

8.3 Results and Discussion

8.3.1 Plasma polymer-coated curatives in carbon black reinforced SE blends

It was demonstrated in Chapter 6 that the curative package of plasma perfluorohexane-coated sulfur together with uncoated CBS substantially increases the mechanical properties of unreinforced SE blends. This curing package is therefore chosen for a trial in carbon black reinforced SE blends, to check the influence of the

presence of carbon black on the performance of plasma-treated curatives.

It can be seen from the rheograms in Figure 8.1 and the stress-strain curves in Figure 8.2 that no appreciable differences in properties are obtained for the carbon black reinforced SE blend, whether straight sulfur or PFH-coated sulfur is applied. Apparently the presence of carbon black in the SE blend undoes the effect of the plasma coating on the properties of such a blend.
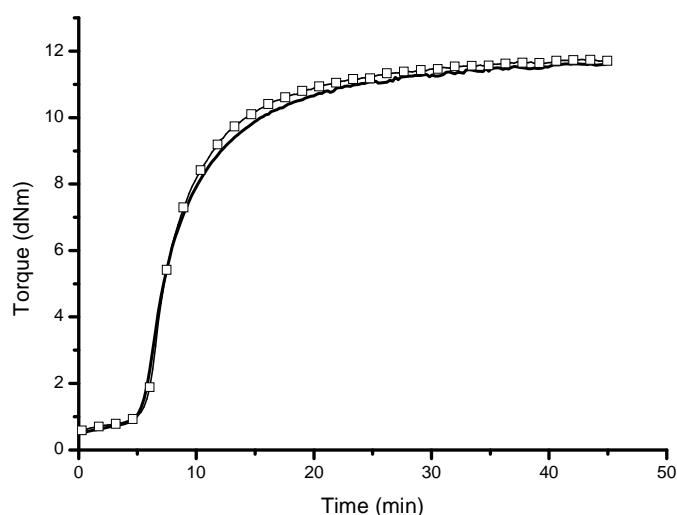

Figure 8.1 Rheograms of the carbon black reinforced SE blends cured with:
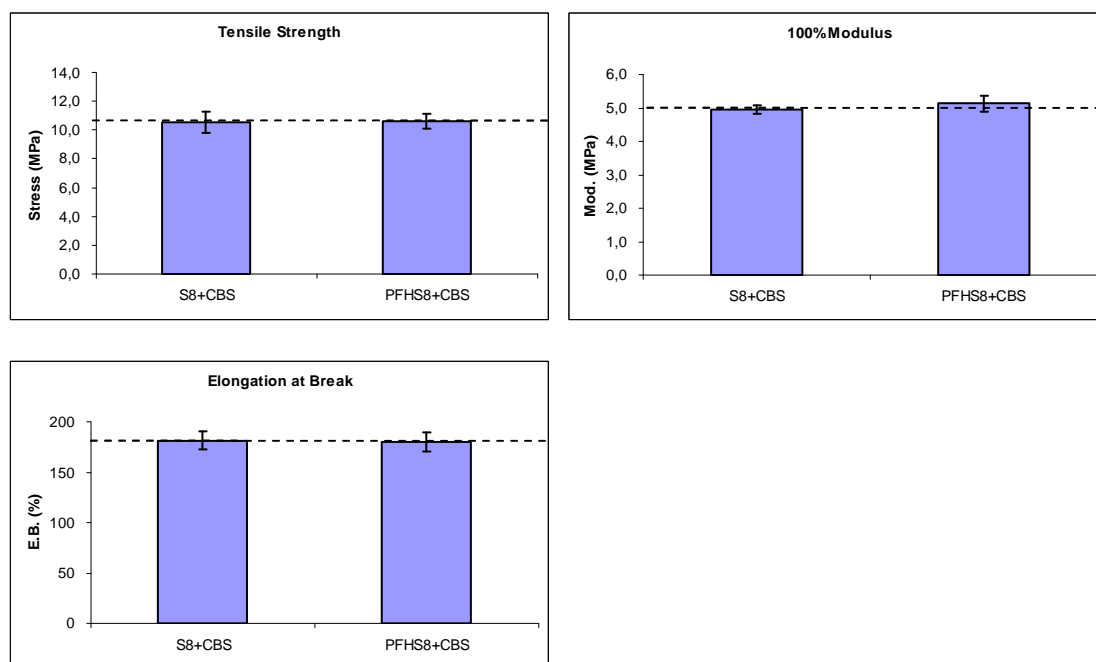(——) S_8+CBS; (—□—) PFHS$_8$+CBS.

Figure 8.2 Stress-strain properties of the carbon black reinforced SE blends cured with different sulfur samples.

To overcome the negative influence of carbon black on the plasma-coated curatives, different curing packages of sulfur and CBS, both modified with various plasma polymers were tested. The curative package of uncoated sulfur and uncoated CBS was used as control. The different curing packages applied in the carbon black reinforced SE and NE blends are listed in Table 8.3.

Table 8.3 Different curative packages applied in the carbon black reinforced SE and NE blends.

No.	Curatives combinations	Sample Code
1	Plasma perfluorohexane-treated sulfur Plasma perfluorohexane-treated CBS	$PFHS_8$+PFHCBS
2	Plasma acetylene-treated sulfur Plasma perfluorohexane-treated CBS	$PPAS_8$+PFHCBS
3	Plasma acetylene-treated sulfur Plasma acetylene-treated CBS	$PPAS_8$+PPACBS
4	Plasma perfluorohexane-treated sulfur Plasma acetylene-treated CBS	$PFHS_8$+PPACBS
5*	Plasma acrylic acid-treated sulfur Plasma perfluorohexane-treated CBS	$PAAS_8$+PFHCBS
6*	Plasma acrylic acid-treated sulfur Plasma acetylene-treated CBS	$PAAS_8$+PPACBS

5 and 6, which contain $PAAS_8$, are only applied in the NE blends based on the results of Chapter 7.

The rheograms of the carbon black reinforced SE blends cured with the different curative packages together with the control are given in Figure 8.3. Compared to the control all the packages of modified curatives provide a slight decrease in maximum torque. The lowest value is found for ($PFHS_8$+ PFHCBS). Except for ($PFHS_8$+ PFHCBS), the other cure packages of the modified curatives give a slightly longer
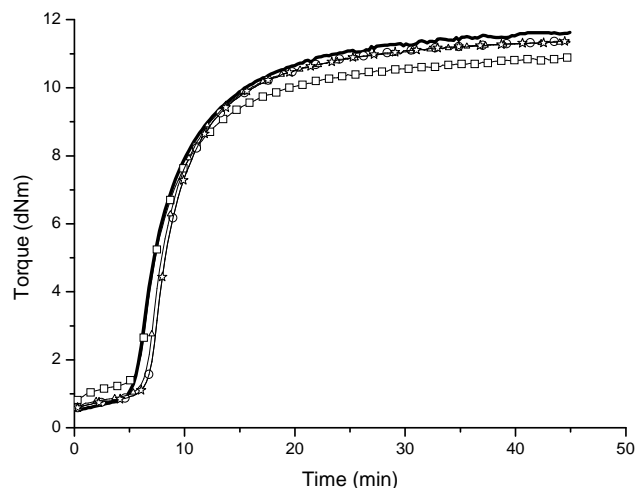
scorch delay compared to the control.

Figure 8.3 Rheograms of the carbon black reinforced SE blends cured with:
(——) control; (—□—) PFHS$_8$+PFHCBS; (—○—) PPAS$_8$+PFHCBS;
(—△—) PPAS$_8$+PPACBS; (—☆—) PFHS$_8$+PPACBS.

The stress-strain properties of the carbon black reinforced SE blends are given in Figure 8.4. Compared to the control, the packages of plasma polymer-modified curatives show appreciably improved tensile strength and elongation at break values. The 200% moduli (M_{200}) of the SE blends cured with plasma polymer-modified curative packages are more than double, compared to the M_{100} of the control, whereas for the control itself no M_{200} is measurable because the elongation at break is less than 200%.

Interestingly, compared to the unreinforced SE blends described in Chapters 5 and 6, the absolute increase in tensile strength falls in the same range of 2-3 MPa for the carbon black reinforced SE blends as well. It is clear, that for the reinforced SE blends, apart from the reinforcing effect of carbon black which increased the tensile strength from a value of 2.5 MPa to 10.0 MPa, the plasma polymer coating provides the same effect on raising the tensile strength as in the unreinforced SE blends.

It has been reported that filler distribution plays a much more important role than the degree of crosslinking in dissimilar rubber-rubber blends containing EPDM. [4,5] The reason why the improvements in properties are still obtained for the carbon black

filled SE blends could therefore be related to a more homogeneous distribution of the carbon black throughout the rubber phases. The crosslinked plasma polymer layer is known to contain radicals trapped in the network of crosslinks between the plasma polymer molecules. These could possibly influence the dispersion of carbon black in the rubber blends. Further investigations are needed to clarify this point in more detail.
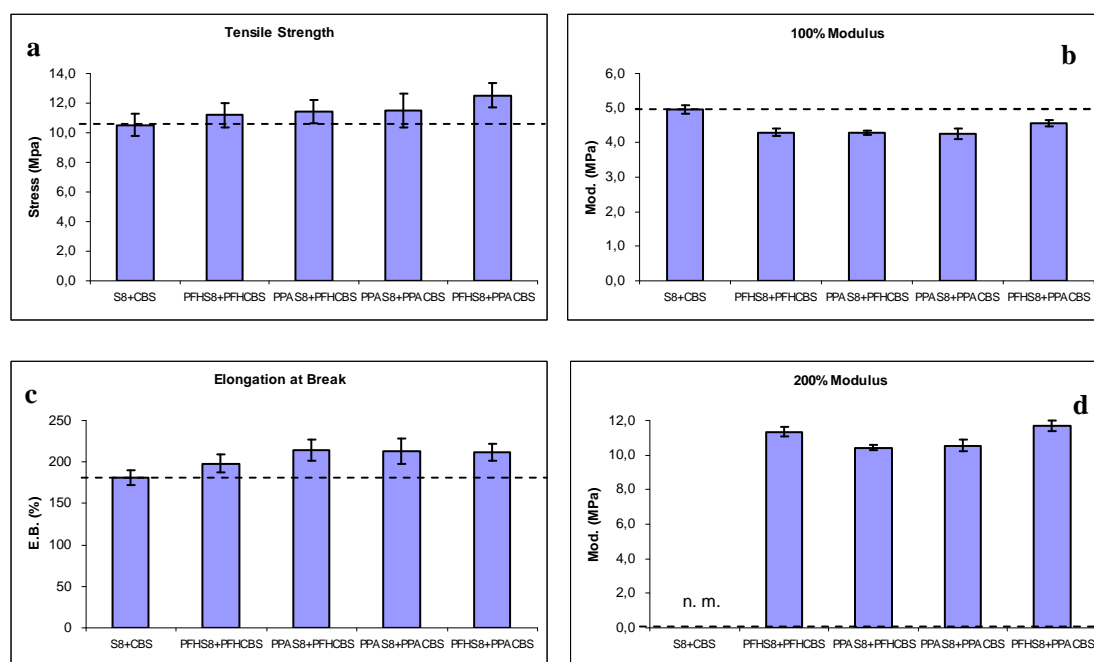
Figure 8.4 Stress-strain properties of the carbon black reinforced SE blends cured with different curative packages.

The rupture energies of the carbon black reinforced SE blends, calculated from the area underneath the full tensile curves in Figure 8.5, are given in Table 8.4. The packages of curatives treated with plasma polymers, all give improved rupture energies. The highest rupture energy is obtained for the combination $PFHS_8+PPACBS$, with an increase of 33% compared to the control.

The crosslink densities of the SE blends cured with different cure packages are also summarized in Table 8.4. No differences exist among the different SE vulcanizates.

Figure 8.5 Stress-strain properties of the carbon black reinforced SE blends cured with:
(——) control; (—□—) PFHS$_8$+PFHCBS; (—○—) PPAS$_8$+PFHCBS;
(—△—) PPAS$_8$+PPACBS; (—✳—) PFHS$_8$+PPACBS.

Table 8.4 Rupture energies and crosslinking densities of the carbon black reinforced
SE blends cured with different curing packages.

Sample code	Rupture energy (a.u)	Crosslink density (%)
Control	876	99.3
PFHS$_8$+PFHCBS	959	99.3
PPAS$_8$+PFHCBS	1107	99.2
PPAS$_8$+ PPACBS	1088	99.3
PFHS$_8$+PPACBS	1163	99.4

(a.u) = arbitrary units

8.3.2 Plasma polymer-coated curatives in carbon black reinforced NE blends

The rheograms of the carbon black reinforced NE blends cured with different curative packages are given in Figure 8.6 together with the control. Compared to the control, all packages of the modified curatives provide an increased maximum torque, opposite to the situation in the SE blends.
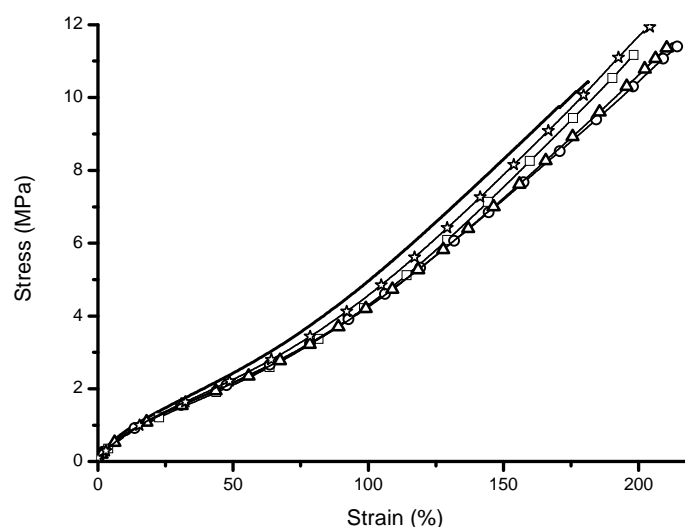
Figure 8.6 Rheograms of the carbon black reinforced NE blends cured with:
(——) control; (—□—) PFHS$_8$+PFHCBS; (—○—) PPAS$_8$+PFHCBS; (—△—) PPAS$_8$+ PPACBS;
(—☆—) PFHS$_8$+PPACBS; (—⊠—) PAAS$_8$+PFHCBS; (—■—) PAAS$_8$+PPACBS.

The tensile strength, elongation at break and moduli of the NE blends cured with different combinations of modified curatives are presented in Figure 8.7. The NE blends cured with the modified curative packages show pronounced improvements in tensile strength and elongation at break values. The 200% moduli of the NE blends cured with plasma-treated curatives are doubled by using the modified curative packages, compared to the 100% modulus of the control, as the 200% modulus of the control is are not measurable by lack of sufficient elongation at break.

Figure 8.7 Stress-strain properties of the carbon black reinforced NE blends cured with different curative packages.

Plasma polymer-treated sulfur, in general, provides more effect in improving the properties of unreinforced NE blends than plasma polymer-treated CBS, as was demonstrated in Chapters 5, 6 and 7. It was further shown in Chapter 7 that the plasma acrylic acid coated sulfur provided the best properties of the unreinforced NE blends. Therefore, it is logical to observe the highest tensile strength and elongation at break for the $PAAS_8$+ PPACBS combination in the carbon black reinforced NE blends as well, see Figures 8.7a and b. It is further surprising that more significant improvements are achieved for the carbon black reinforced NE blends than for the carbon black reinforced SE blends.

The rupture energies calculated by integrating the area under the full stress-strain curves, in Figure 8.8, are given in Table 8.5. The largest improvement is obtained for the cure package of $PAAS_8$+ PPACBS with an increase of 90 %.
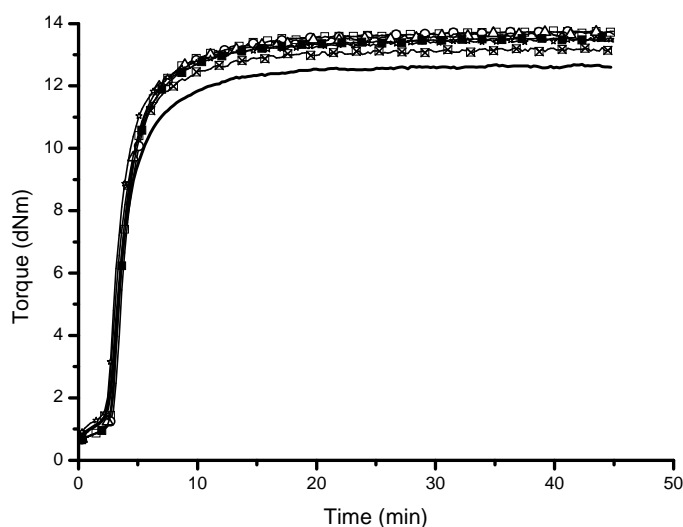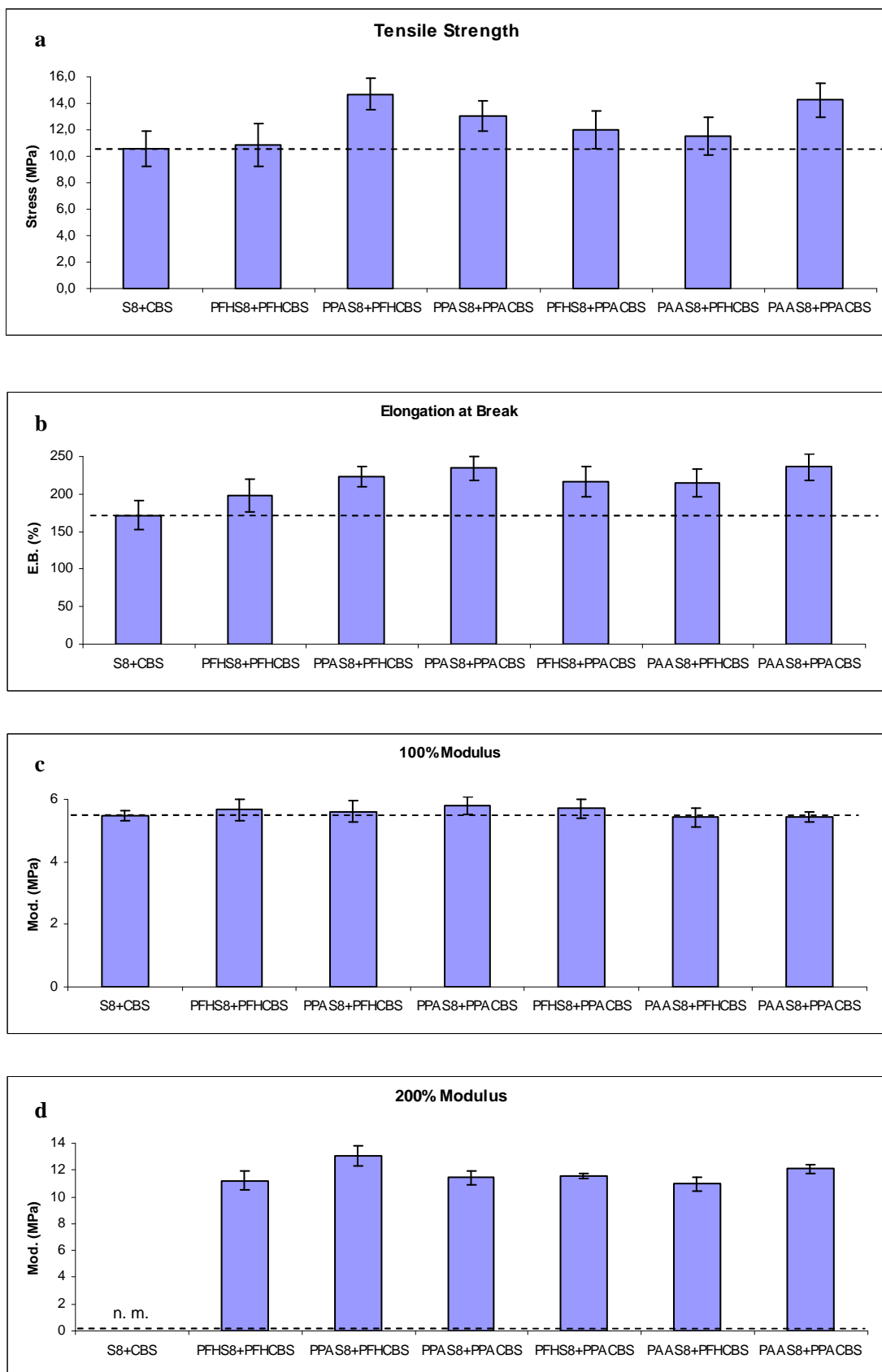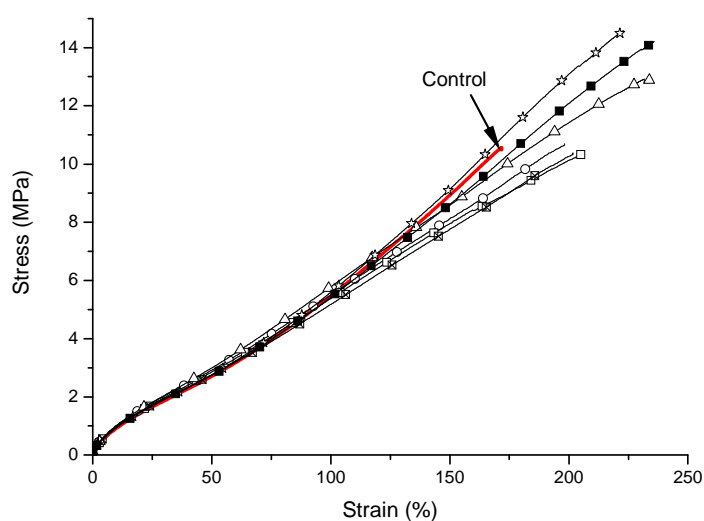

Figure 8.8 Stress-strain properties of the carbon black reinforced NE blends cured with: (——) control; (—□—) $PFHS_8$+PFHCBS; (—○—) $PPAS_8$+PFHCBS; (—△—) $PPAS_8$+ PPACBS; (—☆—) $PFHS_8$+PPACBS; (—⊠—) $PAAS_8$+PFHCBS; (—■—) PAAS8+PPACBS.

The crosslink densities of the NE blends cured with the different curative combinations are also summarized in Table 8.5. As no appreciable differences were obtained in the levels of crosslink density of the different vulcanizates, the improvements in the mechanical properties indicate a more balanced distribution of

crosslinks over the rubber phases along with a more homogeneous carbon black dispersion over the different rubber phases.

Table 8.5 Rupture energies and crosslink densities of the carbon black reinforced NE blends cured with different curative packages.

Sample code	Rupture energy (a. u)	Crosslink density (%)
Control	851	99.3
$PFHS_8$+PFHCBS	1094	99.0
$PPAS_8$+PFHCBS	1341	99.0
$PPAS_8$+PPACBS	1586	99.1
$PFHS_8$+PPACBS	1526	99.2
$PAAS_8$+ PFHCBS	1266	98.9
$PAAS_8$+ PPACBS	1621	99.2

(a.u) = arbitrary units

Although a general increase is achieved for all combinations of curatives, the degree of improvement is not same among the different curative combinations. Clearly, the nature of the monomer applied for the plasma treatment also plays an essential role in determining the performance of the treated curatives. A possible change in distribution of carbon black in the dissimilar blends may have resulted from its interaction with the plasma polymer coating. It can be stated that the improvement in the properties of carbon black reinforced rubber blends may not simply be due to improved co-vulcanization. Further investigation is again necessary to obtain a clear insight in all phenomena involved.

8.4 Conclusions

In the carbon black reinforced SE blends, it was not possible to obtain increased blend mechanical properties by using plasma perfluorohexane-modified sulfur with unmodified CBS as curative package. However, appreciable improvements in

properties were realized by using a vulcanization package of curatives, where both are modified with a plasma polymer coating. Even larger improvements were achieved in the carbon black reinforced NE blends. This is opposite to the situation as was observed for the unreinforced rubber blends. It is clear that the more or less homogeneous distribution of carbon black over the different rubber phases, possibly influenced by the plasma polymer coating on the curatives, plays an important role here as well. More investigations are needed to elucidate the mechanisms behind these changes.

8.5 References

[1]   Y. Schwob, *Rev. Gen. Caout. Plast.*, **1994**, 71, 70.

[2]   A.N. Gent, J.A. Hartwell, *Rubber Chem. Technol.,* **2003**, 76, 517.

[3]   T. Mathew, Ph.D. Thesis, University of Twente, Enschede, the Netherlands, 2008.

[4]   P.M. van de Ven, J.W.M. Noordermeer, Rubber World, September, **2000**, 55.

[5]   H. Zhang, Ph.D. Thesis, University of Twente, Enschede, the Netherlands, 2009.

Chapter 9

Blooming Study on sulfur in Natural Rubber

It was demonstrated in the previous chapters that the performance of sulfur, after being surface-modified with plasma polymers, shows an improved performance in dissimilar rubber blends.

It was of interest to carry out a blooming study to check the influence of a plasma polyacetylene and plasma polyperfluorohexane coating on the blooming behavior of sulfur. Plasma encapsulated sulfur is capable of eliminating blooming and provides especially better performance than insoluble sulfur when the compounds are processed at higher temperatures.

9.1 Introduction

"Blooming" is the exudation and commonly crystallization of compounding ingredients on the surface of a cured or uncured piece of rubber. It happens only when a partly soluble additive is used at a level in excess of its solubility at a given temperature. Crystallization may be energetically more favorable at the surface of the rubber than in the bulk. As crystallization occurs at the surface, a concentration gradient between the layer immediately underneath the surface (a saturated "solution") and the bulk of the rubber (a supersaturated "solution") exists. Consequently, further blooming will occur at the surface until the concentration of the component reaches the solubility limit throughout the whole article. The solutions of ingredients in rubber are similar in nature to solutions in low-molecular weight liquids but more stable. [1,2]

Blooming is useful in some cases; -e.g. films formed on a surface as a result of blooming protect rubber from aging. The antioxidants and waxes protect vulcanized rubber from ozone aging by forming coatings by blooming. [2, 3]

However, in the production of e.g. tires and belts, blooming reduces the tackiness of the stock, which causes difficulties in forming multi-ply articles. In the production of molded articles blooming of ingredients causes non-uniform stresses to be built in. Blooming also results in stains on overcoat fabric, on the surface of colored rubbers and so on. Especially, the blooming of sulfur (S_8) is often desired to be suppressed, as this vulcanizing agent considerably reduces the adhesiveness and stickiness of unvulcanized rubber. [2, 4]

It is claimed that sulfur blooming can be limited by the use of insoluble sulfur. Insoluble sulfur is, by definition, sulfur that is insoluble in carbon disulfide. It is generally understood that insoluble sulfur has a polymeric structure. The polymer chains are consisting of up to several thousand sulfur atoms. It is different from soluble sulfur, which is in crystalline form. Although the use of insoluble sulfur eliminates blooming, the drawback of it is that at the transition temperature of about 105 ^{o}C -110 ^{o}C, insoluble sulfur converts into soluble sulfur (S_8) and loses its effect in bloom reduction. It is usual in practice that a calendar or extrusion speed has to be

decreased to keep the temperature of the rubber compound below this transition temperature. This results in a drop in productivity and the dispersibility of insoluble sulfur is also deteriorated. [4, 5]

The conversion rate of insoluble sulfur into soluble sulfur is normally accelerated in the presence of oil with a weight percent of 1-30%. Young and Randall claimed that insoluble sulfur can be stabilized by adding elemental iodine to the oil. [5]

Besides the method of using insoluble sulfur to reduce blooming, Hoshino et al. [4] claimed that the use of metal-alkylxanthate as a surface-active agent and thus capable of keeping the supersaturated sulfur within the rubber composition in a coagulated form, is also effective in reducing sulfur bloom. They claim a preferred amount of 0.5 - 5%. Another patented method describes the use of sulfur donors, which have the difficulty to be expensive, which limits their use. [4]

Another serious problem caused by the use of soluble sulfur in rubber formulations is that of bin scorch. So-called "bin scorch" occurs for uncured rubber stocks when kept in storage after having been fully compounded. As the uncured rubber composition is temperature sensitive, curing, i.e. crosslinking, may be prematurely initiated to some extent when the storage temperature is not properly controlled. [5]

As demonstrated in the previous chapters, the surface properties of sulfur can be altered by plasma polymerization. The objective of this study is to check whether plasma coatings of sulfur with polyacetylene and polyperfluorohexane may also have a positive reducing effect on the tendency of sulfur blooming.

9.2 Experimental Part

9.2.1 Materials

Natural rubber (NR SMR CV) was used. Zinc-oxide was purchased as commercial grade from Sigma Aldrich; stearic acid was also obtained from Sigma Aldrich. N-cyclohexylbenzothiazole-2-sulphenamide (Santocure® CBS) and insoluble sulfur (Ctx HS OT 20) were provided by Flexsys, Belgium. Carbon black (N330) was provided by Cabot, the Netherlands. Rubber makers sulfur (S_8) was purchased from

Sigma Aldrich, with a particle size smaller than 100 mesh (150 μm). S_8 was surface modified with plasma polyacetylene polymer in the experimental set-up as described in Chapter 5, with 150W power, 31 Pa monomer pressure during 60 mins: coded PPAS$_8$. S_8 was surface modified by plasma polyperfluorohexane polymer, with 180W power, 27 Pa monomer pressure and 90 mins: coded PFHS$_8$. The formulations of the different rubber compounds used in this study are given in Table 9.1. According to Brimblecombe, [6] the solubility of sulfur in NR is below 2 phr at room temperature. Consequently, the dosage of sulfur used in the NR compound is far above its solubility limit. This high amount of sulfur accelerates the blooming process to a reasonable observation time period.

Table 9.1 Formulations of NR compounds (phr).

Ingredient	1-S$_8$	2-IS	3-PPAS$_8$	4-PFHS$_8$
NR	100	100	100	100
Carbon black (N330)	50	50	50	50
ZnO	5	5	5	5
Stearic acid	2	2	2	2
CBS	1	1	1	1
S$_8$	7	-	-	-
Ctx HS OT 20	-	8.75	-	-
PPAS$_8$	-	-	7	-
PFHS$_8$	-	-	-	7

9.2.2 Methods

9.2.2.1 Masterbatch preparation

A natural rubber masterbatch was prepared in an internal mixer (5L Intermix). The mixer temperature was set at 50 $^{\circ}$C. A load factor of 70% and a rotor speed of 33 rpm were used. The elastomer was added at 0 min. After 1 minute of mastication, ZnO, stearic acid and half the amount of the carbon black were added. The other half

amount of carbon black was added at 2.5 min. Sweeping was done at 4 min. and the compound was dumped at 5 min. The dump temperature was in the range of $140\,^{o}$C to $160\,^{o}$C.

9.2.2.2 Heat treatment and blooming observation

To mimic situations of real production processes in a calendar or extruder, a temperature treatment was carried out in a 390 ml Brabender Plasticorder internal mixer at respectively $110\,^{o}$C, $120\,^{o}$C and $130\,^{o}$C. The rotor speed was set at 30 rpm. The curatives were added after 3 minutes plastization of the masterbatch. The compound was dumped at 6 minutes and quickly sheeted out on a Schwabenthan two roll mill (15×33 cm, Polymix 80) with a friction ratio of 1:1.25. Then the sheet was placed on an aluminium foil, without touching the top surface. The development of blooming was observed during storage at room temperature after certain time intervals: 15min., 2hours, 1day, 2days, 6days, 2weeks, and 3weeks. Scorch times were measured with a Mooney viscometer (MV-2000) from Alpha Technologies.

9.3 Results and Discussion

9.3.1. Blooming rate of sulfur after heat treatment at 110 ^{o}C in the Brabender

The incorporation of curatives was intentionally performed in the internal mixer instead of on a two roll mill in order to mimic real production processes in a calendar or extruder, where heat builds up before curing takes place. The heat treatment will greatly accelerate the blooming of sulfur and make it proceed in a reasonable time period for observation.

The control (compound 1-S_8), as expected, shows the worst blooming phenomena, as can be seen in Figure 9.1. The total surface was covered with crystallized sulfur after 3 weeks of storage at RT, which gave the surface a kind of silver-white appearance.

Figure 9.1 Compound 1-S_8 plasticized at 110 ^{o}C after 3 weeks storage at RT.

Blooming was significantly reduced in compound 2-IS, as shown in Figure 9.2: only a few dots of bloomed sulfur appeared after three weeks. These results are in accordance with what is widely known in the rubber industry, that the distribution of insoluble sulfur remains unchanged after dispersion. There is no concentration gradient formed and migration does not occur.

Figure 9.2 Compound 2-IS plasticized at 110 ^{o}C after 3 weeks storage at RT.

The images of compounds 3-$PPAS_8$ and 4-$PFHS_8$ are shown in Figure 9.3 and Figure 9.4, respectively. It is clear that $PPAS_8$ and $PFHS_8$ show a somewhat reduced blooming compared to S_8, however not as good as insoluble sulfur. Compound 4-$PFHS_8$ has a better blooming performance compared to compound 3-$PPAS_8$.

Figure 9.3 Compound 3-PPAS$_8$ plasticized at 110 ^{o}C after 3 weeks storage at RT.
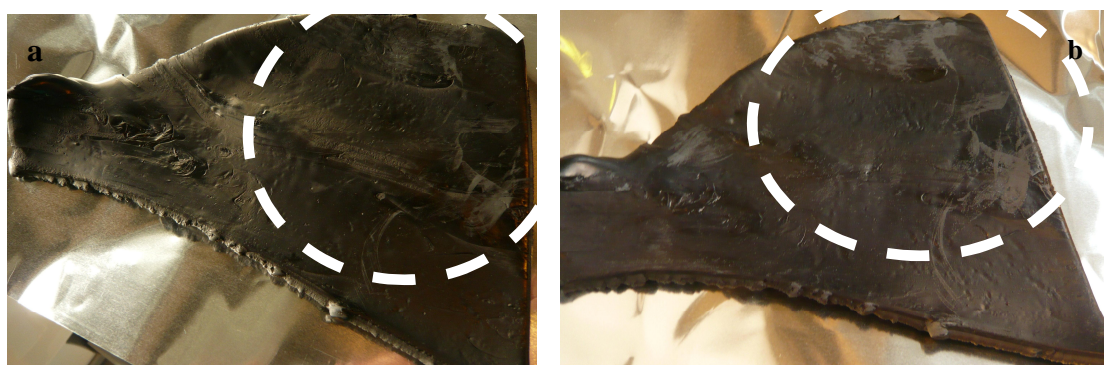

Figure 9.4 Compound 4-PFHS$_8$ plasticized at 110 ^{o}C, after (a) 2 hours; (b) 3 weeks storage at RT.

The blooming rates of the different NR compounds after plastization at 110 ^{o}C for 6 mins. are summarized in Table 9.2. Although there was some increase in temperature for all compounds relative to the set temperature of the mixer, as indicated by the increased temperature after 3 mins. plastization, a much higher increase in temperature was found for compound 4-PFHS$_8$. For compound 1-S$_8$, blooming is clearly getting worse with time, which is a sign of continuous migration of sulfur from the bulk to the compounds' surface. This was much less for the other three compounds. In these compounds the migration of sulfur is reduced or even prohibited. For insoluble sulfur, it is the bulky molecular structure, which stops the diffusion. In case of the plasma polymer coated sulfur, it is due to the coating, which limits the migration of sulfur. The plasma polymer itself has a high molecular weight and has a

better compatibility with the rubber polymers compared to sulfur. Overall, as long as the sulfur aggregates are sealed in the plasma polymer shell, blooming is eliminated.

Table 9.2 Blooming rate of NR compounds after treatment at ~110 ^{o}C.

Compound/properties	1-S$_8$	2-IS	3-PPAS$_8$	4-PFHS$_8$
Set temperature (^{o}C) of Brabender	100	100	100	100
Measured temperature (3min.)	104	106	108	118
Measured temperature (6min.)	107	108	109	119
Bloom at:				
15 min.	Δ	0	0	Δ
2 hrs.	Δ	0	0	Δ
1 day	✕	0	Δ	Δ
2 days	✕	0	Δ	Δ
6 days	✕✕	0	Δ	Δ
2 weeks	✕✕	0	✕	Δ
3 weeks	✕✕	Δ	✕	Δ

0 : *no bloom*

Δ : *bloom on a tiny part of the surface*

✕ : *bloom on quite some areas of the surface*

✕✕ : *bloom on total surface*

9.3.2. Blooming rate after heat treatment at 120 ^{o}C in the Brabender

The bloom rates of the different NR compounds plasticized at 120 ^{o}C are presented in Table 9.3. Compared to the same compounds treated at 110 ^{o}C, compound 1-S$_8$ and 2-IS show similar blooming rates, compound 3-PPAS$_8$ shows a reduced blooming rate. Compound 4-PFHS$_8$ was scorched after the heat treatment and could not be processed

further on the two-roll mill. Apparently, $PFHS_8$ accelerates the vulcanization of NR, similar to its scorch reduction observed for SBR and EPDM in Chapter 6.

Table 9.3 Blooming rate of NR compounds after treatment at ~120 °C.

Compound/properties	1-S_8	2-IS	3-$PPAS_8$
Set temperature (°C) of Brabender	110	110	110
Measured temperature (3min.)	n.m.	118	116
Measured temperature (6min.)	n.m.	120	117
Bloom at:			
15 min.	✕	0	0
2 hrs.	✕	0	0
1 day	✕	0	Δ
2 days	✕✕	0	Δ
6 days	✕✕	0	Δ
2 weeks	✕✕	0	Δ
3 weeks	✕✕	0	Δ

Symbols as in Table 9.2.

n.m.: not measured.

9.3.3. Blooming rate after heat treatment at 130 °C in the Brabender

The bloom rates of the different NR compounds plasticized at 130 °C are given in Table 9.4. Due to the high processing temperature of 130 °C, IS has lost its bloom reduction properties after the heat treatment and behaved exactly the same as S_8, as shown in Figure 9.5: compound 1-S_8 and 2-IS, respectively. On the other hand, compound 3-$PPAS_8$ still showed the best blooming rate reduction, where no bloom could be observed even after 3 weeks storage.

A possible explanation for the reduced blooming behavior of $PPAS_8$, after the heat treatment of 130 °C, is that the shear force generated during the mixing is decreased

for the higher mixing temperature. As a result, more sulfur agglomerates coated with plasma polymers survive after the mixing. Consequently, they act either as a kind of large molecule with a much slower migration rate compared to the uncoated sulfur, or as a more compatible particle relative to the rubber matrix. Compound 4-PFHS$_8$ was not tested under these conditions due to its possible vulcanization during the heat treatment.

Table 9.4 Blooming rate of NR compounds after treatment at ~130 ^{o}C.

Compound/properties	1-S$_8$	2-IS	3-PPAS$_8$
Set temperature (^{o}C) of Brabender	120	120	120
Measured temperature (3min.)	125	127	125
Measured temperature (6min.)	127	129	128
Bloom at:			
15 min.	✕	✕	0
2 hrs.	✕	✕	0
1 day	✕	✕	0
2 days	✕	✕	0
6 days	✕	✕	0
2 weeks	✕	✕	0
3 weeks	✕	✕	0

Symbols as in Table 9.2.

Figure 9.5 Compound 2-IS plasticized at 130 ^{o}C after 3 weeks storage at RT.

Figure 9.6 Compound 3-PPAS$_8$ plasticized at 130 ^{o}C after 3 weeks storage at RT.

9.3.4. Bin scorch

The bin scorch was measured for compounds 1-S$_8$, 2-IS and 3-PPAS$_8$, plasticized at 110 ^{o}C. As compound 4-PFHS$_8$ was proved to be too scorchy for such a NR compound, the bin scorch of this compound was not checked. The scorch time: t$_5$, measured with a Mooney viscometer, was used as an indicator for the bin scorch. The results are shown in Figure 9.7. It is clear that all compounds show no premature vulcanization or scorch during the period of storage. The test was not further conducted for the compounds treated at 120 and 130 ^{o}C, as the viscosities of these compounds were too high for the instrument.
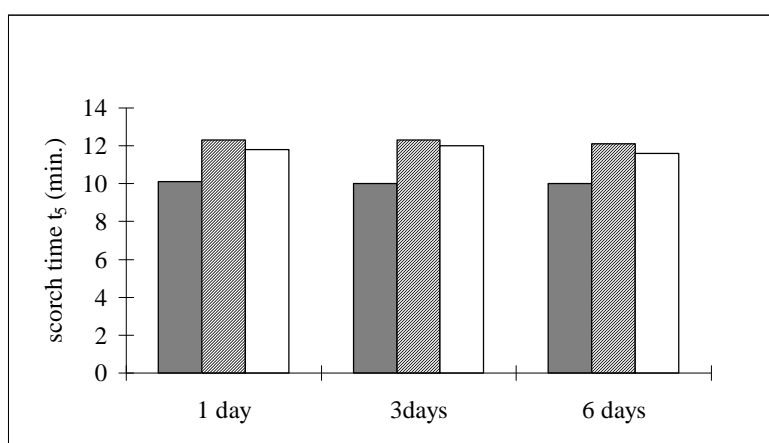

Figure 9.7 Bin Scorch (t$_5$) of NR compounds vs. storage time.
(■) 1-S$_8$; (▨) 2-IS; (□) 3-PPAS$_8$.

9.4. Conclusions

Significant blooming was observed for the control compound 1-S_8, for which the whole surface was covered with sulfur crystals after 3 weeks storage at room temperature. Insoluble sulfur eliminates blooming at a processing temperature of maximum 120 ^{o}C. It is confirmed in this study that the blooming rate of insoluble sulfur is highly dependent on the heat treatment temperature. Insoluble sulfur behaves the same with respect to blooming as soluble sulfur (S_8) in case of a heat treatment temperature $\geqslant$130 ^{o}C. At these temperatures most of the insoluble sulfur converts to soluble sulfur within 3 minutes.

The blooming behavior of different plasma polymer-encapsulated sulfur samples also show a dependence on the heat treatment temperature. The polyacetylene plasma-coated sulfur provides the best blooming reduction for the processing temperature of 130 ^{o}C. This may be due to the fact that the shear forces generated during mixing are decreased due to a lower viscosity of the rubber at higher temperatures. Consequently, the plasma polymer shells on the agglomerates of sulfur remain intact to a greater extent. As a result, migration of sulfur is stopped and blooming is avoided.

The plasma polyperfluorohexane-coated sulfur appears not suitable for this application, as the compound 4-$PFHS_8$ gets scorched during the heat treatment. The shorter scorch time of plasma polyperfluorohexane-coated sulfur compared to the uncoated sulfur was also seen in Chapter 6 in synthetic rubbers. This could to be attributed to the specific nature of the perfluoro-carbon plasma polymers, where probably either a higher amount of radicals or HF are trapped inside the plasma polymer molecules which activate the sulfur cure.

No appreciable bin scorch was seen for all tested compounds during the storage period of 6 days employed in this study, which means that premature vulcanization was not initiated in all the compounds tested.

9.5 References

[1]   F.I. Hoover, B.H. To, R.N. Datta, A.J. de Hoog, N.M. Huntink, A.G. Talma *Rubber Chem. Technol.,* **2003**, 76, 747.

[2]   A.S. Kuzminskii, L.S. Feldshtein, S.A. Reitlinger, *Rubber Chem. Technol.,* **1962**, 35,147.

[3]   S.H. Nah, A.G. Thomas, *Rubber Chem. Technol.,* **1981**, 54, 255.

[4]   U.S. 4,242,472 (1980), to Bridgestone Tire Co. Ltd., Tokyo, JP; invs.: H. Taakashi, I. Setsuko, T. Seisuke.

[5]   U.S. 4,238,470 (1980), to Stauffer Chemical Company, Westport, CT, USA; invs.: Young, A. Randall.

[6]   A. Brimblecombe, *Kautsch. Gummi Kunstst.*, **1996**, 49, 354.

Summary

In industrial applications, different rubber types are often blended to fine-tune or optimize the property portfolio required for successful performance of articles. Considering the complexity of a rubber blend compound, wherein numerous additives are involved, vulcanization or cure mismatch often occurs as an outcome of inhomogeneous distribution of the curatives or imbalanced reactivities of the different rubber phases towards the curatives.

The main objective of the present project was to overcome the cure mismatch in dissimilar rubber blends by controlled distribution of curatives, surface treated curatives through plasma polymerization. Three different monomers with different polarity are applied for the plasma polymerization in order to modify the curatives' surface to either polar or apolar. The performance of the plasma polymer treated curatives are evaluated in both unreinforced and carbon black reinforced dissimilar rubber blends. Dependent on the particular combinations of plasma monomers, improvements are obtained in dissimilar rubber blends using the plasma treated curatives.

Chapter 1 gives a general introduction into rubber technology from a historical point of view. The aim of the research is described together with the structure of the thesis.

An overview of the literature published in the fields of rubber blends, covulcanization, reinforcing fillers and the state of the art of micro-encapsulation is given in **Chapter 2.** Plasma polymerization is introduced in detail with its historical development, mechanism, and especially recent applications towards surface

modification of rubber additive powders.

Chapter 3 provides a solubility study on various curatives in different rubbers, measured with an easy and effective method based on weight up-take by the migration of curative molecules into slightly pre-crosslinked rubbers. The experimental results correlate well with calculated solubility parameter differences. The study provides valuable data for predicting the distribution of curatives in the different phases of dissimilar rubber blends.

Chapter 4 describes a mixing study carried out by applying the solubility knowledge of curatives in rubbers to improve the properties of unreinforced 50/50 w/w blends of SBR/EPDM (SE) and NBR/EPDM (NE). Different mixing procedures are performed based on the same overall recipe for each rubber blend. The curatives are incorporated into a certain phase of rubber before final blending, in an attempt to control their distributions for optimal mechanical properties. Large improvements are achieved for the SE blends, not for the NE blends.

In **Chapter 5**, the surface modification of both sulfur and CBS through plasma polymerization with acetylene is described. As a result of the plasma surface treatment, the surface energies of sulfur and CBS are decreased and brought closer to the range of the rubber polymers involved in this study. Improvements in the mechanical properties are obtained in straight NBR and EPDM compounds, but hardly in straight SBR. A better co-vulcanisation is achieved in the SE blends with the plasma polyacetylene micro-encapsulated sulfur and CBS, however, there are practically no appreciable improvements obtained in the NE blends.

A very un-polar monomer perfluorohexane is used for the plasma encapsulation of sulfur and CBS in **Chapter 6**. Unique features are achieved compared to the modification using acetylene as monomer. The mechanical properties of SE blends are significantly improved by using plasma poly-perfluorohexane coated curatives. Solubility measurements are carried out with plasma perfluorohexane micro-encapsulated sulfur and CBS in the different rubbers studied. The solubility changes, as predicted from the theory, can nicely be used to interpret the improved

performance of the rubber blends by using these poly-perfluorohexane coated additives for the SE blends. For NE blends, the effect of plasma poly-perfluorohexane treatment on curatives is compromised by the cure rate mismatch between the two rubbers involved, which results in no appreciable improvement in final properties.

Improvements in properties of unreinforced NE blends are finally achieved with plasma polyacrylic acid treated sulfur, as described in **Chapter 7**. It was confirmed by ToF-SIMS that a plasma polymer with very high molecule weight is formed for the samples treated for two hours. As a smaller solubility difference between the NBR and the EPDM phases results by using the plasma acrylic acid modified sulfur, a more homogeneous distribution of sulfur is expected. A better covulcanization is achieved as the coating also reduces the migration of the curatives between the different rubber phases. The high polarity and acidity of acrylic acid may also contribute to the unique increase in the properties of the NE blends.

Chapter 8 provides a study of the application of several combinations of various plasma coated sulfur and CBS, in carbon black reinforced dissimilar rubber blends. The improvements achieved in the unreinforced rubber blends are again found by using both plasma coated sulfur and plasma coated CBS in carbon black filled blends. Interestingly, a bigger increase in properties is achieved in NE blends instead of in SE blends.

A blooming study is presented in **Chapter 9**. The blooming behavior of plasma polyacetylene and polyperfluorohexane treated sulfur was determined in carbon black reinforced natural rubber and compared to soluble and insoluble sulfur. It is demonstrated that the plasma coating can also stop sulfur migration from the bulk to the surface of the rubbers, which results in a reduction of blooming. Polyacetylene plasma coated sulfur provides the best blooming reduction for the processing temperature of 130 $^{\circ}$C. The plasma polymer shells on the agglomerates of sulfur remain intact to a greater extent in order to obtain a reduction of blooming. This has the advantage that less accurate control of the mixing temperature is needed for these materials compared to insoluble sulfur, which reverts into soluble sulfur around 110 $^{\circ}$C.

In Chapter 5, 6 and 7, three different monomers: acetylene, perfluorohexane and acrylic acid are used as monomers for plasma surface treatment. Generally, the plasma treated curatives provide better performance in the SE blends compared to the untreated ones. It is proven that a certain degree of coverage is necessary for the treated curatives to show an effect in their performance in dissimilar rubber blends. It would be useful to quantify this level of coverage as the amount of deposited coating, to further optimize the reaction conditions.

Better covulcanization is apparently achieved by using plasma treated curatives in the dissimilar blends of SE and NE, since the overall crosslink density is similar to the identical blends cured with untreated curatives. However, it would still be nicer to differentiate the distribution of crosslinks in various rubber phases to further proof this point. A mechanistic study may also be useful, in order to obtain a deeper insight into the vulcanization reactions with the plasma polymer coated curatives.

Finally, it is worthwhile to combine the work in this study with the previous works on the plasma treated reinforcing fillers, carbon black and silica. Further improvements in properties of dissimilar blends are expected by combining the plasma treated curatives and reinforcing fillers all together. As plasma polymerization is demonstrated to be an effective method in modifying the surface properties of curatives without changing its bulk properties, it is also interesting to apply the obtained know-how from this research in a large scale production trial.

Samenvatting

In dit laatste hoofdstuk wordt een samenvatting gegeven van het onderzoek dat in dit proefschrift is beschreven.

Tot slot wordt er een aantal suggesties voor verder onderzoek gegeven.

10.1   Het onderzoek.

In industriële toepassingen worden verschillende soorten rubber vaak gemengd om de eigenschappen van rubber te optimaliseren en te verfijnen, om zo te komen tot een succesvolle toepassing van artikelen vervaardigd van rubber.

De complexiteit van een rubbermengsel waarin verscheidene additieven worden gebruikt in aanmerking genomen, vindt "cure mismatch" vaak plaats als gevolg van ongelijkmatige verdeling van de vulkanisatieadditieven of ten gevolge van de niet uitgebalanceerde reactiviteit van de verschillende rubbersoorten ten opzichte van de vulkanisatieadditieven.

Het hoofddoel van dit project was om deze "cure-mismatch" in rubbermengsels van ongelijke rubbers op te lossen door het bewerkstelligen van een gelijkmatige verdeling van, met van een plasma polymere schil voorziene vulkanisatieadditieven. Er werden drie monomeren met verschillende polariteit toegepast in de plasmapolymerisatie, met als doel het oppervlak van de vulkanisatieadditieven te veranderen in hetzij polair hetzij a-polair.

De eigenschappen van de met plasmapolymeer gecoate vulkanisatieadditieven werden onderzocht in zowel niet gevulde als roet gevulde rubbermengsels. Afhankelijk van de specifieke combinaties van plasma monomeren, werden verbeteringen in rubbermengsels verkregen door gebruik te maken van de met plasma

polymeer gecoate vulkanisatie-additieven.

## 10.2.	Algemene samenvatting

In hoofdstuk 1 wordt een algemene introductie gegeven in de rubbertechnologie vanuit een historisch perspectief.

In hoofdstuk 2 wordt een overzicht gegeven van de literatuur die is gepubliceerd op het gebied van rubbermengsels, co-vulkanisatie en versterkende vulstoffen en de stand van zaken op het gebied van micro-encapsulatie.

Een onderzoek naar de oplosbaarheid van verscheidene vulkanisatie additieven, gemeten met behulp van een eenvoudige en zeer doeltreffende methode, gebaseerd op gewichtstoename ten gevolge van migratie van vulkanisatie additieven in licht gevulkaniseerde rubbers, wordt beschreven in hoofdstuk 3. De experimentele resultaten komen goed overeen met de berekende oplosbaarheidparameters ($\Delta\delta$). Het onderzoek heeft waardevolle gegevens opgeleverd om de verdeling van de vulkanisatie additieven in de verschillende rubbers te voorspellen.

Hoofdstuk 4 beschrijft onderzoek naar het op verschillende manier mengen van vulkanisatieadditieven in de verschillende rubbers die in de rubbermengsels gebruikt worden, door het toepassen van de in hoofdstuk 3 verworven kennis van de oplosbaarheid van de vulkanisatieadditieven. Op deze manier werd gekeken of de eigenschappen van niet versterkte 50:50 mengsels van SBR en EPDM (SE) en NBR en EPDM (NE) rubber verbeterd konden worden. Verschillende mengprocedures zijn uitgevoerd, om uiteindelijk voor alle mengsels uit te komen op dezelfde samenstelling van het eindmengsel.

De vulkanisatieadditieven zijn toegevoegd aan een van de rubbers uit het mengsel voor het uiteindelijk mengen van de rubbers, dit in een poging om hun verdeling over de verschillende rubbers te controleren, om zo te komen tot optimale rubbereigenschappen.

Voor de SE-mengsels werden grote verbeteringen verkregen, maar niet voor de NE-mengsels.

In hoofdstuk 5 wordt de oppervlaktemodificatie van zowel zwavel als CBS door middel van plasma gepolymeriseerd acetyleen beschreven. Als gevolg van de plasma

poly-acetyleen coating is de oppervlaktespanning van zwavel en CBS verlaagd en komen die daardoor beter overeen met de oppervlakte-energieën van de in deze studie gebruikte rubbersoorten. Verbeteringen in de mechanische eigenschappen werden verkregen in zowel puur NBR en puur EPDM, maar nauwelijks in puur SBR. In de SE mengsels werd een betere co-vulkanisatie verkregen met plasma acetyleen polymeer gecoat zwavel en CBS. In de NE mengsels daarentegen werden geen noemenswaardige verbeteringen gemeten.

De plasma polymerisatie van het zeer apolaire monomeer perfluorohexaan voor het encapsuleren van zwavel wordt beschreven in hoofdstuk 6. Unieke eigenschappen werden hiermee verkregen vergeleken met het plasma acetyleen gecoate zwavel.

De mechanische eigenschappen van de SE mengsels werden significant verbeterd door het gebruik van met plasma poly-perfluoro hexaan geincapsuleerd zwavel.

Oplosbaarheidmetingen in de verschillende bestudeerde rubbers zijn met de plasma poly-perfluorohexaan gecoate zwavel en CBS uitgevoerd. De veranderingen in de oplosbaarheid in de verschillende rubbers, zoals voorspeld op basis van de theorie, konden gebruikt worden om de verbeterde prestatie van deze plasma poly-perfluoro hexaan gecoate additieven in de SE mengsels te verklaren. Bij de NE mengsels wordt het effect van de plasma poly-perfluoro hexaan gecoate additieven teniet gedaan door het grote verschil in de uithardingssnelheid van NBR en EPDM, waardoor geen noemenswaardige verbeteringen in de uiteindelijke eigenschappen werden waargenomen.

Verbeteringen in de eigenschappen van niet met vulstof versterkte NE mengsels werden uiteindelijk bereikt middels met plasma polyacrylzuur gemodificeerd zwavel, zoals beschreven in hoofdstuk 7.

TOF-SIMS analyse aan de monsters die twee uur met plasma waren behandeld, bevestigde dat plasma acrylzuur polymeren met een hoog molecuul gewicht werden gevormd aan het oppervlak van de vulkanisatieadditieven. Door gebruik te maken van plasma acrylzuur gemodificeerd zwavel, ontstaat er een geringer verschil in oplosbaarheid in de NBR en EPDM fase, waardoor een meer homogene verdeling van de zwavel mag worden verwacht. Er wordt op deze manier een betere co-vulkanisatie

bereikt, aangezien de coating de migratie van de zwavel tussen de verschillende rubberfasen vermindert.

De hoge polariteit en de zuurgraad van acrylzuur zullen ook bijgedragen hebben aan de unieke verbetering van de eigenschappen van de NE mengsels.

Hoofdstuk 8 bevat een studie naar de toepassing van verscheidene combinaties van met plasmapolymeer gecoate additieven, zwavel en CBS, in met roet versterkte rubber mengsels. De in niet roetgevulde mengsels gevonden verbeteringen werden in met roetgevulde rubber mengsels, behandeld met de met plasma polymeer gecoate additieven, opnieuw waargenomen. Opmerkelijk genoeg werd er nu een grotere verbetering in eigenschappen in de NE mengsels gemeten in plaats van in de SE mengsels, zoals waargenomen in de niet met roet gevulde mengsels.

In hoofdstuk 9 wordt een "blooming" onderzoek beschreven. Het "blooming" gedrag, dat wil zeggen het uitzweten van een chemicalie, van zwavel gecoat met plasma poly acetyleen en plasma poly perfluorohexaan werd bepaald in roet gevuld natuur rubber (NR) en vergeleken met oplosbaar en onoplosbaar zwavel.

Er werd aangetoond dat de plasma polymere coating ook de migratie van zwavel naar het oppervlak van de rubber kan tegengaan, hetgeen resulteert in een afname van de "blooming". Zwavel gecoat met plasma gepolymeriseerd acetyleen geeft de beste afname van het "bloom" gedrag bij verwerking bij 130°C. De plasma polymere schil rond de zwavelagglomeraten blijft voor een groter deel intact bij deze temperatuur, hetgeen resulteert in een vermindering van het "bloom" gedrag. Dit heeft als voordeel dat de controle van de temperatuur tijdens het mengen minder precies hoeft te worden aangehouden, vergeleken met de verwerking van onoplosbaar zwavel waarbij dit wel nodig is omdat dat bij 110°C omlegt naar oplosbaar zwavel.

10.3.   Suggesties voor verder onderzoek

In de hoofdstukken 5, 6 en 7 worden drie verschillende monomeren, te weten acetyleen, perfluoro hexaan en acrylzuur, gebruikt in de plasma polymerisatie oppervlaktebehandeling. In het algemeen geven de met plasma polymeer gecoate vulkanisatieadditieven een betere werking in de SE mengsels vergeleken met de niet gecoate vulkanisatieadditieven. Er werd bewezen dat er een zekere mate van

bedekking van het oppervlak van de behandelde additieven nodig was om een effect te laten zien in hun werking in rubber mengsels. Het zou zinvol zijn om de bedekkingsgraad na de behandeling goed te kunnen vaststellen als de hoeveelheid neergeslagen polymeer, om zo de reactiecondities en de werking verder te verbeteren. Blijkbaar wordt een betere co-vulkanisatie verkregen wanneer plasma polymeer gecoate vulkanisatie additieven worden gebruikt in de vulkanisatie van rubber mengsels, zoals SE en NE, aangezien de totale crosslink-dichtheid gelijk is aan die van de mengsels gevulkaniseerd met onbehandelde additieven, op basis van de gemeten delta torque. Het zou echter mooier zijn om de crosslink dichtheid van de verschillende rubbers te kunnen differentiëren, teneinde dit punt te kunnen bewijzen.

De opheldering van het mechanisme zou zinvol zijn om zodoende een beter inzicht te verkrijgen in de vulkanisatiereacties met de plasma polymeer gecoate vulkanisatie-additieven.

Tenslotte zou het de moeite waard zijn om de resultaten van dit onderzoek te combineren met de resultaten van de studies met de plasma polymeer gecoate vulstoffen silica en roet. Verdere verbeteringen in eigenschappen zouden verwacht mogen worden door gebruik te maken van deze combinaties. Aangezien gebleken is dat plasma polymerisatie aantoonbaar een effectieve methode is om de oppervlakte eigenschappen te veranderen, zonder de "bulk"-eigenschappen te veranderen, is het ook interessant om de uit dit onderzoek verkregen kennis te testen in een commerciële productie.

Symbols and Abbreviations

δ	Solubility parameter
δ_d	Solubility component from dispersive forces
δ_p	Solubility component from polar forces
δ_h	Solubility component from hydrogen bonding
$\overline{\Delta\delta}$	Difference in solubility parameter
γ	Surface energy
ϕ	Volume fractions
$\overline{\Delta\delta}$	Absolute difference in solubility parameters
ΔH_m	Enthalpy of mixing
ΔG_m	Gibbs free energy change of mixing
ΔS_m	Entropy change of mixing
D	diffusion coefficient
F	Molar or volume flow rate
M	Molecular weight
P_s	Parachor
W	Electrical power input
$W/(F \cdot M)$	power input parameter
AFM	Atomic force microscopy
a.u	Arbitrary units
BR	Butadiene rubber
CB	Carbon black
CBS	N-cyclohexylbenzothiazole-2-sulfenamide
CM	Chlorinated polyethylene

CR	Chloroprene rubber
DCBS	N-dicyclohexylbenzothiazole-2-sulphenamide
DCP	Dicumyl peroxide
DMTA	Dynamic Mechanical Thermal Analysis
DSC	Differential Scanning Calorimetry
DTG	Differential Thermal Gravimetry
E.B.	Elongation at break
EM	Electron Microscopy
EPDM	Ethylene-Propylene-Diene rubber
GC	Gas Chromatography
GLC	Gas Liquid Chromatography
IR	Isoprene rubber
IR	Infrared spectroscopy
IIR	Isoprene-Isobutylene copolymer
IS	Insoluble sulfur
MPa	Mega pasca
MBT	2-mercaptobenzothiazole
NBR	Acrylonitrile-Butadiene rubber
NMR	Nuclear magnetic resonance
NR	Natural Rubber
phr	Parts per hundred rubber
R.E	Rupture energy
RF	Radio frequency
RT	Room temperature
PAA	Plasma polyacrylic acid
PE	Polyethylene
PFH	Plasma polyperfluorohexance
PPA	Plasma polyacetylene

PS	Polystyrene
PVA	Polyvinyl alcohol
RPA	Rubber process analyzer
SANS	Small-angle Neutron Scattering
SAXS	Small-angle X-ray Scattering
SBR	Styrene butadiene rubber
SEM	Scanning electron microscopy
TEM	Transmission Electron Microscopy
TGA	Thermogravimetric analysis
TBBS	N-tert-butyl-benzothiazolesulfenamide
TMTD	Tetramethylthiuram disulfide
ToF-SIMS	Time-of-flight secondary ion mass spectroscopy
XPS	Scanning X-ray Photoelectron Spectroscopy
ZDBC	Zinc dibutyl dithiocarbamate
ZDEC	Zinc diethyl dithiocarbamate

Bibliography

Journal papers

1. R. Guo, A.G. Talma, R.N. Datta, W.K. Dierkes and J.W.M. Noordermeer, *Solubility Study of Curatives in Various Rubbers*, **Eur. Pol. J.**, 2008, 44, 3890.

2. R. Guo, A.G. Talma, R.N. Datta, W.K. Dierkes and J.W.M. Noordermeer, *A Theoretical and Experimental Study on Solubility of Curatives in Rubbers*, **Macromol. Materials Eng.**, 2009, http://dx.doi.org/10.1002/mame.200800370

3. R. Guo, A.G. Talma, R.N. Datta, W.K. Dierkes and J.W.M. Noordermeer, *A Phase Blending Studyon Rubber Blends Based on the Solubility Preference of Curatives,* **Macromol. Materials Eng.**, 2009, accepted in May.

4. R. Guo, A.G. Talma, R.N. Datta, W.K. Dierkes and J.W.M. Noordermeer, *Enhanced Properties of Dissimilar Rubber Blends using Microencapsulated Sulfur through Acetylene Plasma Polymerization,* **Macromol. Materials Eng.**, 2009, submitted in May.

5. R. Guo, A.G. Talma, R.N. Datta, W.K. Dierkes and J.W.M. Noordermeer, *A Novel Surface Modification of Sulfur by Plasma Polymerization and its application in Dissimilar Rubber-Rubber Blends,* **Macromolecules**, 2009, to be submitted.

6. R. Guo, A.G. Talma, R.N. Datta, W.K. Dierkes and J.W.M. Noordermeer, A study of plasma surface modification on vulcanization accelerator and its performance in rubber and rubber-rubber blends, **Polymer**, 2009, in preparation.

7. R. Guo, A.G. Talma, R.N. Datta, W.K. Dierkes and J.W.M. Noordermeer, Applications of plasma polymer encapsulated curatives in carbon black filled rubber system, **Eur. Pol. J.**, 2009, in preparation

Conference proceedings

1. R. Guo, A.G. Talma, R.N. Datta, W.K. Dierkes and J.W.M. Noordermeer, Surface modification of curatives by plasma polymerization for controlled distribution in eslatomer blends, Proceedings of Dutch Polymer Days, Lunteren, the Netherlands, Feb, 2006.

2. R. Guo, A.G. Talma, R.N. Datta, W.K. Dierkes and J.W.M. Noordermeer, Solubility study of curatives in various rubbers, Proceedings of International Rubber Conference, Kuala Lumpur, 2008.

3) R. Guo, A.G. Talma, R.N. Datta, W.K. Dierkes and J.W.M. Noordermeer, Theoretical and practical study on solubility of curatives in rubbers, Proceeding s of Dutch polymer Days, Lunteren, the Netherlands, Feb, 2009.

Curriculum vitae

Rui Guo was born on 23rd March, 1975 in Urumqi, Xingjiang, China. She obtained her Bachelor in 1999 in Shanghai Jiaotong University. After that She worked in AHI warehouse (Shanghai) Co. Ltd. for almost two years. Her master study was carried out in both Shanghai Jiaotong University and University of Twente (the Netherlands) from 2002 to 2005. She obtained Master of Science from University of Twente in 2004.

In May 2005, she started her Ph.D under the supervision of Prof. Dr. Ir. J.W.M. Noordermeer at the University of Twente, the Netherlands. Her mentor is Dr. Auke. Talma. The topic of the research was "Improved Properties of Dissimilar Rubber-Rubber Blends using Plasma Polymer Encapsulated Curatives". The research was funded by Dutch Technology Foundation (STW). The results of this research are described in this thesis. From Oct 2009, the author has started working in Henkel, Shanghai, China as Senior chemist in the Adhesive Research department.

Acknowledgements

This PhD work described in this thesis is the fruit of four years of work in University of Twente, the Netherlands. Looking back of this eventful journey, there are so many people who had given their helps and consideration during the four years.

First of all, I would like to thank my promoter, prof. dr. ir Noordermeer, who offered me the opportunity to carry out my PhD research at the Elastomer Technology and Engineering group. I really have learned a lot from you and I will never forget your vivid rubber course, your suggestions during so many discussions. I respect your scientific attitude toward research and I admire your careful and critical checks with my thesis writing. I am really thankful for your understanding and support all along with my research and life.

I would like to give my special thanks to my co-promotor, dr. Auke Talma. I am very thankful for your continuous confidence in my research work. You always gave me the courage to go further with new ideas. Although you are so busy, you spent a lot of time for discussion and gave me many brilliant ideas.

Dear dr. Rabin Datta, you have helped a lot with my research and you always have great ideas for my work. It was very difficult to face the fact that you had left us but I will remember what you told to "see life in different angle". Thanks also to Sumana-san for giving support in the elemental analysis.

I would like to thank dr. Wilma Dierkes for her support during these years. You were always so patient and willing to help in all kinds of matters.

Prof. dr. van Ooij, I am happy to finally meet in University of Cincinnati. Thank you for taking much time with me to carefully interpret so many ToF-SIMS spectra. Your enthusiasm at research, as well as applying technology to real life has impressed

I specially thank all my Chinese friends for making my stay so memorable. First I would like to thank my flat-mate: Jing, like people always said a friend in need is a friend indeed. Thank you for being so considerate in daily life and giving me advice in all respects; Hongmei, we had so many time together and you are always helping me; I will always remember our friendship. Yan, Jing and Hanquan, Bofei, Yang, Wei, we had great times during our travels. And all the friends that I have met in Enschede: Zhou wei, Yujie, Qi, Lanti, Hao, Rong. Chao, Zhao Wei, Chunlin, Yi, Tian, Xin, Bon-Hua and Hui.

Finally I would like to express my deepest gratitude to my family. Dear Chenglei, it is finally the end of this work. I know it would not be possible without your love, care and support. My dear parents: Guo Zhong-shu and Guo Yü-ru, I am thankful for your love and support in all respect. My dear parents in law: Lu Kang-wei and Yuan Jing-he, thank you for being understanding and thank you for taking such a good care of Lu Yi.

Rui